University of Strathclyde Glasgow

De-risking Development of Hot Sedimentary Aquifer Geothermal Resources: a Case Study of the Chester Formation Sandstone, UK

by

Maëlle Brémaud

Submitted in fulfilment of the requirements for the degree of

Doctor of Philosophy (Ph.D.)

Department of Civil and Environmental Engineering

University of Strathclyde, Glasgow

13 August 2025

Declaration

This thesis is the result of the author's original research. It has been composed by the author and has not been previously submitted for examination which has led to the award of a degree.

13 August 2025

Acknowledgments

There are so many people I would like to acknowledge and thank both professionally and personally. First, I would like to express my deepest gratitude to my supervisors Dr. Neil Burnside and Prof. Zoe Shipton for their unwavering support, guidance, and profound belief in my abilities. I firmly believe the combination of your individual experiences, areas of expertise, and traits was a key asset in the success of the PhD. Neil, thank you for always taking time to meet and discuss whenever I needed it, providing new angles to the PhD, reviewing manuscripts, and assisting with grant applications; all of this while taking care of two young children! Zoe, I am grateful for your time, manuscript edits, and unvaluable guidance throughout this journey that significantly contributed to my growth, not only as a PhD student but also as a person. I am especially appreciative for your enthusiasm and support during fieldwork in chilly Cheshire – classic geology at its best!

I also wish to extend my sincere thanks to the technical support I received in Strathclyde's CEE laboratories. Namely, Mara Knapp and Jim Francis for their availability, patience and guidance with our (sometimes) pretty atypical setup ideas and for rock shipments; and James Minto for the technical advice and assistance with some devices.

I would like to acknowledge the University of Strathclyde International Strategic Partner (ISP) Studentship for funding my PhD research. I am also truly grateful to Strathclyde EPSRC IAA funding for supporting part of the research in Strathclyde's laboratories and in GFZ's lab in Potsdam. I would like to extend my sincere thanks to the Professor John Dunbar International Research Prize 2023 for providing financial support for my participation in the World Geothermal Congress 2023 in Beijing.

Thanks are due to Martin Pujol, Trey Meckel, Cees Willems, Eric Tenthorey, and Graeme Beardsmore who provided support or access to a substantial amount of data for me to include in the database. Without your help my dataset (and associated results) would have looked a bit miserable!

Many thanks to the British Geological Survey, especially Mike Spence and the team at the Keyworth National Geological Repository, for providing access to rock specimens and their assistance during core sampling.

I would also like to express my sincere gratitude to everyone at GFZ for their warm welcome and support during the three months I spent in Potsdam. Special thanks go to Sven Fuchs for his supervision and advice; Claire Bossennec for hosting me, providing valuable technical and scientific advice, and for her friendship; Fiorenza Deon for conducting and interpreting the XRD scans; and Robert Peksa for the technical support.

Thank you to my colleagues at JRG Energy for their continuous support, and for providing learning and work experience opportunities.

I would like to recognise the help I received from two MSc students throughout the PhD. Thanks to Taylor and Hannah for your assistance with data collection and lab measurements, respectively. Thanks are also due to FAFFers for their support and direct or indirect help with the PhD. In particular, I would like to thank my fellow geothermal mates with whom I shared doubts, but also valuable learning experiences and laughter, through many conferences and geological trips. Special thank you to Sally and Dan for memorable Geolidays in China, and to Mohamed for fruitful geology discussions. My gratitude also goes out to all my fellow PhDs in the CEE Department for chats, advice and shared laughter that made this journey truly enjoyable.

Many thanks to my friends, both in Glasgow and back home, for their relentless support and for helping we unwind when I needed it the most. A special thank you goes to Cathiane, Léna, Thomas – I value our friendship more than you know (don't get too cocky though!).

Last but far from least, I would like to thank my family for their unwavering encouragement and love, and for supporting me no matter what. Thank you, Mum and Dad, for always believing in me, always listening even through you hadn't got a clue what I was wittering on about. Special thanks to the best sister ever. Thank you for always being an inspiration since we were kids. Now, it's your time to shine and complete your PhD!

Abstract

Hot sedimentary aquifer (HSA) systems have the potential to play a substantial role in the future energy supply of numerous countries, contributing to decarbonation efforts and the achievement of Net Zero targets. However, the advancement of HSAs is impeded by a broad spectrum of risks. This thesis systematically examines these risks through an analysis of HSA projects worldwide, and proposes strategies to mitigate risks that should contribute to reducing project failure rates. A global database has been compiled, incorporating key parameters from 256 HSA projects across eight countries: Australia, Croatia, Denmark, France, Germany, Poland, the Netherlands, and the UK. The analysis reveals that 26% of these projects have failed, predominantly due to geological and hydrogeological (39%), financial (26%) and technical factors (25%). Notably, geology and hydrogeological data are often underreported by geothermal operators. Almost one quarter of both failed and operational HSA projects have implemented mitigation or remediation strategies, leading to a general decline in failure rates over time. The database findings highlight the necessity of thorough geological site characterisation prior to drilling, continuous borehole monitoring, technological advancements to manage geochemical and technical challenges, and the widespread adoption of risk insurances mechanisms. Additionally, the thesis identifies a lack of standardised terminologies for HSA systems, along with the need for improved regulatory frameworks and enhanced data accessibility.

To address existing knowledge gaps and support risk mitigation in HSA exploration, the Chester Formation of the Cheshire Basin is examined as an HSA case study. The thermal, mineralogical and petrophysical properties of this promising geothermal reservoir are comprehensively characterised. Results indicate that samples collected at outcrop exposures generally exhibit similar properties to core samples from the shallow subsurface, apart from thermal conductivity that tends to be higher in core samples. This suggests that preliminary geothermal assessments can be conducted cost-effectively using outcrop samples, reducing the reliance on

borehole drilling. This approach has the potential to reduce investment risks and facilitate geothermal development. Thermal properties are commonly measured in the lab at ambient temperatures and under unsaturated conductions. Thermal properties of Chester Formation samples are measured at (1) elevated temperature and (2) water-saturated conditions to evaluate potential differences with ambient measurements. Additionally, an innovative experimental setup is developed and benchmarked for measuring thermal properties under in situ reservoir conditions. This setup enables a comparative evaluation of thermal conductivity under both high-temperature and water-saturated conditions, against conventional ambient-temperature measurements on dry samples. Integrating in situ thermal property measurements should enhance the accuracy of geothermal resource characterisation and heat flow predictions, reducing uncertainties and investment risks associated with geothermal projects.

Publications Arising from the Thesis

In Journals

Brémaud, M., Burnside, N. M., Shipton, Z., Willems, C. J. L., Pujol, M., & Bossennec, C. (2025). Global database of hot sedimentary aquifer geothermal projects: De-risking future projects by determining key success and failure criteria in the development of a valuable low-carbon energy resource. *Geoenergy*. https://doi.org/10.1144/geoenergy2024-031

Brémaud, M., Burnside, N. M., Shipton, Z., Bossennec, C., Fuchs, S., & Deon, F. (2025). Bridging Surface and Subsurface: Comparative Analysis of Outcrop and Core Samples from the Chester Formation for Geothermal Exploration. *Geothermics*, under review. SSRN Preprint. 10.2139/ssrn.5177375

In Conference Proceedings

Brémaud, M., Burnside, N. M., Shipton, Z. K., & Willems, C. J. (2023, September). De-risking database for hot sedimentary aquifers. In *World Geothermal Congress 2023*. https://pureportal.strath.ac.uk/en/publications/de-risking-database-for-hot-sedimentary-aquifers

Presentations related to the thesis

- Poster presentation at the European Geothermal PhD Days (EGPD) 2023, Glasgow, UK (in person)
- Poster presentation at the All Energy - Dcarbonise Exhibition and Conference 2023, Glasgow, UK (in person)

- Oral presentation at the Energy Geoscience Conference (EGC) 2023, Aberdeen, UK (in person)
- Poster presentation at the World Geothermal Congress (WGC) 2023, Beijing, China (in person)
- Oral presentation at the UK Geothermal Symposium 2024, London, UK (virtual)

Co-authorship

Burnside, N. M., Andrews, B., Brémaud, M., Deeming, K. B., Flude, S., Gillen, C., ... & Whittington, D. (2023). Lessons from mine water geothermal projects across Central Scotland. In *World Geothermal Congress 2023*. https://pureportal.strath.ac.uk/en/publications/lessons-from-mine-water-geothermal-projects-across-central-scotla

Contents

List of Figures

List of Tables

List of Abbreviations

ADEME	French Environment and Energy Management Agency
AFPG	French Association of Geothermal Professionals
AZU	Croatian Hydrocarbon Agency
BGS	British Geological Survey
BHT	Bottom-hole-temperature
CAPEX	Capital Expenditure
CHP	Combined Heat and Power plant
COP	United Nations Framework Convention on Climate Change
CPB	Chester Pebble Beds
DEVEX	Development Expenditure
DST	Drill stem-tests
EEG	German Renewable Energy Sources Act
EGS	Enhanced Geothermal System
GSA	Geothermal System Assessment
HDR	Hot Dry Rock
HIP	Heat In Place
HSA	Hot Sedimentary Aquifer
IEA	International Energy Agency
IGA	International Geothermal Association
IPCC	Intergovernmental Panel on Climate Change
IRENA	International Renewable Energy Agency
LIAG	The Leibniz Institute for Applied Geophysics

LTR	Long-Term Risk insurance
mbgl	meters below ground level
MD	Measured Depth
NIMBY	Not In My Backyard
OFGEM	Office of Gas and Electricity Markets
OPEX	Operational Expenditure
ORC	Organic Rankine Cycle
PRISMA	Preferred Reporting Items for Systematic Reviews and Meta-Analyses
RO	Research Objective
RQ	Research Question
SEPA	Scottish Environmental Protection Agency
SSG	Sherwood Sandstone Group
STR	Short-Term Risk insurance
TCS	Thermal Conductivity Scanner
TCU	Temperature Control Unit
TNO	Dutch Organization for Applied Scientific Research
TPS	Transient Plane Source
TVD	True Vertical Depth
UKGEOS	UK Geoenergy Observatory
UNFC	United Nation Framework for Classification for Resources
USD	United States Dollar
VDR	Virtual Data Room
WIP	Water Immersion Porosimetry

XRD	X-Ray Diffraction

Parameters

c_p	Specific heat capacity (J kg^{-1} K^{-1})
k	Intrinsic permeability (m^2 or mD)
PI	Productivity Index (m^3/h/bar)
Q	Volumetric flow rate (l/s or m^3/s)
q	Heat Flow (W m^{-2})
T	Transmissivity (Dm)
α	Thermal diffusivity (m^2/s)
λ	Thermal conductivity (W m^{-1} K^{-1})
μ	Dynamic viscosity of a fluid (Pa.s)

Units

EJ	Exajoule
GWe	Gigawatt of electricity
GWth	Gigawatt thermal
kV	Kilovolt
kWe	Kilowatt of electricity
kWh	Kilowatt-hour
kWth	Kilowatt thermal
M	Million
mA	Milliampere

MW	Megawatt
MWh	Megawatt-hour
MWth	Megawatt thermal
PWh	Petawatt-hour
TW	Terawatt
TWh	Terawatt-hour

CHAPTER 1
General Introduction

Suitable aquifers underlay 16% of the Earth's land surface and store an estimated 110,000–1,400,000 PWh (400,000–1,450,000 EJ) that could theoretically be used for direct heat applications. […]

Despite the potential, geothermal direct heat supplies only 0.15% of the annual global final energy consumption. […]

The mismatch between potential and developed geothermal resources is caused by high upfront costs, decentralised geothermal heat production, lack of uniformity among geothermal projects, geological uncertainties, and geotechnical risks.

Intergovernmental Panel on Climate Change (IPCC)
Sixth Assessment Report (2022), Ch. 6

1.1. Project Overview and Rationale

In 2023, global energy consumption reached 183 TWh, with a fossil fuel (i.e., coal, oil and natural gas) share of 77% (Energy Institute - Statistical Review of World Energy (2024); Smil (2017)). Transitioning to low-carbon energy sources faces an additional challenge from growing global energy demand, which is increasing at a rate of 1 to 2% per year (Richie et al., 2020). The Intergovernmental Panel on Climate Change (IPCC) has identified carbon emissions from fossil fuels as the main driver of global warming, accounting for 91% of total emissions in 2022 (Hausfather and Friedlingstein, 2022). To tackle climate change, world leaders convened at the 21st Conference of Parties to the United Nations Framework Convention on Climate Change (COP21) in France in December 2015, where they negotiated the landmark Paris Agreement. This treaty set long-term goals to

pursue efforts in “limiting the rise in global temperature to 2°C above pre-industrial levels” and demonstrates a shift towards net-zero greenhouse gas emissions worldwide. To limit global warming, COP21 stakeholders declared that emissions must peak before 2025 for a decline of 43% by 2030. COP21 goals required all legally bound parties to work together and achieve an effective energy transition with a progressive abandoning of fossil fuels in aid of renewable energies.

Between 2015 and 2023, the share of renewables in global energy consumption increased modestly from 9.8% to 13.7% (Energy Institute - Statistical Review of World Energy (2024); Smil (2017)). COP28, held in Dubai from 30 November to 13 December 2023, emphasised the insufficient progress made to address climate change, especially to reduce greenhouse gas emissions. Leaders called to speed up the transition away from fossil fuels to renewables, and a ’Double Down, Triple Up’ campaign was launched to triple global renewable energy capacity and double energy efficiency by 2030.

Geothermal energy meets many criteria to become a major renewable energy source. It provides a low-carbon, clean, sustainable energy, and can operate all year-round at a competitive cost, no matter the weather. The land occupancy of a geothermal installation is very low (7.5 km^2/TWh, McDonald et al., 2009), and the energy produced can be used for both heating purposes and electricity generation, and sometimes value-added mineral extraction such as lithium. In 2023, geothermal accounted for 0.5% of global renewable-based energy generation, with a power generation capacity of 16,355 GWe and a heating and cooling capacity of 173,303 GWth (IGA, 2023). Between 2015 and 2020, geothermal heating and cooling showed an annual increase of c. 9% while geothermal electricity generation has increased at an annual rate of 3.5% (IRENA and IGA, 2023). According to IPCC (2007), geothermal energy has the potential to fulfil approximately 8% of the global electricity demand and provide energy services to 17% of the world's population.

Amongst all geothermal systems, Hot Sedimentary Aquifers (HSAs) offer a huge potential for low-carbon heat and occasionally power generation. HSA are hot

reservoir rocks that are porous enough to hold large volumes of water, and permeable enough to maintain economically viable production levels without extensive reservoir engineering. Such systems can be found in nearly every country and their potential exploitation could significantly influence future energy provision worldwide (Limberger et al., 2018). Indeed, 50% of global energy consumption is dedicated to heating and nearly two thirds of heating still rely on fossil fuels (Briens and Martinez-Gordon, 2023). HSAs typically incur lower development costs compared to other geothermal systems due to shallower drilling targets, higher borehole flow rates, and the utilisation of established and conventional technologies (Barnett, 2009).

Despite these benefits, the development of Hot Sedimentary Aquifers has been slowed down by various factors. Public acceptance and engagement can play a crucial role in geothermal growth, especially in areas where geothermal development has triggered earthquakes (Wallquist and Holenstein, 2015). While HSA projects are less likely to induce seismic events since they do not involve hydraulic fracturing as used in some other geothermal systems (Gehringer and Loksha, 2012), the risk of induced seismicity is not entirely absent (Kivi et al., 2022). Regulatory constraints and economic risks are also influencing the modest growth of the geothermal industry, especially due to due high upfront costs and long lead time (Gehringer and Loksha, 2012). However, geological uncertainties associated with a geothermal reservoir usually constitute the main obstacle to a broader development of Hot Sedimentary Aquifers (Gehringer and Loksha, 2012; Witter et al., 2019). Temperature, thermal conductivity, permeability, and volume are the most critical subsurface parameters for defining a geothermal resource, and the distribution and localisation of permeability within a geothermal reservoir is significantly influenced by its lithologic distribution and geological structure (Witter et al., 2019). Thermal conductivity is a critical parameter influencing the efficiency of heat transfer within the reservoir, and thus the long-term performance of geothermal systems (Blázquez et al., 2017; García-Noval et al., 2024; Marelis, 2017; Sipio and Bertermann, 2018; van Rijn, 2018). Inaccurately

characterising this parameter can lead to overestimated resource longevity and increased project risk.

Although subsurface exploration technologies have significantly advanced, accurately predicting the exact reservoir characteristics and properties (i.e., depth, extent, geometry, productivity, thermal conductivity, permeability, etc.) remains a considerable challenge and therefore induces exploration risks (Gehringer and Loksha, 2012).

1.2. Project Aims, Research Questions and Objectives

The primary aim of this thesis was to identify, quantify, and offer recommendations to limit the risks associated with the exploration of Hot Sedimentary Aquifer systems ; thereby contributing to practical advancements in the renewable energy sector. Research was performed using publicly available information from currently operational and shut-down projects. In addition, new data on thermal properties were collected from a case study site with the aim of exploring how such properties can be most effectively measured.

Research questions (RQ) and research objectives (RO) of the thesis were thus defined as follows:

RQ 1: How much does geology contribute to project failure in HSAs?

- **RO 1.1:** Identify countries that hold a significant HSA potential and availability of open-access data, and use this data to develop a comprehensive database.
- **RO 1.2:** Determine key predictive parameters (or combinations thereof) that have had an impact on the success or failure of an HSA geothermal project.
- **RO 1.3:** Identify key information gaps that must be addressed.

RQ 2: What approaches can be employed to facilitate the advancement of HSA systems?

- **RO 2.1:** Examine the diverse classification and definitions of geothermal systems.
- **RO 2.2:** Investigate the global accessibility and reporting of geothermal data.
- **RO 2.3:** Explore current energy regulations in identified countries and their impact on geothermal development.
- **RO 2.4:** Elaborate on the mitigation and remediation strategies that contributed to the prevention of project failures.

RQ 3: How well can outcrop sample data be used to predict subsurface conditions in HSA geothermal reservoirs?

- **RO 3.1:** Secure comparative samples from outcrop and borehole.
- **RO 3.2:** Complete analysis on new mineralogical, thermal and petrophysical data of a potential HSA reservoir.
- **RO 3.3:** Compare the results of outcrop and core sample measurements.
- **RO 3.4:** Determine the suitability of outcrop samples use for reservoir properties assessment.

RQ 4: How can thermal property assessments be improved to enhance the characterisation of HSA geothermal reservoirs?

- **RO 4.1:** Conduct ambient experiments and test reproducibility across international laboratories.
- **RO 4.2:** Develop a new methodology for measuring thermal conductivity under water-saturated and different temperature conditions.

- **RO 4.3:** Investigate the individual effects of saturation and temperature on thermal properties and evaluate the difference compared to ambient conditions.
- **RO 4.4:** Evaluate the value of performing in situ thermal conductivity analysis instead of measurements at ambient conditions.

1.3. Thesis Structure

This thesis is composed of eight main chapters (Fig. 1-1). The main results are presented in Chapters 3, 6 and 7 and are written as individual journal articles which have been accepted for publication (Chapter 3), submitted (Chapter 6), or will be submitted (Chapter 7) in peer-reviewed international journals. Each results chapter of the thesis has its own abstract, introduction, methods, results, discussion, and conclusion. Bridging text was written to link these chapters and provide context to the main aims and objectives of the thesis. Contents of the submitted/accepted chapters inevitably contain some overlap, and they were written as first-person plural as they were intended for publication. I am primarily responsible for the work in each paper, with specific contributions of co-authors explicitly outlined in the introduction preceding each manuscript.

The chapters are as follows:

Chapter 1 provides an overview of the research topic, and a description of the research aim with the research questions and research objectives involved in achieving the aim.

Chapter 2 reviews the current state of geothermal energy, with a focus on hot sedimentary aquifers. It introduces the fundamental principles and thermodynamics of geothermal energy. This Chapter examines the key components of a geothermal system and their reservoir properties to assess

geothermal resource potential. Additionally, the classification of geothermal resources and applications are discussed. Finally, public perception and risk management in geothermal development are explored.

Chapter 3 presents a comprehensive database of hot sedimentary aquifer systems in eight countries. It addresses key knowledge gaps on the risks associated with the development of hot sedimentary aquifer systems that restrain their further growth. Notably, Chapter 3 provides key parameters responsible for the failure of HSA projects, thereby supporting the success and viability of such prospects. This study also highlights the poor accessibility of geothermal data and reporting globally, as well as a lack of standard harmonisation regarding the classification of geothermal systems.

Chapter 4 partially builds on Chapter 3 and explores the geological context of the Chester Formation in the Cheshire Basin (UK), which is the case study site investigated in Chapter 6 and 7. This Chapter also provides an evaluation of the geothermal potential of the Cheshire Basin, and details the sampling methods for collecting samples of the Chester Formation.

Chapter 5 addresses the materials and methods used to analyse the Chester Formation rock cores and outcrop samples described in Chapter 4. The samples were examined for mineralogy, petrophysical and thermal properties. The mineralogical composition of the samples was approached using X-ray diffraction and optical microscopy, while thermal conductivity was measured using the thermal conductivity scanner and the transient plane source method. Water Immersion Porosimetry (WIP) and image analysis were utilised to determine porosity, while the permeability of the samples was evaluated using an air permeameter.

Chapter 6 provides a comparative analysis of reservoir properties measured on samples from cores and outcrop exposures to assess the transferability of outcrop-derived data to subsurface conditions. Outcrop and core samples from the Chester

Formation were analysed for mineralogy, petrophysical, and thermal properties using X-ray diffraction, optical microscopy, porosity, permeability, and thermal conductivity tests. This study aims to fill a research gap and improve geothermal exploration by enhancing accuracy while reducing resource risk. If outcrop and core sample properties are similar or comparable, then key geothermal data to be obtained cost-effectively without drilling, reducing investment risks and supporting geothermal project development.

Chapter 7 presents a comparative evaluation of thermal conductivity measurements on the Chester Formation samples under various conditions: ambient temperature in the dry state, in situ reservoir temperature in the dry state, ambient temperature in water-saturated conditions, and in situ reservoir temperature in water-saturated state. This study investigates the impact of temperature and water saturation parameters both separately and simultaneously to evaluate the value of performing in situ thermal analysis instead of measurements at ambient conditions. Associated implications for geothermal reservoir assessment are then discussed.

Chapter 8 concludes the thesis by discussing the major research findings and addressing the established research questions. Additionally, it presents recommendations on key strategies for mitigating the risks associated with HSA geothermal systems, and suggests directions for future research.

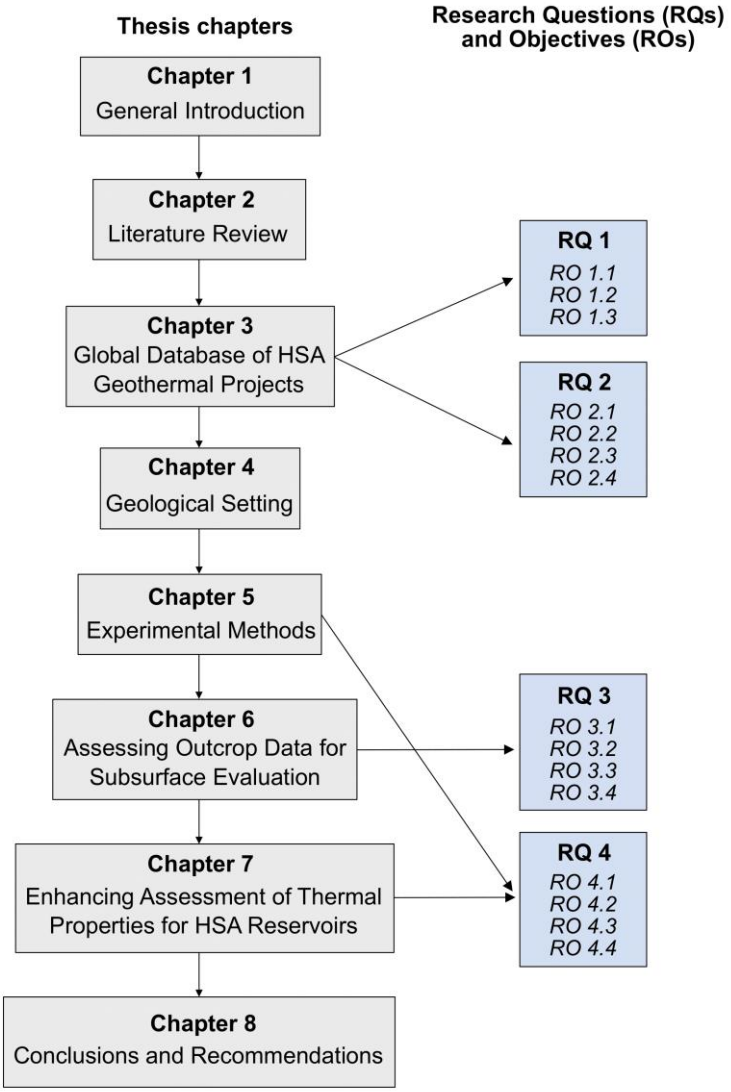

Figure 1-1 : Flow diagram of the structure of the thesis

1.4. References

Barnett, P. (2009). Large scale hot sedimentary aquifer (HSA) geothermal projects. *Presentation to Victoria Energy Conference*. https://hotcopper.com.au/data/oldanns/2009/HRL/30fcbb08-c66c-4db4-807b-f1c497b865a0-HRL213165.pdf

Blázquez, C. S., Martín, A. F., Nieto, I. M., & González-Aguilera, D. (2017). Measuring of thermal conductivities of soils and rocks to be used in the

calculation of A geothermal installation. *Energies*, *10*(6). https://doi.org/10.3390/en10060795

Briens, F., & Martinez-Gordon, R. (2023). Heating. International Energy Agency (IEA). https://www.iea.org/energy-system/buildings/heating

Energy Institute - Statistical Review of World Energy (2024); Smil (2017) – with major processing by Our World in Data. “Primary energy from hydropower” [dataset]. Energy Institute, “Statistical Review of World Energy”; Smil, “Energy Transitions: Global and National Perspectives” [original data].

García-Noval, C., Álvarez, R., García-Cortés, S., García, C., Alberquilla, F., & Ordóñez, A. (2024). Definition of a thermal conductivity map for geothermal purposes. *Geothermal Energy*, *12*(1), 17.

Gehringer, M., & Loksha, V. (2012). Geothermal handbook: Planning and Financing Power Generation. https://www.esmap.org/sites/esmap.org/files/DocumentLibrary/FINAL_Geothermal%20Handbook_TR002-12_Reduced.pdf

Hausfather, Z., & Friedlingstein, P. (2022). Analysis: Global CO2 emissions from fossil fuels hit record high in 2022. Carbon Brief. https://www.carbonbrief.org/analysis-global-co2-emissions-from-fossil-fuels-hit-record-high-in-2022/#:~:text=Fossil%20CO2%20emissions%20represent%20the,the%20same%20as%20fossil%20emissions.

IGA. (2023). IGA unveils new key Geothermal Power & Direct Use data. IGA. https://www.lovegeothermal.org/global-geothermal-update-2023-iga-unveils-new-key-geothermal-power-direct-use-data/

IPCC. (2007). Climate Change 2007: Mitigation of Climate Change. www.ipcc.ch/site/assets/uploads/2018/03/ar4_wg3_full_report-1.pdf

IRENA, & IGA. (2023). Global geothermal market and technology assessment. International Renewable Energy Agency and International Geothermal Association. https://mc-cd8320d4-36a1-40ac-83cc-3389-cdn-endpoint.azureedge.net/-/media/Files/IRENA/Agency/Publication/2023/Feb/IRENA_Global_geothermal_market_technology_assessment_2023.pdf?rev=37e6de031c98489f9bf17880cf9e8858

Kivi, I. R., Pujades, E., Rutqvist, J., & Vilarrasa, V. (2022). Thermal stressing is likely to reactivate distant faults in hot sedimentary aquifers.

Limberger, J., Boxem, T., Pluymaekers, M., Bruhn, D., Manzella, A., Calcagno, P., Beekman, F., Cloetingh, S., & van Wees, J. D. (2018). Geothermal energy in deep aquifers: A global assessment of the resource base for direct heat utilization. In *Renewable and Sustainable Energy Reviews* (Vol. 82). https://doi.org/10.1016/j.rser.2017.09.084

Marelis, A. A. (2017). *Energy capacity of a geothermal reservoir.*

McDonald, R. I., Fargione, J., Kiesecker, J., Miller, W. M., & Powell, J. (2009). Energy Sprawl or Energy Efficiency: Climate Policy Impacts on Natural Habitat for the United States of America. PLoS ONE.

Richie, H., Rosado, P., & Roser, M. (2020). Energy Production and Consumption: Explore data on how energy production and use varies across the world. Our World in Data. https://ourworldindata.org/energy-production-consumption

Sipio, E. di, & Bertermann, D. (2018). Thermal properties variations in unconsolidated material for very shallow geothermal application (ITER project). *International Agrophysics*, *32*(2). https://doi.org/10.1515/intag-2017-0002

van Rijn, S. (2018). *Breakthrough time of a geothermal reservoir.*

Wallquist, L., & Holenstein, M. (2015). Engaging the Public on Geothermal Energy. World Geothermal Congress, Melbourne, Australia, 19-25 April 2015, April.

Witter, J. B., Trainor-Guitton, W. J., & Siler, D. L. (2019). Uncertainty and risk evaluation during the exploration stage of geothermal development: A review. In Geothermics (Vol. 78). https://doi.org/10.1016/j.geothermics.2018.12.011

CHAPTER 2
Literature Review

2.1. Introduction

This chapter reviews the current state of geothermal energy –in particular hot sedimentary aquifers–, starting with an introduction to its principles and thermodynamics. The distinct components of a geothermal system will then be presented, as well as their reservoir properties that are crucial to assess the potential of a geothermal resource. An overview of various geothermal resource classifications and applications is then provided, which are essential for determining their efficiency. Additionally, this chapter addresses public perception and risk management in geothermal development, highlighting the importance of understanding risks and learn from failures to expand its use worldwide.

Through a comprehensive literature review, the chapter aims to provide a thorough understanding of the social, scientific, technical and risks dimensions of the geothermal sector.

2.2. Geothermal Energy

Ethymologically, “geothermal” is derived from the ancient Greek “γῆ” (guê) meaning “Earth”, and “θερμός” (thermos) meaning “hot”. It corresponds to the thermal energy contained within the Earth body.

2.2.1. Thermal Dynamics in Geothermal Systems

“To understand the thermal structure of the earth, knowledge of the thermal properties of the material that constitutes the interior of the earth is indispensable.”

Ki-Iti Horai (1971)

In this section, an introduction on heat production and distribution within the various layers of the Earth is provided through the description of key properties and concepts including heat flow, temperature, and thermal conductivity.

2.2.1.1. Heat Flow

Thermal processes govern plate tectonics and associated activities at plate boundaries (Huenges, 2010), and provide a constraint to the lithospheric rheology (Houseman et al., 1981) and the internal state and dynamics of the mantle (Kellogg et al., 1999; Davies, 1989). Therefore, a comprehension of the Earth's thermal budget is of great significance to understand the global dynamics of the planet and is also valuable for various applications such as geothermal energy (Muffler and Cataldi, 1978).

The natural heat of the Earth primarily comes from (1) the decay of naturally radioactive elements such as uranium, potassium, and thorium within the crust and the mantle, (2) the primordial heat left over from the formation of the Earth that is emanating from the core, and (3) the secular cooling of the mantle (Furlong and Chapman, 2013; Huenges, 2010).

Over the past decades, the global heat budget of the Earth has been successively estimated to be in the range of 46 TW (Jaupart et al., 2007; Jaupart and Mareschal, 2003) to 47 TW (Davies and Davies, 2010). Heat flow models typically break down heat flow values between the continents and the oceans. In the model proposed by Davies and Davies (2010), 15 TW are dissipated across the continental lithosphere and c. 32 TW are released across the oceanic lithosphere (Furlong and Chapman, 2013) (Fig. 2.1).

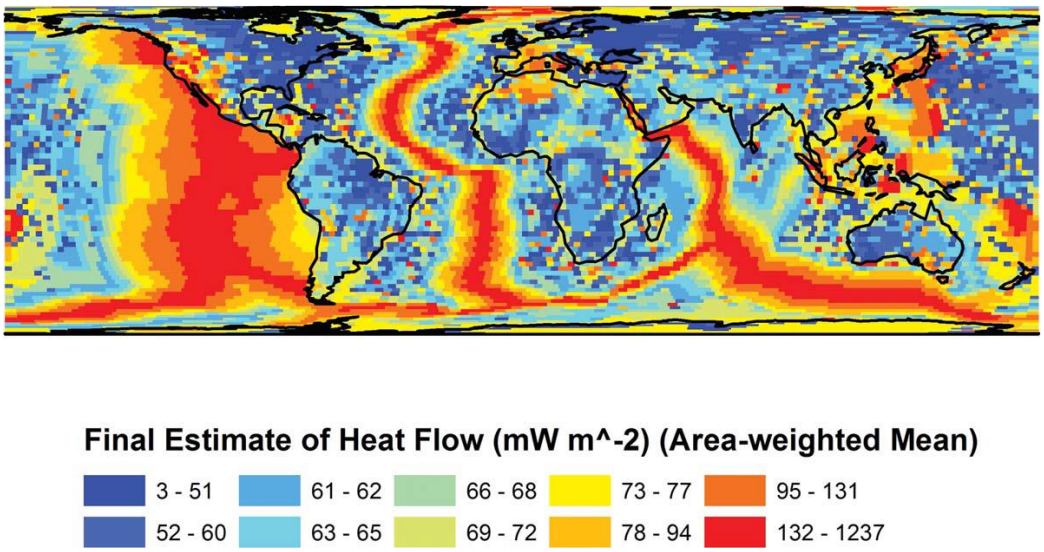

Figure 2-1: Global heat flow map (Davies, 2013)

The main heat transfer mechanisms of the Earth are radiation, conduction, and convection; the three of them working together to transfer heat efficiently. Heat conduction is the transfer of energy from a warmer substance to a colder one through direct contact. It is the main process of heat transfer for solids. In convective systems, the heat transfer occurs by the movement of fluids. The warmer and less dense parts of the fluid ascend, while the cooler and denser parts sink, resulting in a circulation pattern that transfers heat. Heat can also be transferred in the form of an electromagnetic radiation, such as the radiant solar energy. However, radiation typically has a negligible impact on processes that occur within the lithosphere (Schön, 2011).

Heat flow prediction within the continental lithosphere and crust is primarily governed by conductive heat transfer (Turcotte and Schubert, 2014; Huenges, 2010). Since geothermal systems occur within the crust, convection and radiation transfer processes will not be further detailed here. The law of heat conduction is also known as Fourier's Law and states that heat flow is the product of thermal conductivity and temperature gradient. It is detailed in its one-dimensional form in Eq. (2-1), with a temperature variation with depth (i.e., in the z direction):

$$q_z = -\lambda \frac{dT}{dz} \tag{2-1}$$

where q_z is the heat flow (W m^{-2}), λ is the thermal conductivity of the material (W m^{-1} K^{-1}) and $\frac{dT}{dz}$ is the geothermal gradient (K/m). In theory, heat flow can then be determined by direct measurements of thermal conductivity and geothermal gradient in a borehole. However, this process has unexpected complexity in many aspects. Penetrating the subsurface to measure temperatures (e.g., by drilling a borehole) produces thermal perturbations that must be considered when measuring temperature. Thermal conductivity measurements done ex-situ, i.e., in a laboratory on rock samples collected from the subsurface, induce errors because of the pressure and temperature variations between their collection depth and the surface (Stein, 2013). If the thermal conductivity and geothermal gradients significantly change with depth (usually as a result of lithology variations within an interval), then the heat flow must be estimated (Stein, 2013).

2.2.1.2. Thermal Conductivity

Thermal conductivity (λ) is the intrinsic ability of a material to transfer or conduct heat. In geothermal systems, the temperature of the extracted fluid, and thus the efficiency and longevity of the operation, is influenced not only by depth and geothermal gradient, but also by the thermal properties of the reservoir rocks. As thermal energy is extracted over time, a cooling front advances into the reservoir, and the rate at which heat is replenished from the surrounding rock is directly controlled by thermal conductivity. This makes it a critical parameter for evaluating long-term heat extraction potential and ensuring sustainable reservoir performance (Blázquez et al., 2017; García-Noval et al., 2024; Murthy et al., 2023; Sipio and Bertermann, 2018).

Features such as fluid composition, rock texture and mineral content induce a significant variability in thermal conductivity for distinct rock types (Pimienta et al., 2018; Schön, 2011), as shown in Fig. 2-2. Therefore, (1) thermal conductivity is likely to be higher for water-saturated materials than (air) dry rocks and (2) a decrease in thermal conductivity is expected with increasing porosity and fracturing (Nagaraju and Roy, 2014; Midttømme and Roaldset, 1999, Schön, 2011). Temperature also impacts thermal measurements, though the behaviour

significantly varies for different rock types. It is broadly acknowledged that thermal conductivity of clastic rocks decreases with increasing temperature, and that this decrease is more pronounced for rocks with higher thermal conductivity at ambient conditions than for rocks with a low thermal conductivity (Vosteen and Schellschmidt, 2003; Labus and Labus, 2018). Other studies (e.g. Chen et al., 2021) suggested that thermal conductivity versus temperature curves may be classified into different groups based on the thermal conductivity value at 25°C and are independent of the lithology. Although it has been observed that thermal conductivity increases approximately linearly with pressure, its effect is somewhat smaller compared to the effect of temperature (Midttømme and Roaldset, 1999; Abdulagatov et al., 2006). This relationship is likely due to an increased grain-to-grain contact with increasing pressure.

The impact of rock texture on thermal conductivity is complex and not well studied (Midttømme and Roaldset, 1999) but is considered as less important than other parameters such as porosity and mineralogy (Somerton, 1992; Brigaud and Vasseur, 1989). Midttømme and Roaldset (1998) identified a linear correlation between the logarithm of grain size and thermal conductivity while studying artificial quartz samples with different grain size fractions. The most critical parameter that must be considered when assessing the effect of rock texture on thermal conductivity is anisotropy. Stratification of sedimentary rocks usually suggests mineralogy or granulometry variations, which could result in substantial anisotropy differences on rock samples (Brigaud and Vasseur, 1989). Two components of the thermal conductivity are defined: one parallel ($k_{\parallel}$) and one perpendicular ($k_{\perp}$) to bedding. In particular, anisotropy of “structural origin” (i.e., influenced by both porosity layering and mineral bedding in the strata) usually shows a $k_{\parallel}$ smaller than $k_{\perp}$, and the anisotropy factor A is defined as the ratio of $k_{\parallel}$ over $k_{\perp}$ (Brigaud and Vasseur, 1989).

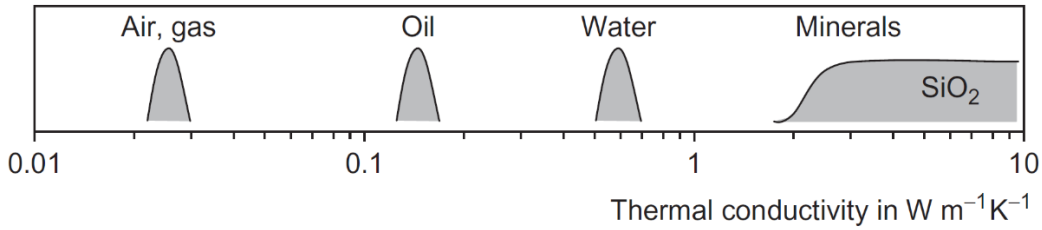

Figure 2-2: Thermal conductivity distribution of fluids (air, gas, oil, and water) and rock-forming minerals (Schön, 2011)

Amongst minerals commonly found in sedimentary rocks, quartz displays a high mean conductivity value of λ = 6.5 W m^{-1} K^{-1} (Clauser, 2006). As a consequence, sandstones usually have higher thermal conductivity than carbonates. The understanding of thermal conductivity values for sedimentary rocks is however still limited (Midttømme and Roaldset, 1999). Schön (2015) compiled the work of various authors and presented thermal conductivity values for sandstones ranging from 0.38 to 6.50 W m^{-1} K^{-1}, while Clark (1966) reported thermal measurements on sandstones between 1.46 and 4.27 W m^{-1} K^{-1}. Thermal conductivity of rocks is typically determined in a laboratory. There is no standard method for measuring thermal conductivity, but the Transient Plane Source (TPS) method and the transient optical scanning technique (TCS) have been used during this study and will be described in Chapter 5.

Several papers investigated the challenges and implications of thermal conductivity measurements at different scales. Gallagher et al. (1997) emphasised that thermal conductivity shows a significant variability based on the study scale. They especially pointed out those small-scale measurements (e.g., on core samples) may not fully capture the large-scale heterogeneity found in sedimentary basins. Such geological areas often exhibit complex layering and lateral variations in lithology which can lead to considerable variations in thermal conductivity across different scales. The potential presence of fractures and variable fluid distribution can also impact thermal conductivity measurements and are not easily captured in small-scale measurements. Wheildon and Rollin (1986) discussed the sampling frequency of a 300m borehole to produce a high-quality heat flow. They

suggested to increase sampling density until the studied reservoir is sufficiently and proportionally represented. The use of models such as mixing laws can also be used to estimate thermal conductivity of heterogeneous geological layers or rocks.

2.2.1.3. Mixing models

Mixing models, also known as mixing laws, are mathematical models used to predict the thermal conductivity of composite materials, such as rocks, that are composed of different minerals with varying thermal conductivities. Mixing models are based on the bulk thermal conductivity of the rock (λ_b), the matrix thermal conductivity of the rock (λ_m), the thermal conductivity of the pore content (λ_p), and the effective porosity of the rock (ϕ). They can be applied at different scales, from the mineral or grain scale up to the lithospheric scale. These laws are especially useful when considering the effects of porosity and fluid saturation in rocks, which is of interest for this thesis. Such models combine the thermal conductivities of the matrix (i.e., the solid part of the rock) and pore filling fluids to predict the thermal conductivity of the layer or the rock (Tatar et al., 2021). Figure 2-3 shows the variation of the conductivity ratio of dry and saturated thermal conductivity measurements with porosity for different rock types (Clauser, 2006). The appropriate mixing law should be selected according to the direction of heat flow, the rock type, and the scale of study.

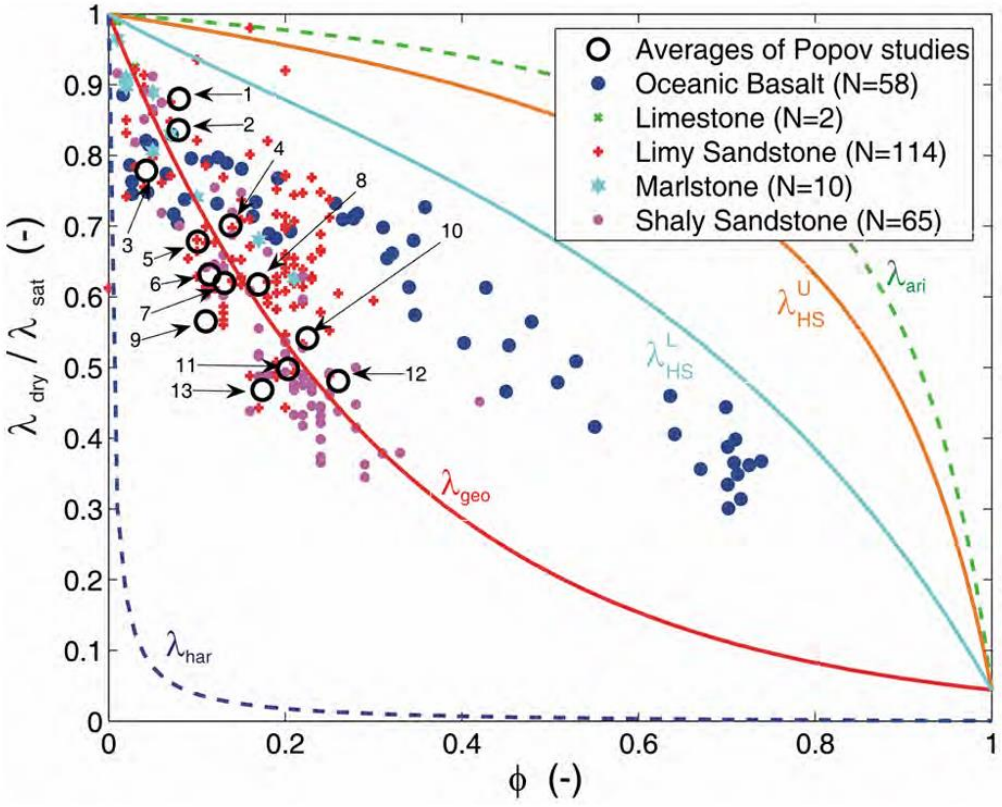

Figure 2-3: Variation of thermal conductivity ratio of dry and saturated measurements with porosity f for different rock types. The curves represent various mixing laws: λ_{har}, λ_{geo}, λ_{HS}^{L}, λ_{HS}^{U}, and λ_{ari} correspond to the harmonic, geometric, upper and lower Hashin-Shtrikman bound, and arithmetic mixing laws, respectively (Clauser, 2006).

Woodside and Messmer (1961a,b) evaluated the geometric mean model, which was firstly proposed by Lichtenecker (1924). The geometrical mean assumes no preferential alignment of phases and provides a reasonable estimate for many heterogeneous materials. The use of this empirical law is thus recommended for assessing the thermal conductivity of sedimentary rocks (Fuchs et al., 2013), and Fig. 2-3 shows a good correlation between sedimentary samples and the geometric model. The equation for the geometric mean is defined as follows (Eq. (2-2)):

$$\lambda_b = \lambda_m^{1-\phi} \cdot \lambda_p^{\phi} \tag{2-2}$$

with λ_b the bulk thermal conductivity, λ_m the matrix thermal conductivity, λ_p the thermal conductivity of the pore content, and ϕ the effective porosity.

2.2.1.4. Other Thermal Properties

Thermal conductivity is connected to three other properties of crucial importance in geothermal studies: specific heat capacity (c_p), thermal diffusivity (α), and density (ρ) of a material. This relationship is shown in Eq. (2-3):

$$\alpha = \frac{\lambda}{c_p \cdot \rho} \tag{2-3}$$

The specific heat capacity is defined as the amount of heat per unit mass needed to raise a material's temperature by 1K. The main unit for specific heat capacity is J/(kg K). Thermal diffusivity controls the time-dependant temperature distribution (m^2/s).

2.2.1.5. Geothermal Gradient and Temperature Measurements

The geothermal gradient is the increase in temperature with increasing depth in the Earth and is commonly given in °C/km. The average temperature gradient across the globe is 25° to 26°C/km (Klemme, 2017; Selley and Sonnenberg, 2015) although values range from c. 18°C to 55°C/km. Areas with high geothermal gradient are typically found along tectonic margins in subduction or continental collision contexts, or over regions where the Moho is at a shallower depth (Busby, 2014; DiPietro, 2013). Factors associated with such areas include ascending magma bodies, crustal thickening, or the unusual presence of the hot mantle at shallower depths. The geothermal gradient is typically calculated using the following formula (Eq. (2-4)):

$$grad\ T = \frac{dT}{dz} = \frac{T_2 - T_1}{z_2 - z_1} \tag{2-4}$$

with $grad\ T$ the geothermal gradient (°C/km), T a temperature at a specific depth (°C), and z a depth at which a temperature measurement was performed (km).

Temperature values are measured using various direct and indirect techniques. In 1850, hand operated maximum-reading mercury thermometers used to be the common way of determining temperature, but such devices implied a tedious

process and a long response time (Jessop, 1990). Electrical thermometers were developed in the second half of the nineteenth century and significantly enhanced the accuracy and precision of the measurements (Prensky, 1992, Jessop, 1990). Another major advancement in temperature measurements occurred in the late 1930s with the introduction by Schlumberger of continuous-recording wireline downhole logging tools (Prensky, 1992). Two types of temperature measurements are of relevance for this thesis, since they were used to calculate the geothermal gradient of the Cheshire Basin (UK): drill stem-tests (DST) and bottom-hole-temperature (BHT) measurements.

A drill-stem test is a standard procedure used in the oil & gas industry to assess the presence of fluids and evaluate the potential productivity of a reservoir by isolating and testing specific zones within a borehole. The DST tool includes various sensors to monitor parameters such as temperature, flow rate, and pressure; as well as a packer to isolate the area of interest. The temperature obtained from a DST is commonly regarded as a reliable approximation of the true formation temperature when the flowing temperature has stabilised (Burley et al., 1984).

A BHT is a single maximum recorded temperature in a borehole and is taken when the logging tool is at the bottom of its run. BHT measurements are of notoriously poor quality because they represent the temperature of the drilling fluid that is usually cooler than the undisturbed temperature of the rock formation (Förster, 2001). Temperature data from hydrocarbon boreholes often come from BHT measurements performed during well logging or testing (Fuchs et al., 2022). In the UK, a catalogue of temperature data (and other subsurface information) was compiled between 1976 and 1988 to assess the geothermal potential of the country, and c. 50% of the temperature collected are BHTs (Burley et al., 1984; Rollin, 1995; Busby et al., 2011). Correction methods can be applied to these non-equilibrated temperatures to obtain the true formation temperature; however, they require the input of various variables that were not often recorded or known. The empirical function used for BHT correction in the UK (from the 4th version of

the UK geothermal catalogue (UKGC)) considers the elapsed time since fluid circulation ended and takes the following form (Eq. (2-5)) (Rollin, 1987):

$$T_{corr} = T_{obs} \cdot \left(1 + \frac{1}{t_{circ}} + \frac{1}{(t_{circ})^2}\right) \quad (2\text{-}5)$$

with T_{obs} the BHT observed, T_{corr} the BHT after correction, and t_{circ} the post-circulation time. All UKGC BHT data with $t_{circ} \geq 5h$ have been corrected using this formula.

2.2.2. Geothermal System

Williams et al. (2011) defined a geothermal system as: "any localised geologic setting where portions of the Earth's thermal energy maybe extracted from a circulating fluid and transported to a point of use". A geothermal system is composed of three main elements: a *heat source*, a *fluid* and a *reservoir* (Dickson and Fanelli, 2013), as illustrated in Fig. 2-4.

Depending on the geological context, the *heat source* can be a magmatic intrusion that rose up to shallow depth or directly related to the increase of temperature with depth (i.e., the geothermal gradient). For example, in the Upper Rhine Graben, Germany, the thinning of the crust and lithospheric mantle triggered a regional increase in the heat flux, resulting in an abnormally high geothermal gradient of up to 100°C/km in some areas (Frey et al., 2022).

The *reservoir* of a geothermal system is usually a volume of permeable and porous rocks often overlain by impermeable rocks, creating a cap (Fig. 2-4).

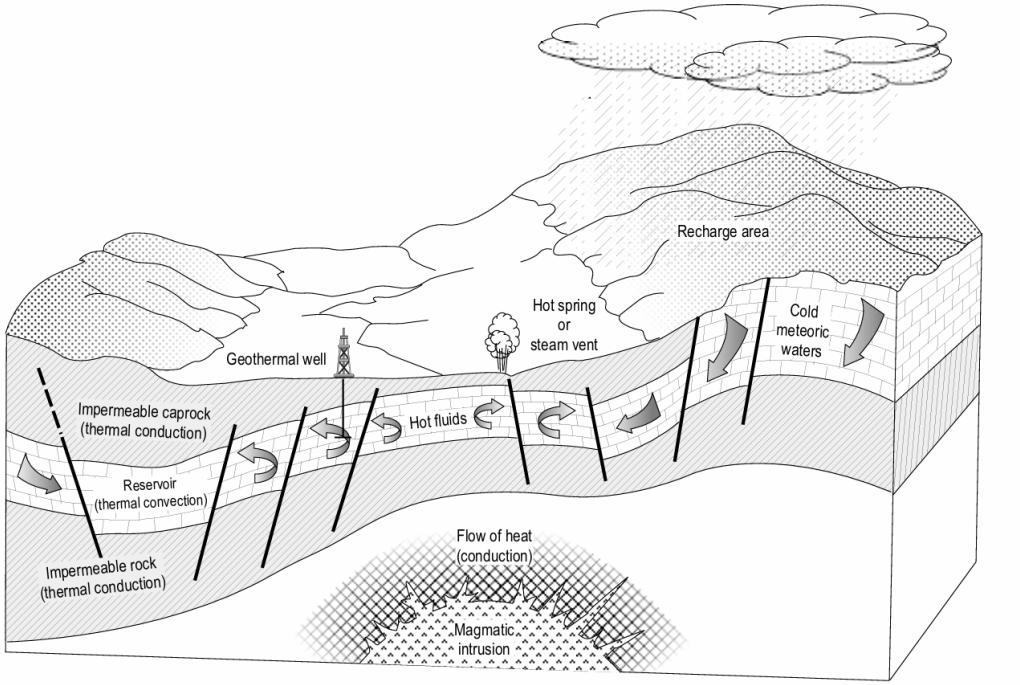

Figure 2-4 : Simplified representation of a geothermal system (Dickson and Fanelli, 2013)

The *fluid* plays a crucial role by transferring the heat from the reservoir to the heat sink – usually the ground surface. In sedimentary systems, it also stores a significant portion of the thermal energy. The main fluid for heat transfer in geothermal systems is water, typically from meteoric or marine water sources (Fig. 2-4). Typically, permeable reservoir rocks are laterally connected to recharge zones to allow fluids to replace the water which is extracted. This recharge results from natural means or artificial events such as the pumping of hot water from a borehole. Where natural or induced recharge is less than extraction rate, produced water is typically reinjected back into the reservoir via a separate dedicated borehole. The natural ways of water escaping in a geothermal system can create surface features, which are apparent evidence of a more complex underground system. Amongst those surface features are geysers, mud pools, hot springs and fumaroles.

2.2.3. Hydrogeological Properties of a Geothermal Reservoir

Understanding the hydrogeological processes in a geothermal reservoir is crucial to appropriately assess, quantify, and potentially exploit the subsurface resource in a sustainable and economic way. A potential reservoir should meet specific petrophysical criteria to be considered as of interest for geothermal exploitation, especially regarding permeability and porosity values. These rock properties are even more critical when appraising naturally porous and permeable sedimentary formations, as is the case in this thesis. In such settings, where the reservoir has not been artificially enhanced, heat is mainly transported by conduction (Gillespie et al., 2013; Moeck, 2014).

Porosity is a measure of the void available within the rock matrix: it corresponds to the ratio of the volume of the pore space to the bulk (pore space and grains) or total volume of a rock (Eq. (2-6)).

$$\phi = \frac{V_p}{V_b} = \frac{V_p}{V_p + V_g} \tag{2-6}$$

where ϕ is porosity, V_p is the pore space volume, V_b is the bulk volume, and V_g is the grain volume. This porosity, also known as *total porosity*, does not provide any information on pore size distribution and connectivity, and is in fact composed of various porosities. Only one of these porosities will be introduced here, as it is the most critical one in appraising a geothermal resource: effective porosity. Unlike total porosity, *effective porosity* is only considering interconnected pores, i.e., the porous volume that directly contributes to the fluid flow. Water-bound to clay particles, and isolated vuggy (i.e., unconnected pores or dead-end pores) porosity is not considered in the effective porosity.

The initial porosity presents in a sediment at the time of deposition or formed during sedimentation is called *primary porosity.* The primary porosity is affected by range of factors including: (1) grain size distribution (uniformity and sorting), (2) grain shape and (3) grain packing (Hook, 2003; Tiab and Donaldson, 2003). The smaller the volume of pore space, the smaller the porosity (Fig. 2-5). Thus,

idealised arrangements to maximise porosity would be loosely packed materials with uniform grains in terms of shape and size, although these arrangements are not likely to be present in real rocks. Primary porosity is dominant in sedimentary rocks such as sandstones. *Secondary porosity* is the post-depositional porosity, i.e., a porosity that formed after the original rock formation process. Post-depositional processes inducing porosity include –but are not limited to– fracturing, diagenesis processes (e.g., dissolution), or weathering (Hook, 2003). Fracture porosity in limestones or tight sandstones can significantly enhance their porosity and therefore boost their potential for a feasible geothermal development.

Although high porosity values (i.e., large volumes of pore space) are key to get a favourable geothermal reservoir, the pore space must be as connected as possible to efficiently transmit the fluid. This critical rock property is termed permeability and is then highly correlated to the geometry of the pore network (Fig. 2-5). Consequently, non-porous rocks have no permeability. Various permeability types come into play according to the scale of study. Matrix permeability is usually measured directly on samples and corresponds to the transfer through sub-centimetre pores and cracks (Katz and Thompson, 1986). At the basin scale, permeability is largely controlled by the architecture of fault zones, and the fracture network (Navelot et al., 2018; Eichhubl et al., 2009). Fracture porosity is mainly impacted by the size, aperture, connection and density of fractures affecting a geological formation.

The flow of a fluid through a porous medium is defined by Darcy's Law (1856).
The constitutive equation is expressed as follows (Eq. (2-7)):

$$q = \frac{Q}{A} = \frac{k}{\mu}\nabla p \qquad (2\text{-}7)$$

where q is the Darcy flux (m/s), Q the volumetric flow rate (m^3/s), A the cross-sectional area (m^2), k the intrinsic permeability (m^2), μ the dynamic viscosity of the fluid (Pa.s), and ∇p the pressure gradient (Pa/m).

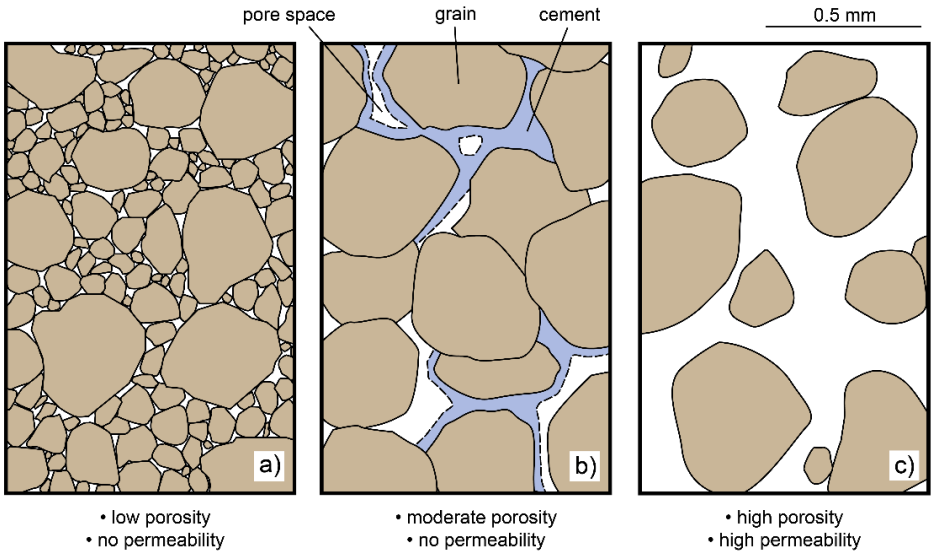

Figure 2-5 : Porosity and permeability in several grain configurations: a) non-uniform grain size and shape, resulting in unconnected few pore spaces; b) relatively homogeneous grain size but precipitation of cement particles decreasing the volume and connectivity of pore space, indicating a medium porosity but no permeability; c) connected pore spaces showing both high porosity and permeability.

Overall, both porosity and permeability of sedimentary rocks generally decrease with increasing depth due to factors such as overburden pressure, compaction and diagenesis (Schön, 2015; Nelson, 1994). Therefore, the main challenge regarding reservoir properties of geothermal systems within sedimentary rocks is to identify resource that (1) are made of high porosity and permeability rocks, (2) are deep enough to hold water at a sufficient temperature to be commercially viable, (3) though not too deep as both porosity and permeability reduce with depth.

2.2.4. Classification of the Geothermal Resource

Geothermal systems are less defined and more complex than hydrocarbon systems (Zarrouk and McLean, 2019). As of 2024, there is still no standard international terminology for geothermal systems, despite this being deplored by many authors in the past decades (Dickson and Fanelli, 2013; Moeck, 2014; Breede et al., 2015, Mijnlieff, 2020). Although various parameters such as depth, temperature, enthalpy, heat transport mechanism, rock type, geology, resource extraction

technology or the environmental-socio-economic viability of a project, can be used to classify geothermal resources; authors often differ in the interpretation of the terms and definitions for each category. In this section, the "hot sedimentary aquifer" category and other criteria directly related to such classification will be explored in more detail, especially in the countries assessed for this study. Figure 2-6 presents specific classifications for geothermal systems based on various parameters.

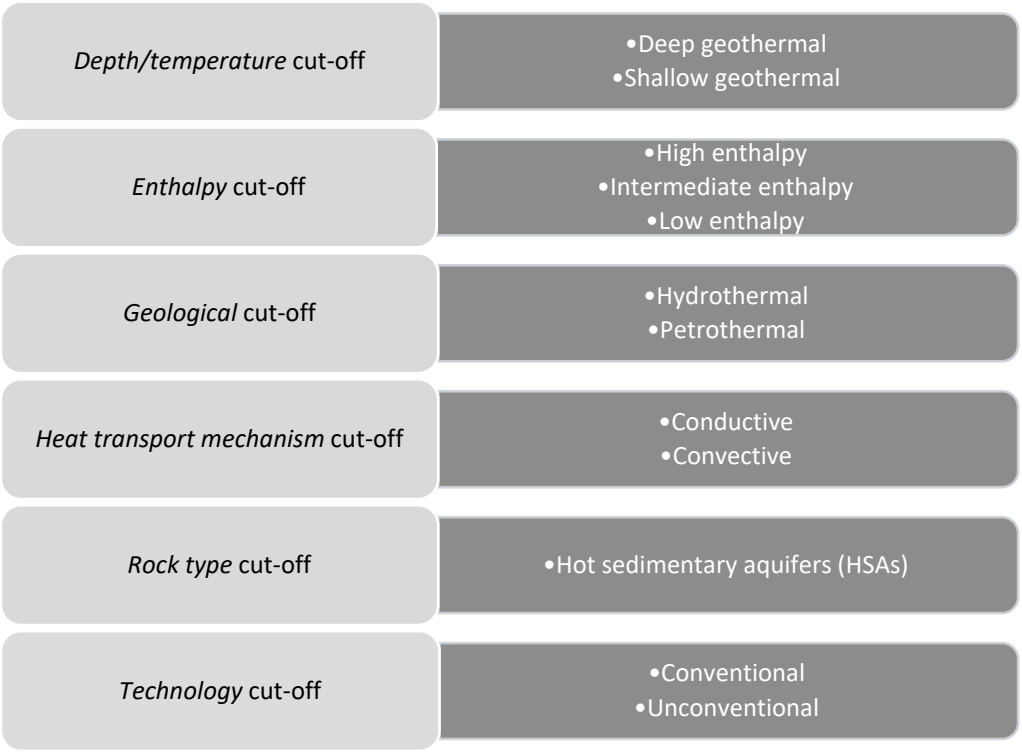

Figure 2-6: Classification of geothermal systems based on specific values for depth and/or temperature, enthalpy, geology, heat transport mechanism, and rock type of the resource; or the technology used to extract the resource.

The term *Hot sedimentary aquifer* (*HSA*) was first used at the end of the 2000s to characterise large and conductive aquifers that are hot enough and have sufficient productivity to constitute a potential geothermal resource (Gillespie et al., 2013). HSAs are conduction-dominated systems typically found in sedimentary basins, although convection is likely to contribute to the water flow for some systems (Moeck, 2014). Typical HSA resources are found at depths down to 4km with groundwater temperatures that usually range from 20°C to 80°C (Gillespie et al.,

2013). However, other minimum temperatures are defined by different authors: 140°C (Barnet, 2009), 130°C (Huddlestone-Holmes and Russell, 2012) or 60°C (Abesser and Walker, 2022). The geothermal community does not agree on a single depth cut-off either: some authors defined HSA depth as > 1.5km (Huddlestone-Holmes, 2014; Abesser and Walker, 2022) or < 4.5km, as permeability will probably be too low at greater depths (Huddlestone-Holmes and Russel, 2012). The hot water produced from HSA resources can be used for heating or/and electricity purposes (Gillespie et al., 2013). Stimulation techniques might be applied to HSA wells to increase the near-wellbore permeability, but they are usually not required (Huddlestone-Holmes and Hayward, 2011). Various geothermal technologies including a hot sedimentary aquifer model are presented in Fig. 2-7.

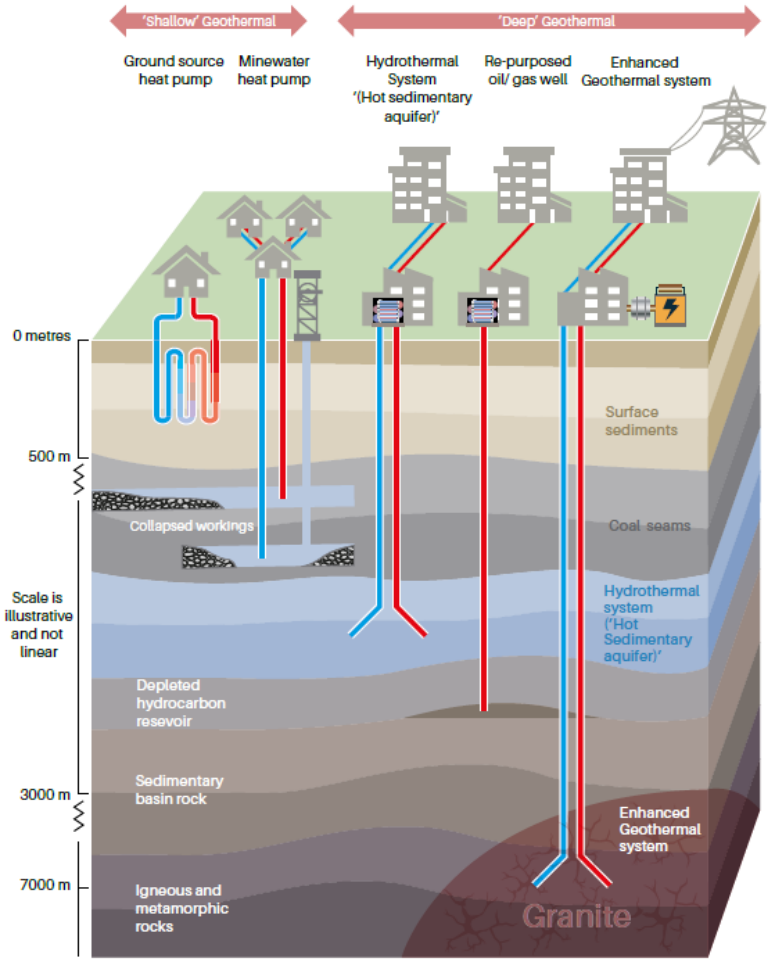

Figure 2-7: Geothermal systems applicable in the UK (Abesser and Walker, 2022)

In the UK, researchers usually refer to HSAs as *deep sedimentary aquifers* (Younger et al., 2015) or *hot sedimentary aquifers* (Gillespie et al, 2013; Comerford et al.

2018). Other authors, such as Hirst (2017), use the Moeck (2014) classification for conduction-dominated geothermal play types and label them *hydrothermal systems*. In 2022, the UK Parliament published a report on geothermal energy where they present *hot sedimentary aquifers* and *hydrothermal systems* as the same category (Abesser and Walker, 2022).

Most authors working on geothermal development in Australia also classify heat stored in sedimentary layers as *hot sedimentary aquifer resources*, as observed in Beardsmore et al. (2023).

In Germany, researchers are often following the Moeck (2014) categories and distinguish between *petrothermal* and *hydrothermal* resources for conduction-dominated plays, based on the ratio between porosity and permeability (Moeck et al., 2020). Thus, HSAs are usually known as *hydrothermal* systems in Germany, although is it confusing whether hydrothermal can sometimes also encompass Enhanced Geothermal Systems (EGS) applied to sedimentary aquifers (Moeck et al., 2020). Authors such as Weber et al. (2015) also refer to such systems as *hydrogeothermal reservoirs*, although it is difficult to find a clear definition for this terminology.

In the Polish geothermal sector, *hydrogeothermal* resources are defined as resources accumulated in underground water reservoirs (Sowizdzal, 2018), which could correspond to HSAs. Those geothermal plays are also labelled as *low-energy geothermal resources* (Pająk et al., 2020) or *low-temperature* but these labels could also be related to igneous rocks (Sowizdzal, 2018).

Mijnlieff (2020) acknowledged the difficulties for the geothermal sector to adhere to widely accepted definitions, and presented five classification schemes for Dutch geothermal plays based on different criteria: (1) *hydrothermal* systems – based on geological characteristics and exploitation strategy (Moeck, 2014); (2) *hot sedimentary aquifers* – based on rock types (Huddlestone-Holmes, 2014; Breede et al., 2015); (3) *conductive play* – based on the main heat transport mechanism (Moeck, 2014); (4) *low-temperature* or *low-enthalpy play* – based on temperature and enthalpy (Dickson and Fanelli, 1990); and (5) *deep geothermal* – based on the

depth (TNO, 2023). In practice, most papers on geothermal projects in the Netherlands mention *hot sedimentary aquifers* or *deep geothermal energy.*

The French classification of geothermal plays is often related to the depth or temperature targeted instead of the geological setting of the system. Boissavy et al. (2019) refer to HSAs as *deep aquifers* or *low-energy geothermal resources,* which can be confusing as most articles describing French geothermal plays do not specify which classification or authors they rely on, the parameter value range or its definition. The same considerations can be applied to the Danish geothermal sector, where authors usually refer to the *deep geothermal energy* or *deep aquifer* potential in Denmark (Røgen et al., 2015; Nielsen et al., 2004).

These variabilities in geothermal terminology and definitions are also observed for concepts such as *deep/shallow geothermal* (Breede et al., 2015; Abesser and Walker, 2022), *hydrothermal/petrothermal* systems (Mijnlieff, 2020; Moeck, 2014; Huenges, 2010; Breede et al., 2015) or *conventional/unconventional* systems (Tester et al., 2006; McCabe et al., 2019; CSIRO and Geoscience Australia, 2012), but will not be detailed here as they are out of scope.

This review of geothermal classification systems highlights significant inconsistencies on the characterisation of hot sedimentary aquifers, which is essentially a result of a lack of standard and internationally recognised geothermal classifications with common criteria. This matter creates confusion when assessing geothermal resources and may be contributing to the slow uptake of geothermal development.

2.2.5. Hot Sedimentary Aquifer Applications

The hot water produced from HSA resources is of relatively low-temperature and typically used for direct-use applications. Indeed, power generation has not historically been cost effective for temperatures below 150°C (McCabe et al. 2019). Conventional uses include district heating, greenhouse heating, aquaculture, food processing or other industrial uses (Lindal, 1973); and the temperature range for each usage is shown in Fig. 2-8. Global installed capacity of geothermal heating

and cooling reached 173,303 MW in 2023 and showed an increase of 44% with respect to 2021 (IGA, 2023). 88% of the global production is in district heating and cooling; 9% in the health, recreation and tourism sector; and 3% for industrial process heat. Other categories represent less of 1% of uses. The local demand and governmental regulations substantially impact the purpose of a geothermal well. Heat cannot be efficiently transported over long distances; therefore, geothermal resources are usually exploited next to high density areas and/or where the heat demand is significant. In the Netherlands, most operational HSA projects produce heat for the greenhouse sector (Godschalk et al., 2020) while in countries such as Denmark, France or Poland, the heat extracted is mainly distributed to district heating networks (Mathiesen et al., 2020; Boissavy et al., 2020; Kępińska, 2020).

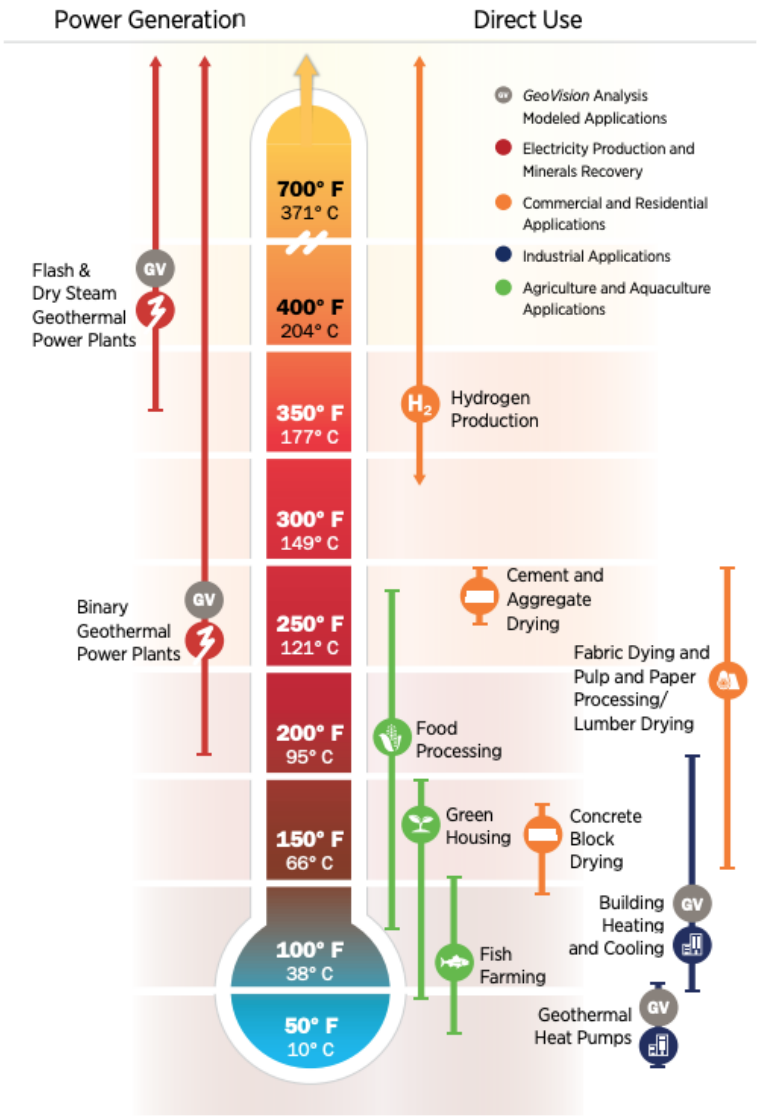

Figure 2-8: Geothermal energy applications and uses (US DOE, 2019; adapted from Lindal, 1973)

Although HSAs are especially suitable for heating applications, the water produced can be used for electricity generation when reservoir temperature and average ambient surface temperature difference is sufficient, e.g. ≥ 90°C in temperate climate regions (Kabeyi, 2019). However, generating power from geothermal systems with temperatures of 80-150°C requires the use of a binary configuration (Moya et al., 2018): the primary fluid –usually hot water– is extracted from the reservoir, the heat is then transferred to a working fluid (which has a lower boiling point) through a heat exchanger, and eventually the vapor drives a turbine and

produces electricity (Dincer, 2018; Stober and Bucher, 2021) (Fig. 2-9). Sometimes, combined heat and power plants (CHP) are designed to get more value out of the geothermal resource, as is the case for many projects in Germany (Weber et al., 2015).

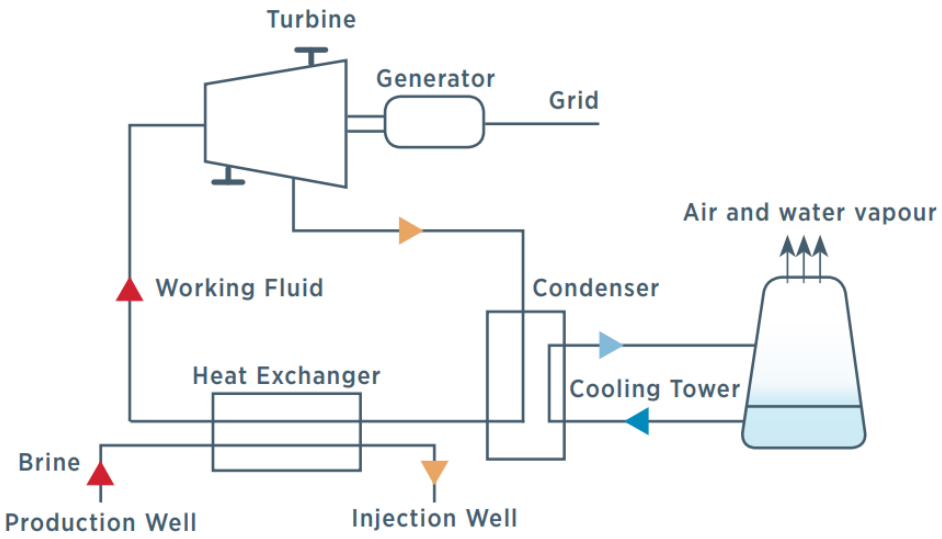

Figure 2-9: Binary cycle power plant (IRENA, 2017)

2.3. Risks Associated with Geothermal Development and Public Perception

This section aims to establish the state-of-the-art regarding the risks related to geothermal energy. An overview on geothermal risk management will be provided, followed by a review of public acceptance and engagement with geothermal energy. Examples of organisations that have developed a "learning from failure" ethos will be described and put into perspective with that of the geothermal industry.

2.3.1. Risk Management in the Geothermal Sector

The International Panel on Climate Change (IPCC, 2011) estimated that by 2050, c. 3% of the global energy demand and 5% of heating and cooling demand should be met by geothermal energy. However, the development of a geothermal project

remains a substantially risky process, the main risk being the risk of failure faced by project developers and operators. Unsuccessful geothermal development can be attributed to various factors such as business risks, seismic risks, well success, pollution risks, competition from oil & gas markets, and assessing risk vs reward (Hanson, 2020). All factors must receive consideration during planning, risk mitigation and feasibility analysis phases. Deinhardt et al. (2021) stated that bankability of a geothermal project is mostly threatened by the geological risk (Deinhardt et al., 2021) (Fig. 2-10).

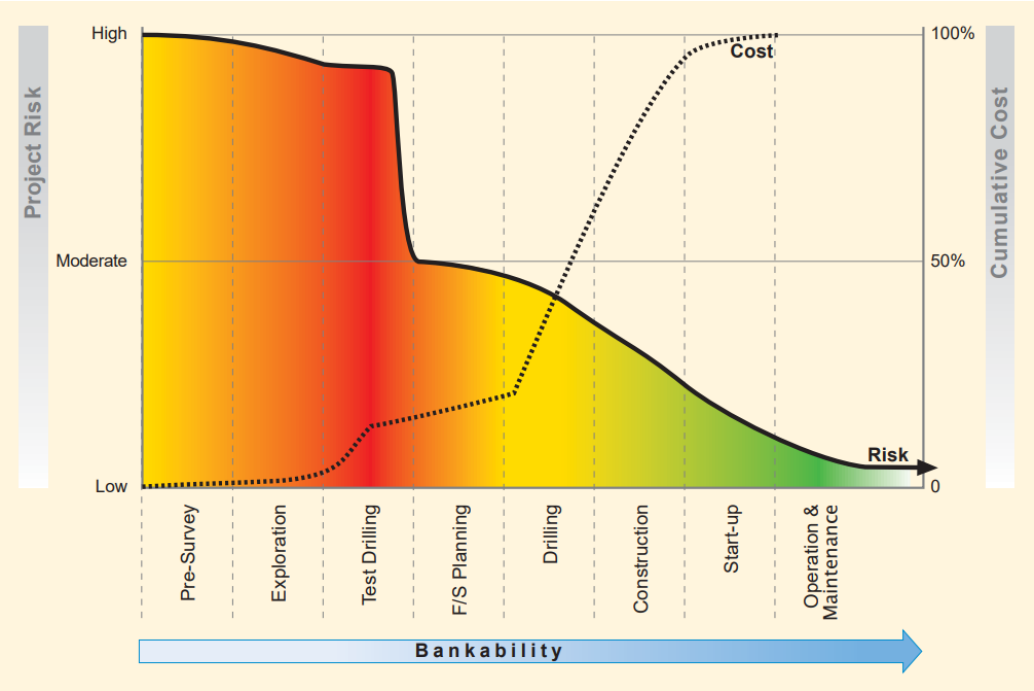

Figure 2-10: Geothermal Project Cost and Risk Profile at various stages of development (Gehringer and Loksha, 2012)

In Germany, the main risks associated with geothermal development have been related to safety and costs. Borehole construction has been at the root of tremors that caused damages in Staufen im Breisgau in 2008 although major technology and knowledge advances of the last decades are substantially reducing the risk (Hockenos, 2020). Public remain concerned about geothermal energy, for instance near Strasbourg (France) where incidents occurred between 2019 and 2021 following the stimulation of a granite for a geothermal power plant. Tremors and earthquakes were classified as “induced events”, and the project faced a strong

opposition from local inhabitants. Local authorities had to put a stop to the geothermal project in December 2020 (Richter, 2020). More recently, induced seismicity associated with the Balmatt geothermal project in Belgium and the Eden Project in the UK has also raised concerns and caused unease among local communities (TWI, 2022; Vergnault, 2022). Although induced seismicity is a major risk in geothermal reservoirs such as Hot Dry Rocks (HDR) or Enhanced Geothermal Systems, it is less likely to occur in HSAs. Indeed, HSAs usually rely on naturally permeable formations and moderate temperature contrasts, reducing the need for high-pressure stimulation and limiting stress or thermal perturbations (Buijze et al., 2020).

Although considerable progress has been made in surface and subsurface exploration technologies, predicting the exact depth of a reservoir, its properties (porosity, permeability, temperature, flow rate, etc) and therefore the exact output from a drilled well remains challenging. There are strong similarities with the exploration challenges of the oil and gas industry, but the main difference lies in the potential returns on investment. The latter are high enough in the petroleum industry to justify the exploration risk, while it is usually not the case for geothermal development (Gehringer and Loksha, 2012). Moreover, petroleum and geothermal well drilling have different reservoir pressures, temperatures, and casing designs. Common issues encountered when drilling a geothermal well are related to the well integrity during the drilling and production phases (Allahvirdizadeh, 2020). Indeed, well barriers play a major role in geothermal project risk due to their long typical life span, which is generally longer than that of a hydrocarbon well.

Cooper and Beardsmore (2008) created a Geothermal System Assessment (GSA) framework that involves four essential geological variables: temperature, rock thermal resistance (insulation), reservoir characteristics, and the working fluid (usually water). These parameters define four areas of risk that control geological productivity. The authors stated that Australian geothermal exploration has mainly focused on two risk factors: temperature and thermal resistance. Little attention

has been directed towards the two others although they are of equally importance when assessing geothermal exploration risk. Therefore, addressing reservoir characteristics and water risk earlier in the evaluation process could limit both risks and costs.

Eventually, technical risks translate to financial risks. The costs of geological studies to assess resource potential and drilling are usually very high for a geothermal developer (Fig. 2-10). As one further progresses in geothermal development stages, a greater understanding of the field characteristics is reached, reducing the risk. Significant investment is often required before knowing whether the geothermal resource has enough potential to recover the costs. Cumulative costs for both exploration and test drilling can account for up to 15% of the overall capital cost (CAPEX), for a relatively high project risk (Fig. 2-10) (Gehringer and Loksha, 2012). Test drilling usually allows for a considerable decrease in the project risk, lowering it to a moderate level. Due to the uncertainty regarding these aspects, funders sometimes lack the risk appetite for becoming involved in such investments (Climate Investment Funds, 2014). The mid-range estimate of investment costs (DEVEX plus CAPEX) is close to US $4 M/MW (Gehringer and Loksha, 2012). Operation and maintenance costs (OPEX) on a geothermal installation are also significant. They are estimated to be in the range of US $3.5 to 10.5 million per year (US $0.009 to 0.027 per generated kWh) for a 50 MW power plant in a developed or developing country (Gehringer and Loksha, 2012). In contrast, OPEX costs for oil and gas projects typically range between US $ 0.0041 and 0.0088 per kWh (Bret-Rouzaut, 2022), although they can vary significantly depending on the scale of operations, the difficulty of extraction or the geographical location (offshore or onshore).

2.3.2. Public Acceptance of Geothermal Energy

Public engagement and perception are becoming increasingly important for successful geothermal development. A local community can influence a geothermal project directly through action groups or indirectly, by defining the political climate and appetite for the technology (Wallquist and Holenstein, 2015).

In specific conditions, public opposition can significantly delay or even cancel geothermal projects. Public perception of geothermal energy is affected by several factors related to the purpose of the project (direct heat use or power production), the coherence of the project with local policies, or the existence (or not) of consultation with the local population (Chavot et al., 2018).

There can be a variety of reasons behind protests. People may feel threatened by water pollution or air emissions (Carr-Cornish and Romanach, 2014). In Hawaii Big Island, opponents condemned geothermal development for cultural and religious reasons (Edelstein and Kleese, 1995), and controversy around geothermal development was raised in France (Alsace) due to induced seismic events (Chavot et al., 2018). As geothermal energy is an emerging technology, worldwide public perception studies are limited, though an increasing number of local analyses are being reported.

A case study in the Palermo province in Sicily (Italy) revealed that the population's opinion was rather positive about the role geothermal energy could play in their region in the future (Pellizzone et al. 2015). However, the main obstacle to geothermal development lay in the high level of uncertainty –as a result of the low level of knowledge– regarding the technology. Local population appreciated taking part in the discussions but regretted a lack of balanced communication and information available, and did not feel prepared enough to play a decisive role in the consultation (Pellizzone et al. 2015). A study perfomed by Chavot et al. (2018) studying social, cultural, and political factors affecting geothermal projects in Alsace (France) using data from public inquiries, media, and interviews came to the same conclusion. Two regions were compared: northern Alsace, where public perception is positive, and Strasbourg, where opposition is strong. The key difference lies in community engagement; successful projects involved local communities in planning, leading to greater acceptance. In Strasbourg, projects initiated without local input led to misunderstandings and opposition, resulting in project failures. It highlights the importance of community involvement for the success of geothermal initiatives.

In Australia, exploratory research conducted by Carr-Cornish and Romanach (2014) to assess the agreement of Australian population with the use of geothermal energy allowed for a better understanding of the public approach to this new technology. Overall, survey participants agreed with the use of geothermal energy (at large) in Australia and the number of people with a positive view increased further after the provision of information. However, most participants would prefer the geothermal boreholes to be located at more than 100 km from their homes.

The results obtained in early surveys might not reflect public perception once the technology is deployed and becomes mature (Siegrist, 2010). Indeed, local populations might have not developed any attitude towards geothermal energy, especially if they have never faced such a technology before (Willems et al., 2020). At the start of the study from Carr-Cornish and Romanach (2014) and prior to any information, participants were "unsure" or "agreed with" geothermal energy. At the end of the process, a higher number of participants approved the use of the technology in Australia (Fig. 2-11).

Start	End			
	Disagree	**Unsure**	**Agree**	**Total**
Disagree	–	–	–	–
Unsure	5% (5)	13% (13)	24% (24)	42% (42)
Agree	2% (2)	6% (6)	50% (50)	58% (58)
Total	7% (7)	19% (19)	74% (74)	100% (100)

Figure 2-11: Attitudes toward geothermal energy technology being used in Australia (from Carr-Cornish and Romanach, 2014)

Reviewing regional and local newspapers and articles can be insightful when considering relatively old projects where no public attitude surveys were made. It is more relevant for areas where geothermal development triggered negative perceptions and opposition because the topic would then be widely covered in the newspapers. Indeed, while media reporting does not directly reflect public perception, research has shown that media reporting is indirectly linked to public

perception because the way it presents a technology is likely to influence reactions (Nisbet et al., 2002). In the UK, public perception of geothermal energy was evaluated by looking at local articles from 1980 to 2018 (Willems et al., 2020). The investigation results show that geothermal energy is a relatively new topic to the UK community, and the newspapers have a positive tone about the geothermal technology: stimulation of the local economy, CO_2 reduction and potential capacity of the projects are frequently mentioned. However, more recent geothermal projects appear not to have the same impact in the local population. Seismic incidents that occurred in January and March 2022 at the Eden geothermal drilling site in Cornwall were reported as having scared the local population: local and national newspapers talk about the tremors as “frightening” (Gatten, 2022).

Disseminating information early on and encouraging the population to take part in the discussion is essential to facilitate the social and political acceptance of a geothermal project (Chavot et al., 2018). It is crucial to build a climate of confidence and transparency between the stakeholders through an early engagement with the community in the project. Diverse subjects and type of geothermal systems are more perceived as a risk depending on the country and the area assessed. As they do not require hydraulic fracturing, hot sedimentary aquifers are not exposed to a high risk regarding induced seismicity but can be subject to the “not in my backyard” (NIMBY) syndrome reported by various studies (Pellizzone et al., 2015; O’Hare, 1977). This concept states that some people support renewable energy (geothermal technology here) as long as it is not in their local residential area. This could be a challenge for the deployment of HSA direct heat use as the drilling sites must be near the end-use application (Carr-Cornish and Romanach, 2014).

2.3.3. Learning From Failure in Diverse Organisations

Many studies have investigated the organisational learning from failures and how it differs from learning from success. Such topics are key for the improvement of every industry or venture, including the geothermal sector. This review is the

starting point of the HSA de-risking approach that will be developed in the following chapters.

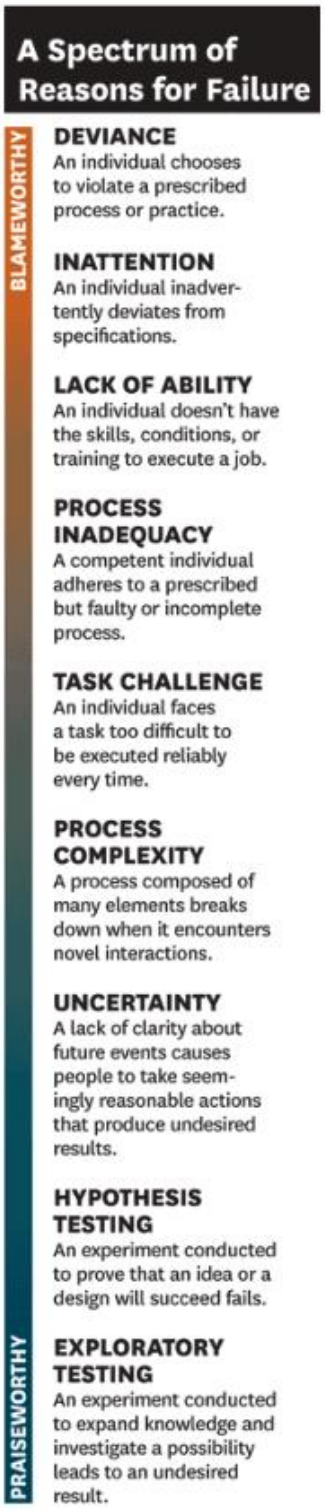

Organisational learning is an iterative, dynamic process by which an organisation creates, retains and transfers knowledge. Failure corresponds to a deviation from expected and desired results, and includes both avoidable errors and the unavoidable negative outcome of experiments and risk taking (Cannon and Edmondson, 2001). When small failures are not accurately identified and thoroughly analysed, the prevention of more significant failures becomes considerably challenging (Tucker and Edmondson, 2003; Sitkin, 1992). Disregarding failures may also lead to their recurrence. Social, psychological and organisational barriers discourage the reporting of failures, while technical barriers such as system complexity can hinder their identification (Cannon and Edmondson, 2005). Once a project failure is identified, some of the best practices include acting quickly (Hart, et al., 1990), offering an explanation (Mattila, 2006), fair treatment (Maxham and Netemeyer, 2002), effective complaint procedures (Tax et al., 1998), fair compensation (Smith et al., 1999), and empowering employees to make amends (Tax et al., 1998).

Figure 2-12 presents failure causes ranging from deviance to deliberate experimentation. Aside from deliberate misconduct, it becomes increasingly challenging, as one moves further down the list, to identify an action that warrants blame. In her study, Edmondson (2011) surveyed executives to estimate the proportion of failures within their organisations that

were genuinely blameable. The executives indicated that only about 2% to 5% of failures fell into this category, whereas when asked about the percentage of failures that were actually treated as blameworthy, their responses ranged from 70% to 90%. Specific focus should be paid to rewarding managers for identifying, reporting and analysing failures.

For serial entrepreneurs, continued engagement within the same industry across successive ventures plays a more critical role in determining later venture success than the results of their previous endeavours (Eggers and Song, 2015). The accumulation of industry-specific experience likely serves as a significant factor contributing to the success of these entrepreneurs. The geothermal industry has also benefited from experience accumulated throughout the decades. Only two decades after its emergence, the French geothermal marked faced a major crisis at the end of the 1980s that implied technical difficulties, financial issues and a global lack of expertise of plant operators. At the beginning of the 2000s, geothermal systems were improved, and technical and financial problems faced during the crisis were solved thanks to geothermal stakeholders that have gained significant experience (Laplaige et al., 2000).

Figure 2-12: A spectrum of reasons from failure (Edmondson, 2011)

There are two main ways to approaching failure: open-loop and close-loop systems (Syed, 2015). In close-loop systems, people do not learn from failure, they repeat the same mistakes over and over. In open-loop systems, data are collected and examined, and failures are seen as building blocks for improving. Syed (2015) contrasted the health care (closed-loop) and aviation (open-loop) industries according to their response to failure and pointed out significant differences in the systems and culture that drive each field. Unlike the health care sphere, the airline industry has used failures as learning opportunities through the establishment of both the necessary culture and system.

In the geothermal industry, reporting failure is not a common practice. Due to the scarcity of detailed published or publicly available data, defining failure modes (i.e.

damage types to the wellhead and/or the downhole construction of a geothermal well) for wells is challenging (Kruszewski and Wittig, 2018). Only a few published studies describe and analyse failures from geothermal projects, and use this for suggesting solutions and areas for improvements. The geothermal energy sector shares a close connection with the oil and gas industry, as both fields employ comparable technologies and expertise. Additionally, the challenges faced and the risks inherent in drilling wells are alike (Kruszewski and Wittig, 2018). The failures and issues faced while developing petroleum projects could therefore greatly benefit the emergent geothermal energy industry, including HSAs.

2.4. Conclusion

The literature review highlighted significant challenges in developing HSA systems, including well integrity issues, unpredictable reservoir behaviour, and high exploration costs that hinder financing and project viability. It also stressed the importance of public acceptance and the need for improved transparency, especially by fostering a culture of learning from failures, an area in which geothermal lags behind other industries. Additionally, the literature review pointed out the lack of consistent terminology for geothermal classifications, particularly for HSAs, which creates confusion and may slow progress in the field.

2.5. References

Abdulagatov, I. M., Emirov, S. N., Abdulagatova, Z. Z., & Askerov, S. Y. (2006). Effect of pressure and temperature on the thermal conductivity of rocks. Journal of Chemical and Engineering Data, 51(1). https://doi.org/10.1021/je050016a

Abesser, C., & Walker, A. (2022). POSTbrief: Geothermal Energy. In Renewable Energy Technologies and Water Infrastructure (Issue April). https://post.parliament.uk/research-briefings/post-pb-0046/

Allahvirdizadeh, P. (2020). A review on geothermal wells: Well integrity issues. In Journal of Cleaner Production (Vol. 275). https://doi.org/10.1016/j.jclepro.2020.124009

Barnett, P. (2009). Large scale hot sedimentary aquifer (HSA) geothermal projects. Presentation to Victoria Energy Conference. https://hotcopper.com.au/data/oldanns/2009/HRL/30fcbb08-c66c-4db4-807b-f1c497b865a0-HRL213165.pdf

Beardsmore, G., Ballesteros, M., Davidson, C., Larking, A., & Pujol, M. (2023). Country Update-Australia. Proceedings World Geothermal Congress 2023.

Blázquez, C. S., Martín, A. F., Nieto, I. M., & González-Aguilera, D. (2017). Measuring of thermal conductivities of soils and rocks to be used in the calculation of A geothermal installation. *Energies*, *10*(6). https://doi.org/10.3390/en10060795

Boissavy, C., Henry, L., Genter, A., Pomart, A., Rocher, P., & Schmidlé-Bloch, V. (2019). Geothermal Energy Use, Country Update for France. European Geothermal Congress, 11–14.

Boissavy, C., Schmidlé-Bloch, V., Pomart, A., & Lahlou, R. (2020). France country update. Proceedings World Geothermal Congress, 1.

Breede, K., Dzebisashvili, K., & Falcone, G. (2015). Overcoming challenges in the classification of deep geothermal potential. In Geothermal Energy Science (Vol. 3, Issue 1). https://doi.org/10.5194/gtes-3-19-2015

Bret-Rouzaut, N. (2022). Economics of Oil and Gas Production. In The Palgrave Handbook of International Energy Economics. https://doi.org/10.1007/978-3-030-86884-0_1

Brigaud, F., & Vasseur, G. (1989). Mineralogy, porosity and fluid control on thermal conductivity of sedimentary rocks. Geophysical Journal International, 98(3). https://doi.org/10.1111/j.1365-246X.1989.tb02287.x

Buijze, L., van Bijsterveldt, L., Cremer, H., Paap, B., Veldkamp, H., Wassing, B. B. T., van Wees, J. D., van Yperen, G. C. N., & ter Heege, J. H. (2020). Review of induced seismicity in geothermal systems worldwide and implications for geothermal

systems in the Netherlands. In *Geologie en Mijnbouw/Netherlands Journal of Geosciences*. https://doi.org/10.1017/njg.2019.6

Burley, A. J., Edmunds, W. M., & Gale, I. N. (1984). Investigation of the geothermal potential of the UK: catalogue of geothermal data for the land area of the United Kingdom.

Busby, J. (2014). Geothermal energy in sedimentary basins in the UK. Hydrogeology Journal, 22(1). https://doi.org/10.1007/s10040-013-1054-4

Busby, J., Kingdon, A., & Williams, J. (2011). The measured shallow temperature field in Britain. Quarterly Journal of Engineering Geology and Hydrogeology, 44(3). https://doi.org/10.1144/1470-9236/10-049

Cannon, M. D., & Edmondson, A. C. (2005). Failing to learn and learning to fail (intelligently): How great organizations put failure to work to innovate and improve. Long Range Planning, 38(3 SPEC. ISS.). https://doi.org/10.1016/j.lrp.2005.04.005

Carr-Cornish, S., & Romanach, L. (2014). Differences in public perceptions of geothermal energy technology in Australia. Energies, 7(3). https://doi.org/10.3390/en7031555

Chavot, P., Heimlich, C., Masseran, A., Serrano, Y., Zoungrana, J., & Bodin, C. (2018). Social shaping of deep geothermal projects in Alsace: politics, stakeholder attitudes and local democracy. Geothermal Energy, 6(1). https://doi.org/10.1186/s40517-018-0111-6

Chen, C., Zhu, C., Zhang, B., Tang, B., Li, K., Li, W., & Fu, X. (2021). Effect of Temperature on the Thermal Conductivity of Rocks and Its Implication for in Situ Correction. Geoflu-ids, 2021. https://doi.org/10.1155/2021/6630236

Clauser, C. (2006). 8.1 The Earth's thermal regime: 8 Geothermal energy. Renewable Energy, 493–548.

Climate Investment Funds. (2014). Accelerating Geothermal Development by Reducing Exploration Risks. https://www.climateinvestmentfunds.org/sites/cif_enc/files/knowledge-documents/kn-ctf-accelerating_geothermal_development_by_reducing_exploration_risks_0.pdf

Comerford, A., Fraser-Harris, A., Johnson, G., & McDermott, C. I. (2018). Controls on geothermal heat recovery from a hot sedimentary aquifer in Guardbridge, Scotland: Field measurements, modelling and long term sustainability. Geothermics, 76. https://doi.org/10.1016/j.geothermics.2018.07.004

Cooper, G. T., & Beardsmore, G. R. (2008). Geothermal systems assessment: understanding risks in geothermal exploration in Australia. PESA Eastern Australasian Basins Symposium III.

CSIRO & Geoscience Australia. (2012). Information for ARENA: Unconventional Geothermal Systems and International Comparisons. https://hotcopper.com.au/data/oldanns/2009/HRL/30fcbb08-c66c-4db4-807b-f1c497b865a0-HRL213165.pdf

Davies, G. F. (1989), Mantle convection model with a dynamic plate: Topography, heat flow and gravity anomalies, Geophys. J. Int., 98, 461–464.

Deinhardt, A., Dumas, P., Schmidle, V., Antoniadis, A., Boissavy, C., Bozkurt, C., Garabetian, T., Hamm, V., Karytsas, S., Kasztelewicz, A., Kepinska, B., Keramiotis, C., Kujbus, A., Leguenan, T., Link, K., Lupi, N., Mendrinos, D., Miecznik, M., Nador, A., … Yildirim, C. (2021). Why De-risking is Key to Develop Large Geothrmal Projects? https://www.georisk-project.eu/wp-content/uploads/2021/07/Final-Report.pdf

Dickson, M. H., & Fanelli, M. (1990). Geothermal energy and its utilization. In Small geothermal resources.

Dickson, M. H., & Fanelli, M. (2013). Geothermal energy: Utilization and technology. In Geothermal Energy: Utilization and Technology (Vol. 9781315065786). https://doi.org/10.4324/9781315065786

Dincer, I. (2018). Comprehensive energy systems. Elsevier.

DiPietro, J. A. (2013). Keys to the Interpretation of Geological History. In Landscape Evolution in the United States. https://doi.org/10.1016/b978-0-12-397799-1.00020-8

Edelstein, M. R., & Kleese, D. A. (1995). Cultural relativity of impact assessment: Native hawaiian opposition to geothermal energy development. Society and Natural Resources, 8(1). https://doi.org/10.1080/08941929509380896

Edmondson, A. C. (2011). Strategies of learning from failure. Harvard Business Review, 89(4).

Eggers, J. P., & Song, L. (2015). Dealing with failure: Serial entrepreneurs and the costs of changing industries between ventures. Academy of Management Journal, 58(6). https://doi.org/10.5465/amj.2014.0050

Eichhubl, P., Davatzes, N. C., & Becker, S. P. (2009). Structural and diagenetic control of fluid migration and cementation along the Moab fault, Utah. AAPG Bulletin, 93(5). https://doi.org/10.1306/02180908080

Förster, A. (2001). Analysis of borehole temperature data in the Northeast German Basin: Continuous logs versus bottom-hole temperatures. Petroleum Geoscience, 7(3). https://doi.org/10.1144/petgeo.7.3.241

Frey, M., Bär, K., Stober, I., Reinecker, J., van der Vaart, J., & Sass, I. (2022). Assessment of deep geothermal research and development in the Upper Rhine Graben. In Geothermal Energy (Vol. 10, Issue 1). https://doi.org/10.1186/s40517-022-00226-2

Fuchs, S., Förster, A., & Norden, B. (2022). Evaluation of the terrestrial heat flow in Germany: A case study for the reassessment of global continental heat-flow data. In Earth-Science Reviews (Vol. 235). https://doi.org/10.1016/j.earscirev.2022.104231

Fuchs, S., Schütz, F., Förster, H. J., & Förster, A. (2013). Evaluation of common mixing models for calculating bulk thermal conductivity of sedimentary rocks: Correction charts and new conversion equations. Geothermics, 47. https://doi.org/10.1016/j.geothermics.2013.02.002

Furlong, K. P., & Chapman, D. S. (2013). Heat flow, heat generation, and the thermal state of the lithosphere. Annual Review of Earth and Planetary Sciences, 41. https://doi.org/10.1146/annurev.earth.031208.100051

Gallagher, K., Ramsdale, M., Lonergan, L., & Morrow, D. (1997). The role of thermal conductivity measurements in modelling thermal histories in sedimentary basins. Marine and Petroleum Geology, 14(2). https://doi.org/10.1016/S0264-8172(96)00068-2

García-Noval, C., Álvarez, R., García-Cortés, S., García, C., Alberquilla, F., & Ordóñez, A. (2024). Definition of a thermal conductivity map for geothermal purposes. *Geothermal Energy*, *12*(1), 17.

Gatten, E. (2022). 'Frightening' earthquake at Cornwall's Eden Project forces halt to drilling. The Telegraph. https://www.telegraph.co.uk/environment/2022/03/10/frightening-earthquake-cornwalls-eden-project-forces-halt-drilling/

Gehringer, M., & Loksha, V. (2012). Geothermal handbook: Planning and Financing Power Generation. https://www.esmap.org/sites/esmap.org/files/DocumentLibrary/FINAL_Geothermal%20Handbook_TR002-12_Reduced.pdf

Gillespie, M. R., Crane, E. J., & Barron, H. F. (2013). Potential for deep geothermal energy in Scotland: study volume 2. In British Geological Survey Geology and Landscape, Scotland Programme Commissioned Report Cr/12/131 (Vol. 2). https://www.gov.scot/publications/study-potential-deep-geothermal-energy-scotland-volume-2/documents/

Godschalk, B., Provoost, M., & Schoof, F. (2020). Netherlands Country Update. Proceedings World Geothermal Congress, 1.

Hanson, P. (2020). Causes of Geothermal Failure: White Paper Teaser. GeoEnergy Marketing.

Hart, C. W., Heskett, J. L., & Sasser, W. E. (1990). The profitable art of service recovery. Harvard Business Review, 68(4).

Hirst, C. M. (2017). The Geothermal Potential of Low Enthalpy Deep Sedimentary Basins in the UK. http://etheses.dur.ac.uk/11979/

Hockenos, P. (2020). Germany's geothermal sector is struggling to take off. Clean Energy Wire. from https://www.cleanenergywire.org/news/germanys-geothermal-sector-struggling-take

Hook, J. R. (2003). An introduction to porosity. Petrophysics, 44(3).

Huddlestone-Holmes, C. (2014). Geothermal Energy in Australia Prepared for the ARENA International Geothermal Energy Group.

Huddlestone-Holmes, C., & Hayward, J. (2011). The potential of geothermal energy.

Huddlestone-Holmes, C., & Russell, C. (2012). AEMO 100% Renewable Energy Study.

Huenges, E. (2010). Geothermal Energy Systems: Exploration, Development, and Utilization. In Geothermal Energy Systems: Exploration, Development, and Utilization. https://doi.org/10.1002/9783527630479

IGA. (2023). IGA unveils new key Geothermal Power & Direct Use data. IGA. https://www.lovegeothermal.org/global-geothermal-update-2023-iga-unveils-new-key-geothermal-power-direct-use-data/

IPCC. (2011). Renewable Energy Sources and Climate Change Mitigation. http://www.ipcc.ch/pdf/special-reports/srren/SRREN_Full_Report.pdf

IRENA (International Renewable Energy Agency) (2017). Project Navigator: Technical Concept Guidelines for Geothermal Projects 2017. IRENA. https://navigator.irena.org/index.html.

Jaupart, C., Labrosse, S., Lucazeau, F., & Mareschal, J. C. (2015). Temperatures, Heat, and Energy in the Mantle of the Earth. In Treatise on Geophysics: Second Edition (Vol. 7). https://doi.org/10.1016/B978-0-444-53802-4.00126-3

Jaupart, C., & Mareschal, J. C. (2003). Constraints on Crustal Heat Production from Heat Flow Data. In Treatise on Geochemistry (Vols. 3–9). https://doi.org/10.1016/B0-08-043751-6/03017-6

Jessop, A. M. (1990). Thermal geophysics. Thermal Geophysics. https://doi.org/10.1016/0264-8172(91)90075-c

Kabeyi, M. J. B. (2019). Geothermal Electricity Generation, Challenges, Opportunities and Recommendations. International Journal of Advances in Scientific Research and Engineering, 5(8). https://doi.org/10.31695/ijasre.2019.33408

Katz, A. J., & Thompson, A. H. (1986). Quantitative prediction of permeability in porous rock. Physical Review B, 34(11). https://doi.org/10.1103/PhysRevB.34.8179

Kellogg, L. H., Hager, B. H., & van der Hilst, R. D. (1999). Compositional stratification in the deep mantle. Science, 283(5409). https://doi.org/10.1126/science.283.5409.1881

Kępińska, B. (2020). Geothermal energy country update report from Poland, 2015–2019. Proceedings, World Geothermal Congress, 1.

Klemme, H. D. (2017). Geothermal Gradients, Heat Flow and Hydrocarbon Recovery. In Petroleum and Global Tectonics. https://doi.org/10.1515/9781400885930-010

Kruszewski, M., & Wittig, V. (2018). Review of failure modes in supercritical geothermal drilling projects. In Geothermal Energy (Vol. 6, Issue 1). https://doi.org/10.1186/s40517-018-0113-4

Labus, M., & Labus, K. (2018). Thermal conductivity and diffusivity of fine-grained sedimentary rocks. Journal of Thermal Analysis and Calorimetry, 132(3). https://doi.org/10.1007/s10973-018-7090-5

Laplaige, P., Jaudin, F., Desplan, A., & Demange, J. (2000). The French Geothermal Experience Review and Perspectives. World Geothermal Congress. Kyushu - Tohoku, Japan May 28-June 10, 2000.

Lichtenecker, K. von. (1924). Der elektrische Leitungswiderstand künstlicher und natürlicher Aggregate. Physikalische Zeitschrift, 25(8), 169–181.

Lindal, B. (1973). Industrial and other applications of geothermal energy. Geothermal Energy.

Mathiesen, A., Nielsen, L. H., Vosgerau, H., Poulsen, S. E., Bjørn, H., Røgen, B., Ditlefsen, C., & Vangkilde Pedersen, T. (2020). Geothermal energy use, country update report for Denmark. Proceedings of the World Geothermal Congress, 1.

Mattila, A. S. (2006). The power of explanations in mitigating the ill-effects of service failures. Journal of Services Marketing, 20(7). https://doi.org/10.1108/08876040610704856

Maxham, J. G., & Netemeyer, R. G. (2002). Modeling customer perceptions of complaint handling over time: The effects of perceived justice on satisfaction

and intent. Journal of Retailing, 78(4). https://doi.org/10.1016/S0022-4359(02)00100-8

McCabe, K., Beckers, Koenraad. J., Young, Katherine. R., & Blair, Nathan. J. (2019). GeoVision Analysis Supporting Task Force Report: Thermal Applications. Quantifying Technical, Economic, and Market Potential of Geothermal District Heating Systems in the United States. NREL (No. NREL/TP-6A20-71715).

Midttømme, K., & Roaldset, E. (1998). The effect of grain size on thermal conductivity of quartz sands and silts. Petroleum Geoscience, 4(2). https://doi.org/10.1144/petgeo.4.2.165

Midttømme, K., & Roaldset, E. (1999). Thermal conductivity of sedimentary rocks: uncertainties in measurement and modelling. Geological Society Special Publication, 158. https://doi.org/10.1144/GSL.SP.1999.158.01.04

Mijnlieff, H. F. (2020). Introduction to the geothermal play and reservoir geology of the Netherlands. In Geologie en Mijnbouw/Netherlands Journal of Geosciences (Vol. 99). https://doi.org/10.1017/njg.2020.2

Moeck, I. S. (2014). Catalog of geothermal play types based on geologic controls. In Renewable and Sustainable Energy Reviews (Vol. 37). https://doi.org/10.1016/j.rser.2014.05.032

Moeck, I. S., Dussel, M., Weber, J., Schintgen, T., & Wolfgramm, M. (2020). Geothermal play typing in Germany, case study Molasse Basin: A modern concept to categorise geothermal resources related to crustal permeability. Geologie En Mijnbouw/Netherlands Journal of Geosciences. https://doi.org/10.1017/njg.2019.12

Moya, D., Aldás, C., & Kaparaju, P. (2018). Geothermal energy: Power plant technology and direct heat applications. In Renewable and Sustainable Energy Reviews (Vol. 94). https://doi.org/10.1016/j.rser.2018.06.047

Muffler, P., & Cataldi, R. (1978). Methods for regional assessment of geothermal resources. Geothermics, 7(2–4). https://doi.org/10.1016/0375-6505(78)90002-0

Murthy, Ch. S. N., Tripathi, A., Dileep, G., & Pal, S. K. (2023). A Review Study of Thermal Conductivity and Influencing Physico-mechanical Properties of Rocks. *International Journal of Mining and Mineral Engineering*, *14*(3). https://doi.org/10.1504/ijmme.2023.10059738

Nagaraju, P., & Roy, S. (2014). Effect of water saturation on rock thermal conductivity measurements. Tectonophysics, 626(1). https://doi.org/10.1016/j.tecto.2014.04.007

Navelot, V., Géraud, Y., Favier, A., Diraison, M., Corsini, M., Lardeaux, J. M., Verati, C., Mercier de Lépinay, J., Legendre, L., & Beauchamps, G. (2018). Petrophysical properties of volcanic rocks and impacts of hydrothermal alteration in the Guadeloupe Archipelago (West Indies). Journal of Volcanology and Geothermal Research, 360. https://doi.org/10.1016/j.jvolgeores.2018.07.004

Nelson, P. H. (1994). Permeability-porosity relationships in sedimentary rocks. Log Analyst, 35(3).

Nielsen, L. H., Mathiesen, A., & Bidstrup, T. (2004). Geothermal energy in Denmark. Geological Survey of Denmark and Greenland Bulletin, 4. https://doi.org/10.34194/geusb.v4.4771

Nisbet, M. C., Scheufele, D. A., Shanahan, J., Moy, P., Brossard, D., & Lewenstein, B. v. (2002). Knowledge, reservations, or promise? A media effects model for public perceptions of science and technology. In Communication Research (Vol. 29, Issue 5). https://doi.org/10.1177/009365002236196

O'Hare, M. (1977). "Not on my block you don't": facilities siting and the strategic importance of compensation. In Public Policy (Vol. 25, Issue 4).

Pająk, L., Tomaszewska, B., Bujakowski, W., Bielec, B., & Dendys, M. (2020). Review of the low-enthalpy lower cretaceous geothermal energy resources in poland as an environmentally friendly source of heat for urban district heating systems. Energies, 13(6). https://doi.org/10.3390/en13061302

Pellizzone, A., Allansdottir, A., de Franco, R., Muttoni, G., & Manzella, A. (2015). Exploring public engagement with geothermal energy in southern Italy: A case study. Energy Policy, 85. https://doi.org/10.1016/j.enpol.2015.05.002

Pimienta, L., Klitzsch, N., & Clauser, C. (2018). Comparison of thermal and elastic prop-erties of sandstones: Experiments and theoretical insights. Geothermics, 76. https://doi.org/10.1016/j.geothermics.2018.06.005

Prensky, S. (1992). Temperature Measurements in Boreholes. An Overview of Engineering and Scientific Applications. The Log Analyst, 33(3).

Richter, A. (2020). New seismic event puts longer pause on geothermal project in Alsace, France. Think GeoEnergy - Geothermal Energy News. https://www.thinkgeoenergy.com/new-seismic-event-puts-longer-pause-on-geothermal-project-in-alsace-france/

Røgen, B., Ditlefsen, C., Vangkilde-Pedersen, T., Nielsen, L. H., & Mahler, A. (2015). Geothermal Energy Use, 2015 Country Update for Denmark. World Geotermal Congress 2015, June.

Rollin, K. E. (1987). Catalogue of geothermal data for the land area of the United Kingdom. Third revision: April 1987. Nottingham, UK, British Geological Survey, 95pp. (Investigation of the Geothermal Potential of the UK, WJ/GE/87/007) (Unpublished)

Rollin, K. E. (1995). A simple heat-flow quality function and appraisal of heat-flow measurements and heat-flow estimates from the UK Geothermal Catalogue. Tectonophysics, 244(1–3). https://doi.org/10.1016/0040-1951(94)00227-Z

Schön, J. H., (2011). Physical Properties of Rocks: A Workbook. In Vasa.

Schön, J. H. (2015). Physical Properties of Rocks: Fundamentals and Principles of Petrophysics (2nd edition). Developments in Petroleum Science (Elsevier), 65.

Selley, R. C., & Sonnenberg, S. A. (2015). Elements of Petroleum Geology. In Elements of Petroleum Geology. https://doi.org/10.1016/C2019-0-04461-5

Siegrist, M. (2010). Predicting the future: Review of public perception studies of nanotechnology. Human and Ecological Risk Assessment, 16(4). https://doi.org/10.1080/10807039.2010.501255

Sipio, E. di, & Bertermann, D. (2018). Thermal properties variations in unconsolidated material for very shallow geothermal application (ITER project). *International Agrophysics*, *32*(2). https://doi.org/10.1515/intag-2017-0002

Sitkin, S. B. (1992). Learning Through Failure: the strategy of Small Losses. In Research in organizational behavior (Vol. 14).

Smith, A. K., Bolton, R. N., & Wagner, J. (1999). A Model of Customer Satisfaction with Service Encounters Involving Failure and Recovery. Journal of Marketing Research, 36(3). https://doi.org/10.1177/002224379903600305

Somerton, W. H. (1992). Thermal properties and temperature-related behavior of rock/fluid systems. Thermal Properties and Temperature-Related Behavior of Rock/Fluid Systems. https://doi.org/10.1016/0377-0273(93)90059-z

Sowizdzal, A. (2018). Geothermal energy resources in Poland – Overview of the current state of knowledge. In Renewable and Sustainable Energy Reviews (Vol. 82). https://doi.org/10.1016/j.rser.2017.10.070

Stein, C. A. (2013). Heat Flow of the Earth. https://doi.org/10.1029/rf001p0144

Stober, I., & Bucher, K. (2021). Geothermal energy: From theoretical models to exploration and development. In Geothermal Energy: From Theoretical Models to Exploration and Development. https://doi.org/10.1007/978-3-030-71685-1

Syed, M. (2015). Black box thinking: why most people never learn from their mistakes -- but some do.

Tatar, A., Mohammadi, S., Soleymanzadeh, A., & Kord, S. (2021). Predictive mixing law models of rock thermal conductivity: Applicability analysis. Journal of Petroleum Science and Engineering, 197. https://doi.org/10.1016/j.petrol.2020.107965

Tax, S. S., Brown, S. W., & Chandrashekaran, M. (1998). Customer evaluations of service complaint experiences: Implications for relationship marketing. Journal of Marketing, 62(2). https://doi.org/10.2307/1252161

Tester, J. W., Anderson, B. J., Batchelor, A. S., Blackwell, D. D., & DiPippo, R. (2006). The Future of Geothermal Energy - Impact of Enhanced Geothermal Systems (EGS) on the United States in the 21st Century. MIT - Massachusetts Institute of Technology.

Tiab, D., & Donaldson, E. C. (2003). Petrophysics: Theory and practice of measuring reservoir rock and fluid transport properties. In Petrophysics: Theory and Practice of Measuring Reservoir Rock and Fluid Transport Properties. Elsevier. https://doi.org/10.1016/B978-0-7506-7711-0.X5000-2

TNO. (2023). ThermoGIS. https://www.thermogis.nl/en

Tucker, A. L., & Edmondson, A. C. (2003). Why hospitals don't learn from failures: Organizational and psychological dynamics that inhibit system change. In California Management Review (Vol. 45, Issue 2). https://doi.org/10.2307/41166165

Turcotte, D., & Schubert, G. (2014). Geodynamics (3rd ed.). Cambridge University Press.

TWI. (2022). *Induced Seismicity at the Balmatt Geothermal Project*. TWI. https://www.twi-global.com/media-and-events/press-releases/2022/induced-seismicity-at-the-balmatt-geothermal-project

US DOE. (2019). GeoVision: Harnessing the heat beneath our feet. US Department of Energy, Washington, DC (United States).

Vergnault, O. (2022). Earthquake near Eden Project was one of 300 man-made "seismic events" since January. *Corwall Live*. https://www.cornwalllive.com/news/cornwall-news/earthquake-near-eden-project-one-6781365

Vosteen, H. D., & Schellschmidt, R. (2003). Influence of temperature on thermal con-ductivity, thermal capacity and thermal diffusivity for different types of rock. Physics and Chemistry of the Earth, 28(9–11). https://doi.org/10.1016/S1474-7065(03)00069-X

Wallquist, L., & Holenstein, M. (2015). Engaging the Public on Geothermal Energy. World Geothermal Congress, Melbourne, Australia, 19-25 April 2015, April.

Weber, J., Ganz, B., Schellschmidt, R., Burkhard, S., & Schulz, R. (2015). Geothermal energy use in Germany. World Geothermal Congress, April.

Wheildon, J., and Rollin, K. E. (1986). Heat Flow, in Downing, R. A., and Gray, D. A., eds., Geothermal Energy: The potential in the United Kingdom. London. HMSO. p. 13.

Willems, C. J. L., Ejderyan, O., Westaway, R., & Burnside, N. M. (2020). Public perception of geothermal energy at the local level in the UK. World Geothermal Congress 2020.

Williams, C. F., Reed, M. J., & Anderson, A. F. (2011). Updating the Classification of Geothermal Resources. Proceedings, Thirty-Sixth Workshop on Geothermal Reservoir Engineering, Stanford University, Stanford, California, January 31 - February 2, 2011.

Woodside, W., & Messmer, J. H. (1961a). Thermal conductivity of porous media. I. Unconsolidated sands. Journal of Applied Physics, 32(9). https://doi.org/10.1063/1.1728419

Woodside, W., & Messmer, J. H. (1961b). Thermal conductivity of porous media. II. Consolidated rocks. Journal of Applied Physics, 32(9). https://doi.org/10.1063/1.1728420

Younger, P. L., Feliks, M. E. J. J., Westaway, R., Mccay, A. T., Harley, T. L., Elliott, T., Stove, G. D. C. C., Ellis, J., Watson, S., & Waring, A. J. (2015). Renewing the Exploration Approach for Mid-Enthalpy Systems: Examples from Northern England and Scotland. Proceedings World Geothermal Congress 2015, April.

Zarrouk, S. J., & McLean, K. (2019). Chapter 2 - Geothermal systems. In Geothermal Well Test Analysis.

CHAPTER 3
Global Database of HSA Geothermal Projects

3.1. Introduction

The literature review identified key insights and knowledge gaps regarding the risks associated with the development of HSA systems. Major risks include well integrity issues and unpredictable reservoir characteristics, all of which contribute to financing challenges. Unlike the oil and gas industry, geothermal projects usually face lower returns on investment, discouraging potential funders. Although technological advancements have improved geothermal risk assessment, high exploration and drilling costs (up to 15% of CAPEX) remain significant barriers for the sector. Addressing geological risks at an earlier stage could enhance project viability, but operational costs (OPEX) also constrain further geothermal development.

Public perception and societal acceptance are crucial for the expansion of geothermal energy, but can be negatively impacted by several factors, such as a limited public knowledge or understanding, a lack of transparency, and inadequate communication with local populations. Such issues can delay or even halt projects and must therefore be carefully considered when planning geothermal developments.

A clear absence of a “learning from failure” ethos was identified in the geothermal sector. While industries such as aviation leverage failures as learning opportunities, the geothermal sector rarely reports unsuccessful projects. This lack of transparency makes it challenging to define failure modes and mitigate risks effectively. While failures may arise from avoidable errors and inherent

uncertainties, identifying and analysing minor failures can prevent more significant setbacks. However, social, psychological, and technical barriers often discourage the reporting of failures, further hindering the growth of geothermal energy. Lessons from the oil and gas industry, which employs similar technologies and face comparable risks, could significantly benefit geothermal projects, particularly HSAs.

Additionally, Chapter 2 highlighted a lack of standardised international terminology for classifying geothermal systems, particularly HSAs. Although geothermal resources can be categorised using various parameters including depth, temperature, enthalpy, heat transport mechanism, rock type, geology, resource extraction technology or the environmental-socio-economic viability of a project; inconsistencies in definitions and interpretations among authors create confusion. In particular, multiple depth and temperature thresholds have been proposed to define HSAs, contributing to ambiguity and potentially hindering the advancement of geothermal development.

By providing and quantifying key parameters associated with the failure of HSA projects, this chapter seeks to address the identified gaps, thereby supporting the success and viability of future HSA prospects. Furthermore, it aims to provide a refined definition of HSA geothermal systems.

This chapter was submitted in September 2024 and accepted for publication in *Geoenergy* (https://doi.org/10.1144/geoenergy2024-031). The published version may differ slightly from the one presented here. I contributed to the paper with: Writing – Original Draft, Writing – Review & Editing, Conceptualization, Methodology, Validation, Investigation, Data Curation, Visualization. Other authors **: NMB:** Writing – Review & Editing, Conceptualization, Methodology, Supervision, Project Administration, Funding Acquisition. **ZKS:** Review & Editing, Conceptualization, Methodology, Supervision. **CJLW:** Writing – Review & Editing, Conceptualization, Resources. **MP:** Writing – Review & Editing, Resources. **CB:** Writing – Review & Editing, Resources.

The dataset is available in Appendix B.

3.2. Publication

Global database of hot sedimentary aquifer geothermal projects: De-risking future projects by determining key success and failure criteria in the development of a valuable low-carbon energy resource

Maëlle Brémaud[1,3], Neil M. Burnside[1], Zoe K. Shipton[1], Cees J. L. Willems[2], Martin Pujol[3], Claire Bossennec[4,5]

[1]Department of Civil and Environmental Engineering, University of Strathclyde, Glasgow G1, 1XJ, UK

[2] N.V. HVC, Jadestraat 1, Alkmaar, 1812 RD, Netherlands

[3]JRG Energy, Level 2, 600 Murray Street, West Perth, 6005, Western Australia, Australia

[4]GFZ German Research Centre for Geosciences, Section 4.8, Geoenergy, Telegrafenberg, Potsdam, 14473, Germany

[5]Laboratoire d'Océanologie et de Géosciences, Université de Lille, 59650, Villeneuve-d'Ascq, France

Correspondence to: Maëlle Brémaud (maelle.bremaud@strath.ac.uk)

Keywords

Hot Sedimentary Aquifer, de-risking, geothermal energy, geology, heat production

Abstract

Hot sedimentary aquifers (HSAs) have huge potential for low-carbon energy supply but remain a relatively untapped resource. For example, HSAs could meet 100 years of UK national heat demand. The main technical barriers to HSA deployment are subsurface risks and associated well completion requirement. Numerous studies and policies have attempted to tackle these hurdles, but the sluggish implementation of HSA projects underscores the need for a deeper understanding

of what works and what does not. Embracing a "learning from failure" ethos, we compiled a comprehensive database of key parameters through a systematic review of publicly available information from 256 HSA projects across eight countries where data were widely available: Australia, Croatia, Denmark, France, Germany, Poland, the Netherlands, and the UK. This database encompasses project specifics, borehole details, geological and hydrogeological parameters, associated risks, and mitigation strategies. Analysis reveals that 26% of HSA projects failed, mainly due to geological and hydrogeological (39% of all reasons), financial (26%) and technical (25%) issues. Mitigation or remediation strategies were implemented by 24% of both failed and running projects, resulting in a general decrease in failure rate over time. Successful projects emphasise the importance of robust pre-drilling site characterisation and ongoing monitoring of the geothermal installations. We recommend the adoption of international standards for geothermal play classification and data reporting to enhance appraisal of HSA prospects. By quantifying key parameters for project failure and success, we hope to derisk and inform better budgeting of HSA endeavours, thereby bolstering the success and viability of future HSA projects.

3.2.1. Introduction

The energy sector is responsible for 35% of global emissions (Bruckner et al., 2014). In 2022, the share of renewable energy in the fossil fuel dominated global energy mix (electricity, transport, and heating) was 12.3% (IEA, 2023). To achieve an effective decarbonisation of energy, a rapid transition to renewable technologies is required. Unlike other intermittent renewable options, geothermal can produce largely weather-independent low-carbon energy for multiple applications such as baseload electricity generation and heating of buildings, greenhouses, and heat for industrial processes. With a technical potential of 800 GWe for electricity and almost 6000 GWth for heat generation by 2050, geothermal energy could supply c. 15% of global electricity needs (IEA, 2024). Geothermal energy produces negligible greenhouse gas emissions (McCay et al., 2019), the comparative land occupancy of a power plant is very low (7.5 km2/TWh, McDonald et al., 2009), and

the global average levelised cost of electricity (USD 71/MWh) is competitive against already widely adopted renewable energy options like offshore wind (USD 84/MWh) and solar PV (USD 57/MWh) (IRENA, 2021).

Various parameters are used to categorise geothermal systems –defined as specific types of geothermal resources characterised by their distinct thermal and geological properties– e.g., depth, temperature, enthalpy, heat transport mechanism, rock type, geology, resource extraction technology or the environmental-socio-economic viability of a project. The geothermal community lacks a common definition and boundaries for each category, except the latter that is internationally agreed via the United Nation Framework Classification for Resources (UNFC) group (Falcone and Conti, 2019). However, this scheme is only relevant for the sustainable management of geothermal resources and does not fit in this study. The introduction of multiple classifications that are not recognised as international standards (Breede et al., 2015) creates confusion which may be contributing to the slow uptake of geothermal development. This paper focuses on a category of geothermal plays called hot sedimentary aquifers (HSAs). The definition of HSAs found in the literature can be ambiguous, so HSAs were identified here as large, conduction-dominated reservoirs found in sedimentary basins. HSAs must be hot enough and have sufficient productivity to constitute a potential geothermal resource (Gillespie et al., 2013); Busby, 2014; Comerford et al., 2018). Stimulation techniques are typically not required due to the targeted completion of wellbores into zones of comparatively high primary or secondary permeability (Huddlestone-Holmes and Hayward, 2011), but they might be applied to some HSA boreholes to increase the near-wellbore permeability, especially in carbonate reservoirs. Some countries use the alternative term hydrothermal systems, although this is not restricted to HSAs and can encompass other geothermal resource types such as volcanic plays or fault systems, as long as the hot water is produced from naturally occurring water-bearing structures (Moeck, 2014; Breede et al., 2015; Huddlestone-Holmes and Hayward, 2011; Acksel et al., 2022).

Based on the literature for HSAs and deep geothermal energy, we defined HSAs as having minimum temperatures of 20°C (Gillespie et al., 2013) and depths of 200 m below ground level (mbgl) (Banks, 2012; AFPG, 2023). These were the shallowest and coolest thresholds found in the literature for HSA or deep geothermal systems. The 200 m cut-off is also used by various countries for energy and water regulations (Tinti et al., 2016; SEPA, 2016; Tsagarakis et al., 2020). This definition intentionally excludes shallower systems utilising heat pumps, as our focus is on deep geothermal reservoirs with distinct drilling and completion risks. HSAs are especially suitable for heating applications, but the water produced can be used for electricity generation when reservoir temperature and average ambient surface temperature difference is sufficient, e.g. ≥ 90°C in temperate climate regions (Kabeyi, 2019). In 2018, 50% of global energy consumption was for heating (IEA, 2019), implying that HSA systems could have a considerable impact in the future energy provision of many countries. In the UK, HSA heat in place (HIP) has been conservatively estimated at 55,834 to 91,112 TWh (Busby, 2014) which if used solely for heat could meet 100 years of current UK demand (OFGEM, 2016). HSAs usually have lower development costs than other geothermal systems thanks to shallower drilling targets, higher borehole flow rates, and use of proven and conventional technology (Barnett, 2009). One of the main barriers for HSA development is related to geological uncertainties. Assessing subsurface thermal resources up to several kilometres below ground can be challenging as the understanding of aquifer properties mainly comes from surface and near-surface data (Gillespie et al., 2013). Information gaps are usually found in rock property, geological, geophysical and borehole data (Witter et al., 2019). These uncertainties, together with financial, technical, and policy concerns, significantly enhance project risk exposure and lead to stakeholder reluctance to invest in HSAs (Gehringer and Loksha, 2012). If not mitigated or addressed, these risks can result in the abandonment of geothermal projects.

Failures can be taken as learning opportunities as is common aviation, amongst other industrial sectors (Syed, 2015). However, in the geothermal industry, reporting failures is not a common practice. In this paper, we present an assessment of operational and closed projects targeting HSAs in eight countries to identify the most important predictive parameters and gaps that must be addressed to de-risk future HSA prospects. For the purpose of this research, failure was defined as follows: At least one of the risks occurs, cannot be mitigated, and leads to the abandonment of a project during its planned lifetime. Regarding research projects, a project is said to have succeeded when only drilled to investigating the geothermal potential of a reservoir and collect data such as temperature gradients or rock cores. If a research borehole aims to demonstrate a favourable productivity and the geothermal reservoir does not meet expectations, it is here classified as a failure. We examined the most common reasons for project failure, and we highlight that organisational learning from failures is key to the improvement of the geothermal sector.

3.2.2. Methodology

3.2.2.1. Systematic Literature Review Methodology

A database of hot sedimentary aquifer heat and electricity projects was built using a systematic literature review approach to examine key parameters associated with successful and unsuccessful projects. An HSA project involves the exploration or development of HSA resources, and fundamentally corresponds to a list of boreholes in the database. A systematic literature review synthetises the current state of knowledge on a topic by methodically compiling information from peer-reviewed and (high quality) grey literature. This research methodology enables the comprehension of the breadth and depth of the area under study, the development of new hypotheses and the identification of research gaps (Xiao and Watson, 2019). The HSA database covers eight countries: Australia, Croatia, Denmark, France, Germany, Poland, the Netherlands, and the UK. Figure 3-1 describes the identification and screening process, based on the Preferred

Reporting Items for Systematic Reviews and Meta-Analyses (PRISMA) standards (Moher et al., 2010; Nguyen et al., 2019). Data were collected from three sources: online databases, research publications and websites. In this work, 'project' refers to a single commercial or research project that may have drilled one or more boreholes, as well as any associated thermal demand. For each country investigated, HSA projects or boreholes were identified during the initial evaluation and screened for more information. More in-depth research was sometimes needed to find out the failure causes of a project: search terms entered into Google and Google Scholar included the name of a project (e.g., "Asten"), name of a borehole (e.g., "GPNE1"), parameters (e.g., "porosity" or "depth"), together with "borehole report", "project", "final report", production test", "closure", or "failure". Only already processed data were included in the database, e.g. we did not compute petrophysical variables (porosity, permeability) from well logs when applicable. Projects initiated after 2022 or without sufficient information such as project name, location or depth were not considered. Initial results for Denmark, the Netherlands, the UK, and Poland were presented in Brémaud et al. (2023) (Appendix A): this paper describes results from an extension of the database into Australia, Croatia, France and Germany, and more in-depth analysis of previously explored countries. Other countries were investigated – Spain, Italy, Hungary, Switzerland, Turkey, China, and Algeria– but they were not included in the database due to a lack of publicly available information, reporting or no existing/past HSA projects. The main data collection sources for each project were different, not least because each nation has its own political, legal and economic circumstances.

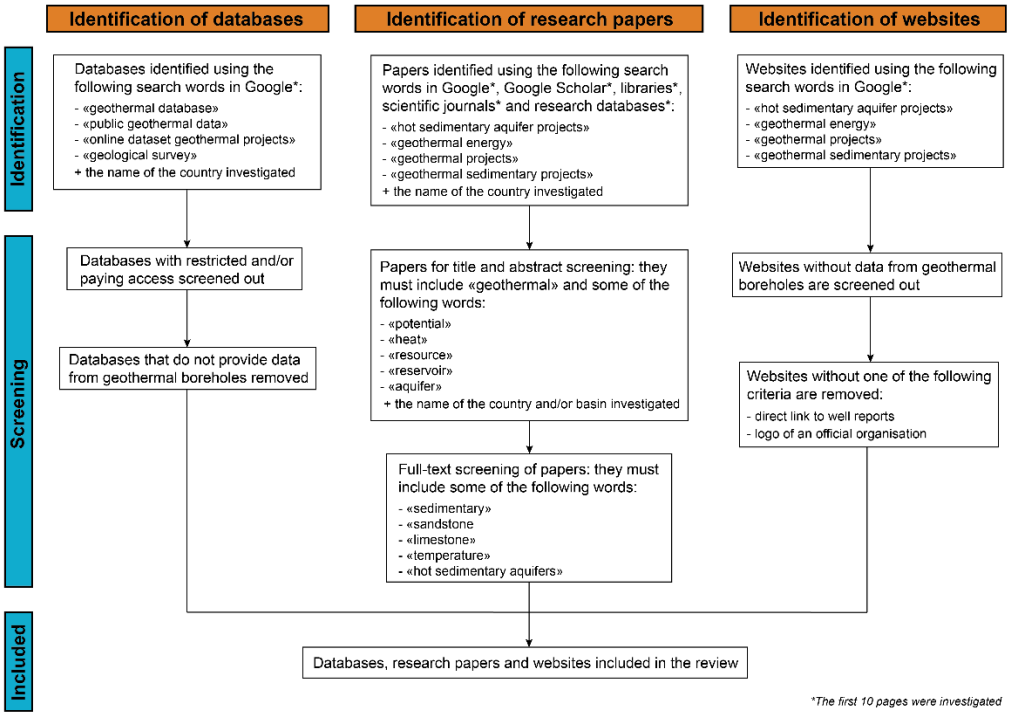

Figure 3-1: Preferred Reporting Items for Systematic reviews and Meta-Analyses (PRISMA) flowchart (Moher et al., 2010) of databases, research papers and websites selection for the systematic literature review.

Data collection was also facilitated by various members of the geothermal community who provided access to restricted-access databases and internal reports, shared their datasets, and reviewed some parts of the HSA database. This was especially true for French, Australian, Dutch, and German geothermal projects.

A systematic literature review requires data quality assessment to evaluate the veracity of data sources and ensure information accuracy. Data collated from published articles, end-of-borehole reports or national geothermal databases are considered the most reliable. Occasionally, detailed information on specific projects was only available on websites that inventoried geothermal projects in one or more countries, which are subject to uncertain quality control measures, so it is acknowledged that these datasets may contain transcribing or other reporting errors. A higher likelihood of erroneous results arises from boreholes

drilled decades ago, when drilling, logging, and testing techniques were less advanced than today.

3.2.2.2. Structure of the Hot Sedimentary Aquifers Database

The HSA database considers a wide range of project and borehole characteristics, and 57 parameters were chosen to describe the project characteristics as accurately as possible. The variables were organised into separate categories (Brémaud et al., 2023, Appendix A): (1) general information on the project/borehole; (2) geology variables; (3) hydrogeological data; (4) risks associated with the project/borehole, and (5) mitigation and remediation measures. Table 3-1 summarises the information collected in the database fields.

Some numerical variables were only provided as a range in publications and reports. Should it happen, the range is recorded in the database, and the median is used for data analysis (Brémaud et al., 2023, Appendix A). For example, Biernat (1993) provided effective porosity and permeability values of respectively 10–30% and 900–1300mD for the Jurassic sandstone reservoir of the Pyrzyce heating plant. In total, 2% of the numerical values of the geological and hydrogeological database parameters were reported only as a range.

Table 3-1: Description of fields for each category of the HSA database

Fields	Description
(1) General	
Project	
Country	Name of the country investigated
Town	Name of the (nearest) town where the borehole is drilled/planned to be drilled
Basin	Name of the geological basin drilled/planned to be drilled
Project	Name of the geothermal project
Use	Specific use of the heat produced, e.g., district heating, greenhouse heating
General use	Broad use of the heat produced, i.e., power only, heat only, research, heat and power, other

Borehole configuration	Type of borehole configuration used in the project, i.e., single borehole, doublet, triplet (etc.)
Heat Capacity (kWth)	Heat generated or planned by the geothermal project
Power Capacity (kWe)	Power generated or planned by the geothermal project
Water disposal	When applicable, network where the pumped water is discharged
Status	Current (2022) status of the project, e.g., active, closed
Outcome	Current (2022) result of the project, e.g., success, failure
Borehole	
Borehole short name	Name of the geothermal borehole
Operator	Name of the organisation/company that is developing the geothermal project
Year	Completion year of the borehole
Closure Year	Year of closure or suspension of the borehole
Total MD (km)	Measured depth of the borehole, i.e. the total length of the wellbore measured along its length
Total TVD (km)	True vertical depth of the borehole, i.e. absolute vertical distance between the rotary table and the end of the wellbore
Target MD (km)	Measured depth of the reservoir, i.e. the length of the wellbore until the middle of the reservoir, measured along its length
Target TVD (km)	True vertical depth of the reservoir, i.e. absolute vertical distance between the rotary table and the mid-reservoir
Coring	Specifies whether cores were collected from the borehole or no (Y/N)
Borehole drilled	Specifies whether a borehole was drilled or not (Y/N). Some of the projects included are in development, or were stopped before the drilling phase
Borehole trajectory	Trajectory of the borehole, i.e., vertical or deviated
Borehole type	Type of borehole, i.e., injector or producer
Flow rate (l/s)	Water flow rate of the borehole
Stimulation	When applicable, specifies which stimulation type was performed in the borehole
Number of sidetracks	When applicable, specifies how many sidetracks were drilled
Target formation/group name	Formation or group name of the reservoir rocks
Member	Member name of the reservoir rocks
(2) Geology	

Age	Age of the reservoir rocks
Lithology	Lithology of the reservoir rocks
Gross aquifer thickness (m)	Total thickness of the reservoir
Net aquifer thickness (m)	Net reservoir interval, i.e. part of the reservoir that has been identified as having a useful capability to store fluids and allow them to flow (Worthington, 2010)
Depositional environment	Depositional environment of the reservoir rocks
Fracturing/Faulting	Specifies any information regarding fractures/faults nearby the borehole
Diagenesis	Specifies any information on reservoir diagenesis
(3) Hydrogeology	
Porosity	Porosity of the reservoir
Permeability (mD)	Permeability of the reservoir
Transmissivity (Dm)	Transmissivity of the reservoir
Skin factor	Skin factor (positive or negative), i.e. region of increased or decreased permeability around the wellbore. Geothermal borehole producing water typically display a negative skin factor (Rutagarama, 2012)
Geothermal gradient (°C/km)	Geothermal gradient in the vicinity of the borehole
Target temperature (°C)	Temperature of the reservoir
Productivity index (m3/h/bar)	Productivity index of the reservoir
Thermal conductivity (Wm-1K-1)	Thermal conductivity of the reservoir
Heat flow (mWm-2)	Heat flow of the reservoir
(4) Risks	
Technical	Problems associated with the technology or processes used in the geothermal project
Geology/Hydrogeology	Issues related to the geological or hydrogeological parameters of the reservoir
Financial	Challenges on the management or allocation of financial resources for a geothermal project
Social	Geothermal risks that are linked to public concerns or interest
Policy	Matters associated with policies and regulations for geothermal projects
(5) Mitigation and remediation	
Sidetracks	Drilling of sidetrack boreholes
Old doublet replaced	Replace an old doublet borehole system with a new one

New borehole added to the project	Add a new borehole to the existing borehole configuration
Refurbishment/improvement work	Perform refurbishment or improvement work on the installations
Back-up reservoir layer	Foresee a fall-back reservoir target in case of issues with the first one
Stimulation	Stimulation or workover of a geothermal borehole
Change in the system use	Modify the planned system use of the geothermal hot water

The "general" section contains essential information about a geothermal project and the borehole(s) drilled, e.g. title, location, timeline, status, capacity, purpose, and the geological formation(s) reached. We distinguished between parameters associated with boreholes (e.g. borehole name, trajectory or type) and fields specific to projects (e.g. capacity, status, outcome). The "geology" and "hydrogeology" categories encompass variables related to the reservoir properties, structure, composition as well as heat and fluid flow properties. The former subclass includes the thickness and lithology of the rocks targeted and provides information regarding potential fault structures or geochemical alteration processes within or near the borehole. Key components of the "hydrogeology" group are typically petrophysical and thermal properties such as productivity, flow rate, porosity, temperature, thermal conductivity, or permeability; all derived from latest available data (e.g. well-tests or production data). The "risks" category encapsulates the potential technical, economic, and socio-political risks faced by projects. Examples of each risk are presented in Table 3-2.

Table 3-2: Detailed classification of the five types of risks catalogued in the database: technical, geology and hydrogeology, financial, social, and policy risks

Risk Category	Examples
Technical	casing/tubing issues, poor condition of the bore, failure of the pumping equipment
Geology/Hydrogeology	Ground deformation, subsidence, fault reactivation, induced seismicity, borehole integrity issues (corrosion, formation damaged, clogging, scaling), aquifer uncertainties, low petrophysical and thermal values, changing or unfavourable groundwater chemistry

Financial	Lack of funding, bankruptcy, not commercially attractive, insufficient number of subscribers, no use of the water nearby
Social	Local communities against the project
Policy	Lack of support by the authorities, wrong decisions, expiration of the drilling permit, environmental awareness, political choices

The "mitigation and remediation" category captures planned interventions for particular project conditions or remediation measures to improve project performance.

3.2.3. Results

Although the HSA database contains information from 57 parameters on collated projects, it must be underlined that none of the projects reported data for all variables in the public domain. Some installations did not provide any data on first-order variables such as the borehole depth, or any information related to the geothermal reservoir, i.e. geological or reservoir parameters. Thus, almost 34% of database cells are blank, rising to 56% for geology and hydrogeology values.

The database collated information on 256 projects targeting HSAs in seven European countries: Croatia, Denmark, France, Germany, Poland, the Netherlands, and the UK; plus, Australia. The target aquifer can be produced using various borehole configurations (e.g., single, doublet or more boreholes), and some boreholes are producing from several geothermal reservoirs. Therefore, from these 256 projects, a total of 464 boreholes and 51 unique target reservoirs from 477 total data entries were reported in the database. 202 boreholes (44%) were drilled in France, followed by Germany (n=88, 19%), Australia (n=64, 14%) and the Netherlands (n=53, 11%). The remaining countries each represent < 6% of the total number of boreholes: 5% (n=22) from Croatia, 4% (n=17) from Poland, and 2% from Denmark (n=10) and the UK (n=8). The results and variables presented in this paper were thus influenced by the prevalence of French projects.

Over half of the projects (56%) used a doublet configuration, i.e., with a producer and an injection borehole. Around one third of the projects (30%) used a single borehole, and the thermally spent water was discharged to surface watercourses, ponds, the sea, transferred to local water network after treatment, or used for agricultural purposes. A triplet configuration was utilised in 18 projects (7%) and could entail two producers and one injector (n=10), or one producer with two injectors (n=8), primarily based on the project requirements for reservoir productivity. The remaining projects (n=18) used more advanced borehole configurations, including, four, five, six, or seven borehole arrays.

3.2.3.1. Growth of Geothermal Exploitation Over Time

Figure 3-2 shows the number of new boreholes (first/lighter bar) and the number of new projects (second/darker and stipple bar) since the 1890s. Only nine projects (corresponding to ten boreholes) were initiated in Australia, Germany and later in France up to 1960. Seven boreholes were artesian, and the hot water is, or was, typically being used for pools and spas. The two remaining boreholes were former oil boreholes drilled in France. The 1960s saw an 11-fold increase in new projects until the end of the 1980s (n=103), mostly due to developments in France (n=81). The first geothermal projects in the Netherlands, Croatia, UK and Denmark were also initiated in 1960–1990. This slowed down in the 1990s with only 19 new projects, although this decade showed a significant increase in new projects in Australia, Germany, Croatia and the first four HSA projects in Poland. The number of new projects increased again in the 2000s (n=30) and 2010s (n=82), a high proportion of them being initiated in the Netherlands, France, Germany, and to a lesser extent in Australia.

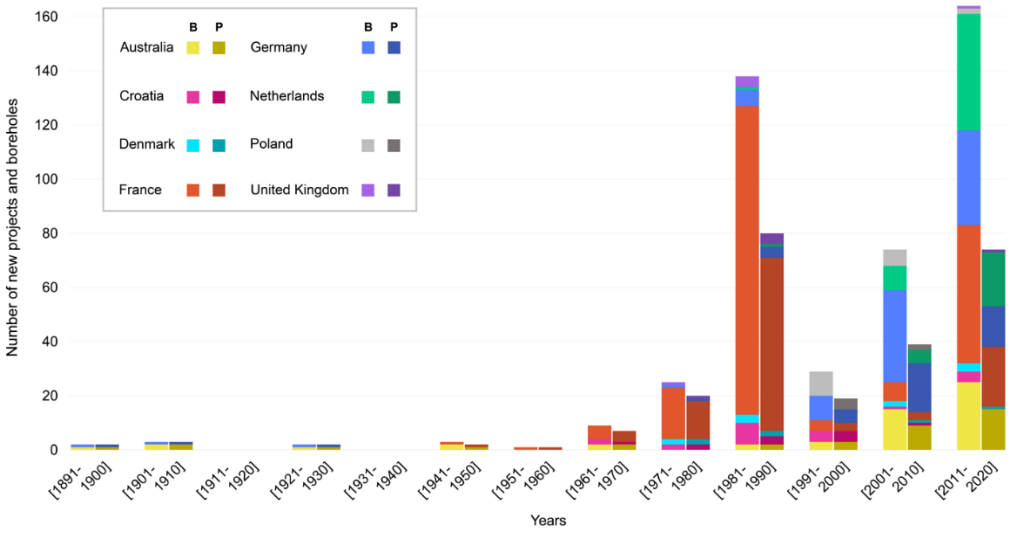

Figure 3-2: Number of new HSA boreholes (first, lighter column) and new HSA projects (second, darker column) per 10 year interval since 1891 for Australia (yellow), Croatia (pink), Denmark (turquoise blue), France (orange), Germany (neon blue), the Netherlands (green), Poland (grey) and the UK (purple). The increase in the ratio of boreholes (B) to projects (P) indicates a greater use of multi-borehole systems.

Most pre-1961 projects were single borehole configurations, and the number of multi-borehole configurations has increased with time (Fig. 3-2). Countries such as France, Germany, the Netherlands, Poland and Australia showed an evolution from around one borehole per project at the onset of geothermal energy development, to twice as many boreholes as projects as the industry matured and environmental regulations were established, especially regarding water disposal. This trend was seen to a lesser extent in Denmark, indicating a greater prevalence of single borehole configurations. The evolution of borehole configuration in Croatia did not show a clear trend in the ratio of boreholes/projects. Though it has a comparatively small number of total projects (n = 6), the UK stood out with a borehole-to-project ratio of 1:1 for each decade, i.e., every one of the 6 UK projects to-date had pursued a single borehole strategy.

3.2.3.2. Geological and Reservoir Parameters

Sixteen parameters depicting the geological characteristics and behaviour of the reservoirs have been included in the HSA database. Figure 3-3 overlays collated

information from HSA boreholes for which basin, lithology, porosity and permeability data were available (179 data points, representing 38% of the total data entries). The two main lithologies shown in Fig. 3-3 are limestone (70%) and sandstone (28%), followed by mixed reservoirs made of claystone and sandstone (2%) or limestone and sandstone (1%). Data are also clustered depending on the 14 geological basins where the boreholes were drilled. The sandstone domain (yellow ellipse in Fig. 3-3) shows an extensive range of permeability versus porosity values (permeability: 1–104 mD and porosity: 8%–38%), largely due to six outlying data points from a borehole in the West Netherlands Basin (purple data points with porosity >20% in Fig. 3-3). In 1987, the first Dutch geothermal borehole was drilled in Asten (the Netherlands) to assess the productivity of six Lower Cenozoic reservoirs for heat applications. Following low transmissivity results, the borehole was eventually abandoned (Mijnlieff, 2020). Limestone reservoirs (green ellipse in Fig. 3-3) have significantly tighter ranges in values (permeability 102 to 104 mD; porosity 4%–24%). 99% (n=124) of the limestone data points come from the Dogger reservoir of the Paris basin (green triangles in Fig. 3-3) and the remaining limestone data point (yellow triangle in Fig. 3-3) corresponds to a borehole drilled in the Carpathian Basin. The black dotted line distinguishes between EGS porosity/permeability domains that require hydraulic stimulation to run (below the line), and those where stimulation is not often used for enhancing permeability (Moeck, 2014). All data points but two are located above the black dotted line. The two points located below the threshold were boreholes initiated in the Otway Basin (Australia) and the Himmerland Graben (the Netherlands) whose projects failed due to unfavourable reservoir conditions.

Figure 3-3 underlines a lack of available petrophysical data. 48% (n=14) of the basins in the database were not represented in Fig. 3-3 as no information was available. Only 3 of these 14 basins show more than 3 data points. Limited data from German (1%), Australian (3%) and Croatian (0%) projects were represented, while 90% of Danish (90%) and 64% of French projects had available petrophysical information. This trend was similar for all geological and hydrogeological parameters, with relatively little information available. Reservoir parameters such

as productivity index, thermal conductivity and heat flow only contained values for 13%, 1% and 1% of the HSA database entries respectively.

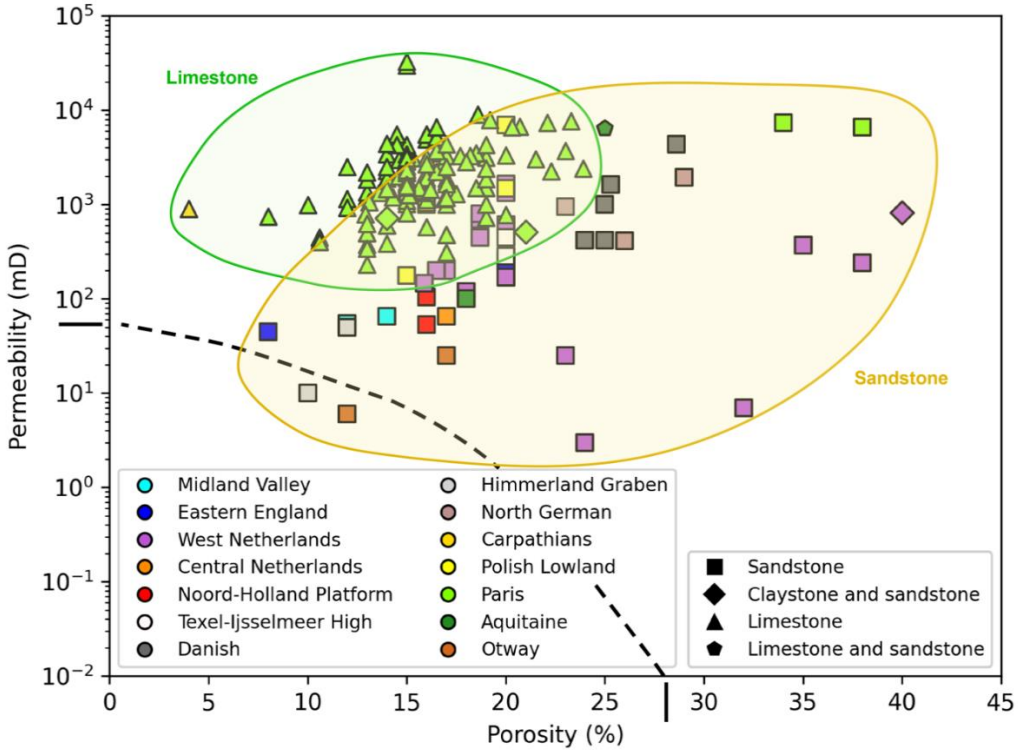

Figure 3-3: Porosity and permeability of various geothermal reservoirs. Porosity/permeability domains characteristic for different reservoir rock types: limestone (green ellipse) and sandstone (yellow ellipse) have been drawn from the data. According to Moeck (2014), the domain below the black dotted line classifies as EGS and therefore requires technical enhancement for producing hot water. The shapes and colours of the data points represent the rock type and the geological basin of the samples, respectively.

3.2.3.3. Unsuccessful Hot Sedimentary Aquifer Projects

Information on failure reporting or analysis was not usually available from operator reports or project stakeholders themselves, but instead was collected from other sources, for instance newspaper reports. Amongst the 256 projects in the database, 26% (n=67) were unsuccessful due to at least one failure, and 11% piled up several issues. The proportion of failed HSA projects varied for each country (Fig. 3-4). The highest failure rate was observed in Danish projects (67%). UK projects also experienced a high rate of failure with five out of eight projects (63%)

that are either no longer active or were never launched. However, this number must be put into perspective as five UK projects were drilled for research purposes with a failure rate of 60%. In comparison, Poland showed a 100% success rate (n=6). The Netherlands, Croatia, France and Australia experienced between 24% and 29% project failures, with 22 projects in France that experienced two or more diverse problems. Germany had the second lowest rate of failure (13%). Yet it should be noted that not all basins in individual nations had the same success rate. All HSA projects initiated in the Perth Basin in Western Australia were still running (as of 2022) while Eromanga Basin projects showed a failure rate of 87.5%. This difference in success rate is likely due to diverse uses of the hot water: the Perth Basin is a mature and well-studied area for geothermal heat production, while the main aim of the HSA projects drilled in the Eromanga Basin is to generate electricity through deeper wells at relatively low temperatures (with regards to electricity production), i.e. 80 to 100°C (Pujol et al., 2015).

It is likely that there was a reporting bias, i.e., an under-reporting of failed projects (Dawson and Dawson, 2018), unless there were regulatory reporting requirements as is the case in the Netherlands (see discussion section). Therefore, these numbers should be taken in context.

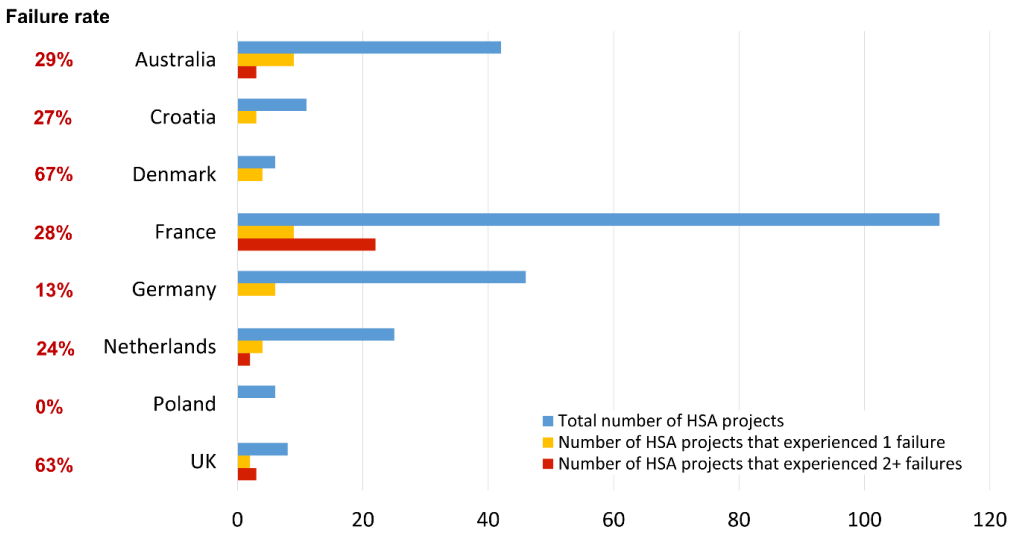

Figure 3-4: Total number of HSA projects (blue) versus the number of HSA projects that experienced one (yellow) or more (red) failures, for each country assessed.

Figure 3-5(a) illustrates the three main reasons for closure or suspension of the 67 failed projects: (i) issues with assessment of geological and/or reservoir properties (39%); (ii) financial decisions (26%); and (iii) technical problems on/in the borehole (25%). Policy decisions (7%) were the remaining reason behind the failure of HSA projects, and 4 projects (3%) did not communicate the causes. No social concerns led to the closure of any of the HSA projects collated (Table 3-1, Fig. 3-5). Most problems encountered in the geological and hydrogeological category were related to chemical degradation of the borehole or unfavourable reservoir parameters (Table 3-2). The proportion of failure causes was different for each country (Fig. 3-5(b)). Project failures from France were due to a blend of financial, technical and geological and hydrogeological reasons. Geological and hydrogeological issues prevailed for Danish, Dutch, British and German failures, while HSA failures in Croatia and Australia were dominated by financial aspects and policy respectively. Unknown failure reasons were greatest for Germany (17%) and Denmark (25%), but this was likely linked to the small number of projects involved (respectively n=6 and n=4).

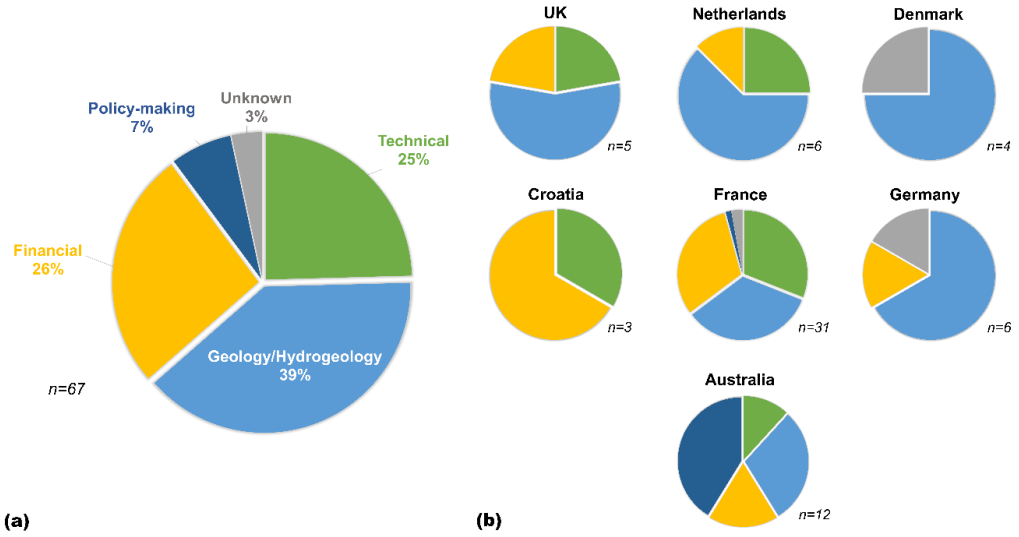

Figure 3-5: Failure categories of unsuccessful HSA projects (a) for the full database and (b) for each of the countries.

Assessing causes of failure during different stages of the project lifecycle is essential. The initial development phase encompasses all project steps from resource exploration to drilling and borehole completion, and when applicable, plant construction and commissioning. The operational phase starts once the project is commissioned and includes reservoir monitoring and operational maintenance until project completion and decommissioning. The three main failure classes display a high percentage of failure during the operational phase, i.e., 72% for the geology and hydrogeology group, and respectively 83% and 84% for the technical and financial categories (Fig. 3-6). Policy is the only exception, with 63% (n=5) of policy-related project failures occurring during the development phase. This was mainly related to a project initiated in 2017 in Winton (Queensland, Australia) to provide 310 kWe to the city and that became the first Australian geothermal power plant in 25 years (Ballesteros et al. 2019). However, the plant never delivered electricity due to commissioning issues and was shut down. The problems encountered by the Winton project contributed to the termination of four nearby projects. Bulloo Shire Council Mayor declared that “all the news that we were getting out of Winton was that it wasn't working yet, to lay off, so we did that” (O'Neal, 2022).

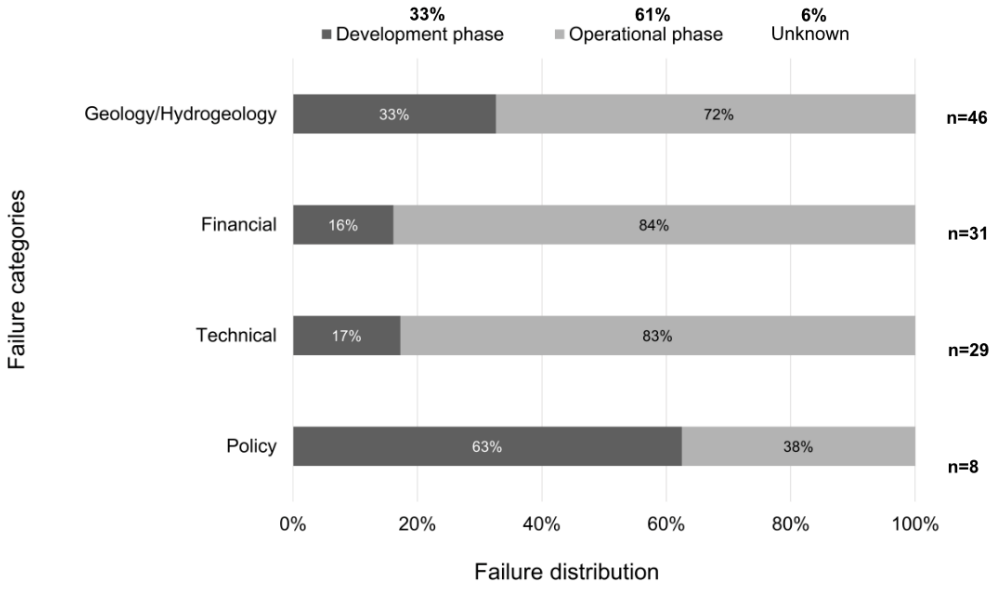

Figure 3-6: Distribution of failures per risk category and project phase

3.2.3.4. Mitigation and Remediation Strategies

More than half of all projects (n=136), including both active and closed projects, had implemented strategies to mitigate encountered risks. Utilised strategies were grouped into seven categories (Table 3-1; Fig. 3-7). The main approaches applied are stimulation on the borehole (59%), the use of sidetrack boreholes (14%) and refurbishment and/or improvement work on one or several boreholes (9%).

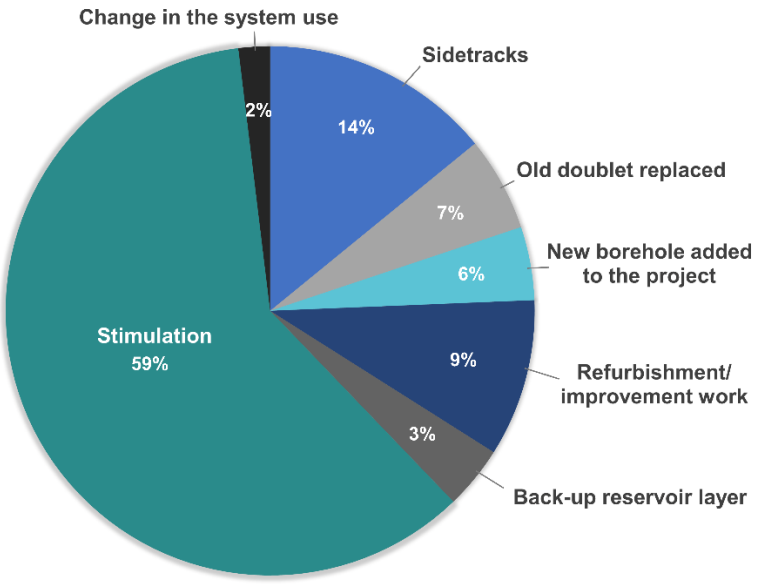

Figure 3-7: Distribution of the seven mitigation and remediation strategies identified

In contrast to hot dry rock systems, HSAs do not necessarily require borehole stimulation. However, 94 projects (37%) required acidizing to establish economically sustainable production rates, and two projects in the Upper Rhine Graben also undertook hydraulic fracturing. Acid stimulation is frequently used in carbonate reservoirs for increasing the permeability and therefore improving the productivity of a borehole by dissolving acid-soluble minerals in the rock matrix. This method had been widely employed in two major geothermal reservoirs included in this study: the Dogger limestones of the Paris Basin (France) (n=75) and the Malm limestones of the Bavarian Molasse Basin (Germany) (n=18). Acidizing was successfully used to increase the yield of 14 boreholes drilled nearby Munich as some of them were only a few kilometres apart (Schumacher and Schulz, 2013). The acidizing stimulation technique had also been designed to cope with borehole damage (Ungemach et al., 2009; Hoefner et al., 1987; McLeod, 1984). In total, 59% of the projects that implemented risk mitigation or remediation measures had used borehole stimulation (Fig. 3-7).

A sidetrack is a secondary borehole drilled from the original as an offshoot (Richardson and Neymeyer, 2013), and is usually completed following technical difficulties, to bypass unusable sections of the borehole, or to explore other geological layers nearby. 22 projects (9%) reported in the database required a sidetrack to be drilled, and 60% of sidetracked boreholes have been drilled in the Netherlands, most following technical issues in the original borehole.

Figure 3-8 presents the distribution per country of all projects that carried out risk mitigation and remediation strategies compared to those which were active in 2022 and the total number of projects. Poland represented only 3% of projects that performed mitigation or remediation, but had the highest rate of implementation, with reconstruction work undertaken on boreholes that were damaged or decommissioned in 4 out of 6 projects (67%). In these cases, borehole refurbishment work was assessed to be a more cost-effective option than drilling

new boreholes (Bujakowski et al., 2020). Other projects in western Europe and Australia also performed improvement work or repairs on geothermal boreholes to fix damaged casing, replace broken pieces, address clogging or changing the submersible pump (Lopez et al., 2010; Dufour and Heederik, 2019; Stuke, 2019).

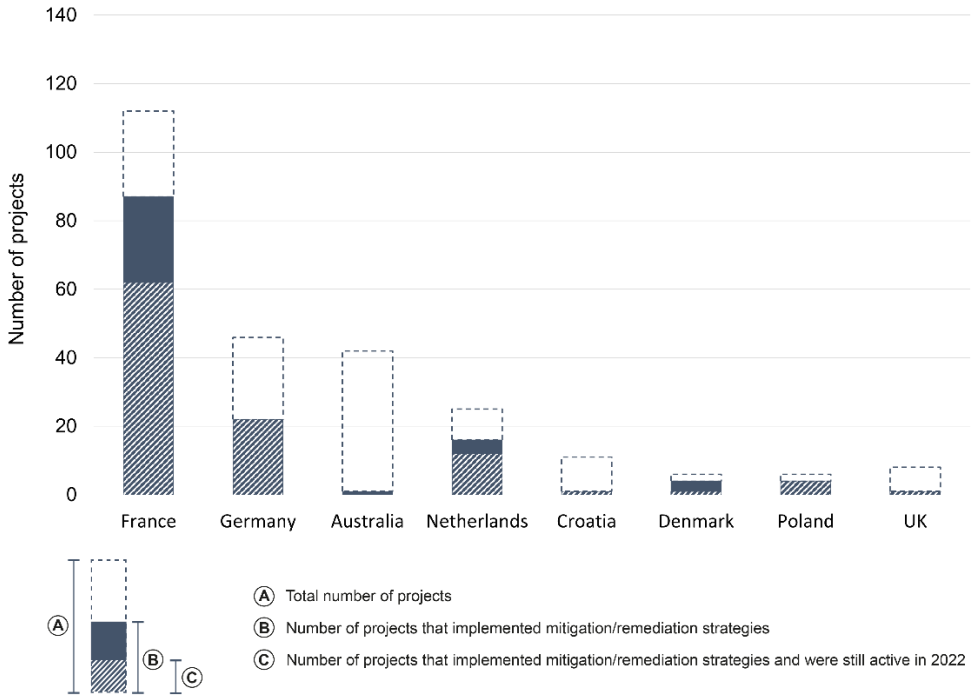

Figure 3-8: Distribution of (C) the projects that implemented mitigation or remediation strategies and are still active today, compared to (B) all the projects that applied those methods, compared to (A) all running and closed HSA projects, per country investigated.

Remediation measures could also involve a renewal of operations: for instance, adding a borehole to the current configuration (6% of all strategies, Fig. 3-7) or decommissioning and replacing a geothermal doublet that has reached its planned lifetime (7% of all strategies, Fig. 3-7) that would provide heat to the same (or a bigger) district heating network. Both strategies had been mostly performed in France, with a share of 71% for the first and 100% for the second approach. In the Paris Basin, nine projects were renewed from 1989–2018 by completely replacing the original doublet. Indeed, the operating permits were for a duration of between 15 and 30 years (Hamm et al., 2019) and completion of new doublets were required to: (1) build more efficient and durable geothermal boreholes with subhorizontal drilling (Ungemach et al., 2019) (2) limit corrosion by using

composite materials (Boissavy et al., 2020); (3) increase heat production (ADEME, 2012, Boissavy et al., 2020); or (4) extend the heating network (ADEME, 2012). For three projects, geothermal installation renewal was carried out in two phases: a new borehole was drilled and used as a doublet with the best performing original borehole, and several years later a new second borehole was drilled and the original borehole was decommissioned (ADEME, 2012). Since 2008, five doublet installations targeting the Dogger limestones in the Paris Basin have drilled a new producer borehole to increase their heat production and are now operating as triplet configurations with two producers and one injector (Lopez et al., 2010).

Defining back-up reservoir layers (3% on Fig. 3-7) was a strategy especially implemented by French geothermal companies to reduce the risks, simplify, and speed up the decision-making in case of problems encountered with the first geological target. Issues were typically linked to the reservoir itself, e.g., the layer could not be found, or the aquifer had less favourable reservoir properties (productivity, flow rate, permeability) than expected. Two HSA projects in the Netherlands and Denmark also had primary and back-up geothermal targets.

When facing technical, geological or economic difficulties, one way to resume or continue exploiting the subsurface geothermal resource is by changing the purpose of the boreholes. This had been done in three projects: two in Germany and one in the UK (Fig. 3-7). The Science Central project in Newcastle-Upon-Tyne, UK was initiated in 2011 and included a 1.8 km deep borehole. The transmissivity of the target Fell Sandstone aquifer was too low to provide space heating for local buildings, as initially planned (Younger et al., 2016). However, this project was not seen by the operators as a failure because it proved that the resource was there. The borehole had been transitioned to a geothermal research site. Newcastle City Council's director of investment and development said that: "It was really exploratory and in essence it has achieved everything that was set out […] about understanding geothermal heat at a 2km depth" (Proctor, 2014). Bruchsal and Unterhaching geothermal projects in Germany both faced economic difficulties after more than a decade of operation. The Bruchsal doublet was drilled in the

Upper Rhine Graben in 1987 and initially suppled heat to a district heating scheme. In the 1990s, both boreholes were stopped following oil prices drops (Herzberger et al., 2010). Energy policies were fundamentally modified in the early 2000s with the renewable energy act (EEG) that came into force (Gründinger, 2017). The Bruchsal project was eventually revitalised, and boreholes were recommissioned in 2003 to provide 500 kWe (Herzberger et al., 2010). In Unterhaching (Bavarian Molasse Basin), the geothermal power plant was built in 2004 to supply electricity and heat to the city. However, electricity generation was not cost-effective, leading to a change in project purpose. Since 2017, the plant solely delivers district heating to c. 7,000 households (Richter, 2018).

These examples demonstrate the utility of risk mitigation and remediation measures to overcome prospective HSA project failure. Amongst all HSA projects in the database that acted to reduce risks, 76% were still active in 2022 (Fig. 3-8) although the results are dissimilar for each country. Croatia, Germany, Poland and the UK show a 100% rate, followed by the Netherlands and France with respectively 75% and 71%, and Denmark and Australia fall behind with 25% and 0%. Of the 24% projects that implemented mitigation and remediation measures and eventually failed, only one of 33 failed for a reason related to the implemented strategy employed. The Sønderborg project (Denmark), drilled in 2013, did not find its initial Bunter Sandstone target reservoir, so opted for a backup completion into the Gassum Formation at a c. 1km shallower depth. This option allowed the installation to deliver district heating for five years. However, the plant never ran as planned due to technical issues in the injection borehole. Fine sand entered the injector and acted as a plug because the screen was initially designed for a deeper and more porous reservoir. In 2018, long-term decreasing injectivity and difficulties in injecting the water back into the reservoir meant the operators eventually closed the geothermal installations (Berg Badstue Pedersen, 2020).

3.2.4. Discussion

3.2.4.1. Evolution of Energy Regulations

Geothermal energy can be classified as a relatively new or unexploited energy source when comparing current exploitation to global potential: in 2023, geothermal accounted for a negligible share (0.5%) of global renewable-based energy generation (IRENA and IGA, 2023) but it has the potential to meet more than 3% of electricity demand and c. 5% of heating and cooling demand by 2050 (Craig and Gavin, 2018). Geothermal energy development goes together with an evolution of energy regulations, but this change is innately linked with the state of play of geothermal technology in each country. No specific legal regulation has yet been implemented for most investigated nations to set guidelines for the geothermal sector.

Poland lacks any geothermal regulation, despite geothermal being recognised as the renewable energy with the highest technical potential (Szalewska, 2021). Thus, shallow and deep geothermal energy are subject to six different laws, although Szalewska (2021) states that the complexity of the legal framework is not a limiting factor for the development of geothermal energy in Poland.

As of 2023, the UK has no legal acknowledgement of geothermal resources and “the absence of a coordinating body for the geothermal application process is seen by stakeholders as a barrier to faster roll out of geothermal projects, and many [of them] have found the regulatory requirements for deep geothermal projects to be somewhat difficult or extremely difficult” (Abesser et al., 2023). This could explain the limited geothermal development in the UK compared to other countries, with only 8 HSA projects identified as of 2022.

In Germany, the exploitation of subsurface heat is regulated by the "Bundesberggesetz" (Federal Mining Act), which covers various aspects of mining activities, including geothermal energy extraction. The Federal Ministry for Economic Affairs and Climate Protection oversees mining activities and energy policies at the federal level. Germany is divided into 16 federal states, each with its

specific regulations and authorities governing geothermal energy and subsurface heat production. At the local level, municipalities and districts may have their own zoning regulations and permits that apply to geothermal projects. The current trend is to harmonise and simplify regulations while also strengthening environmental impact monitoring (Stemmle et al., 2024). The evolution of the regulations has a direct impact in the geothermal development in Germany with an increase in number of projects and boreholes throughout the last two decades (Fig. 3-2).

The growth of the geothermal sector is also inherently correlated with the use of the subsurface by other industries. An intensive expansion of the coal industry caused the failure of two HSA projects in Australia (Fig. 3-5(b)). In the 1950s, two boreholes in the Gippsland Basin (Victoria State) were used to process water in paper manufacturing, but regional coal mining activities caused substantial dewatering that led to decommissioning of several geothermal installations in the area (King et al., 1987). In 1989, the Mulka power plant, the first geothermal Organic Rankine Cycle (ORC) plant designed and built in Australia, was shut down after only three years of operation because the land was bought as a mining lease (Popovsky, 2013).

Oil price fluctuations have significantly impacted the geothermal market, as evidenced by the repercussions of the 1973 oil crisis. This is particularly clear in France, where in the 1970s HSA projects were shut down during the operational phase (Fig. 3-6). The drop in oil prices, technical difficulties and corrosion issues encountered by those geothermal installations in the 1980s and the 1990s (Laplaige et al., 2000) ultimately led to the closure of 21 projects (8% of total projects) in the Paris basin. Early Dogger aquifer geothermal projects faced considerable sulphide mineral scaling problems, with plant operators needing more expertise to face resulting technical and financial issues (Laplaige et al., 2000). Since the 2000s, the rate of failure decreased seven-fold in the Paris Basin, with only three projects (12.5% of projects in the Paris Basin) closed following an issue. Corrosion and scaling phenomena have been controlled thanks to

technological improvements (Lopez et al., 2010), and geothermal stakeholders have gained experience throughout the decades.

Since the 1980s and following several energy crises (Fig. 3-9), the French geothermal market also considerably benefited from several insurance and risk mitigation schemes that helped limit financial risk and reassure potential investors. Two complementary mechanisms, i.e., short-term risk (STR) and long-term risk (LTR) insurance, were implemented to cover geological risks during the rise of geothermal district heating in France (Fig. 3-2, Fig. 3-9). The STR covered total or partial failure of the first borehole drilled. Success or failure are there based on a temperature/flow rate zone. Simultaneously, the LTR was focused on long-term exploitation, especially covering the risks related to the degradation of the installations and the reservoir exploitability (Boissavy and Laplaige, 2018). The Geothermal Guarantee Fund was launched in 2005 as a revision of the STR and LTR funds. From 2009, the development of renewable heat production facilities and heating networks in France are also supported by the Renewable Heat Fund in order to meet 32% of renewables by 2030 (ADEME, n.d.). This success story inspired other European countries to set up their governmental funds for supporting the launching of geothermal heating projects: in 2010, the Netherlands introduced a government guarantee scheme on drilling risks, followed by the Stimulation Sustainable Energy production scheme two years later (Mijnlieff et al., 2013) that facilitated completion of 43 geothermal boreholes (Fig. 3-2). These schemes were critical for the advancement of deep geothermal in the Netherlands (Boissavy and Laplaige, 2018).

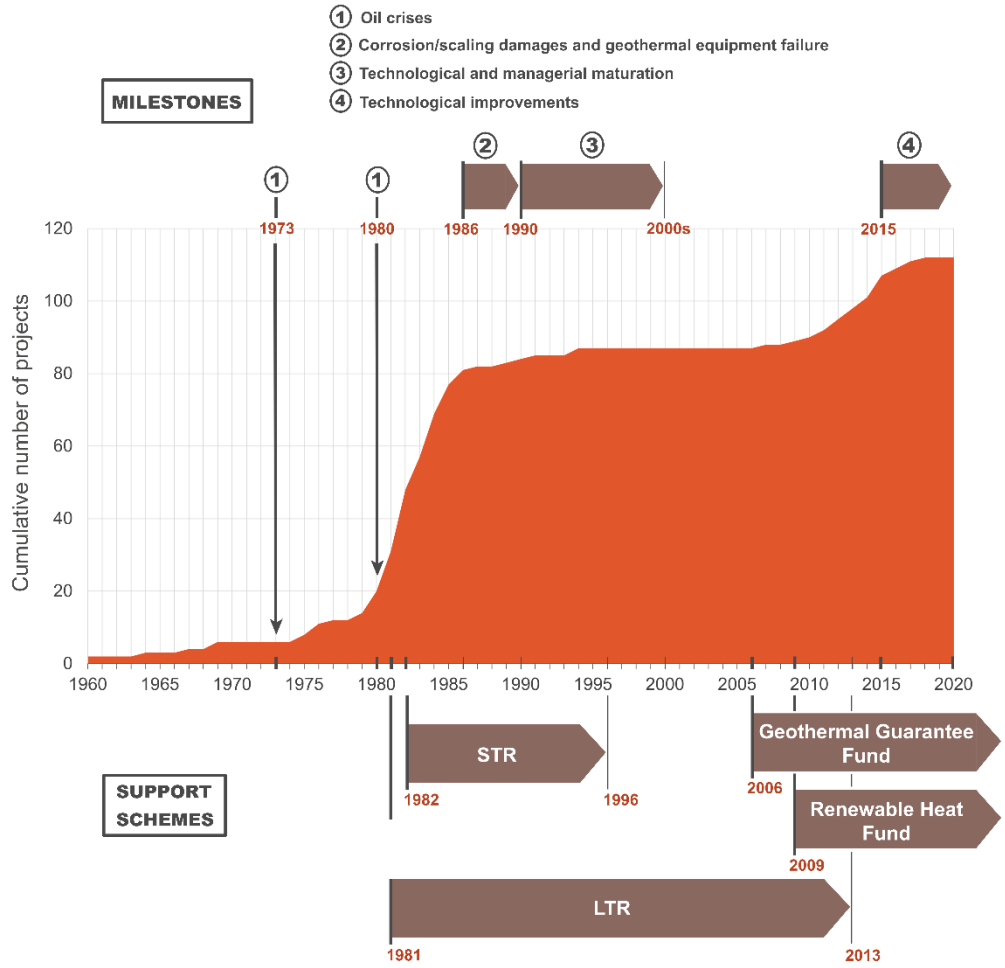

Figure 3-9: Risk mitigation and HSA market development in France since the 1960s

3.2.4.2. Lessons Learned from Mitigation/Remediation Measures and Failures in Hot Sedimentary Aquifer Plays

Building a "learning from failure" culture requires operators to report consistently and perform detailed failure analysis to ensure the proper lessons are learned (Edmondson, 2011). However, this is not a common practice in the geothermal industry, and HSA projects included in this study did not often reveal details on encountered issues. Without a mechanism for reporting, there is limited opportunity for future projects to learn from previous failures. The analysis of the main failure modes for the compiled HSA projects clearly showed that geology and hydrogeology accounted for the highest proportion of the failure causes (Fig. 3-5). Indeed, the profitability of a geothermal project is mainly threatened by the

resource (i.e. subsurface conditions and geological structure) risk (Deinhardt et al., 2021). As shown in Fig. 3-10, the costs of geological studies to assess resource potential and test drilling are usually very high for the developer. The development cost of a geothermal project is usually between 4.5 M USD and 5.5 M USD per installed megawatt (DiPippo, 2016) and drilling expenditures in hydrothermal electricity projects typically account for 25%–50% of CAPEX costs (Tester et al., 2006). However, as geothermal development stages progress, a greater understanding of the field characteristics is reached, reducing the risk (in theory). In Fig. 3-10, we highlighted a higher number of failures (and therefore risks) during the operational phase (61%) than during the development phase (33%) (Fig. 3-10, Fig. 3-6) of a project. Figure 3-10 is based on Gehringer and Loksha (2012) who displayed a very low risk at the end of the development phase (blue curve in Fig. 3-10), and seemingly no additional cost for the operational phase. This may be because they decided to mostly focus on the development stage, while we included both in our study, or because we included another 12 years of data. Throughout this work, we also showed that assessing the risks and acting prior to any major failure was an efficient lever to preventing the closure of HSA installations. Such measures were applied in 63 projects (25% of total projects) and 80% of these projects remained active in 2022. An adequate monitoring of the installations (both surface and borehole) can significantly improve the understanding of the condition of the infrastructures. It also helped to avoid potential failures through renovation or improvement work on the geothermal installations (22% of all measures), or decisions to be taken based on reservoir changes (add another borehole, 10% of all measures; replace a doublet, 13% of all measures; change the use of the heat, 5% of all measures). Richardson and Neymeyer (2013) provided insights gleaned from various geothermal projects and especially stated that borehole monitoring and management are of key importance.

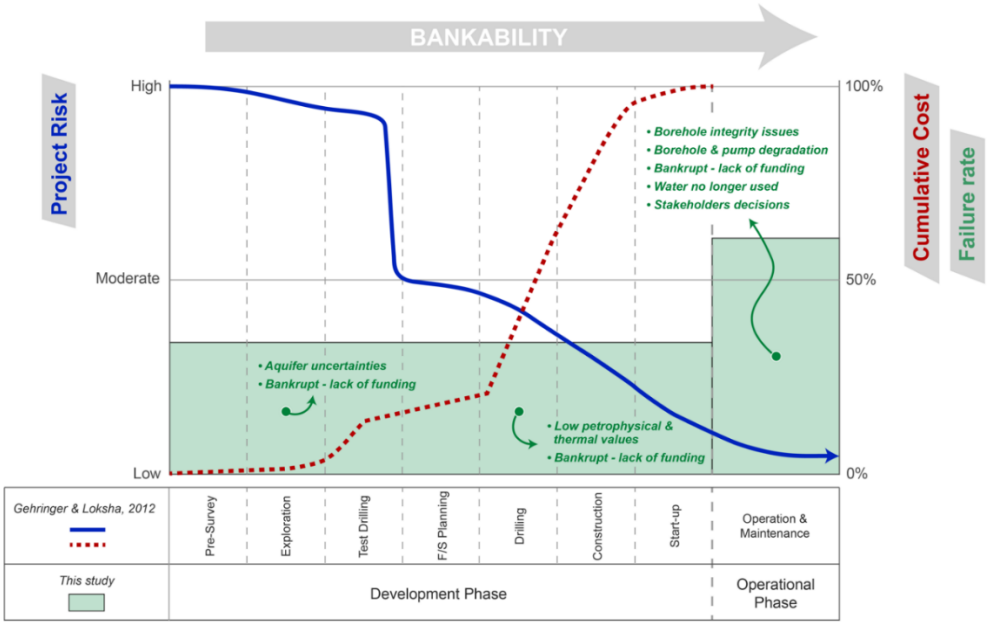

Figure 3-10: Geothermal Project Cost, Risk Profile and Failure Rate at various stages of development and operational phases. Project risk and cost profiles (blue and dashed red lines respectively) are from Gehringer and Loksha (2012). Failure rate and reasons (green) are findings from this study.

The HSA database showed that geological and hydrogeological data were significantly lacking, either not measured or not reported by geothermal operators. This significant gap of crucial data might encourage developers or governments to invest more in exploratory geological studies at the early development stage of a geothermal project or region to limit any issues linked with reservoir and geological aspects. It should also encourage operators to carry out regular monitoring to avoid borehole integrity issues such as clogging or corrosion, and technical problems with the installations.

However, although huge progress has been made in surface and subsurface exploration technologies, prognoses of the depth of a reservoir, its properties (porosity, permeability, temperature, flow rates, etc.) as well as the output from a geothermal borehole remain uncertain until the first borehole is drilled. There are similar challenges in the hydrocarbon industry, though the returns on geothermal investment are comparatively small, making risk more economically unpalatable and therefore more likely to result in project termination (Gehringer and Loksha,

2012). Cumulative costs for exploration and test drilling can account for up to 15% of the overall capital cost, for a near-halving from high to moderate project risk (Fig. 3-10; Gehringer and Loksha 2012). Due to these uncertainties, funders sometimes lack the risk appetite for becoming involved in such investments (Climate Investment Funds, 2014). Balancing the probability of success against the cost of failure is key to reach the best expected outcome (Gehringer and Loksha, 2012). Success stories such as the maturation of French know-how during the early stages of geothermal energy can also be used as a model for helping other countries grow their geothermal sector.

Public concerns did not result in the cessation of any of the 256 projects in the HSA database (Fig. 3-6). There can be a variety of reasons that can negatively influence public appetite for geothermal developments: project location (Carr-Cornish and Romanach, 2014; Edelstein and Kleese, 1995), distrust between parties involved (Willems et al., 2020), and fears over induced seismicity. The latter is partially a legacy of failed enhanced geothermal system (EGS) projects which have demonstrably triggered earthquakes and caused damage to surface infrastructure (e.g., Burnside et al., 2019 ; Edwards et al., 2015; Trutnevyte and Wiemer, 2017; Westaway and Burnside, 2019). Triggered seismicity at EGS projects has apparently had little negative influence on public opinion of HSA projects, but it is crucial that prospective operators ensure full and transparent dialogue with local stakeholders to outline prospective project risks and mitigations.

3.2.4.3. Geothermal Data Collection and Availability

Reporting standards, data availability and type are highly variable depending on historic timing and national location of geothermal project. Amongst countries investigated in this study, France and the Netherlands stood out by providing open or on-demand, free of charge access to a national database that integrates widely ranging data and knowledge on heat or electricity production from geothermal resources.

In the Netherlands, geophysical, borehole and production/injection data are supplied to the Geological Survey of the Netherlands (TNO) and made publicly available online (www.nlog.nl) no more than five years after acquisition (Kombrink et al., 2012). This mandate to make data available came out from the 2003 Mining Law. Published information includes seismic data, production and injection data, field and production licences of developed fields, maps and models, and core and borehole data. The online database usually provides a wide range of data for reported boreholes: original end-of-borehole reports, lithological logs, well-test reports and sometimes water analysis and reports on palynology and diagenesis evolution (TNO, 2023).

In France, the “Système de bancarisation et de suivi des opérations de géothermie de basse énergie en France métropolitaine” (SYBASE) Project has been in operation since 2018 and includes data and knowledge on geothermal boreholes across mainland France. It has been developed from the previous 2002 “Dogger base” database which recorded information on geothermal installations targeting the Dogger limestone aquifer in the Ile-de-France region. Unlike the Dutch geothermal database, the full SYBASE database access is restricted to government administration organisations, Agence de l'Environnement et de la Maîtrise de l'Energie (ADEME, the French agency for ecological transition), and licenced subsurface engineering consultancies. Public access is provided to limited data (e.g. technical information on the boreholes and targeted reservoir, temperature and sometimes transmissivity) through the “Geothermie Perspectives” website (Hamm et al., 2019). We have been given access to the full geothermal database as an exception for this study, which includes end-of-well reports, sometimes combined with geological and production test reports.

To a lesser extent, Germany and some Australian states also grant access to geothermal databases. Germany has been moving towards a more open data policy, especially with the Geologie Datengesetz (Geology Data Act), which came into effect on June 30, 2020. This new law replaces the 1934 Repositories Act (Lagerstättengesetz, LagerstG) and governs tasks related to geological mapping at

both the federal and state levels. It focuses on making geological data accessible to the public, particularly datasets older than ten years. Despite the positive intentions of the law, its practical implementation has faced challenges. This is mainly due to limited financial resources available to the responsible institutions, making it difficult to efficiently manage the workload required to comply with the law's provisions (pers. comm. 2022). GeotIS (www.geotis.de) is the information system that provides knowledge on the use and potential of geothermal energy in Germany via a map interface. It is based on data from boreholes (geothermal, oil and gas, mining) and porosity, permeability, temperature and structural data processed into 3D subsurface models (LIAG, 2023). A table compiling all geothermal installations plus specific information for each operation can also be accessed. However, no raw report has been provided, and reservoir data are missing. The situation in Australia differs from state to state. For example in South Australia, all open-source geothermal exploration data is available on the SARIG (https://map.sarig.sa.gov.au/); it includes well completion reports, company exploration reports, geophysical surveys and other raw and interpreted geoscientific data. In other states such as Western Australia, availability of data varies. For direct-use projects, only limited data is available in the public domain. Well Completion Reports and Exploration activity reports for projects undertaken under the Petroleum and Geothermal Energy Resources Act 1967 is available on WAPIMS (https://wapims.dmp.wa.gov.au/wapims) in a database containing primarily oil and gas data that is only released sometime after the exploration works takes place for confidentiality reasons. The earliest release date for the well's basic data and reports is two years from the end of the activity. Release provisions for basic survey's data can vary according to survey type, permit type, and commercial intent (exclusivity). The earliest release is three years from the end of the activity. Confidentiality periods of up to 15 years may apply. Most recently however, the Department of Mine and Environmental Regulation started compiling geothermal-specific database as part of its Carbon Dioxide Geological Storage Atlas project (https://wapims.dmp.wa.gov.au/WAPIMS/Search/CO2StorageAtlas).

Accessing relevant information for nations with no central data repository or open-access geothermal data requirements is much more challenging. The Agencija Za Ugljikovodike (AZU, Croatian Hydrocarbon Agency) does hold a free-of-charge geothermal database with access to all borehole reports, seismic and GIS data of geothermal operations in Croatia (AZU, 2023); however, the Croatian Geothermal Virtual Data Room (VDR) is only available to collaborators of Croatian university-led research or potential investors. HSA data from Croatia, Denmark, Poland, the UK and, to a certain extent, Australia (direct-use projects in Western Australia) were mainly retrieved from research publications and reports, although these often lack details and typically only provide an overview of current and past projects. However, a new trend is emerging in the last decade, with more countries planning to invest in geothermal energy resulting in more data becoming available, which in turn enables a better understanding of the state of play of the technology.

In addition to significant challenges with data availability and accessibility, the geothermal industry also lacks common definitions on reported as well as a misalignment of collection methodologies between various geothermal organisations. Such issues, especially regarding industry data (e.g., capacity or production variables) at a global scale, lead to misunderstandings and uncertainties in the resulting geothermal values conveyed (Krieger et al., 2022). Our analysis was based on the hot sedimentary aquifer definition previously specified: large and conduction-dominated sedimentary reservoirs of depths ≥ 200m and temperatures ≥ 20°C with elevated heat flow and sufficient productivity to constitute a potential geothermal resource. The outcomes of this study would be impacted by the alteration of geological, temperature and depth thresholds. An explicit definition of an international standard for classifying such geothermal plays, and to a wider extent all geothermal systems would remove ambiguities, greatly enhance appraisal of potential HSA prospects, and promote worldwide opportunities for geothermal resource development.

3.2.5. Conclusion

In this paper, we presented the Hot Sedimentary Aquifer database which captured data from 256 geothermal projects across 19 sedimentary basins in eight countries (Australia, Croatia, Denmark, France, Germany, Poland, the Netherlands, and the UK). Information was collated using a systematic literature review approach and classified in various categories. The following points are key lessons for the sector:

- 26% (n = 67) of the projects of the HSA database have failed and 39% of these failures were related to geological or hydrogeological factors. Financial and technical issues were responsible for 26% and 25%, respectively, of unsuccessful projects. This emphasises the importance of site characterisation prior to drilling to limit geological and reservoir risks, borehole monitoring and technological improvements to effectively manage geochemical and technical issues, and widespread application of risk insurances.

- 24% (n=61) of HSA projects implemented remediation or mitigation techniques to reduce the chances of failure, which proved useful as 80% of these 61 projects were active as of 2022. The main measures were the drilling of sidetrack boreholes (32%) and renovation and/or improvement work on the geothermal installations (22%). Poland stood out from other studied countries by using risk reduction measures in 67% of its HSA projects.

- The database did not hold values for all projects and variables, with nearly 34% of the data missing. In particular, 56% of geological and hydrogeological values were lacking, whereas these variables were responsible for almost 40% of failed projects. This exposes the poor accessibility of geothermal data and reporting globally. Similarly to Dickinson and Ireland (2023), we argue that better data availability is key for a proper risk assessment of HSA projects and more broadly the expansion of geothermal energy worldwide.

- Reported values, including success rates and data availability, varied considerably across countries and over time; mainly driven by (i) regulatory regimes, such as proper law-making to make energy data publicly available and encourage geothermal development, and (ii) technological evolution, such as drilling techniques and corrosion reduction measures. The development of hot sedimentary aquifers requires consistent support to companies, primarily through financial schemes to limit the risks. Therefore, risk mitigation schemes that were implemented in France since the 1980s considerably contributed to the development of renewable energies and even inspired other countries, such as the Netherlands, to set up their fund.

We explored the accessibility of HSA project information across the world. Ultimately, HSA database construction was limited by lack of open access data for countries other than the eight mentioned above. Although we consider the database broadly representative of all HSA projects, analytical outcomes may be influenced by additional data from other countries. Therefore, the database could be improved with new countries such as the USA and extra parameters such as drilling technology, borehole design or total project cost. For the HSA to optimise learning opportunities from previous project successes and failures, we recommend that nations/organisations follow the example of France and the Netherlands, plus Australia and Germany to a lesser extent (state-dependent regulations) which have set the standard for governmental policies, data reporting and have thriving HSA industries as a result.

Author Contributions

MB: Writing – Original Draft, Writing – Review & Editing, Conceptualization, Methodology, Validation, Investigation, Data Curation, Visualization. **NMB:** Writing – Review & Editing, Conceptualization, Methodology, Supervision, Project Administration, Funding Acquisition. **ZKS:** Review & Editing, Conceptualization, Methodology, Supervision. **CJLW:** Writing – Review & Editing, Conceptualization,

Resources. MP: Writing – Review & Editing, Resources. **CB:** Writing – Review & Editing, Resources.

Competing Interests

The authors declare that they have no conflict of interest.

Acknowledgements

This work is funded by an International Strategic Partner (ISP) Research Studentship for 2021/2024. The Authors would also like to thank Virginie Hamm from BRGM for providing access to the entirety of the SYBASE database and Eric Tenthorey (Geoscience Australia) for his help with Australian geothermal data and contacts.

References

Abesser, C., Gonzalez Quiros, A., & Boddy, J. (2023). *The case for deep geothermal energy-unlocking investment at scale in the UK: a deep geothermal energy white paper: detailed report*.

Acksel, D., Amann, F., Bremer, J., Bruhn, D., Budt, M., Bussmann, G., Görke, J.-U., Grün, G., Hahn, F., Hanßke, A., Kohl, T., Kolditz, O., Regenspurg, S., Reinsch, T., Rink, K., Sass, I., Schill, E., Schneider, C., Shao, H., … Will, H. (2022). *Roadmap for Deep Geothermal Energy for Germany: Recommended Actions for Policymakers, Industry and Science for a Successful Heat Transition*. file:///C:/Users/maell/Downloads/Roadmap%20Deep%20Geothermal%20Energy%20for%20Germany%20FhG%20HGF%2010102022.pdf

ADEME. (n.d.). *Funding*. Retrieved April 12, 2024, from https://www.ademe.fr/en/our-missions/funding/

ADEME. (2012). *French know-how in the field of geothermal energy*. https://geodeep.fr/wp-content/uploads/2020/05/ADEME_French_Know-how-Geothermal-Energy.pdf

AFPG. (2023). *La géothermie en France - Étude de filière 2023*. https://www.afpg.asso.fr/lafpg-publie-ledition-2023-de-letude-de-filiere-geothermie-la-geothermie-en-france/

AZU. (2013). https://azu.hr/en-us/data-room/.

Ballesteros, M., Pujol, M., Walsh, F., & Teubner, J. (2019). Geothermal Energy Electricity Generation in Australia: Recent Developments and Future Potential. *Australian Geothermal Energy Association*.

Banks, D. (2012). An introduction to thermogeology: Ground source heating and cooling: Second edition. In *An Introduction to Thermogeology: Ground Source Heating and Cooling: Second Edition*. https://doi.org/10.1002/9781118447512

Barnett, P. (2009). Large scale hot sedimentary aquifer (HSA) geothermal projects. *Presentation to Victoria Energy Conference*. https://hotcopper.com.au/data/oldanns/2009/HRL/30fcbb08-c66c-4db4-807b-f1c497b865a0-HRL213165.pdf

Berg Badstue Pedersen, M. (2020). Sønderborgs geotermianlæg ude af drift i to år: Her er synderen. *Energy Supply*. https://www.energysupply.dk/article/view/741788/sonderborgs_geotermianlaeg_ude_af_drift_i_to_ar_her_er_syndere

Biernat, H. (1993). Geothermal waters utilization in the Pyrzyce power plant. *Technika Poszukiwań Geologicznych, Geosynoptyka i Geotermia*.

Boissavy, C., & Laplaige, P. (2018). The successful geothermal risk mitigation system in France from 1980 to 2015. *Transactions - Geothermal Resources Council*, *42*.

Boissavy, C., Schmidlé-Bloch, V., Pomart, A., & Lahlou, R. (2020). France country update. *Proceedings World Geothermal Congress*, 1.

Breede, K., Dzebisashvili, K., & Falcone, G. (2015). Overcoming challenges in the classification of deep geothermal potential. In *Geothermal Energy Science* (Vol. 3, Issue 1). https://doi.org/10.5194/gtes-3-19-2015

Brémaud, M., Burnside, N. M., Shipton, Z. K., & Willems, C. J. L. (2023, April). De-risking database for hot sedimentary aquifers. *World Geothermal Congress 2023*.

Bruckner, T., Bashmakov, I. A., Mulugetta, Y., Chum, H., De la Vega Navarro, A., Edmonds, J., Faaij, A., Fungtammasan, B., Garg, A., & Hertwich, E. (2014). Energy systems Climate Change 2014: Mitigation of Climate Change. Contribution of Working Group III to the Fifth Assessment Report of the Intergovernmental Panel on Climate Change ed OR Edenhofer et al. *Cambridge and New York: Cambridge University Press. Available at: Https://Www. Ipcc. Ch/Pdf/Assessment-Report/Ar5/Wg3/Ipcc_wg3_ar5_chapter7. Pdf*.

Bujakowski, W., Bielec, B., Miecznik, M., & Pająk, L. (2020). Reconstruction of geothermal boreholes in Poland. In *Geothermal Energy* (Vol. 8, Issue 1). https://doi.org/10.1186/s40517-020-00164-x

Burnside, N. M., Westaway, R., Banks, D., Zimmermann, G., Hofmann, H., & Boyce, A. J. (2019). Rapid water-rock interactions evidenced by hydrochemical evolution of flowback fluid during hydraulic stimulation of a deep geothermal borehole in granodiorite: Pohang, Korea. *Applied Geochemistry*, *111*. https://doi.org/10.1016/j.apgeochem.2019.104445

Busby, J. (2014). Geothermal energy in sedimentary basins in the UK. *Hydrogeology Journal*, *22*(1). https://doi.org/10.1007/s10040-013-1054-4

Carr-Cornish, S., & Romanach, L. (2014). Differences in public perceptions of geothermal energy technology in Australia. *Energies*, *7*(3). https://doi.org/10.3390/en7031555

Climate Investment Funds. (2014). *Accelerating Geothermal Development by Reducing Exploration Risks*. https://www.climateinvestmentfunds.org/sites/cif_enc/files/knowledge-documents/kn-ctf-accelerating_geothermal_development_by_reducing_exploration_risks_0.pdf

Comerford, A., Fraser-Harris, A., Johnson, G., & McDermott, C. I. (2018). Controls on geothermal heat recovery from a hot sedimentary aquifer in Guardbridge, Scotland: Field measurements, modelling and long term sustainability. *Geothermics*, *76*. https://doi.org/10.1016/j.geothermics.2018.07.004

Craig, W., & Gavin, K. (2018). *ICE Themes Geothermal Energy, Heat Exchange Systems and Energy Piles*. ICE Publishing.

Dawson, P., & Dawson, S. L. (2018). Sharing successes and hiding failures: 'reporting bias' in learning and teaching research. *Studies in Higher Education*, *43*(8). https://doi.org/10.1080/03075079.2016.1258052

Deinhardt, A., Dumas, P., Schmidle, V., Antoniadis, A., Boissavy, C., Bozkurt, C., Garabetian, T., Hamm, V., Karytsas, S., Kasztelewicz, A., Kepinska, B., Keramiotis, C., Kujbus, A., Leguenan, T., Link, K., Lupi, N., Mendrinos, D., Miecznik, M., Nador, A., … Yildirim, C. (2021). *Why de-risking is key to develop large geothermal projects? GEORISK Projet*. https://www.georisk-project.eu/wp-content/uploads/2021/07/Final-Report.pdf

DiPippo, R. (2016). Geothermal Power Generation: Developments and Innovation. In *Geothermal Power Generation: Developments and Innovation*. https://doi.org/10.1016/C2014-0-03384-9

Dufour, F. C., & Heederik, J. P. (2019). Early geothermal exploration in the Netherlands 1980–2000. *European Geothermal Congress*.

Edelstein, M. R., & Kleese, D. A. (1995). Cultural relativity of impact assessment: Native hawaiian opposition to geothermal energy development. *Society and Natural Resources*, *8*(1). https://doi.org/10.1080/08941929509380896

Edmondson, A. C. (2011). Strategies for learning from failure. *Harvard Business Review*, *89*(4), 48–55.

Edwards, B., Kraft, T., Cauzzi, C., Kästli, P., & Wiemer, S. (2015). Seismic monitoring and analysis of deep geothermal projects in st Gallen and Basel, Switzerland. *Geophysical Journal International*, *201*(2). https://doi.org/10.1093/gji/ggv059

Falcone, G., & Conti, P. (2019). Regional and country-level assessments of geothermal energy potential based on UNFC principles. *Proceedings*.

Gehringer, M., & Loksha, V. (2012). *Geothermal handbook: Planning and Financing Power Generation*. https://www.esmap.org/sites/esmap.org/files/DocumentLibrary/FINAL_Geothermal%20Handbook_TR002-12_Reduced.pdf

Gillespie, M. R., Crane, E. J., & Barron, H. F. (2013). Potential for deep geothermal energy in Scotland: study volume 2. In *British Geological Survey Geology and Landscape, Scotland Programme Commissioned Report Cr/12/131* (Vol. 2). https://www.gov.scot/publications/study-potential-deep-geothermal-energy-scotland-volume-2/documents/

Gründinger, W. (2017). The Renewable Energy Sources Act (EEG). In *Drivers of Energy Transition*. https://doi.org/10.1007/978-3-658-17691-4_6

Hamm, V., Maurel, C., Treil, J., & Hameau, S. (2019). *: Sybase project-Banking system and monitoring of low-energy geothermal operations in mainland France-Final report*.

Herzberger, P., Münch, W., Kölbel, T., Bruchmann, U., Schlagermann, P., Hötzl, H., Wolf, L., Rettenmaier, D., Steger, H., Zorn, R., Seibt, P., Möllmann, G.-U., Sauter,

M., Ghergut, J., & Ptak T. (2010). The Geothermal Power Plant Bruchsal. In *Proceedings World Geothermal Congress*.

Hoefner, M. L., Fogler, H. S., Stenius, P., & Sjoblom, J. (1987). ROLE OF ACID DIFFUSION IN MATRIX ACIDIZING OF CARBONATES. *JPT, Journal of Petroleum Technology*, *39*(2). https://doi.org/10.2118/13564-PA

Huddlestone-Holmes, C., & Hayward, J. (2011). *The potential of geothermal energy*.

IEA. (2019). *Renewables 2019: Analysis and Forecast to 2024*. https://www.iea.org/reports/renewables-2019

IEA. (2023). *Renewables share of total energy supply in the Net Zero Scenario, 2010-2030*. IEA. https://www.iea.org/data-and-statistics/charts/renewables-share-of-total-energy-supply-in-the-net-zero-scenario-2010-2030-2

IRENA. (2021). *Renewable Energy Power Generation Costs 2020*. www.irena.org/-/media/Files/IRENA/Agency/Publication/2021/Jun/IRENA_Power_Generation_Costs_2020.pdf

IRENA, & IGA. (2023). *Global geothermal market and technology assessment*. International Renewable Energy Agency and International Geothermal Association. https://mc-cd8320d4-36a1-40ac-83cc-3389-cdn-endpoint.azureedge.net/-/media/Files/IRENA/Agency/Publication/2023/Feb/IRENA_Global_geothermal_market_technology_assessment_2023.pdf?rev=37e6de031c98489f9bf17880cf9e8858

Kabeyi, M. J. B. (2019). Geothermal Electricity Generation, Challenges, Opportunities and Recommendations. *International Journal of Advances in Scientific Research and Engineering*, *5*(8). https://doi.org/10.31695/ijasre.2019.33408

King, R. L., Ford, A. J., Stanley, D. R., Kenley, P. R., & Cecil, M. K. (1987). *Geothermal resources of Victoria* (T. and R. Department of Industry & Victorian Solar Energy Council, Eds.). Victoria, Government Publ.

Kombrink, H., Ten Veen, J. H., & Geluk, M. C. (2012). Exploration in the Netherlands, 1987-2012. *Geologie En Mijnbouw/Netherlands Journal of Geosciences*, *91*(4). https://doi.org/10.1017/S0016774600000317

Krieger, M., Kurek, K. A., & Brommer, M. (2022). Global geothermal industry data collection: A systematic review. *Geothermics*, *104*. https://doi.org/10.1016/j.geothermics.2022.102457

Laplaige, P., Jaudin, F., Desplan, A., & Demange, J. (2000). The French Geothermal Experience Review and Perspectives. *World Geothermal Congress. Kyushu - Tohoku, Japan May 28-June 10, 2000*.

LIAG. (2023). *GeotIS.* www.geotis.de

Lopez, S., Hamm, V., Le Brun, M., Schaper, L., Boissier, F., Cotiche, C., & Giuglaris, E. (2010). 40 years of Dogger aquifer management in Ile-de-France, Paris Basin, France. *Geothermics*, *39*(4). https://doi.org/10.1016/j.geothermics.2010.09.005

McCay, A. T., Feliks, M. E. J., & Roberts, J. J. (2019). Life cycle assessment of the carbon intensity of deep geothermal heat systems: A case study from Scotland. *Science of the Total Environment*, *685*. https://doi.org/10.1016/j.scitotenv.2019.05.311

McDonald, R. I., Fargione, J., Kiesecker, J., Miller, W. M., & Powell, J. (2009). Energy Sprawl or Energy Efficiency: Climate Policy Impacts on Natural Habitat for the United States of America. *PLoS ONE*.

McLeod, H. O. (1984). MATRIX ACIDIZING. *JPT, Journal of Petroleum Technology*, *36*(13). https://doi.org/10.2118/13752-pa

Mijnlieff, H. F. (2020). Introduction to the geothermal play and reservoir geology of the Netherlands. In *Geologie en Mijnbouw/Netherlands Journal of Geosciences* (Vol. 99). https://doi.org/10.1017/njg.2020.2

Mijnlieff, H., Ramsak, P., Lako, P., Groen, B. in't, Smeets, J., & Veldkamp, H. (2013). Geothermal energy and support schemes in The Netherlands. *European Geothermal Congress 2013*.

Moeck, I. S. (2014). Catalog of geothermal play types based on geologic controls. In *Renewable and Sustainable Energy Reviews* (Vol. 37). https://doi.org/10.1016/j.rser.2014.05.032

Moher, D., Liberati, A., Tetzlaff, J., & Altman, D. G. (2010). Preferred reporting items for systematic reviews and meta-analyses: The PRISMA statement. *International Journal of Surgery*, *8*(5). https://doi.org/10.1016/j.ijsu.2010.02.007

Nguyen, H., Manolova, G., Daskalopoulou, C., Vitoratou, S., Prince, M., & Prina, A. M. (2019). Prevalence of multimorbidity in community settings: A systematic review and meta-analysis of observational studies. *Journal of Comorbidity*, *9*. https://doi.org/10.1177/2235042x19870934

OFGEM. (2016). *Ofgem's Future Insights Series, the Decarbonisation of Heat*. https://www.ofgem.gov.uk/sites/default/files/docs/2016/11/ofgem_future_insights_programme_-_the_decarbonisation_of_heat.pdf

O'Neal, D. (2022). Council launches legal action over $4m geothermal plant that's never delivered power. *ABC News*. from https://www.abc.net.au/news/2022-05-30/winton-council-legal-action-geothermal-plant failure/101093796

Popovsky, J. (2013). First Australian Geothermal Plant-Mulka Case Study. *Australian Geothermal Energy Conference*, *November*.

Proctor, K. (2014). *Giant 2km borehole project fails to bring hot water to Newcastle businesses*. ChronicleLive. https://www.chroniclelive.co.uk/news/north-east-news/giant-2km-borehole-project-fails-8189518

Pujol, M., Ricard, L. P., & Bolton, G. (2015). 20 years of exploitation of the Yarragadee aquifer in the Perth Basin of Western Australia for direct-use of geothermal heat. *Geothermics*, *57*. https://doi.org/10.1016/j.geothermics.2015.05.004

Richardson, I., & Neymeyer, A. (2013). *Deep geothermal review study: Final report*.

Richter, A. (2018). Equipment of Kalina geothermal power plant of Unterhaching to be sold. *Think GeoEnergy - Geothermal Energy News*. https://www.thinkgeoenergy.com/equipment-of-kalina-geothermalpower-plant-of-unterhaching-to-be-sold

Rutagarama, U. (2012). The role of well testing in geothermal resource assessment. *United Nations University*.

Schumacher, S., & Schulz, R. (2013). Effectiveness of acidizing geothermal wells in the south German molasse basin. *Geothermal Energy Science*, *1*(1). https://doi.org/10.5194/gtes-1-1-2013

SEPA. (2016). *SEPA's requirements for activities related to geothermal energy – Consultation*. https://www.sepa.org.uk/media/219431/sepa-s-requirements-for-activities-related-to-geothermal-energy-consultation-document.pdf

Stemmle, R., Lee, H., Blum, P., & Menberg, K. (2024). City-scale heating and cooling with aquifer thermal energy storage (ATES). *Geothermal Energy*, *12*(1). https://doi.org/10.1186/s40517-023-00279-x

Stuke, J. (2019). *Humboldt-Sprudel im Kurpark verstopft: 50 Meter langer Pfropfen ist schuld*.

https://www.nw.de/lokal/kreis_minden_luebbecke/bad_oeynhausen/22557993_50-Meter-langer-Pfropfen-hat-den-Humboldt-Sprudel-verstopft.html

Syed, M. (2015). *Black box thinking: why most people never learn from their mistakes -- but some do*.

Szalewska, M. (2021). Legal aspects of geothermal energy use in Poland. *Comparative Law Review*, *27*. https://doi.org/10.12775/CLR.2021.017

Tester, J. W., Anderson, B. J., Batchelor, A. S., Blackwell, D. D., & DiPippo, R. (2006). The Future of Geothermal Energy - Impact of Enhanced Geothermal Systems (EGS) on the United States in the 21st Century. *MIT - Massachusetts Institute of Technology*.

Tinti, F., Pangallo, A., Berneschi, M., Tosoni, D., Rajver, D., Pestotnik, S., Jovanović, D., Rudinica, T., Jelisić, S., Zlokapa, B., Raimondi, A., Tollari, F., Zamagni, A., Chiavetta, C., Collins, J., Chieco, M., Mercurio, A., Marcellini, F., Mrvaljević, D., & Meggiolaro, M. (2016). How to boost shallow geothermal energy exploitation in the adriatic area: The LEGEND project experience. *Energy Policy*, *92*. https://doi.org/10.1016/j.enpol.2016.01.041

TNO. (2023). *NLOG.* www.nlog.nl

Trutnevyte, E., & Wiemer, S. (2017). Tailor-made risk governance for induced seismicity of geothermal energy projects: An application to Switzerland. *Geothermics*, *65*. https://doi.org/10.1016/j.geothermics.2016.10.006

Tsagarakis, K. P., Efthymiou, L., Michopoulos, A., Mavragani, A., Anđelković, A. S., Antolini, F., Bacic, M., Bajare, D., Baralis, M., Bogusz, W., Burlon, S., Figueira, J., Genç, M. S., Javed, S., Jurelionis, A., Koca, K., Ryżyński, G., Urchueguia, J. F., & Žlender, B. (2020). A review of the legal framework in shallow geothermal energy in selected European countries: Need for guidelines. *Renewable Energy*, *147*. https://doi.org/10.1016/j.renene.2018.10.007

Ungemach, P., Antics, M., & Davaux, M. (2019). Subhorizontal well architecture and geosteering navigation enhance well performance and reservoir evaluation A field validation. *Proceedings, 44th Workshop on Geothermal Reservoir Engineering, Stanford University, Stanford, California*.

Ungemach, P., Antics, M., & Lalos, P. (2009). Sustainable geothermal reservoir management practice. *Transactions - Geothermal Resources Council*, *33*.

Westaway, R., & Burnside, N. M. (2019). Fault "corrosion" by fluid injection: A potential cause of the November 2017 MW 5.5 Korean Earthquake. *Geofluids*, *2019*. https://doi.org/10.1155/2019/1280721

Willems, C. J. L., Ejderyan, O., Westaway, R., & Burnside, N. M. (2020). Public perception of geothermal energy at the local level in the UK. *World Geothermal Congress 2020*.

Witter, J. B., Trainor-Guitton, W. J., & Siler, D. L. (2019). Uncertainty and risk evaluation during the exploration stage of geothermal development: A review. In *Geothermics* (Vol. 78). https://doi.org/10.1016/j.geothermics.2018.12.011

Worthington, P. F. (2010). Net pay-what is it? What does it do? How do we quantify it? How do we use it? *SPE Reservoir Evaluation and Engineering*, *13*(5). https://doi.org/10.2118/123561-PA

Xiao, Y., & Watson, M. (2019). Guidance on Conducting a Systematic Literature Review. In *Journal of Planning Education and Research* (Vol. 39, Issue 1). https://doi.org/10.1177/0739456X17723971

Younger, P. L., Manning, D. A. C., Millward, D., Busby, J. P., Jones, C. R. C., & Gluyas, J. G. (2016). Geothermal exploration in the Fell Sandstone Formation (Mississippian) beneath the city centre of Newcastle upon Tyne, UK: The Newcastle Science Central Deep Geothermal Borehole. *Quarterly Journal of*

Engineering Geology and Hydrogeology, *49*(4). https://doi.org/10.1144/qjegh2016-053

CHAPTER 4
Geological Setting

Chapter 3 highlighted the key role of geology in the success or failure of an HSA project. Amongst all recommendations is a thorough geological characterisation of a potential geothermal site before drilling to effectively reduce geological and reservoir risks. In this chapter, a case study of the Chester Formation in the Cheshire Basin (UK) is presented, providing geological context and evaluating the geothermal potential of this hot sedimentary aquifer. The sampling methods for collecting Chester Formation rocks will also be detailed.

4.1. Introduction

To date, the only geothermal project delivering heat for direct use in the UK is in Southampton. This project has been producing water at 76°C since 1988 with a current heat capacity of 2.2 MWth. The Southampton scheme targets the Triassic Sherwood Sandstone reservoir in the Wessex Basin (Busby, 2014) at a depth of c. 1.7km, which is one of the primary geothermal aquifers with a significant HSA potential in the UK. The Sherwood Sandstone Group (SSG) is primarily found in the Cheshire Basin and the Wessex Basin.

In this section, the geological context of the Cheshire Basin will be detailed and an evaluation of the geothermal potential of this hot sedimentary aquifer will be performed based on publicly available studies.

4.2. Geological Context of the Study Area

The Cheshire Basin is a complex NE-SW trending half-graben located in northwest England that was initiated during the Permian age (Fig. 4-1). The basin structure has been studied and described using geophysical tools such as seismic reflection

(Plant et al., 1999). The southeast margin of the basin is significantly faulted, and the cumulative throw goes up to 4 km, while its western margin is relatively unfaulted (Figs. 4-1, 4-2) (Chadwick, 1997; Busby, 2014). The burial history of the Cheshire basin has been examined by numerous authors, including Mikkelsen and Floodpage (1997), Evans et al. (1993), Plant et al. (1999), and Vincent and Merriman (2004). As one of the lowermost formations of the Sherwood Sandstone Group, the maximum burial depth of the Chester Formation is broadly comparable to that of the SSG as a whole. Depth of burial of the SSG exhibits significant variability across the basin, ranging from more than 5000 m in the deepest southeastern parts of the basin to approximately 1000 m at the basin margins.

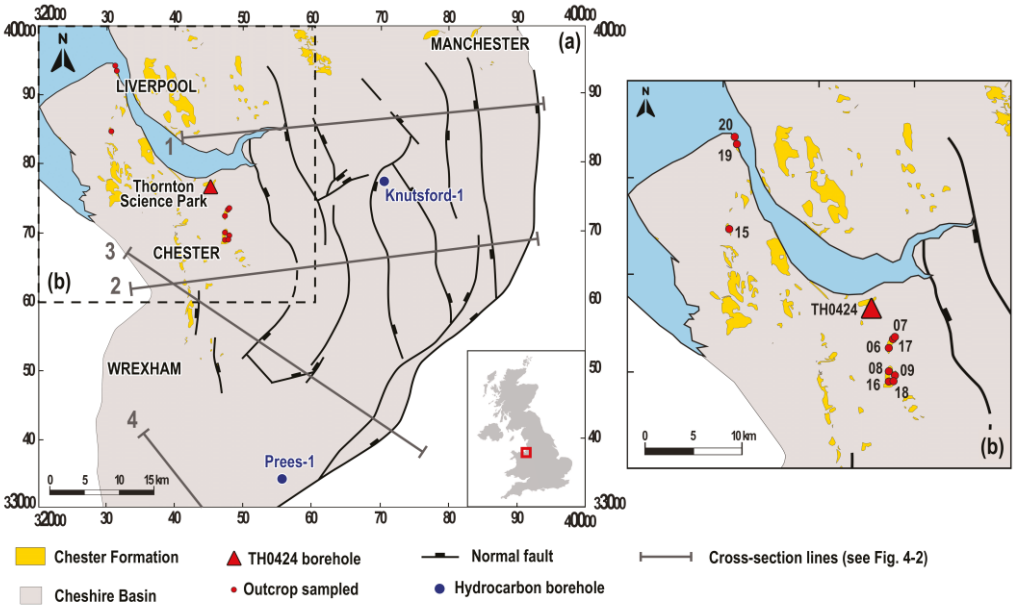

Figure 4-1: (a) Distribution of the Chester Formation in the Cheshire Basin and (b) zoom in the area of interest within the basin. Basin structure is reproduced from Mikkelsen and Floodpage (1997). Locations of the core and outcrop samples collected in this study are displayed by the red triangle and red circles respectively. Two hydrocarbon boreholes are shown in blue: Knutsford-1 and Prees-1.

Knutsford-1 and Prees-1 (Fig. 4-1) are deep hydrocarbon exploration boreholes drilled in the early 1970s to explore the potential of Permo-Triassic sandstone reservoirs (Evans et al., 1993). They reached depths of 3 km and 3.8 km respectively, but were both unsuccessful and were abandoned (Brown, 2023). In the Knutsford-1 borehole that was drilled in a relatively deep part of the Cheshire

Basin (Fig. 4-3), maximum burial depth of the SSG is estimated at about 4000 m (Figs. 4-3, 4-4).

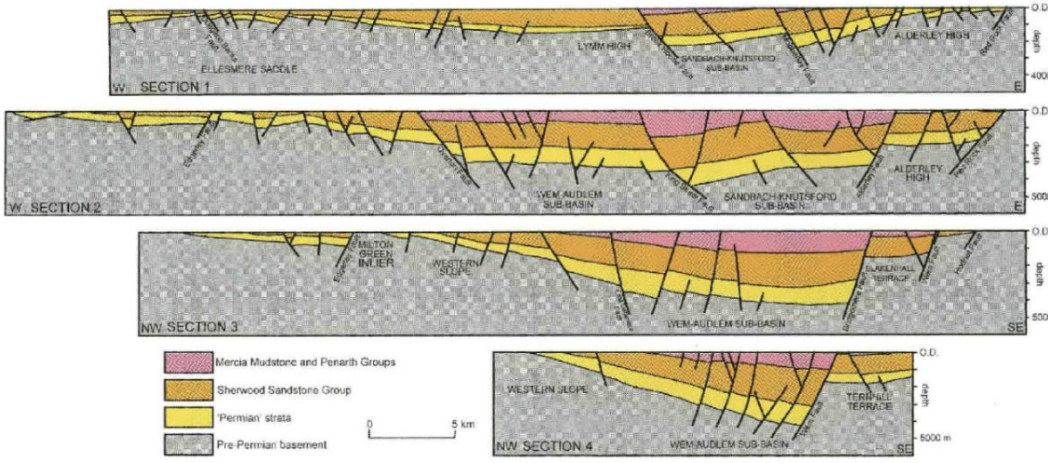

Figure 4-2: Cross sections through the Cheshire Basin highlighting the main structural features and faults within the basin (Plant et al., 1999). Line locations and orientations are shown in Fig. 4-1.

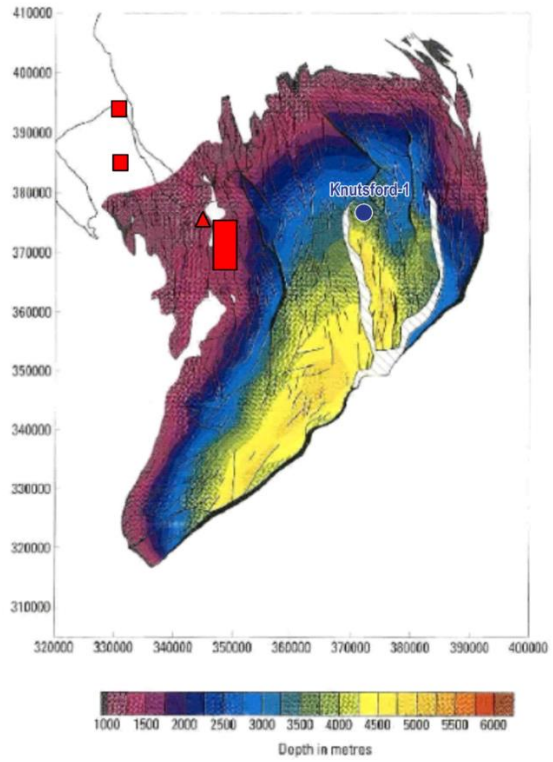

Figure 4-3: Structure-contour map restored to maximum burial depth at the base of the Sherwood Sandstone Group (after Plant et al., 1999). Red triangle shows the location of the

TH0424 borehole, and red squares and rectangle display the position of the outcrop exposures sampled. The map was generated by adding a gridded isopach map of eroded overburden, derived from compaction curve analysis and borehole density/sonic log data to present-day depth grids. These calculations, validated by contouring results and regional palaeotemperature studies, restored the basin's configuration at the time of maximum burial.

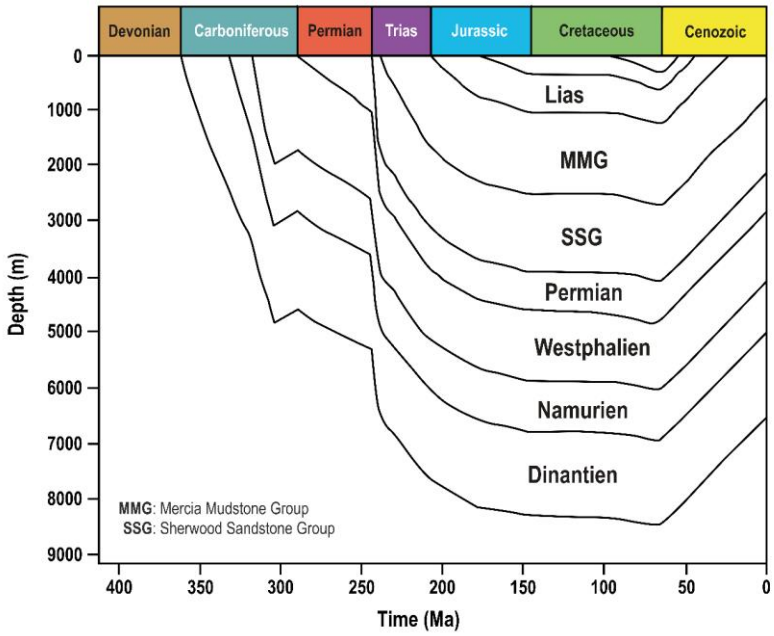

Figure 4-4: Burial history model of the Knutsford-1 borehole (after Mikkelsen and Floodpage, 1997)

Sedimentary infill is mainly composed of Permian (Collyhurst Sandstone) and Triassic (Sherwood Sandstone Group, SSG) successions and locally Early Jurassic strata. In Early Triassic times, the SSG was deposited as a large river system flowing northward from northern France to Britain (Warrington, 1970; Wills, 1970). In the Cheshire Basin, the SSG consists of four formations: the Kinnerton Sandstone Formation, the Chester Formation, the Wilmslow Sandstone Formation, and the Helsby Formation (Fig. 4-5) (Warrington et al., 1980). The Early-Triassic Chester Formation is composed of river-sourced pebbly sandstones that show a progressive change in lithology northwards (Mikkelsen and Floodpage, 1997; Ambrose et al., 2014). In the Cheshire Basin, the Chester Formation or Chester Pebble Beds (CPB) mostly consists of cross-bedded sandstones and conglomerates

interbedded with mudstone strata. Conglomerates with quartzite pebbles and a reddish-brown sandy matrix are usually found at the base of the formation, followed by interbedded sandstone and conglomerates in the middle, and sandstones and pebbly sandstones in the upper part (Ambrose et al., 2014). In addition to these coarser deposits, other lithofacies within the Chester Pebble Beds are fine- to medium-grained sandstones with cross-bedding or laminations, reflecting deposition under lower energy fluvial conditions (Jones and Ambrose, 1994; Benton et al., 2002; Ambrose et al., 2014).

Diagenetic regimes observed in the Cheshire Basin are categorised based on the framework established by Schmidt and McDonald (1979). The authors distinguish between *eodiagenesis* wherein diagenetic reactions are primarily influenced by near-surface conditions prior to burial; *mesodiagenesis*, where diagenetic reactions are primarily influenced by subsurface conditions during burial; and *telodiagenesis*, which encompasses diagenetic processes governed by near-surface conditions following uplift or basin inversion. While the paragenesis sequence of the Sherwood Sandstone Group across the UK has been extensively investigated (Burley, 1984; Rowe and Burley, 1997; Holmes et al., 1983; Knox et al., 1984; Schmid et al., 2004; Mckinley et al., 2013), relatively few studies have focused on the Cheshire Basin. Moreover, the Chester Formation has not been the primary focus of research within the Sherwood Sandstone Group.

Plant et al. (1999) conducted a comprehensive multi-disciplinary study of the Cheshire Basin, including a detailed paragenesis sequence of the SSG that is subdivided into eight sequences of events of mineralogical features. However, the complete set of events or characteristics associated with a diagenetic episode may not be observed in every sample, borehole, or location. The main characteristics of each diagenetic episodes are summarised in Fig. 4-6.

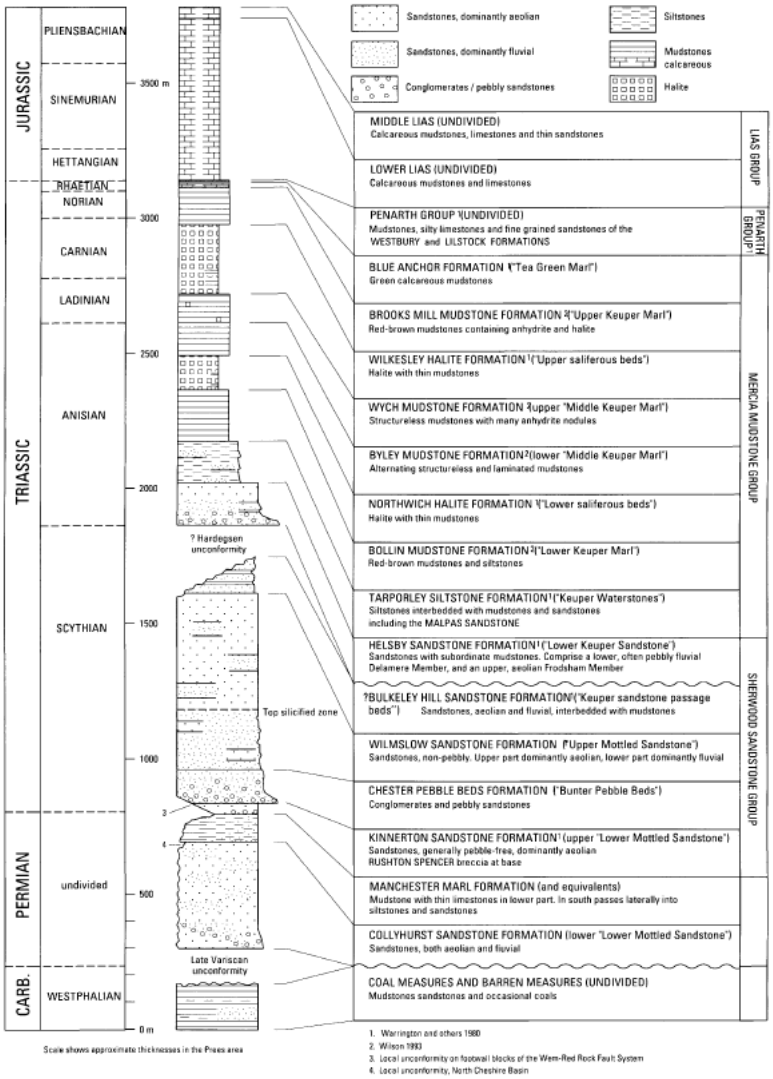

Figure 4-5: Lithostratigraphic column of the central Cheshire Basin (Evans et al., 1933)

Diagenetic episode		Principal characteristics	Stage
DE1	*a*	Shallow/near-surface red-bed diagenesis with development of infiltrated cutans, haematite grain coatings, anatase. Preceded compaction and closely associated with DE1b.	Eodiagenesis
	b	Micronodular non-ferroan dolomite and calcite cements (pedogenic dolocrete and calcrete). These are often interbanded or intercalated with DE1a, and are enclosed within later DE features. Expansive near-surface fabrics which preceded and are affected by later compaction effects.	Diachronous
DE2		Early diagenetic (limited burial) precipitation of pore-lining and grain-replacive smectite (now preserved only as illite, illite-smectite or corrensite) + minor K-feldspar and quartz overgrowths. Only very minor compaction effects prior to authigenesis.	Early Mesodiagenesis
DE3		Recrystallisation of early carbonate cements and precipitation of idiomorphic non-ferroan dolomite and calcite overgrowth cements. Precipitation of ferroan dolomite as late-stage overgrowths. Alteration of Ti-Fe minerals to anatase. Minor compaction effects prior to authigenesis.	Shallow burial
DE4		Precipitation of locally major quartz ± K-feldspar and albite overgrowths and cements. Minor pyrite authigenesis and alteration of Ti-Fe minerals to anatase, closely preceded the main quartz authigenesis. Possibly several generations of quartz and feldspar.	Middle Mesodiagenesis
DE5		Precipitation of major pore-filling evaporite cement (anhydrite ± possibly halite–anhydrite observed in deep basin area, inferred elsewhere). Possibly both prior to, and during, maximum burial compaction.	Moderate burial
DE6	*a*	Precipitation of non-ferroan dolomite, progressively becoming ferroan dolomite then ankerite in several stages, each separated by periods of carbonate corrosion. Cements and fracture mineralisation, postdating main compaction.	Late Mesodiagenesis Deep burial and tectonic fracturing
	b	Anhydrite cementation and fracture mineralisation.	
	c	Complex quartz overgrowth and colloidal silica (chalcedonic) cements and silification ± baryte ± carbonate ± minor/trace Cu-S, Ag-S, Ag-Se, Cu-Ag-Se, Co-Ni-As-S, molybdenite, cobaltite, cinnabar, sphalerite, pyrite and galena mineralisation restricted to fault rocks and adjacent wall-rocks. Accompanied by dissolution of evaporite cement in adjacent wall-rocks.	
	d	Major Cu-Fe-S mineralisation (chalcopyrite, pyrite and other Cu-Fe sulphides) ± minor Ag-S, Hg-S, Bi-S in fractures and associated wall-rocks ± minor quartz, chalcedony, baryte.	
	e	Complex precipitation of major weakly ferroan calcite ± baryte as major cements closely associated with fracture mineralisation.	
	f	Galena-baryte fracture mineralisation.	
DE7		Dissolution of evaporite cements, and some dissolution of feldspar grains. Precipitation of minor fibrous illite in rejuvenated porosity. Migration of liquid hydrocarbons.	
DE8		Telodiagenetic alteration in recent and present-day near-surface groundwater regime at basin margins: late-stage oxidative dissolution of carbonate cements; oxidation of sulphide mineralisation and associated precipitation of secondary iron and manganese oxyhydroxide alteration products; detrital feldspar dissolution and kaolinite authigenesis. Oxidative (supergene) alteration of major Cu-Pb mineralisation areas produced a very complex assemblage of secondary alteration products dominated by Fe and Mn oxyhydroxides, malachite, azurite, chrysocolla, dioptase, amorphous hydrated Cu-Al silicate gel, mimetite, pyromorphite, plumbogummite, cerrusite, hydrocerrusite and smithsonite.	Telodiagenesis Tertiary to present uplift

Major fault-related mineralisation around basin margins (Alderley, Clive, Bickerton Hills etc.)

Figure 4-6: Summary of the principal characteristics of each Diagenetic Episode in the SSG of the Cheshire Basin (Plant et al., 1999)

4.3. Geothermal Potential

Sherwood sandstone strata are found in many places in Wales, England and southwest Scotland and constitute a major target for geothermal development in the UK as they host aquifers at depths of ≤ 3 km which contain groundwater at up to 80°C (Hirst, 2017). Regional modelling of the Cheshire basin has estimated the geothermal resource to range between 44.1 and 75×10^{18} J (Downing and Gray, 1986; Rollin et al., 1995; Jackson, 2012), representing approximately 23% of the

UK's available Hot Sedimentary Aquifers (HSAs) resource (Brown, 2020). However, a recent study by Brown (2023) showed a new estimation of the resource to be between 91 and 144x10^{18} J by using a geothermal gradient of 27°C/km in the basin (against 20°C/km for the former estimate).

In the late 1970s, the Cheshire Basin became of great interest regarding its hydrocarbon potential (Mikkelsen and Floodpage, 1997), though not many boreholes have been drilled within the basin. Knutsford-1 and Prees-1 encountered the Chester Formation (Colter and Barr, 1975; Colter, 1978; Penn, 1987; Evans et al., 1993) at 1.87 km and 2.73 km respectively, with a thickness of ca. 170 m. Porosity and hydraulic conductivity data of the Chester Fm. compiled from several literature sources (Allen et al., 1997; Plant et al., 1999; Downing and Gray, 1986) show a wide range of values from various data: outcrops, well-logs, or rock cores. Despite these geological investigations, little information is available regarding the general petrophysical (e.g., porosity, permeability, mineralogy) or specific thermal (e.g., conductivity, diffusivity) reservoir properties of this formation, which control subsurface heat flow and are key for the geothermal system performance.

4.4. Rock sampling

Rock borehole cores and outcrop samples of the Chester Formation were collected within the Cheshire Basin to (1) gain information on the geothermal potential of the geological formation by determining its petrophysical and thermal properties, and to (2) assess the usefulness of rock outcrops as surface analogues for their deep counterparts. If the thermal properties of outcrop and core samples prove to be similar, then key geothermal data could be collected relatively easily and at very little cost, providing vital information to de-risk capital investment decisions for the development of geothermal projects.

Using the BGS geological maps and the Street View option in Google Maps, outcrops of the Chester Formation were located, and 17 samples were collected

(Fig. 4-1). These outcrops exhibited diverse degrees of preservation due to differential varying weathering conditions, nature of the outcrop (natural vs engineered; inland vs coastal) conditions, facies characteristics, stratification features, degrees of induration, and fracturing patterns. Six lithotypes were sampled: sand-dominated (massive) horizons, laminated horizons, cross-bedded horizons, pebble-rich horizons, and one mud-dominated horizon. In addition, a single pebble from a pebble-rich horizon was also examined. The samples display a considerable variability in many aspects: grain shape (rounded to angular), size (clay to medium-coarse sand), and sorting (very well sorted to moderately sorted), sedimentary features (cross-bedding, mud clasts, or soft-sediment deformation), and proportion of pebbles. Pebble-rich samples generally exhibited medium to coarse grain sizes with pebbles with a long axis up to 10cm, while the sandy samples were characterised by fine to fine-medium grain sizes.

Rock cores collected for this study were obtained from the TH0424 borehole that was drilled to a total depth of 100 m in November 2021 (Fig. 4-1). The borehole is one of many open bedrock boreholes for geophysical and hydrogeological investigations on the UKGEOS Cheshire site at the Thornton Science Park. The main exploration target of the borehole was the Triassic Sherwood Sandstone and especially the Chester Formation located near the surface in this area. A selection of interest zones in the borehole core was made following the features of the outcrop samples already collected. A total of 21 samples were sub-cored from the original borehole core, at depths from 22.8 to 96.6 meters below ground level (mbgl). Detailed descriptions and pictures of the samples are provided in Appendix 6.

All collected samples originate from the same main fault block (Fig. 4-1) and are located in relatively close proximity to one another. Their location in the northwestern portion of the Cheshire Basin –its shallowest section– suggests that these samples are likely to have undergone less burial than those from the Knutsford-1 borehole (Fig. 4-3). Based on previous studies (Plant et al., 1999), it is estimated that the burial depth of the SSG did not exceed 1750 m at this location.

Most outcrop samples are located slightly further to the southeast compared to core samples and therefore may have experienced slightly greater burial depths due to their position within the basin.

The sampling strategy aimed to capture the lithological and textural heterogeneity of the Chester Formation, ensuring that both outcrop and borehole samples represented the range of depositional and diagenetic features observed in this unit mentioned in section 4.2. Outcrop locations were selected to maximise variability in exposure type, weathering state, and structural integrity. Within each location, samples were chosen based on the lithofacies identified in the literature: sand-dominated (massive) horizons, laminated horizons, cross-bedded horizons, pebble-rich horizons, and one mud-dominated horizon. In addition, a single pebble from a pebble-rich horizon was also examined. This approach was designed to capture the full range of lithofacies present and to account for the heterogeneity of the Chester Formation within the Cheshire Basin.

For borehole core sampling, intervals were selected to match, as closely as possible, the range of lithofacies identified in the outcrop samples, including laminated, cross-bedded, sand-dominated, and pebble-rich horizons. This facilitated a comparative analysis between surface and subsurface materials across equivalent lithotypes. Although there is inherent risk of sampling bias in any targeted selection, the strategy employed here aimed to minimise this by covering a wide range of lithological features. By prioritising representativeness, this sampling strategy enhances the validity of any conclusions drawn about the comparability of outcrop and core samples.

Overall, the approach balances practicality with scientific rigour, striving to eliminate bias where possible while explicitly acknowledging and accounting for natural heterogeneity in the formation. This careful strategy supports the wider objective of evaluating outcrop analogues as a tool for geothermal resource assessment prior to the cost-intensive process of drilling.

4.5. Conclusion

Chapter 4 established the geological context of the Chester Formation (Sherwood Sandstone Group) within the Cheshire Basin and evaluated its geothermal potential. The depositional environment, burial history, and structural setting of the Chester Formation were reviewed. Representative rock samples from both outcrops and a shallow borehole (UKGEOS Cheshire) were collected from the same fault block for further analysis. These samples support the assessment of the suitability of the Chester Formation as an HSA reservoir and test whether surface outcrops can serve as reliable analogues for reservoir conditions at depth.

4.6. References

Allen, D. J., Brewerton, L. J., Coleby, L. M., Gibbs, B. R., Lewis, M. A., MacDonald, A. M., Wagstaff, S. J., & Williams, A. T. (1997). The physical properties of major aquifers in England and Wales. *British Geological Survey*, *Technical*.

Ambrose, K., Hough, E., Smith, N. J. P., & Warrington, G. (2014). Lithostratigraphy of the Sherwood Sandstone Group of England, Wales and south-west Scotland. British Geological Survey Research Report RR/14/01.

Benton, M., Cook, E., & Turner, P. (2002). Permian and Triassic red beds and the Penarth Group of Great Britain. Geological Conservation Review Series, 24.

Brown, C. S. (2020). Modelling, characterisation and optimisation of deep geothermal energy in the Cheshire basin (Doctoral dissertation, University of Birmingham).

Brown, C. S. (2023). Revisiting the Deep Geothermal Potential of the Cheshire Basin, UK. In Energies (Vol. 16, Issue 3). https://doi.org/10.3390/en16031410

Burley, S. D. (1984). Patterns of diagenesis in the Sherwood Sandstone Group (Triassic), United Kingdom. Clay Minerals, 19(3). https://doi.org/10.1180/claymin.1984.019.3.11

Busby, J. (2014). Geothermal energy in sedimentary basins in the UK. Hydrogeology Journal, 22(1). https://doi.org/10.1007/s10040-013-1054-4

Chadwick, R. A. (1997). Fault analysis of the Cheshire Basin, NW England. Geological Society Special Publication, 124. https://doi.org/10.1144/GSL.SP.1997.124.01.18

Colter, V. S. (1978). Exploration For Gas in the Irish Sea. Geol Mijnbouw, 57(4).

Colter, V. S., & Barr, K. W. (1975). Recent Developments in the Geology of the Irish Sea and Cheshire Basins. Geol, 1.

Downing, R. A., & Gray, D. A. (1986). Geothermal resources of the United Kingdom. Journal of the Geological Society, 143(3). https://doi.org/10.1144/gsjgs.143.3.0499

Evans, D. J., Rees, J. G., & Holloway, S. (1993). The Permian to Jurassic stratigraphy and structural evolution of the central Cheshire Basin. Journal - Geological Society (London), 150(5). https://doi.org/10.1144/gsjgs.150.5.0857

Hirst, C. M. (2017). The Geothermal Potential of Low Enthalpy Deep Sedimentary Basins in the UK. http://etheses.dur.ac.uk/11979/

Holmes, I., Chambers, A. D., Ixer, R. A., Turner, P., & Vaughan, D. J. (1983). Diagenetic processes and the mineralization in the triassic of Central England. Mineralium Deposita, 18(2 Supplement). https://doi.org/10.1007/BF00206485

Jackson, T. (2012). Geothermal potential in great Britain and northern Ireland. Sinclair Knight Merz: Sydney, NSW, Australia.

Jones, N. S., & Ambrose, K. (1994). Triassic sandy braidplain and aeolian sedimentation in the Sherwood Sandstone Group of the Sellafield area, west Cumbria. Proceedings of the Yorkshire Geological Society, 50(1), 61-76.

Knox, R. W. O., Burgess, W. G., Wilson, K. S., & Bath, A. H. (1984). Diagenetic influences on reservoir properties of the Sherwood Sandstone (Triassic) in the

Marchwood geothermal borehole, Southampton, UK. Clay Minerals, 19(3). https://doi.org/10.1180/claymin.1984.019.3.12

Mckinley, J. M., Ruffell, A. H., & Worden, R. H. (2013). An Integrated Stratigraphic, Petrophysical, Geochemical and Geostatistical Approach to the Understanding of Burial Diagenesis: Triassic Sherwood Sandstone Group, South Yorkshire, UK. In Linking Diagenesis to Sequence Stratigraphy. https://doi.org/10.1002/9781118485347.ch10

Mikkelsen, P. W., & Floodpage, J. B. (1997). The hydrocarbon potential of the Cheshire Basin. Geological Society Special Publication, 124. https://doi.org/10.1144/GSL.SP.1997.124.01.10

Penn, I. E. (1987). Geophysical logs in the stratigraphy of Wales and adjacent offshore and onshore areas. Proceedings of the Geologists' Association, 98(4). https://doi.org/10.1016/S0016-7878(87)80072-X

Plant, J. A., Jones, D. G., & Haslam, H. W. (1999). The Cheshire Basin: basin evolution, fluid movement and mineral resources in a Permo-Triassic rift setting. British Geological Survey.

Rollin, K. E., Kirby, G. A., & Rowley, W. J. (1995). Atlas of geothermal resources in Europe: UK revision. British Geological Survey, Regional Geophysics Group.

Rowe, J., & Burley, S. D. (1997). Faulting and porosity modification in the Sherwood Sandstone at Alderley Edge, northeastern Cheshire: An exhumed example of fault-related diagenesis. Geological Society Special Publication, 124. https://doi.org/10.1144/GSL.SP.1997.124.01.20

Schmid, S., Worden, R. H., & Fisher, Q. J. (2004). Diagenesis and reservoir quality of the Sherwood Sandstone (Triassic), Corrib Field, Slyne Basin, west of Ireland. Marine and Petroleum Geology, 21(3). https://doi.org/10.1016/j.marpetgeo.2003.11.015

Schmidt, V., & McDonald, D. A. (1979). The role of secondary porosity in the course of sandstone diagenesis.

Vincent, C. J., & Merriman, R. J. (2004). Thermal modelling of the Cheshire Basin using BasinModTM.

Warrington, G. (1970). The stratigraphy and palaeontology of the “Keuper” Series of the central Midlands of England. In Quarterly Journal of the Geological Society of London (Vol. 126, Issues 1–4). https://doi.org/10.1144/gsjgs.126.1.0183

Warrington, G., MG, A. C., RE, E., WB, E., HC, I. C., & PE, K. (1980). A correlation of Triassic rocks in the British Isles.

Wills, L. J. (1970). The Triassic succession in the central Midlands in its regional setting. In Quarterly Journal of the Geological Society of London (Vol. 126, Issues 1–4). https://doi.org/10.1144/gsjgs.126.1.0225

CHAPTER 5
Experimental Methods

5.1. Introduction

This chapter addresses the materials and methods used to analyse the Chester Formation rock cores and outcrop samples described in Chapter 4. In order to gain a complete understanding of the reservoir behaviour and characteristics, samples were examined for mineralogy, petrophysical and thermal properties using a range of techniques. The mineralogical composition of the samples was assessed using two methods: X-ray diffraction, and optical microscopy. The petrophysical properties of the samples were quantified by Water Immersion Porosimetry (WIP), image analysis (porosity) and an air permeameter. Thermal diffusivity and

conductivity measurements are taken on dry and water-saturated samples at both ambient laboratory and increased reservoir temperature conditions. Two thermal measurement techniques were used: the thermal conductivity scanner and the transient plane source method.

5.2. Mineralogy

5.2.1. X-Ray Diffraction

Identification and quantification of the mineralogical species composing the rock samples has been assessed through X-Ray Diffraction (XRD) analyses. X-Ray Diffraction (XRD) is an analytical technique that provides advanced information on the chemical composition and crystallographic structure of rock samples. Crystalline structures exhibit a systematic and periodic arrangement of atoms in a three-dimensional lattice. Within these structures, atoms are regularly spaced, resulting in distinct planes of atoms separated by consistent interplanar distances. These interplanar spacings are characteristic of specific crystalline species (Buerger, 1942; Klug and Alexander, 1954; Cullity, 1956).

The sample is crushed, then X-rays are generated by a cathode ray tube and directed towards the powder. When conditions meet Bragg's Law (Eq. (5-1)) the incident rays interact with the sample to produce constructive interference (and a diffracted ray).

$$2d\ \sin\theta = n * \lambda \qquad (5\text{-}1)$$

Bragg's Law relates the lattice spacing in a crystalline sample d and the angle of the diffracted beam θ to the order of diffraction n and the wavelength of the electromagnetic radiation λ (Fig. 5-1). Next, these diffracted X-rays are detected, examined, and tallied. Because the powdered material has a random orientation, all possible diffraction directions of the lattice are obtained by scanning the sample through a range of 2θ angles. The conversion of the diffraction peaks to interplanar

spacings enables mineral identification, by comparing these spaces with industry-standard reference patterns. (Fig. 5-2).

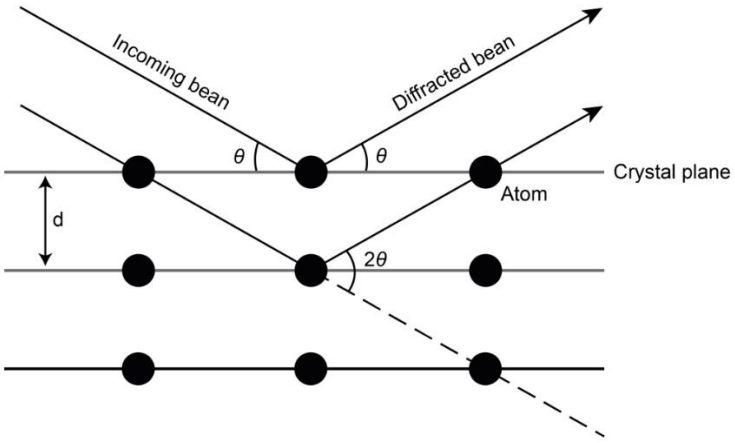

Figure 5-1: Scheme of electrons diffraction from Bragg's Law

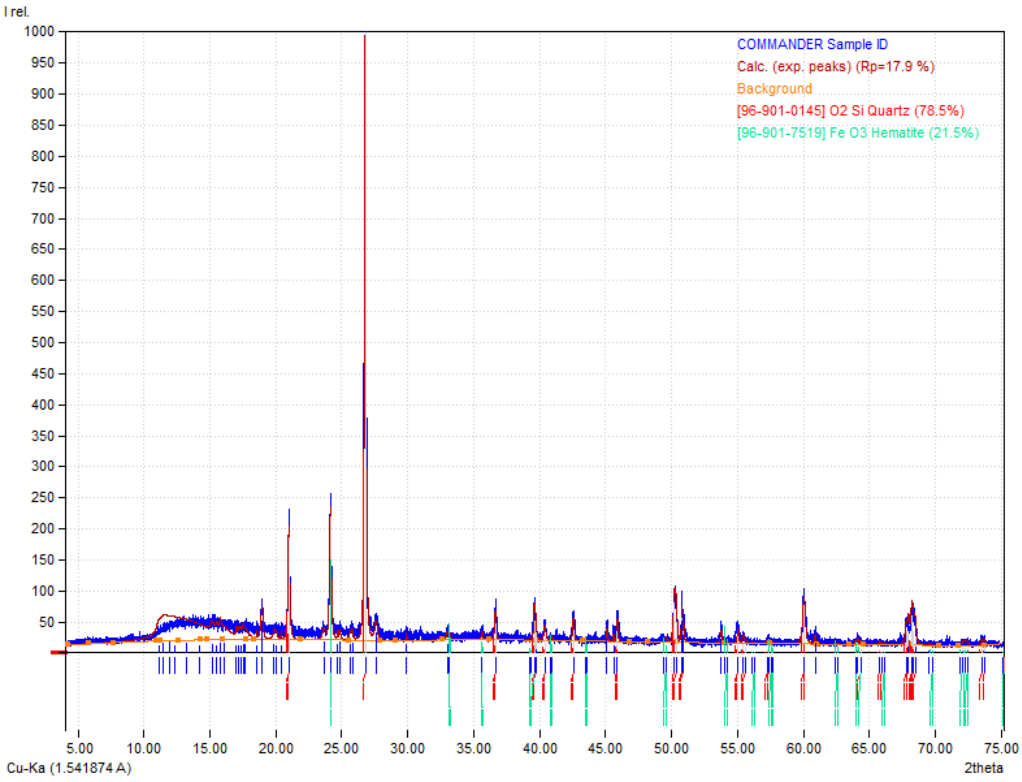

Figure 5-2: Example of an X-ray diffraction spectrum

5.2.2. Optical Microscopy

Thin section descriptions were carried out using an optical microscope under plane-polarised and cross-polarised light. This technique was used to capture the mineral composition of the samples by counting points on high-resolution photomicrographs of thin sections. Thin sections were impregnated with a blue dye to facilitate porosity identification and stained to highlight carbonate minerals. The point counting process was carried out using JMicrovision software (Roduit, 2007) on an arbitrary grid (Fig. 5-3), and was stopped once two conditions were met: a minimum of 500 points had been counted, and (2) the class percentages stabilised as observed in the evolution plot. The standard deviation for point counting in a homogenous rock sample is calculated using Eq. (5-2) (Plas and Tobi, 1965):

$$\sigma = \sqrt{\frac{f(100-f)}{n}} \tag{5-2}$$

where f is the percentage of a class and n is the total number of points counted. According to Plas and Tobi (1965), the 68% confidence interval lies between f+σ and f-σ, the 95% confidence interval between f+2σ and f-2σ, and the 99.7% confidence interval between f+3σ and f-3σ.

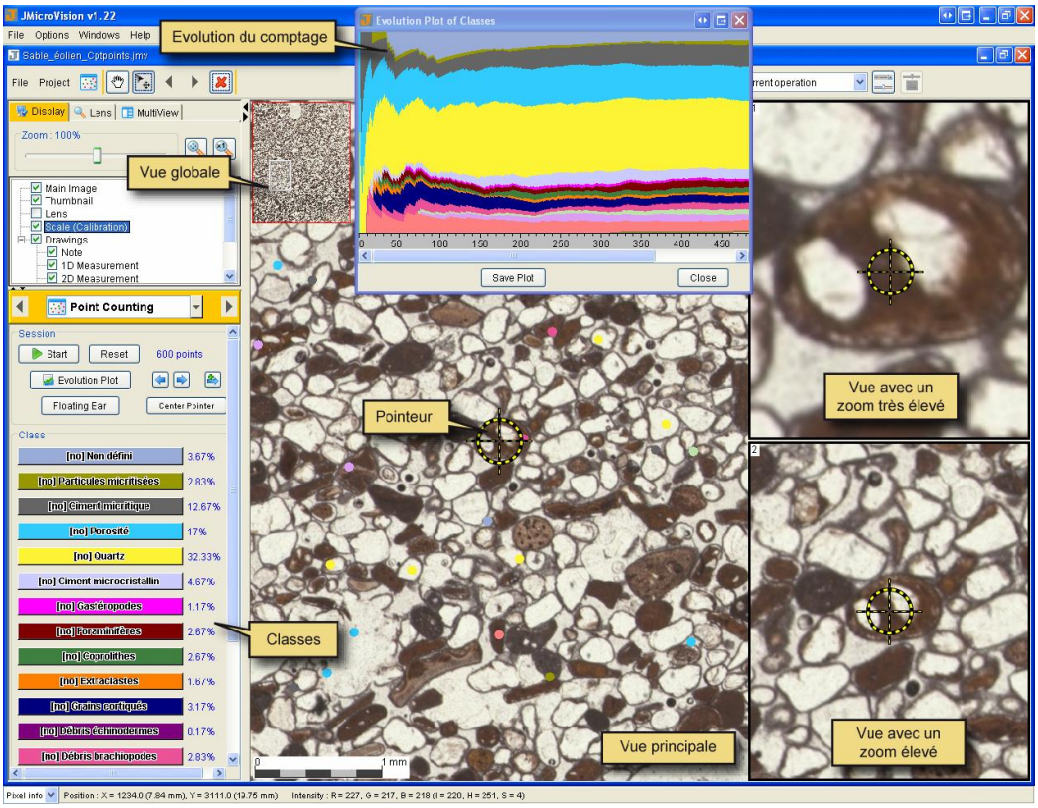

Figure 5-3: Example of point counting of an aeolian sand photomicrograph (Roduit, 2007)

5.3. Petrophysical Characterisation

5.3.1. Porosity

Porosity can be computed using various direct or indirect techniques. In this study, porosity was characterised using the Water Immersion Porosimetry (WIP) procedure. It has also been estimated from image analysis of photomicrographs.

5.3.1.1. Water Immersion Porosimetry

The Water Immersion Porosimetry (WIP) procedure requires that the samples must first be dried at 60°C in an oven for a minimum of 24h (Bloomfield et al., 1995) until their weight remains steady. Then the dry weight (m_{dry}) is measured. In a second step, the samples are saturated with water within a sealed vacuum desiccator for 48h (Fig. 5-4). Two weights are computed from each saturated sample: the saturated mass (m_{sat}) and the submerged mass (m_{hydro}). The saturated mass is measured by removing the sample from the water and weighing

it directly on a scale. The submerged mass is obtained by placing the sample in a mesh container fully submerged in water, which is suspended from the scale using a wire. During measurement of m_{hydro}, the sample must remain completely underwater.

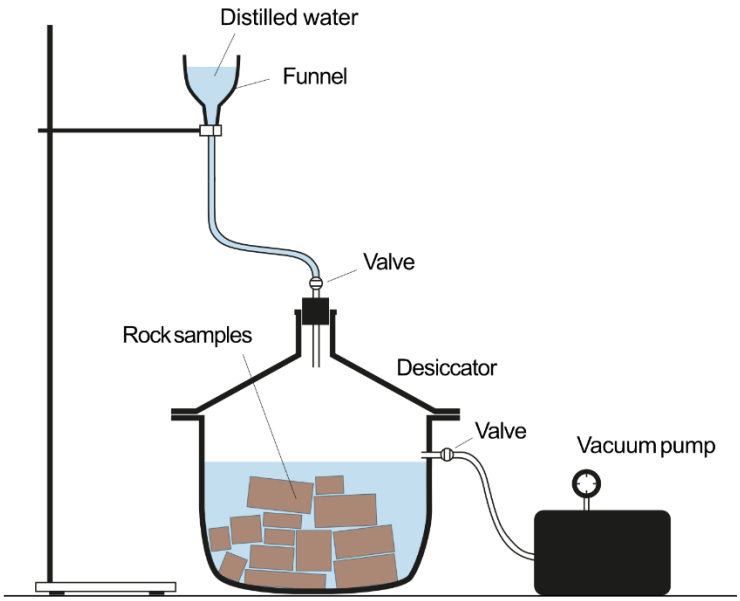

Figure 5-4: Scheme of the water saturation system using a desiccator

The pore volume (V_p) and sample volume (V_i) are then calculated from Eq. (5-3) and Eq. (5-4) respectively:

$$V_p = \frac{m_{sat} - m_{dry}}{\rho_{water}} \tag{5-3}$$

$$V_i = \frac{m_{sat} - m_{hydro}}{\rho_{water}} \tag{5-4}$$

Porosity is eventually determined using V_p and V_i as shown in Eq. (5-5):

$$\phi = \frac{V_p}{V_i} \cdot 100 \tag{5-5}$$

The uncertainty of the methods is estimated with <0.5 abs-%. A significant limitation of this method is the difficulty for the water to displace air from the smallest nanometre-sized pores (Anovitz and Cole, 2015). The molecular diameter of 2.9Å is considered as the lower limit for water accessibility. Water immersion porosimetry is measuring the effective porosity of a material (Bloomfield et al., 1995; A.P.I., 1998).

5.3.1.2. Thin Section Porosity

Porosity was computed through mineral point counting (see above). This approach captures total optical porosity (TOP), which usually corresponds to an approximation of total porosity (White et al., 1998, Grove et al., 2011). However, TOP tends to underestimate total porosity, as micropores and isolated pores are not easily detected (Halley, 1978).

5.3.2. Permeability

The permeability measurement method used is based on gas injection into the samples and therefore represents an apparent gas permeability.

The air permeameter apparatus measures the matrix permeability and the effective fracture apertures on rock samples. The NER's TinyPerm 3 is a portable handheld air permeameter that allows easy and quick measurements on core or outcrop samples. Like a syringe, air is sucked out from the device with a single stroke while pressing its rubber nozzle against the rock. The syringe volume and the transient vacuum pulse created at the sample surface are monitored and measurements are instantaneously stored and displayed on a mobile Android device supplied with the air permeameter (Fig. 5-5). Data provided include date, GPS coordinates, barometric pressure, temperature, humidity, sample pictures and permeability.

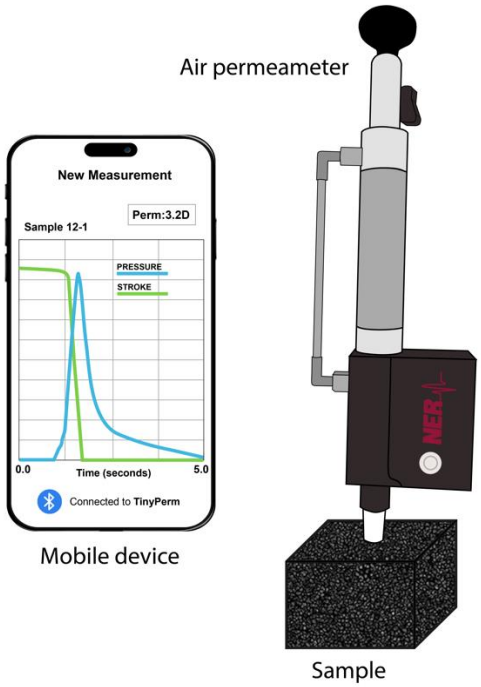

Figure 5-5: Scheme of the TinyPerm device and a measurement display

5.4. Thermal Analyses

5.4.1. Transient Optical Scanning

Thermal conductivity measurements using the TSCAN thermal conductivity scanner were performed on dry and saturated samples at ambient laboratory conditions. For the first series of measurements, the samples were dried in an oven at 60°C for a minimum of 24h, before conductivity was measured. Then, for measurements of conductivity of saturated samples, they were submerged in a water-filled, sealed vacuum desiccator for 48h (Fig. 5-4).

The Thermal Conductivity Scanner (TCS) uses the optical scanning technology developed by Yuri Popov in the 1980s (Popov et al., 1999). Each sample must be painted in black along the scanning line chosen to ensure a complete absorption of infrared heating. The sample is then placed between two standards of known thermal conductivity (also painted in black) on the scanning platform, and all

samples are scanned by a concentrated mobile heat source. The movable device includes a “cold” infrared sensor that measures the initial temperature, the heat source, and a “hot” infrared sensor with two channels: one measures the maximum temperature inline, and the other measures the temperature some millimetres beside the scanning line (Fig. 5-6). The scanner unit moves at a constant speed behind the samples, calculates the maximum temperature rise (θ) and continuously generates a conductivity profile. The maximum temperature rise (θ) is described by Eq. (5-6):

$$\theta = \frac{Q}{2\pi \cdot x \cdot \lambda} \tag{5-6}$$

where Q is the heat source power, x is the distance between the heat source and the sensors, and λ the thermal conductivity.

The thermal conductivity of the sample (λ_i) is then calculated from Eq. (5-7):

$$\lambda_i = \lambda_R \left(\frac{\theta_R}{\theta}\right) \tag{5-7}$$

where λ_R and θ_R are the thermal conductivity and the maximum temperature rise of a reference standard respectively.

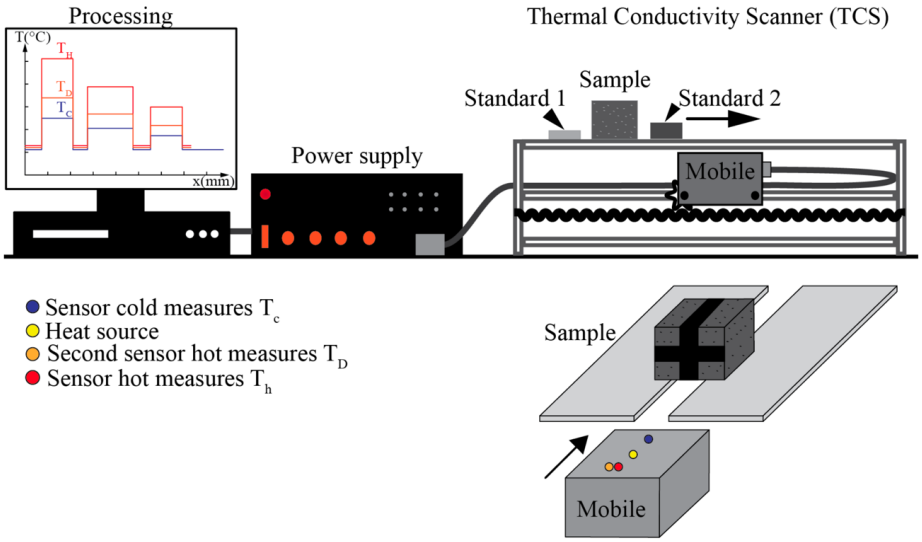

Figure 5-6: Scheme of the optical scanning apparatus (Navelot, 2018)

The accuracy of the device is given with 3% (for a confidential probability of 0.95) for thermal conductivity and 5% for thermal diffusivity.

5.4.2. Transient Plane Source Method

Thermal analysis with a Hot Disk device was carried out on dry and on saturated samples both under ambient laboratory and increased reservoir temperature conditions.

5.4.2.1. Measurements on unsaturated samples

The Hot Disk TPS 1500 and 2500 S are designed for precision analysis of thermal conductivity, thermal diffusivity, and specific heat capacity of many material types. The instrument follows the Transient Plane Source (TPS) method, also referred to as the Hot Disk method or the Gustafsson Probe, after Silas E. Gustafsson who invented this technique in 1986. The TPS method uses a transiently heated plane sensor with an electrically conducting circular double spiral etched out of a thin Nickel foil, that is used as both a resistance thermometer and a heat source. The disk is sandwiched between two thin sheets of an electrical insulator such as polyimide (Kapton), mica, aluminium nitride, or aluminium oxide, with different radii depending on the type of material analysed. It is recommended for the

diameter of the sample to be no less than twice that of the sensor, and the thickness of the sample to be no less than the radius of the sensor. During the measurements, the sensor is fitted between two pieces of identical samples to be tested, and an electric current is run through the spiral which raises both its temperature and resistance (Fig. 5-7). Thermal properties (thermal conductivity, thermal diffusivity and specific heat capacity) of the sample are then deduced by monitoring the resulting temperature increase (Zheng et al., 2020).

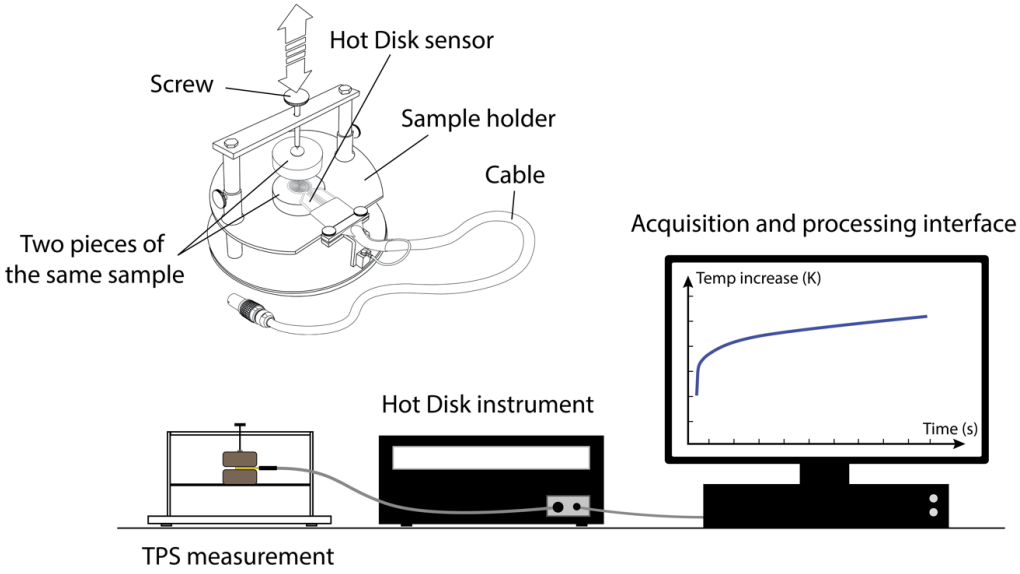

Figure 5-7 : Schematic of a Hot Disk measurement at ambient temperature

In this study, two Kapton Hot Disk Sensors have been used: 5501 F2 (radius: 6.4mm) for the largest samples, and 5465 F1 (radius: 3.2mm) for the thinnest and smallest ones. The thermal conductivity analyses on dry samples under increased reservoir (temperature) conditions required the use of a temperature control unit (TCU). The convection oven has a maximum chamber temperature of 600°C with a stability of ±0.5°C and is automatically controlled via the Hot Disk Desktop application. The analysed under in situ temperature conditions, at three temperature steps: 50°C, 70°C, and 90°C. Analyses on saturated samples under reservoir conditions will be described in the following section.

The Hot Disk device has an accuracy of ±5%, with measurement reproducibility within ±2%.

5.4.2.2. Measurements on water-saturated samples

Two innovative experimental setups were developed to analyse saturated samples under elevated temperatures using the transient plane-source method. Prior to thermal analysis, samples were submerged in a water-filled, sealed vacuum desiccator for 48h to ensure full saturation. Both setups incorporated:

- A heated bath with a temperature controller
- Vertical placement of the sensor to prevent submersion of the cable-sensor connection, positioned between two samples pieces
- Clamp(s) to secure the sample pieces together
- A manual control of temperature stability at four temperature steps: 30, 50, 70, and 90°C

The first setup (Experiment A) was designed at the GFZ Thermal Petrophysics Lab in Potsdam, Germany. A Polystat CC2 heated circulating bath was used, ensuring superior temperature homogeneity. The samples were held together with a single clamp (Fig. 5-8a).

The second experiment (Experiment B) was conducted in the CEE Laboratory at the University of Strathclyde and employed a JB Nova convection water bath. To minimise condensation water loss, the bath was covered with a lid, leaving a small gap to accommodate the sensor cable. An extended version of the 5501 sensor was employed with the cable-sensor connection positioned 10 cm above the water level to reduce risk of moisture ingress. The sample pieces were fastened around the sensor using two clamps (Fig. 5-8b).

The advantages and drawbacks of each set up are summarised in Table 5-1.

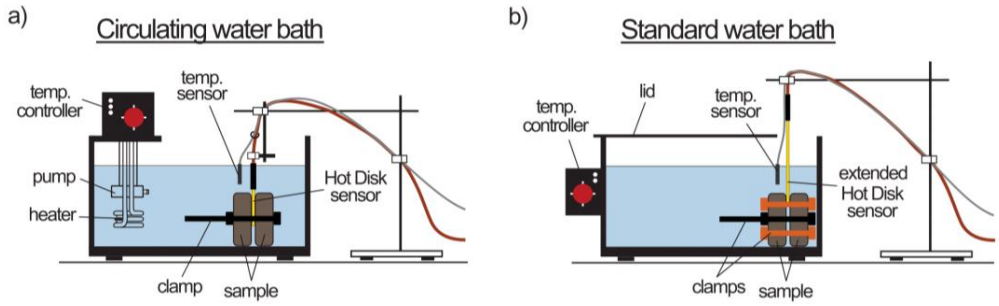

Figure 5-8: Comparison of the two experimental set ups designed to measure thermal conductivity under water-saturated conditions at different temperature steps. Temperature and Hot Disk sensor cables are connected to the Hot Disk instrument, as shown in Fig. 5-7 a) Experiment A: Circulating water bath with a pump and a heater. b) Experiment B: Standard (convection) water bath with a lid and an extended Hot Disk sensor.

Table 5-1: Advantages and disadvantages of each setup tested

	Advantages	Drawbacks
Experiment A	• Temperature homogeneity	• Instability of the setup • Heat loss • Unsuitable clamp • Water bubbles on the sensor surface
Experiment B	• Lid to reduce heat loss • No water flow • Setup stability • Suitable clamps	• Unstable temperature • Water bubbles on the sensor surface

5.5. Conclusion

This chapter presented the experimental methods used to characterise the mineralogical, petrophysical, and thermal properties of the Chester Formation sandstone samples. The techniques and instruments used are summarised in Table 5-2.

Table 5-2 : Summary of experimental methods and instruments used to characterise the Chester Formation samples

Property	Mineralogical composition	Porosity	Permeability	Thermal properties
Apparatus or technique	• X-ray diffraction • Optical microscopy by point counting	• Water immersion technique • Thin section porosity by point counting	TinyPerm 3 Air Permeameter	• TSCAN Thermal Conductivity Scanner • Hot Disk TPS 1500 • Hot Disk TPS 2500 S

5.6. References

Anovitz, L. M., & Cole, D. R. (2015). Characterization and analysis of porosity and pore structures. In Pore Scale Geochemical Processes. https://doi.org/10.2138/rmg.2015.80.04

A.P.I. (1998). Recommended practices for core analysis. API Recommended Practice, 40 ED. 2 REV.

Bloomfield, J. P., Brewerton, L. J., & Allen, D. J. (1995). Regional trends in matrix porosity and dry density of the Chalk of England. Quarterly Journal of Engineering Geology, 28(Suppl. 2). https://doi.org/10.1144/gsl.qjegh.1995.028.s2.04

Buerger, M. J. (1942). X-ray Crystallography.

Bustin, R. M., Bustin, A. M. M., Cui, X., Ross, D. J. K., & Pathi, V. S. M. (2008). Impact of shale properties on pore structure and storage characteristics. Society of Petroleum Engineers - Shale Gas Production Conference 2008. https://doi.org/10.2118/119892-ms

Cullity, B. D. (1956). Diffraction I: The directions of diffracted beams. Elements of X-ray Diffraction, 1, 84.

Grove, C., & Jerram, D. A. (2011). JPOR: An ImageJ macro to quantify total optical porosity from blue-stained thin sections. Computers and Geosciences, 37(11). https://doi.org/10.1016/j.cageo.2011.03.002

Halley, R. B. (1978). Estimating pore and cement volumes in thin section. Journal of Sedimentary Research, 48(2). https://doi.org/10.1306/212f7504-2b24-11d7-8648000102c1865d

Klug, H. P., & Alexander, L. E. (1954). Diffraction procedures for polycrystalline and amorphous materials. NY: John Wiley and Sons, 687.

Navelot, V. (2018). Caractérisations structurale et pétrophysique d'un système géothermique en contexte volcanique d'arc de subduction. Exemple de l'archipel de Guadeloupe. Phd thesis, Université de Lorraine. 11, 153, 170, 172, 503

Nelson, P. H. (2009). Pore-throat sizes in sandstones, tight sandstones, and shales. AAPG Bulletin, 93(3). https://doi.org/10.1306/10240808059

Orellana, L. F., Nussbaum, C., Grafulha, L., Henry, P., & Violay, M. (2022). Physical characterization of fault rocks within the Opalinus Clay formation. Scientific Reports, 12(1). https://doi.org/10.1038/s41598-022-08236-7

Plas, L., & Tobi, A. C. (1965). A chart for judging the reliability of point counting results. American Journal of Science, 263(1), 87-90.

Popov, Y. A., Pribnow, D. F. C., Sass, J. H., Williams, C. F., & Burkhardt, H. (1999). Characterization of rock thermal conductivity by high-resolution optical scanning. Geothermics, 28(2). https://doi.org/10.1016/S0375-6505(99)00007-3

Roduit, N. (2007). JMicroVision : un logiciel d'analyse d'images pétrographiques polyvalent. PhD thesis, Université de Genève. 149, 177, 275, 513

White, J. v., Kirkland, B. L., & Gournay, J. P. (1998). Quantitative porosity determination of thin sections using digitized images. Journal of Sedimentary Research, 68(1). https://doi.org/10.2110/jsr.68.220

Zheng, Q., Kaur, S., Dames, C., & Prasher, R. S. (2020). Analysis and improvement of the hot disk transient plane source method for low thermal conductivity materials. International Jour-nal of Heat and Mass Transfer, 151. https://doi.org/10.1016/j.ijheatmasstransfer.2020.119331

CHAPTER 6
Assessing Outcrop Data for Subsurface Evaluation

6.1. Introduction

As outlined in Chapter 3, geological factors are the primary contributors to the failure of hot sedimentary aquifer (HSA) projects, accounting for 39% of unsuccessful cases. Key geological issues included, but were not limited to, borehole integrity challenges (e.g., corrosion, clogging, and formation damaged) and unfavourable reservoir characteristics (e.g., porosity, transmissivity). These findings emphasise the critical importance of thorough site characterisation prior to drilling to mitigate uncertainties associated with geological and reservoir conditions.

Additionally, the analysis of the HSA database revealed a substantial lack of geological and hydrogeological data, that were unmeasured or unreported by geothermal operators. This major gap in yet fundamental information underscores the need for increased investment by developers or governmental bodies in early-stage geological investigations.

Despite significant advancements in surface and subsurface exploration technologies, uncertainties persist regarding reservoir depth, properties (e.g., porosity, permeability, temperature), and the expected performance of geothermal boreholes until initial drilling is conducted. Notably, exploration and test drilling costs can constitute up to 15% of the total capital investment of a geothermal project, for a near-halving from high to moderate project risk. Due to these uncertainties, funders sometimes lack the risk appetite for becoming involved in such investments.

Building upon the geological characterisation of the Chester Formation and methods presented in previous chapters, this chapter presents a comparative analysis of outcrop and core samples from the same geological formation. The analysis examines the thermal, petrophysical, and mineralogical properties of these samples to (1) provide new geological data of an HSA system, and (2) assess the extent to which outcrop-derived data can serve as proxies for subsurface reservoir conditions. The findings of Chapter 6 aim to improve the reliability of geothermal resource assessments, reduce exploration costs, and facilitate the wider adoption of geothermal energy.

This chapter was submitted in *Geothermics* in March 2025. My contributions to the paper included: Conceptualization, Formal analysis, Investigation, Methodology, Validation, Visualization, Writing – original draft, Writing – review & editing. Other Authors: **Neil Murray Burnside:** Conceptualization, Funding Acquisition, Supervision, Writing – review & editing. **Zoe Kai Shipton:** Conceptualization, Supervision, Writing – review & editing. **Claire Bossennec:** Investigation, Visualization, Writing – review & editing. **Sven Fuchs:** Supervision, Writing – review & editing. **Fiorenza Deon:** Investigation, Writing – review & editing.

6.2. Publication

Bridging Surface and Subsurface: Comparative Analysis of Outcrop and Core Samples from the Chester Formation for Geothermal Exploration

Maëlle Brémaud[1,2], Neil M. Burnside[1], Zoe K. Shipton[1], Claire Bossennec[3], Sven Fuchs[4], Fiorenza Deon[4]

[1]Department of Civil and Environmental Engineering, University of Strathclyde, Glasgow G1, 1XJ, UK

[2]JRG Energy, 6B Waipāhīhī Avenue, Hilltop, Taupō 3330, New-Zealand

[3]Laboratoire d'Océanologie et de Géosciences, Université de Lille, 59650, Villeneuve-d'Ascq, France

[4]GFZ German Research Centre for Geosciences, Section 4.8, Geoenergy, Telegrafenberg, Potsdam, 14473, Germany

Correspondence to: Maëlle Brémaud (maelle.bremaud@strath.ac.uk)

Keywords

geothermal energy, reservoir properties, outcrop analogues, Chester Formation, Cheshire Basin, resource risk.

Abstract

Hot sedimentary aquifers (HSAs) offer a sustainable alternative for geothermal energy, but exploration risks remain a major challenge. To mitigate this risk, the use of outcrop samples as analogues for subsurface reservoir properties has gained attention. However, outcrop samples are often influenced by surface weathering and altered conditions that may not accurately represent in situ reservoir conditions. This study compares outcrop and core samples from the Chester Formation in the Cheshire Basin, UK, to assess the transferability of outcrop-derived data to reservoir conditions. Seventeen outcrop samples and twenty-one core samples were analysed for mineralogy, petrophysical, and thermal properties. Results show that while outcrop samples exhibit some variability due to surface weathering, they generally offer comparable mineralogical and petrophysical properties to core samples. The mean thermal conductivity values for core samples are 2.15 ± 0.01 W m^{-1} K^{-1} and 2.07 ± 0.02 W m^{-1} K^{-1} when measured using device A and device B respectively, whereas outcrop samples exhibit lower mean values of 1.74 ± 0.01 W m^{-1} K^{-1} and 1.72 ± 0.03 W m^{-1} K^{-1} using device A and B. Variations are also observed between different lithotypes. These findings highlight the potential of outcrop samples for early-stage geothermal exploration, offering a cost-effective alternative to drilling and providing key insights into the depositional environment and lithological composition of the reservoir. This approach could improve the accuracy of subsurface predictions and reduce exploration costs, ultimately supporting the growth of the geothermal sector by de-risking investment decisions.

6.2.1. Introduction

As many countries commit to Net Zero emissions in the coming decades, hot sedimentary aquifers (HSA) offer a reliable and sustainable energy alternative to fossil fuels, particularly for heat, the most difficult component of energy sector to decarbonise. Despite significant advancements in subsurface understanding driven by technological innovations and enhanced expertise, geothermal development is still subject to diverse risks across all project phases (Gehringer and Loksha, 2012; Witter et al., 2019). The resource or exploration risk refers to the uncertainty associated with the identification and estimation of a geoenergy resource, e.g., the exact depth, productivity, and architecture of the reservoir. This has been a common challenge for the hydrocarbon industry, but the risk-appetite in geothermal development is far lower due to comparatively limited returns on investment (Gehringer and Loksha, 2012), creating a major economic barrier and impeding growth of the sector. In hot sedimentary aquifers, geology and hydrogeology factors are responsible for 39% of the failures observed in existing and past projects (Brémaud et al., 2024).

To mitigate resource risk during the appraisal of geothermal resources, it is crucial to achieve a more comprehensive characterisation of subsurface properties. However, drilling into HSAs, or any geothermal reservoir, involves high upfront capital costs, which can increase significantly with depth. The financial burden can be prohibitive, particularly for exploratory wells that might not yield viable resources (Gehringer and Loksha, 2012). To address these challenges and effectively reduce resource risks, extensive research has been conducted to investigate the applicability of outcrop samples in predicting in situ reservoir properties. While these studies have been predominantly applied to oil and gas reservoirs (Flint and Bryant, 1993; Eschard and Doligez, 1993; Aigner et al., 1996), they have recently been extended to geothermal fields (Reyer, 2014; Weydt et al., 2018; Bauer et al., 2017; Peacock et al., 2022). Outcrop analogues can allow for a better understanding and prediction of reservoir characteristics and fluid-flow behaviour including depositional settings, structural patterns, and reservoir

properties. However, several challenges significantly constrain the effective application of such studies:

- Outcrop samples are exposed to surface conditions such as weathering and surface-related fracturing. Rock weathering can alter the thermal, petrophysical, and mineralogical properties, potentially deviating from those of samples under in situ reservoir conditions.
- While outcrop analogues are often selected from the same formation as the subsurface reservoir, differences in burial, stress, and alteration histories can create significant variability, leading to outcrop data being dismissed for the wrong reasons. This highlights the need for an integrated approach: outcrops provide invaluable insights into 3D structural features at the sub-seismic scale, while core data and geological models can bridge the gap between these observations and subsurface variability in pressure, burial, stress conditions, and geological evolution. Combining these elements allows for a more robust and accurate reservoir characterisation.
- Subsurface rocks experience specific saturation conditions as well as elevated pressures and temperatures that influence their physical and thermal behaviour (cf., Norden et al., 2020). Outcrop samples are at ambient conditions and may not replicate these in situ effects accurately. While some studies have investigated reservoir properties of both outcrop samples and cores of the same formation, few have conducted experiments replicating in situ reservoir conditions to directly assess how closely outcrop-derived properties align with those measured in the subsurface.
- The process of extrapolating outcrop-derived data to deep reservoir conditions lacks a standardised framework.

This study aimed to address some of these gaps through a comparative analysis of outcrop and core samples from the same geological formation. Filling this research gap is essential for enhancing the cost-effectiveness and accuracy of geothermal exploration, ultimately reducing the resource risk and supporting the growth of

the geothermal sector. Indeed, if reservoir properties of outcrop and core samples prove to be similar or comparable, key geothermal data could be collected relatively easily and at very little cost (i.e., without the need for borehole drilling). Such findings would provide vital information to de-risk capital investment decisions for the development of geothermal projects.

6.2.2. Geological Setting

HSA resources in the UK are mainly associated with deep onshore Mesozoic basins such as the Cheshire, Eastern England, and Wessex basins. The Cheshire Basin is a complex NE-SW trending half-graben in northwest England. It was initiated during the Permian and is predominantly filled with fluvial and aeolian sandstones, including the Sherwood Sandstone Group (SSG) of late Permian-early Triassic age. The Cheshire Basin has been widely investigated and exploited for its copper mineralisation (Warrington, 1980), halite (Pugh, 1960), and hydrocarbon (Mikkelsen and Floodpage, 1997) potential. It also contains one of the main potable aquifers in the UK (Downing, 1993). Regional modelling of the Cheshire basin has estimated the geothermal resource to range between 44.1 and 75 EJ (Downing and Gray, 1986; Rollin et al., 1995; Jackson, 2012), representing approximately 23% of the UK's available Hot Sedimentary Aquifer (HSA) resource (Brown, 2020).

The Chester Formation, also known as Chester Pebble Beds, is one of the basal formations of the SSG, as shown in Fig. 6-1. It is a red-bed sequence derived from a braidplain environment (Radley and Coram, 2016) broadly dated to the Late Permian - Middle Triassic age (Warrington and Ivimey-Cook, 1992). This system was sustained by a northward-flowing braided river network, which transported metaquartzite clasts originating from the Armorican Massif in France across distances exceeding 400 km.

The Chester Pebble Beds comprise conglomerates, pebbly sandstones and sandstones, with the abundance of pebbles decreasing to the north (Plant et al., 1999). Horizontally bedded gravels indicate deposition in longitudinal sheet bars,

while flat- and cross-bedded gravels represent mid-channel bars in confined braided channels. These facies are primarily found in the southeast of the basin. Thick cross-bedded pebbly sandstones that also occur in this area and extend northward, represent transverse bar and dune deposits in braided river channels (Steel and Thompson, 1983; Thompson, 1970; Thompson et al., 1985). The rocks are typically light brown to red-brown and exhibit significant lithological variability, even in a single locality, as expected from complex fluvial facies.

The detrital mineralogy of the Chester Formation comprises major quartz with K-feldspar, chert grains and lithic clasts (including chert, quartzite, volcanic fragments) (Plant et al., 1999). The formation is often cemented by calcite or dolomite, and clay (forming coatings or disseminated within the sandstone matrix) has been regularly observed.

The Cheshire Basin has experienced a complex geological history of burial and inversion, meaning that a complete diagenetic record may not be preserved. Furthermore, identifying diagenetic processes and constructing a paragenetic sequence is particularly challenging for rocks deposited in basin-margin settings, as these environments often undergo a more complex history of fluid-rock interactions compared to deeper, more central areas of a basin (Plant et al., 1999). In the SSG, eodiagenetic and early mesodiagenetic processes usually led to a reduction in primary intergranular pore space due to mechanisms such as compaction, initial pressure solution, grain overgrowth, and cementation. Subsequent mesodiagenetic processes removed some of the previously formed cements and dissolved unstable framework grains, which contributed to the development of secondary porosity (Plant et al., 1999).

The northern part of the Cheshire Basin exhibits a nearly symmetrical structure, whereas in the south, prominent basin-margin normal faults contributed to a pronounced basin asymmetry. The SSG is found along the basin margins and over a large area to the north, with the Chester Formation exclusively outcropping in the north and northwest (Fig. 6-2).

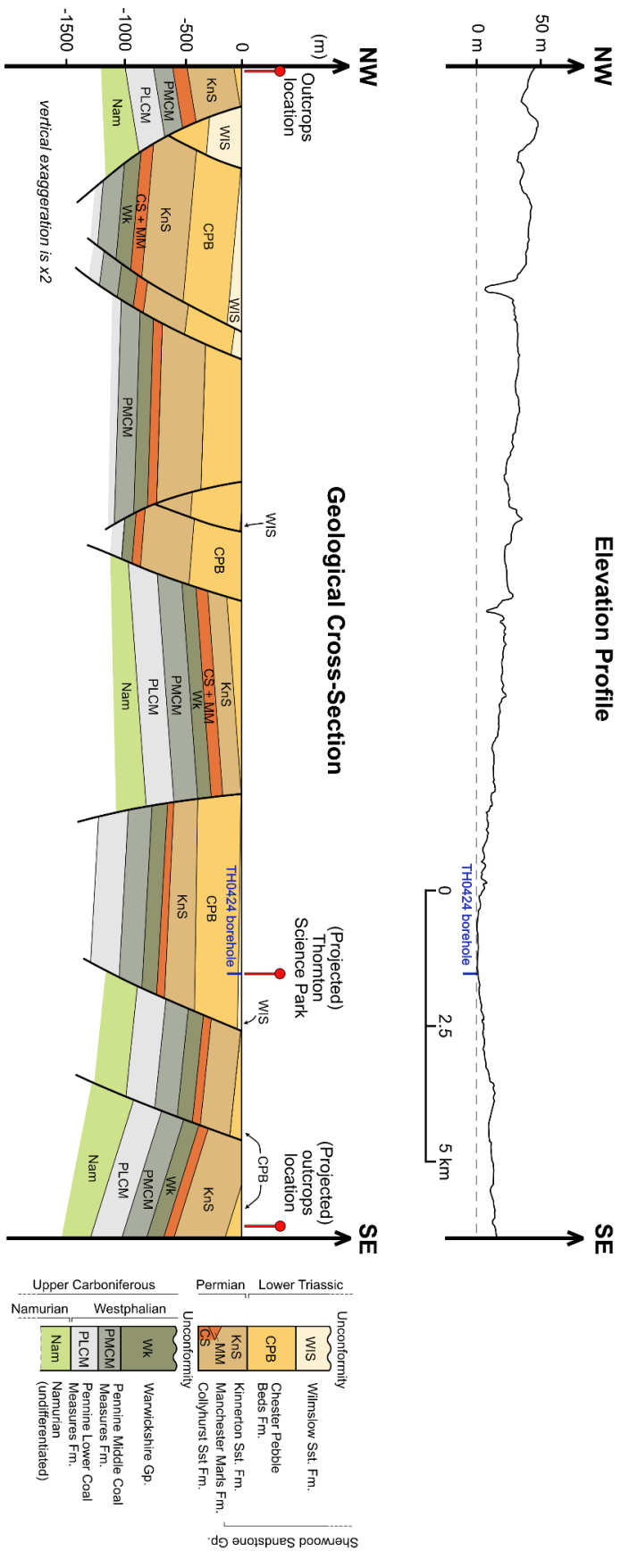

Figure 6-1: Northwest-southeast true topography section and vertically exaggerated geological cross-section of the area of study. The section line is shown in Fig. 6-2. Two sampling locations, located 1 to 2 km apart from the cross section, are projected onto the section line. However, the geological characteristics at these locations are assumed to be comparable to the those represented in the cross-section. The geological cross-section was constructed using three geological sheets, two of which are outdated and lack detailed information. Consequently, the section is characterised by numerous approximations. The geological log presented on the right side of the cross-section exclusively details the formations identified on the cross-section.

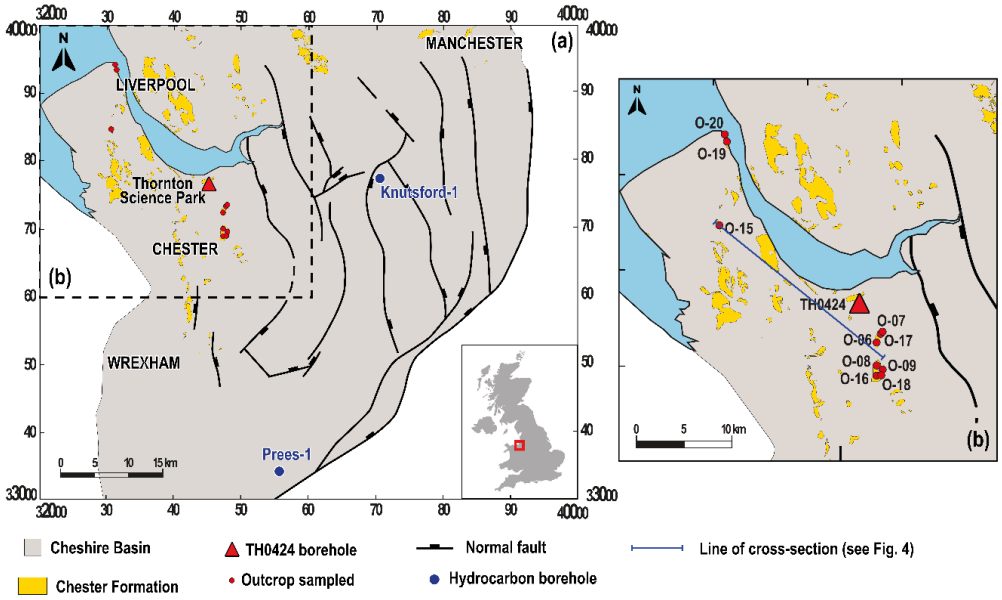

Figure 6-2: (a) Distribution of the Chester Formation in the Cheshire Basin and (b) zoom in on area of interest within the basin. Basin structure is reproduced from Mikkelsen and Floodpage (1997). Locations of the core and outcrop samples collected in this study are displayed by the red triangle and red circles respectively.

6.2.3. Methods: Sampling and Analytical Procedure

6.2.3.1. Sample Location and Collection

We collected and compared core and outcrop samples of the Chester Formation from six lithotypes: sand-dominated horizons, laminated horizons, cross-bedded horizons, pebble-rich horizons, one mud-dominated horizon, and one pebble from the pebble-rich horizons. Using BGS geological maps and the Street View option in Google Maps, outcrops of the Chester Formation were identified along roadways across the northern Cheshire Basin (red dots on Fig. 6-2). These outcrops exhibited diverse weathering conditions, facies characteristics, stratification features degrees of induration and fracturing patterns (Fig. 6-3). Sixteen outcrop samples were collected and display a significant variability in many aspects: rock texture, induration, grain shape and sorting, pebble content, or sedimentary structures.

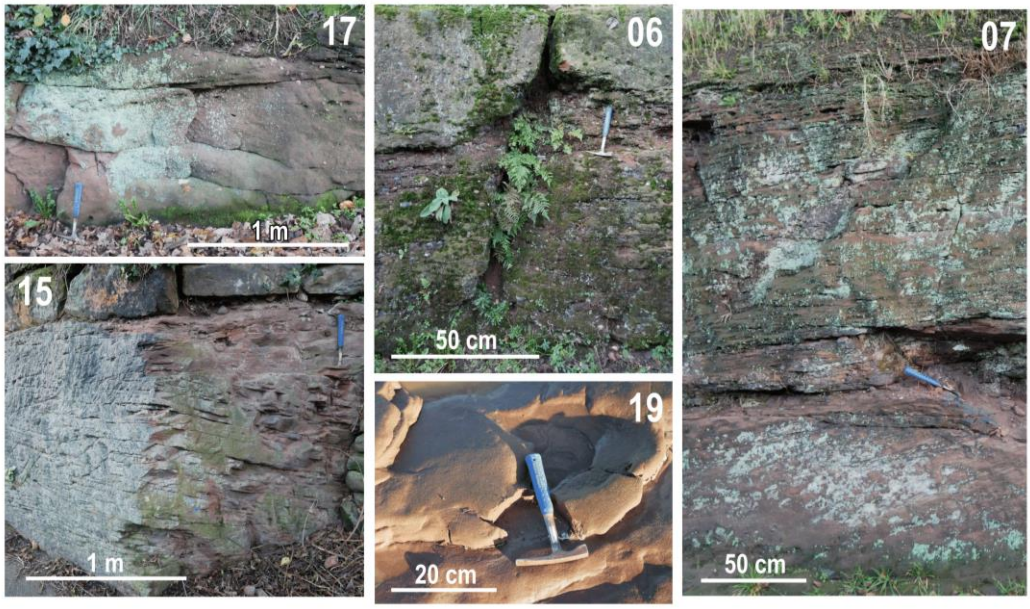

Figure 6-3: Examples of the Chester Formation outcrop exposures sampled in the Cheshire Basin. Numbers refer to sample localities in Fig. 6-2.

Core samples were obtained from an open bedrock borehole drilled for geophysical and hydrogeological research at the UKGEOS Cheshire site at Thornton Science Park (red triangle in Fig. 6-2). The TH0424 borehole was drilled to a total depth of 100 m in November 2021 to target the Chester Formation. The entire length of the borehole was cored, resulting in a 100 m core with a diameter of 90 mm. A total of twenty-one samples, each with a diameter of 5 cm, were sub-cored from the original borehole core, from depths between 22.8 and 96.6 meters below ground level (mbgl). A selection of zones of interest was made following the features of the outcrop samples already collected, to maintain the same variability amongst both sample sets.

Core samples were identified by their BGS sampling ID, which begins with "SSK1537", and samples from outcrops were designated by a number followed by a suffix such as "-1, -2 or -3" (e.g., 19-1). Multiple samples collected from the same outcrop exposure share the same number and are distinguished by their suffix (e.g., 07-1 and 07-2). Detailed descriptions and pictures of the samples are provided as supplementary information to this paper (Appendix C).

The elevation profile shown in Fig. 6-1 reveals minimal topographical difference amongst the sampling sites, which include both outcrop locations and core samples from the TH0424 borehole at the Thornton Science Park. The topography of the area varies between 0 and c. 50 m. The geological cross section indicate that the outcrops are part of the lower Chester Formation, while the core samples are situated within the upper part of the formation (Fig. 6-1). Additionally, several normal faults in the area exhibit a relatively significant throw of 400 to 500 m while others exhibit negligible displacements.

6.2.3.2. Analytical Techniques

The mineralogical composition of the samples was appraised using X-Ray Diffraction (XRD) and optical microscopy. Ten samples (five outcrop samples and five rock cores) were selected to capture the lithological variability of the Chester Formation and crushed with an agate mortar to powder. A ball milling machine was avoided to preserve the integrity and crystallinity of the mineral assemblage. The samples were measured with a D6 Phaser XRD. The device features a copper tube, and the patterns were collected at 20 kV and 5 mA. For the measurements, a 0.6 mm divergence slit, a 2.5 mm detector slit, and a 2.5° anti-scatter slit were chosen. The patterns were collected from $2\theta = 4°$ to 75° with a 0.012° step. Each sample was measured for approximately 90 minutes to guarantee a low noise and a reliable result. Prior to measurement, a corundum standard was used to calibrate the device and validate the exact position of the peaks. The patterns were semi-quantitatively interpreted using Match! software, and a database of structures was used to identify and assign the peaks to the mineral phases. The semi-quantitative interpretation of the patterns indicates the occurrence of the main minerals forming the specimen. To detect and identify accessory minerals (usually with a concertation below 2 or 3 wt.%), a thin section of each XRD-assessed sample was prepared and inspected using optical microscopy (50x to 100x) to refine interpretation of XRD results.

The ten thin sections were impregnated with a blue dye to assess porosity, and stained to reveal carbonate minerals. Thin section descriptions were carried out

using an optical microscope under plane-polarised and cross-polarised light. Mineral composition of the samples was approached by counting points on high-resolution pictures of the thin rock sections using the JMicrovision software (Roduit, 2007). Point counting was performed on an arbitrary grid to account for all elements regardless of their size and was stopped when: (1) reaching at least 500 points; and (2) the proportion of each class stabilises. The standard deviation for point counting in a homogenous rock is given by Eq. (6-1) (Plas and Tobi, 1965):

$$\sigma = \sqrt{\frac{f(100-f)}{n}} \tag{6-1}$$

where f is the percentage of a class and n is the total number of points counted. Plas and Tobi (1965) provide a 68% confidence interval between f+σ and f-σ, a 95% confidence between f+2σ and f-2σ, and a 99.7% confidence interval between f+3σ and f-3σ.

Thermal conductivity was determined on dry samples under ambient conditions (20°C, 1 atm) using the transient plane source method (TPS, Gustafsson, 1991). Measurements were made using a Hot TPS 2500 S, with a sensor composed of a thin circular nickel foil double spiral, functioning as both a resistance thermometer and a heat source. This disk has a radius of 6.4 mm and is enclosed between two Kapton insulating layers. Rock samples were cut in half, ensuring that both resulting pieces had flat surfaces for optimal contact with both sides of the sensor. An electric current passed through the spiral induces a rise in its temperature and resistance. By monitoring this temperature rise, the thermal properties of the sample can be determined. To test the reproducibility of results and verify the reliability of the TPS method and Hot Disk equipment, measurements were conducted at two facilities: (1) Stratchlyde's Civil and Environmental Engineering Laboratory; and GFZ Thermal Petrophysics Lab. For expediency, these are referred to as Lab A (Strathclyde) and Lab B (GFZ) in associated results, e.g., thermal conductivity results are noted as λ_A and λ_B respectively. 37 core and outcrop samples were analysed at Lab A, while 32 samples were measured at Lab B. Five samples were excluded from analysis at Lab B due to their small size, which made

them unsuitable for measurement with the available sensors. Five repeats were performed per sample (within +/- 3%), and this measurement error is displayed as bars in the figures and mentioned in the text. According to the manufacturer, the accuracy of the Hot Disk device is given with +/- 5%, and the reproducibility of the measurements is within +/- 2% (Gustafsson, 1991).

A petrophysical characterisation of the rocks was performed throughout porosity and permeability analyses. Porosity was determined using the water immersion porosimetry (WIP) method and thin section analysis. WIP requires the samples to be oven dried until a consistent dry weight is reached and recorded. Samples where then water-submerged within a sealed vacuum desiccator, to obtain a saturated weight. Effective porosity of samples was determined by subtracting the dry weight from saturated weight of each sample. Measurements were made on 35 samples, the mudstone sample (SSK153715) and one friable sandstone sample (16-2) were discarded. The uncertainty of the method is estimated from repeated experiments with a porosity error of ± 0.5 percentage points (Bloomfield et al., 1995). Porosity estimation was also performed on the ten samples selected for XRD analysis using point-counting on associated thin sections (magnification of 50x to 100x).

Permeability measurements were carried out on 32 samples using a New England Research TinyPerm 3 transportable air permeameter. Five samples were discarded (06-1, 06-2, 07-2, 16-3, 18-1) due to their small size and/or irregular surfaces that prevent adequate contact with the device rubber nozzle of the device. The rubber nozzle of the TinyPerm 3 was pressed against the rock surface and air was evacuated from the device in a single stroke. The syringe volume and the transient vacuum pulse generated at the sample interface were continuously monitored and corresponding permeability is calculated. A minimum of five measurements were performed per sample, and mean matrix permeabilities are displayed in Table 3. The manufacturer does not specify accuracy and reproducibility values for the TinyPerm 3; however, its accuracy was evaluated against other gas permeameters in a study conducted by Filomena et al. (2014).

6.2.4. Results

6.2.4.1. Mineralogy

6.2.4.1.1. Petrographic Description

The mineralogical composition of the selected sandstone samples (Table 6-1, Fig. 6-4) reveals significant variability in mineral phase distribution. Quartz is the dominant mineral across all samples, with values ranging from 55.4% to 66.6%, confirming its primary role in the framework of the studied sandstones. K-feldspar shows moderate variation, with values between 7.1% and 19.2%, indicating a feldspathic influence in certain samples. Plagioclase constitutes a minor fraction of the mineral assemblage, with Na-rich plagioclase content varying between 1.0% and 11.7%, while Ca-rich plagioclase ranges from 1.0% to 3.9%. Iron oxides occur in varying concentrations, reaching up to 6.8% in some samples, potentially indicating a diagenetic oxidation. Clay minerals are heterogeneously distributed, with content ranging from 2.0% to 15.6%. They are predominantly associated with cross-bedded and laminated lithofacies. Calcite is absent in surface samples but is found in borehole specimens, particularly within cross-bedded and pebble-rich sandstones. Porosity values exhibit considerable variability, ranging from 3.1% to 15.6%.

Mineralogical trends differ according to lithotype, influencing the overall texture and diagenetic characteristics. Cross-bedded sandstones (outcrop samples 7-01, 15-1, 16-2; and borehole samples SSK153713, SSK153718, and SSK153722) exhibit high quartz content (49.3 to 66.6%), moderate K-feldspar concentrations (5.7 to 22.3%), with borehole samples containing comparatively high clay mineral (reaching a maximum of 15.6% in SSK153713) and calcite (reaching a maximum of 11.6% in SSK153722) contributions. Porosity of cross-bedded sample remains moderate to low, typically ranging between 3.1 and 15.6%.

Pebble-rich sandstones (samples 8-01 and SSK153721) contain quartz content ranging from 55.4 to 66.9%, and K-feldspar values between 8.9% and 19.2%. These samples show relatively low clay content, between 3.2% and 9.8%, but a high

presence of iron oxides (1 to 6.8%). Calcite is found in SSK153721 (up to 7.8%), and porosity of both pebble-rich samples varies between 6.8% and 12.3%.

Laminated sandstones (sample SSK153725), show the highest K-feldspar concentrations, peaking at 22.8%, with quartz values between 56.9% and 60.5%. Clay content is moderate (5.9 to 7.3%), while calcite constitutes up to 5.1% of the total mineralogical composition. Porosity is comparatively low, between 3.4% and 4.6%, potentially related to finer laminations.

Sand-dominated sample 20-2, exhibits quartz content between 55.6 and 60.1% but a broad porosity range, from 6.6 to 15.6%. K-Feldspar content varies from 12.3 to 20%, reflecting a feldspathic-rich composition.

These findings provide insights into the depositional and diagenetic processes that shaped the mineralogical and structural properties of the studied sandstones.

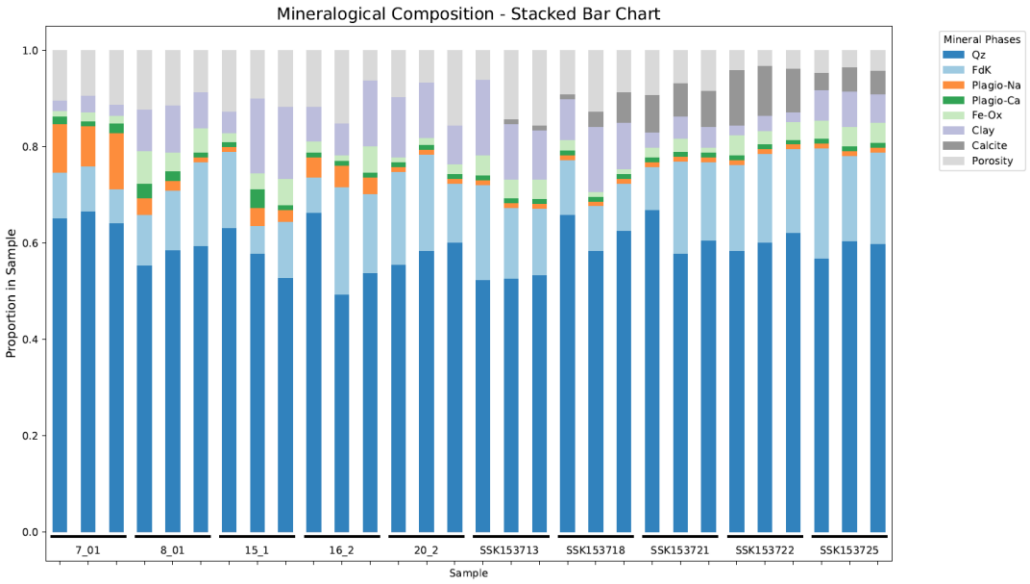

Figure 6-4: Mineral proportion for the Chester Fm thin sections analysed

Table 6-1: Mineralogical composition and porosity of ten (five outcrop samples and five sub-cores) samples of the Chester Formation obtained from thin section point counting, with three micrographs analysed per thin section.

Sample ID	Lithotype	Photomicrograph number	Quartz (%)	K-Feldspar (%)	Na-Plagioclase (%)	Ca-Plagioclase (%)	Fe-Ox (%)	Clay (%)	Porosity (%)	Calcite (%)
07-1	cross-bedded	1	65.2	9.5	10.1	1.5	1.2	2.1	10.4	0
		2	66.6	9.4	8.3	1	1.9	3.5	9.3	0
		3	64.1	7.1	11.7	2	1.5	2.4	11.2	0
08-1	pebble-rich	1	55.4	10.5	3.4	3.1	6.8	8.5	12.3	0
		2	58.6	12.4	2	2	3.9	9.8	11.3	0
		3	59.4	17.4	1	1	5.1	7.4	8.7	0
15-1	cross-bedded	1	63.2	15.8	1	1	1.9	4.5	12.6	0
		2	57.9	5.7	3.7	3.9	3.4	15.4	10	0
		3	52.8	11.6	2.5	1	5.5	15	11.6	0
16-2	cross-bedded	1	66.3	7.4	4.1	1	2.3	7.3	11.6	0
		2	49.3	22.3	4.5	1	1.1	6.7	15.1	0
		3	53.8	16.4	3.5	1	5.4	13.7	6.2	0
20-2	sand-dominated	1	55.6	19.2	1	1	1.1	12.5	9.6	0
		3	58.4	20	1	1	1.5	11.5	6.6	0
		2	60.1	12.3	1	1	2	8	15.6	0
SSK153713	cross-bedded	1	52.4	19.7	1	1	4.2	15.6	6.1	0
		2	52.7	14.7	1	1	3.8	11.6	14.2	1
		3	53.4	13.8	1	1	4.1	10.1	15.6	1
SSK153718	cross-bedded	1	65.9	11.4	1	1	2.2	8.4	9.1	1
		2	58.4	9.3	1	1	1	13.5	12.6	3.2
		3	62.6	9.8	1	1	1	9.6	8.7	6.3
SSK153721	pebble-rich	1	66.9	8.9	1	1	2	3.2	9.2	7.8
		2	57.8	19.2	1	1	2.7	4.6	6.8	6.9
		3	60.6	16.2	1	1	1	4.3	8.4	7.5
SSK153722	cross-bedded	1	58.4	17.9	1	1	4.1	2	4	11.6
		2	60.1	18.5	1	1	2.7	3.1	3.1	10.5
		3	62.2	17.3	1	1	3.7	2	3.8	9
SSK153725	laminated	1	56.9	22.8	1	1	3.7	6.4	4.6	3.6

6.2.4.1.2. X-Ray Diffraction Patterns

No significant differences are observed through XRD analysis between core and outcrop samples regarding the dominant mineral composition (Table 6-2). However, these two sample types can be differentiated based on hematite and clay content: hematite is identified solely in outcrop samples, while clay minerals are found exclusively in core samples. No major trends are identified based on the lithotype, although pebble-rich samples generally exhibit lower K-feldspar content compared to other lithotypes.

XRD analysis exclusively characterises the mineralogical composition of the matrix, whereas point counting on thin sections provides the composition of the whole rock, i.e., matrix and pores. Observations at the thin-section scale further support XRD findings, revealing a predominantly quartz-dominated matrix with localised occurrences, hematite, clay minerals, and calcite in one core sample. Variations in the proportions of minor minerals −such as feldspars or clays− between both

methods may be attributed to sample heterogeneity and scale-related factors, as thin sections and powders originate from distinct and limited portions of a given sample.

Table 6-2: Mineralogical composition of ten (five outcrop samples and five sub-cores) samples of the Chester Formation, obtained from XRD analysis.

Sample ID	Lithotype	Quartz (%)	K-Feldspar (%)		Na-Plagioclase (%)	Hematite (%)	Clay (%)	Calcite (%)
			Sanidine	Microcline	Albite			
07-1	cross-bedded	95		5				
08-1	pebble-rich	89			3	8		
15-1	cross-bedded	79				21		
16-2	cross-bedded	92	8					
20-2	sand-dominated	97	3					
SSK153713	cross-bedded	85	6		5		4	
SSK153718	cross-bedded	98	2					
SSK153721	pebble-rich	97						3
SSK153722	cross-bedded	65	35					
SSK153725	laminated	76	12				12	

6.2.4.2. Thermal Properties

Thermal conductivity measurements on dry samples are presented in Table 6-3. Thermal conductivity values λ_A are in the range 1.23 to 2.99 W m^{-1} K^{-1} with a mean of 1.98 ± 0.01 W m^{-1} K^{-1}, while λ_B values are in the range 1.07 to 2.90 W m^{-1} K^{-1}, with a mean of 1.96 ± 0.02 W m^{-1} K^{-1}. Figure 6-5 shows a good correlation (R^2 = 0.9225) between thermal conductivity values obtained from the two different devices.

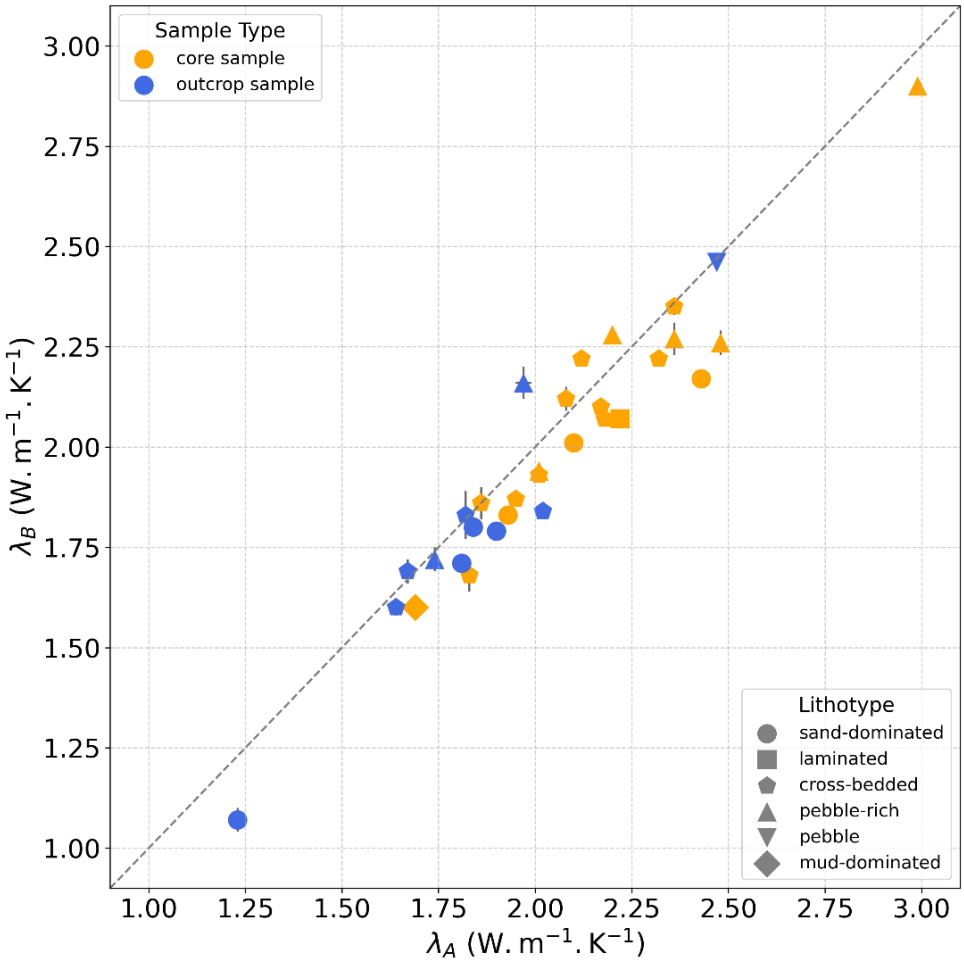

Figure 6-5: Comparison of thermal conductivity values using the TPS technique at Lab A (λ_A, x axis) and Lab B (λ_B, y axis). Conductivities were measured on dry samples at ambient lab conditions on two sample types: samples from outcrop exposures (blue markers) and core (orange markers) samples. The rock lithotypes are displayed as different marker shapes. Error bars representing repeated measurements are displayed in black, and are often smaller than the sample marker.

The mud-dominated sample SSK153715 exhibits a thermal conductivity of 1.69 ± 0.01 W m^{-1} K^{-1} when measured with device A and 1.60 ± 0.01 W m^{-1} K^{-1} with device B. Sandstone samples demonstrate higher mean thermal conductivity values, which vary according to the lithotype. Sand-dominated samples have a mean conductivity of 1.79 ± 0.01 W m^{-1} K^{-1} with device A, while laminated, cross-bedded and pebble-rich sandstones show mean values of 2.22 ± 0.00, 1.99 ± 0.01 and 2.25 ± 0.01 W m^{-1} K^{-1} respectively, with the same apparatus. Thermal analysis

performed on the second device exhibits a similar trend, albeit with slightly lower conductivity values (Fig. 6-6).

Table 6-3: Thermal and petrophysical properties measured on Chester Formation samples from outcrop exposures and cores.

Sample type	Sample ID	Lithotype	Thermal conductivity λ_A (W m^{-1} K^{-1})	Thermal conductivity λ_B (W m^{-1} K^{-1})	Air Permeability (mD)	Water Immersion Porosity (WIP, %)
Core sample	SSK153718	cross-bedded	2.17	2.10	1428	19.7
Core sample	SSK153716	cross-bedded	2.01	1.93	261	20.8
Core sample	SSK153729	pebble-rich	2.36	2.27	3036	17.7
Core sample	SSK153713	cross-bedded	1.83	1.68	9086	24.5
Core sample	SSK153724	cross-bedded	2.12	2.22	45	16.5
Core sample	SSK153728	sand-dominated	2.43	2.17	2397	19.8
Core sample	SSK153717	cross-bedded	2.08	2.12	475	18.3
Core sample	SSK153720	sand-dominated	2.10	2.01	6486	22.5
Core sample	SSK153711	cross-bedded	1.95	1.87	1381	23.8
Core sample	SSK153712	sand-dominated	1.84	1.80	6788	25.3
Core sample	SSK153722	cross-bedded	2.32	2.22	1	12.8
Core sample	SSK153727	cross-bedded	2.36	2.35	1166	17.8
Core sample	SSK153714	sand-dominated	1.93	1.83	8885	25.0
Core sample	SSK153715	mud-dominated	1.69	1.60	7	-
Core sample	SSK153707	cross-bedded	1.86	1.86	3909	21.4
Core sample	SSK153730	pebble-rich	2.20	2.28	2405	18.2
Core sample	SSK153723	pebble-rich	2.48	2.26	171	15.3
Core sample	SSK153725	laminated	2.22	2.07	2	13.9
Core sample	SSK153719	cross-bedded	2.18	6	3261	20.3
Core sample	SSK153721	pebble-rich	2.99	2.90	1021	14.7
Core sample	SSK153726	pebble-rich	2.01	1.94	4747	20.0
Outcrop sample	06-1	sand-dominated	1.68	-	-	26.2
Outcrop sample	06-2	sand-dominated	1.23	1.07	-	30.6
Outcrop sample	06-3	pebble	2.47	2.46	49	7.4

Outcrop sample	07-1	cross-bedded	1.96	-	1449	23.0
Outcrop sample	07-2	cross-bedded	1.82	1.83	-	22.2
Outcrop sample	08-1	pebble-rich	1.97	2.16	2157	21.1
Outcrop sample	08-2	pebble-rich	1.74	1.72	24539	24.9
Outcrop sample	09-1	sand-dominated	1.84	1.80	322	20.5
Outcrop sample	15-1	cross-bedded	1.67	1.69	3073	22.4
Outcrop sample	16-1	cross-bedded	2.02	1.84	2635	23.1
Outcrop sample	16-2	cross-bedded	1.64	1.60	285	-
Outcrop sample	16-3	cross-bedded	1.90	-	-	19.2
Outcrop sample	17-1	sand-dominated	1.45	-	49834	26.7
Outcrop sample	18-1	sand-dominated	1.42	-	-	19.8
Outcrop sample	19-1	sand-dominated	1.90	1.79	1335	22.5
Outcrop sample	20-2	sand-dominated	1.81	1.71	480	22.8

Core samples exhibit thermal conductivity ranges between 1.69 and 2.99 W m^{-1} K^{-1} using device A, and from 1.23 to 2.47 W m^{-1} K^{-1} using device B. In general, core samples exhibit higher thermal conductivity values compared to outcrop samples (Fig. 6-6), with means of c. 2.1 m^{-1} K^{-1} and c. 1.8 m^{-1} K^{-1}, respectively, irrespective of the device used. Pebble-rich sandstone samples show the highest conductivities, although this trend is more pronounced in core samples than in outcrop samples, as depicted in Fig. 6-5. Notably, two samples deviate significantly from the overall trend: a sand-dominated sample collected from an outcrop exposure exhibits notably low conductivity, while a pebble-rich sandstone core sample displays the highest conductivity (Fig. 6-5).

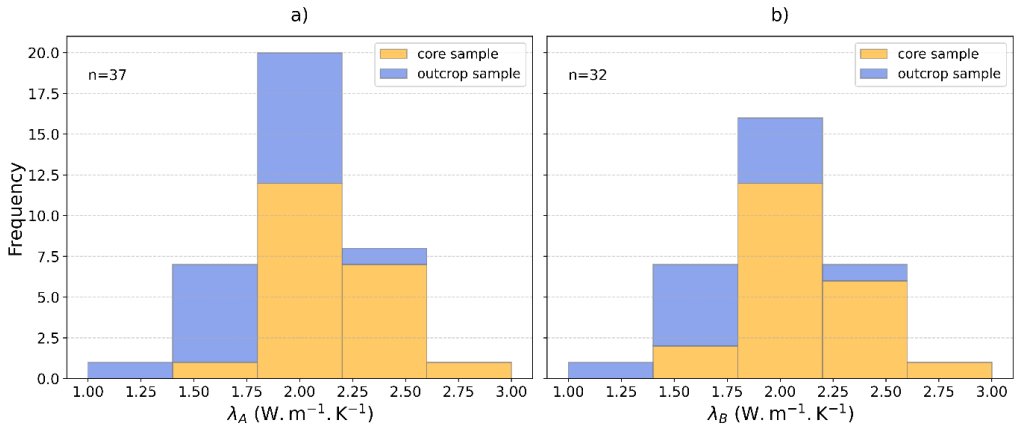

Figure 6-6: Stacked bar charts comparing thermal conductivity values using a) device A (λ_A) and b) device B (λ_B). Core samples are displayed in orange and outcrop samples in blue. The total number of samples analysed is presented in the upper-left corner of each figure.

Given the comparable thermal conductivity values obtained from devices A and B, only the measurements acquired using device A will be considered and analysed in the subsequent sections. This selection is justified by the greater number of samples analysed with device A, resulting in a more comprehensive dataset for petrophysical and thermal assessments.

6.2.4.3. Petrophysical Analysis

Effective porosity for all rock samples ranges between 7.4 and 30.6% (Table 6-3, Fig. 6-7). Permeability values span from $5x10^{-1}$ to $5x10^{4}$ mD with a mean value of $5x10^{3} \pm 3x10^{2}$ mD (Table 6-1, Fig. 6-7). Figure 8 shows that the data exhibit the expected overall increase in permeability with increasing porosity. Pebbly sandstone samples display lower porosities compared to other samples, likely influenced by their pebble content. In contrast, no clear trend is observed among the remaining lithotypes. Outcrop samples exhibit a higher mean porosity (22.2% and 23.2% without the pebble) compared to core samples (19.4%) (Fig. 6-7, Fig. 6-8). The mean permeability of outcrop samples (7.8×10^{3} mD) is also slightly higher than that of core samples (2.7×10^{3} mD) (Fig. 6-7).

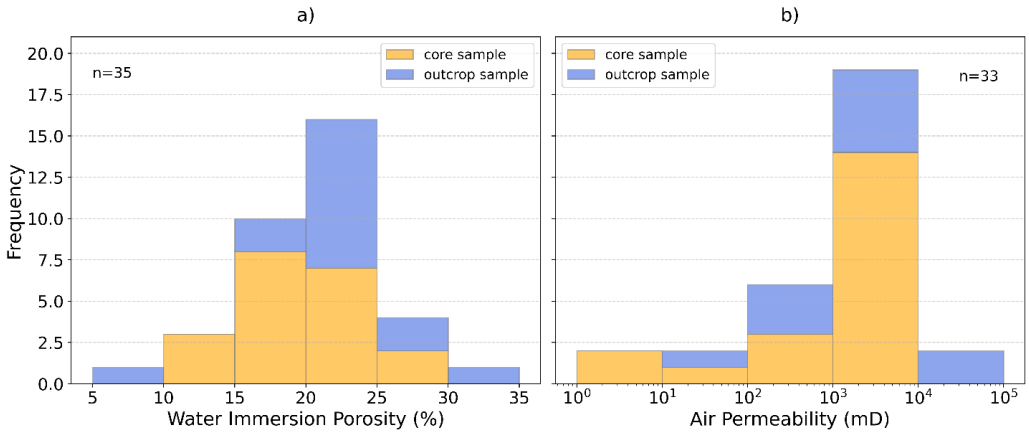

Figure 6-7: Stacked bar chart of a) effective porosity (using the WIP technique) and b) air permeability for samples from cores (orange) and outcrop exposures (blue). The total number of samples analysed is presented in the upper-right or -left corner of each figure.

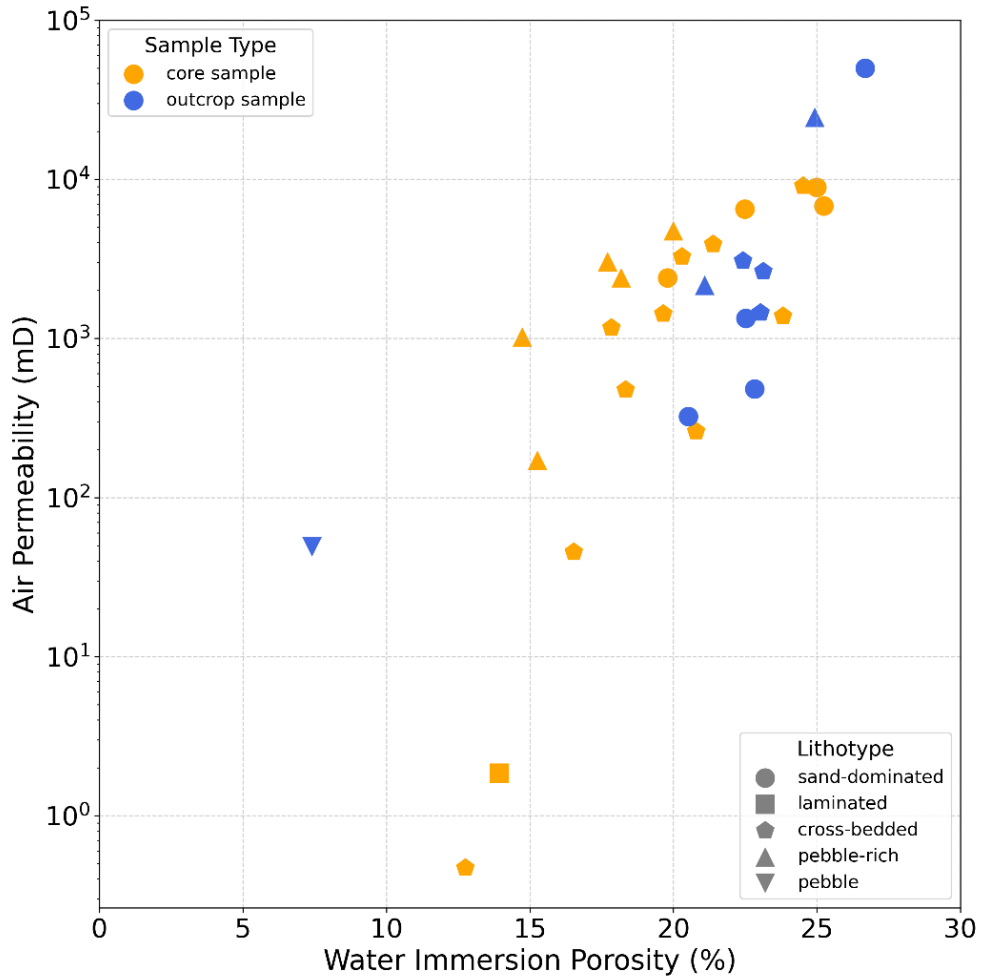

Figure 6-8: Plot of air permeability as a function of porosity (using the water immersion method). Results are discredited depending on the sample origin (different colours) and the lithotypes (different shapes).

Two sandstone core samples exhibit relatively low porosity and permeability (Fig. 6-8). These samples exhibit distinct physical properties: while the cross-bedded sample has a grey coloration (as opposed to the typical reddish) and likely underwent a leaching process, the second sample –characterised by horizontal laminations– features layers enriched in darker minerals layers (hematite). More information on the samples is provided as supplementary information to this paper (Appendix C).

Porosity was additionally computed through point-counting performed on photomicrographs for ten samples, comprising five samples from outcrop exposures and five samples from core material (Table 6-1). Samples taken at surface exposures exhibit higher porosities than samples from core samples (Fig. 6-9).

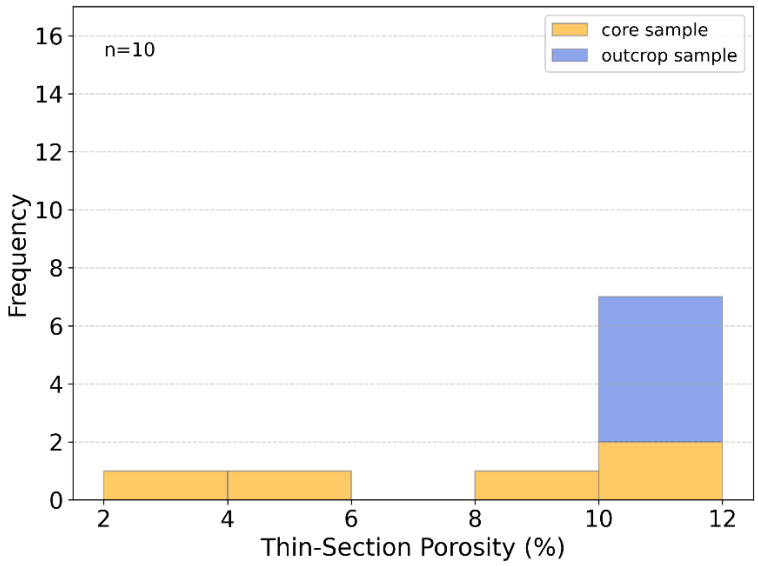

Figure 6-9: Histogram of thin section porosity values for five samples from cores (orange) and five outcrop exposure specimens (blue). The total number of samples analysed is presented in the upper-right or -left corner of each figure.

Notably, porosity derived from thin-section analysis are two to three times lower than WIP results from the same samples (Fig. 6-10). This misalignment can be attributed to various factors, including differences in measurement scale, and the heterogeneous nature of sandstone pore systems. Thin-section analysis captures two-dimensional, localised porosity, often missing micropores observed in bulk measurements Additionally, thin sections analysis may be affected by sample preparation artifacts that can alter the true porosity proportion, and is reliant on petrographer interpretation, particularly when the blue-dyed porosity is not distinctly visible (Cather et al., 1991). In contrast, the WIP method reflects the interconnected pore network across the entire sample (Bloomfield et al., 1995). However, samples containing surface vugs may experience liquid loss during weighing, leading to an underestimation of the pore volume (A.P.I., 1998). Porosity measurements obtained using the WIP technique are deemed more accurate and are consequently selected for use in the subsequent analyses.

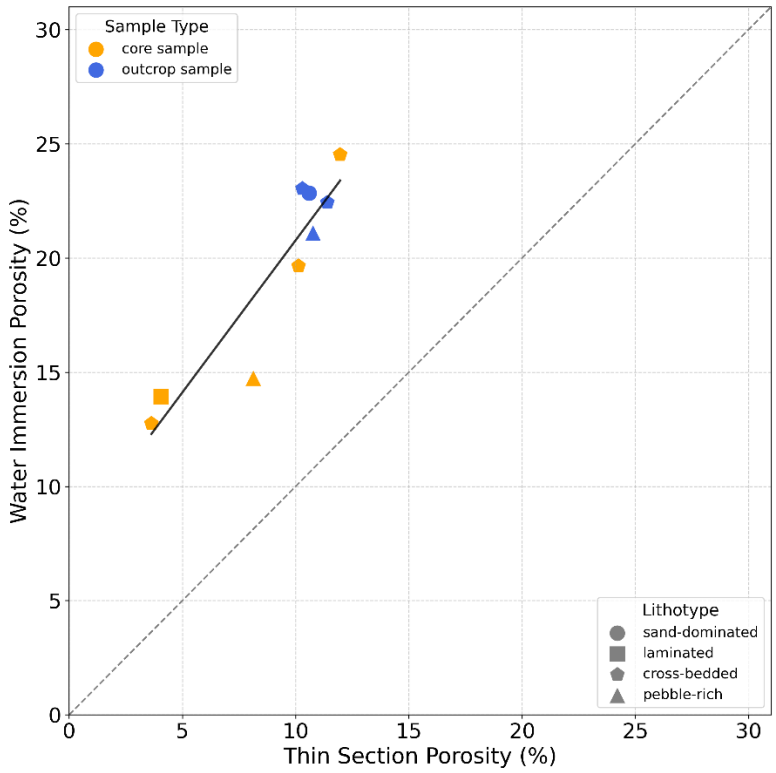

Figure 6-10: Comparison of porosities measured using two methods: water immersion porosimetry (y axis) and porosity calculated from thin sections (x axis) from outcrop samples

(orange markers) and core samples (blue markers). The rock lithotypes are shown through various marker shapes.

Figure 6-11 shows a decrease in thermal conductivity with increasing effective porosity. Samples collected from outcrops exhibit higher porosities and lower conductivities than core samples. The two sample groups are well defined, though the pebble sample collected at an outcrop exposure is a clear outcrop outlier with low porosity and relatively high thermal conductivity. All lithotypes exhibit a similar trend.

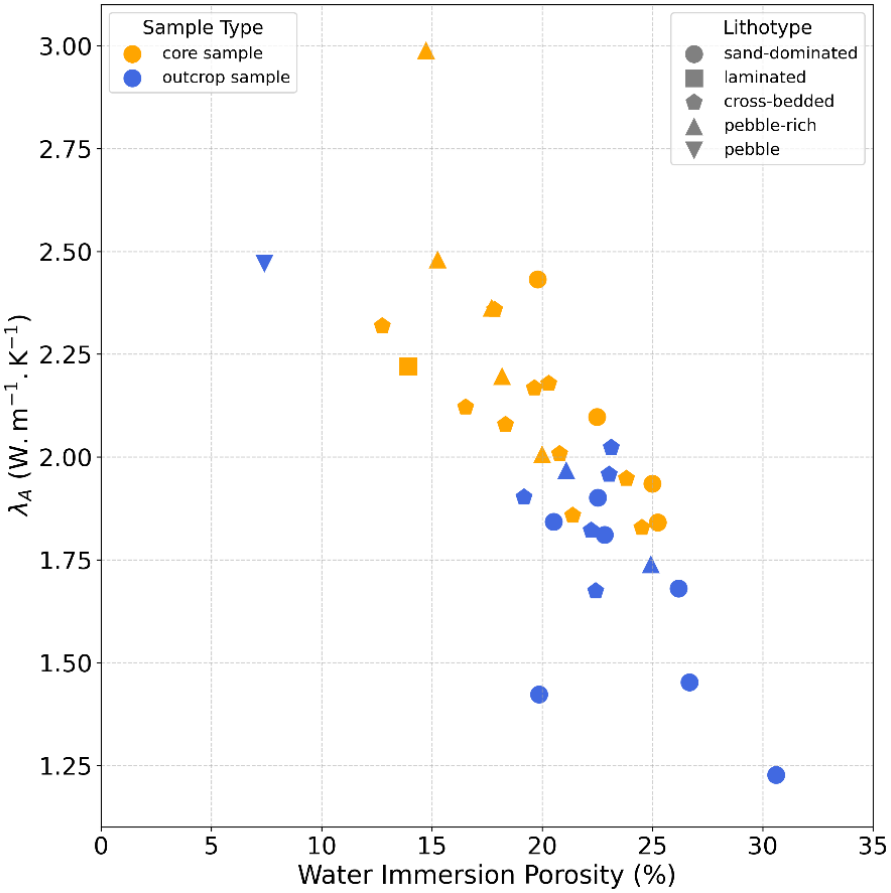

Figure 6-11: Comparison of the thermal conductivity measured using the TPS device A (x axis) and porosity using the water immersion porosity technique (y axis) for both sample types (outcrop samples and core samples).

6.2.5. Discussion

6.2.5.1. Statistical Comparison of Core and Outcrop Sample Properties

Following all measurements, a t-test is used to determine whether there is a significant difference between the means values of rock core and outcrop samples and if yes, how they are related. The Student t-test or t-test was developed by William Sealy Gosset in 1908 and is defined in the following equation (Eq. (6-2)) (Student, 1908):

$$t = \frac{M_c - M_o}{S_{pooled}} \tag{6-2}$$

where M_c is the mean of the core samples, M_o is the mean of the outcrop samples and S_{pooled} is the pooled standard error for the t-test that can be calculated using Eq. (6-3).

$$S_{pooled} = \sqrt{\left(\frac{S_c}{\sqrt{N_c}}\right)^2 + \left(\frac{S_o}{\sqrt{N_o}}\right)^2} \tag{6-3}$$

where S_c is the standard deviation of the core samples, N_c is the number of core samples, S_o is the standard deviation of the outcrop samples, and N_o is the number of outcrop samples.

Null hypothesis states that there is no difference between each sample type and can be defined as follows (Eq. (6-4)):

$$\text{Ho:} \quad p_c - p_o = 0 \tag{6-4}$$

where p_c and p_o are the measured properties of the core samples and outcrop samples respectively.

T-distribution tables provide a critical t-value of $t_c = 2.04$ at a level of confidence of 0.95 for a degree of freedom df defined as follow (Eq. (6-5)) (Moore et al., 2009):

$$df = N - P \tag{6-5}$$

where N is the population size (i.e., the number of samples), and P is the number of parameters to estimate (i.e., 2 – outcrop and core samples).

The t-test value (t) is then compared to the critical t-value (t_c). If the computed t value is above t_c, the null hypothesis is rejected, indicating a significant difference between the means of outcrop and core samples for a given property. The mean permeability and porosity values without the outliers are selected. A t-test is computed for three properties: porosity, permeability and thermal conductivity, and results are given in Table 6-4.

Table 6-4: t-test values for thermal and petrophysical properties of the Chester Formation sandstone investigated

Property	Air Permeability	WIP	Thermal conductivity λ_A	Thermal conductivity λ_B
***t*-value**	1.13	1.87	3.96	2.49

The analysis of petrophysical properties reveal no statistically significant difference between the mean porosities and permeabilities of core and outcrop samples, as indicated by $t < t_c$. In contrast, the t-test for thermal conductivity results in the rejection of the null hypothesis (H_0), demonstrating a notable discrepancy in the measured mean values between the two sample types: thermal conductivity values are generally higher for core samples compared to outcrop samples.

6.2.5.2. Variability in Thermal and Petrophysical Measurements

The use of the Hot Disk apparatus is subject to various potential sources of error, including human error, analytical error, and rock heterogeneity. Analytical error can be approached by conducting repeated measurements with the same apparatus, and incorporating manufacturer provided measurement error ranges. For example, the accuracy of the TPS device is assessed through five thermal measurements per sample. The results demonstrate high device precision, with standard deviations of 0.00 to 0.02 W m^{-1} K^{-1} for twenty-four means

measurements of 1.65 to 2.73 W m^{-1} K^{-1}. Whenever feasible, thermal, mineralogical, and petrophysical measurements are repeated to enhance the reliability of the data.

Rock heterogeneity represents a critical source of variability in thermal and petrophysical measurements for both core and outcrop samples. Sandstone samples, particularly those that originate from fluvial depositional environments, exhibit significant heterogeneity. Fluvial facies such as channels, levees, floodplains, and overbank deposits are characterised by distinct sedimentological properties. The dynamic nature of fluvial systems, involving migrating channels and variable flow velocities, generates a complex patchwork of sandstone and finer-grained deposits. These variations influence grain size, sorting, sedimentary structures, and lithological distribution, and consequently petrophysical properties. Additionally, depositional processes like bar or levee formation in braided systems create lateral and vertical heterogeneity in lithology, porosity, and permeability (Bjørlykke, 2015; Bridge and Tye, 2000). Post-depositional diagenetic alterations further enhance variability by unevenly modifying original rock characteristics, leading to potential substantial differences in properties either between neighbouring samples or within a single sample.

In this study, the heterogeneity of the geological formation is addressed by collecting and comparing petrophysical, mineralogical and thermal properties of samples from six distinct lithotypes identified within the Chester Formation: pebble-rich, sand-dominated (massive), cross-bedded, laminated, mud-dominated, and a single pebble. Pebble-rich samples stand out with higher thermal conductivity and lower porosity values than the other lithotypes, while no other major differences in properties are observed between the remaining lithotypes.

To further evaluate rock heterogeneity, the Hot Disk sensor placement is systematically varied across the samples. The analysis is performed on six samples –three cores and three outcrops– at four distinct sensor positions, with five measurements taken at each location. Standard deviations range from 0.03 to 0.19

W m^{-1} K^{-1}, with the highest variability observed in two of the pebbly sandstone samples that exhibit standard deviations of 0.09 and 0.19 W m^{-1} K^{-1} (Table 6-5).

Table 6-5: Variability of the sensor placement generating high standard deviations of thermal conductivity values for six samples of the Chester Formation

Sample type	Sample ID	Lithotype	Thermal conductivity λ_A (W m^{-1} K^{-1})	
			Value	Standard deviation
core	SSK153714	Sand-dominated	1.95	0.03
	SSK153723	Pebble-rich	2.61	0.09
	SSK153720	Sand-dominated	2.10	0.04
outcrop sample	08-1	pebble-rich	2.09	0.19
	19-1	Sand-dominated	1.88	0.03
	08-2	pebble-rich	1.71	0.03

The measured petrophysical and thermal properties of rocks can also vary significantly depending on the size of the sample and the scale of observation (Schön, 2015). Permeability measurements at small scales, such as those obtained from core or outcrop samples, primarily reflect matrix permeability. In contrast, reservoir-scale measurements, often derived from well tests, typically exhibit higher permeability values due to the influence of fracture networks and larger flow pathways (Berkowitz, 2002). Similarly, porosity assessments conducted at different scales −such as thin-section analysis, core or outcrop measurements, or reservoir-scale evaluation− can yield disparate results. These discrepancies arise because each method evaluates different pore structures and may exclude or emphasize certain features, such as low-porosity cemented zones or high-porosity fractured layers (which dominate at larger scales).

Key geological factors contributing to these scale-dependent differences include fracturing, anisotropy and heterogeneity (Schön, 2015). Variations in these factors can also lead to thermal conductivity values at the regional scale that deviate substantially from laboratory measurements (Clauser and Huenges, 1995; Li et al., 2024; Adl-Zarrabi et al., 2010). Although core and outcrop samples are relatively comparable in scale, diagenetic alteration or surface weathering can influence the

petrophysical and thermal properties of outcrop samples, potentially introducing additional variability.

6.2.5.3. Diagenetic Parasequence and Associated Petrophysical Controls

The diagenetic parasequence of the analysed samples reveals a complex diagenetic history influenced by multiple processes and is summarised in Table 6-6. Early diagenesis features the development of coatings composed of detrital clay cutans impregnated with red-brown iron oxide (Fig. 6-12a). These clay-iron oxide coatings play a crucial role in preserving intergranular porosity by inhibiting cementation. The iron oxide is responsible for the reddish-brown coloration of samples from which the thin sections originate. Iron-rich oxides, prevalent near grain contacts, reflect oxidative weathering and precipitation from pore waters during early stages of diagenesis. Only sample SSK153722 of pale green-grey colour does not exhibit any iron oxide coating, that has probably been leached by reducing mesodiagenetic fluids (Plant et al., 1999). Another early diagenesis process involves the development of concentric-structured dolomitic nodules (Fig. 6-12b). As described by Plant et al. (1999), these nodules usually contain iron-oxide staining through intricate spheroid structures and radial-fibrous fabrics.

Table 6-6: Principal features observed in the Chester Formation samples for each diagenetic regime

Diagenesis Stage	Main characteristics observed
Eodiagenesis	• Clay-Iron oxides coating • Dolomite micronodules
Mesodiagenesis	• Quartz overgrowths • Calcite cementation • Feldspar dissolution and precipitation in clay minerals • Development of secondary porosity
Telodiagenesis	• Oxidative dissolution of carbonate cements in outcrop samples • Development of pore-lining fibrous illite

A major mesodiagenetic cementation episode is recorded in the samples studied. Evidence of compaction is found on quartz grains of all thin sections. Pressure

solution at grain contacts and overgrowths significantly contribute to reduced pore space and tighter grain packing (Fig. 6-12c). In contrast to the outcrop samples, calcite cementation is observed in all core samples analysed. Calcite is filling intergranular spaces, leading to substantial reductions in porosity (Fig. 6-12d). This cementation represents a late diagenetic process associated with deeper burial conditions. In most samples, feldspar grains exhibit significant alteration and dissolution; sometimes resulting in secondary porosity (Fig. 6-12a).

Late-telodiagenetic alteration is likely recorded in the surface samples, characterised by an oxidative dissolution of carbonate cements. This process has also been documented by Holmes et al. (1983) in Triassic formations across various basins in Central England. A less plausible hypothesis for the absence of calcite in outcrop samples is associated with the part of the Chester Formation sampled by the cores. The observed variation in calcite content could be a primary depositional difference, as the upper section of the Chester Formation may inherently contain lower calcite concentrations than the lower section exposed at outcrop (Fig. 6-1). However, all samples are within proximity to one another (maximum 30 km) and are situated in the same part of the basin. Moreover, the fault displacements have resulted in only small variations in stratigraphic depth (on the order of a few hundred meters), making it unlikely that differential burial diagenesis accounts for the observed discrepancy. Consequently, the first hypothesis is more plausible than the second. Some samples, such as SSK153722 (Fig. 4d), exhibit fibrous illite growth within uncemented pores. While pore-lining illite has a minor effect on porosity, it can have a pronounced impact on permeability: its alignment along pore walls can narrow pore throats, impeding fluid flow (Neasham, 1977).

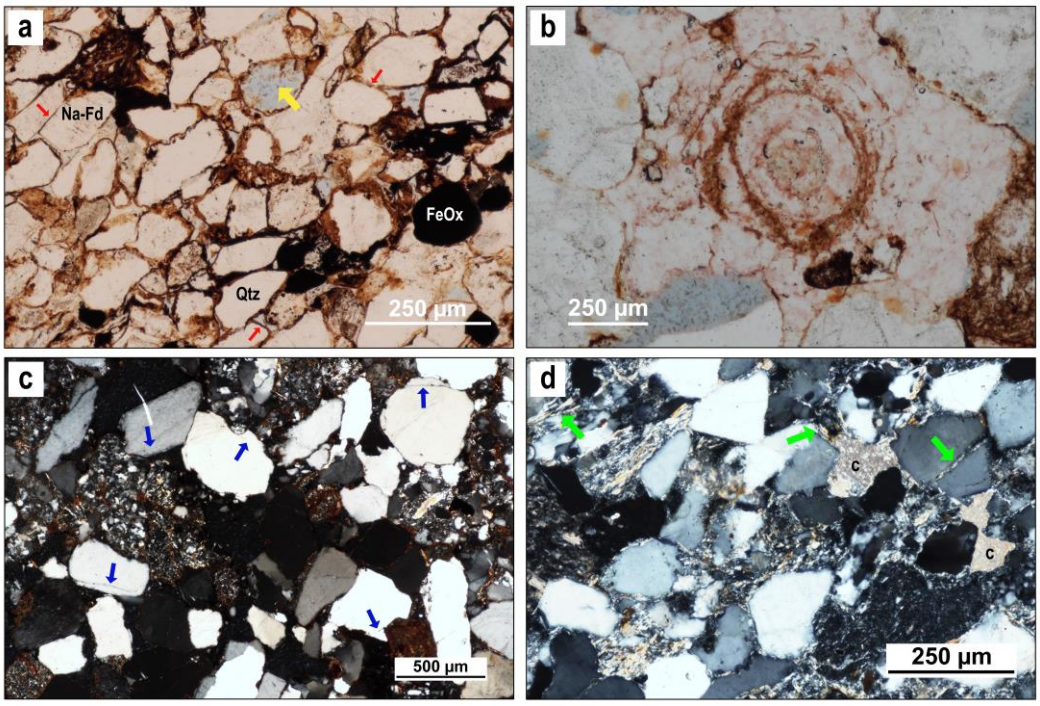

Figure 6-12: Paragenesis observations on Chester Formation surface and subsurface samples through optical microscopy. (a) PPL photomicrograph (sample SSK153725) of iron oxides (FeOx) and clay cutans impregnated with iron oxides (red arrows). The yellow arrow indicates secondary porosity resulting from the partial dissolution of a feldspar; (b) PPL photomicrograph (sample SSK153721) of a concentric-structured dolomitic nodule; (c) XPL photomicrograph (sample 15-1) of abundant quartz overgrowths (blue arrows); (d) XPL photomicrograph (sample SSK153722) of calcite cementation (denoted by 'c') and pore-lining illite (green arrows).

Core and outcrop samples of the Chester Formation show comparable diagenetic evolution, with the primary distinction being the dissolution of calcite cement in outcrop samples due to surface weathering. Variations in petrophysical properties are predominantly governed by mineral composition and microstructural characteristics. Quartz, as the principal mineral phase, enhances the mechanical stability the rock framework. Its high thermal conductivity (~6 to 8 W m^{-1} K^{-1}) significantly influences the overall thermal conductivity of the rock. In contrast, feldspar alteration, leads to the formation of clay minerals. These newly formed clays tend to reduce permeability by obstructing pore spaces. Additionally, their presence decreases porosity by filling voids within the rock matrix (Schön, 2011). The lower thermal conductivity of clay minerals (~0.5 to 2 W m^{-1} K^{-1}) compared to

feldspars (~2 to 3 W m^{-1} K^{-1}) further contributes to a decrease in the thermal conductivity of the samples.

Thermal conductivity is strongly controlled by lithotype and grain connectivity. Pebble-rich sandstones, particularly in core samples, exhibit slightly higher thermal conductivity (2.25 ± 0.01 W m^{-1} K^{-1}). This is likely due to enhanced grain-to-grain contact. Laminated and cross-bedded sandstones display intermediate thermal conductivity values (2.22 ± 0.00 and 1.99 ± 0.01, respectively), attributed to variations in grain packing and mineral distribution. The precipitation of clay minerals tends to reduce thermal conductivity, whereas calcite cementation enhances it by occluding pore spaces and increasing intergranular contact.

These findings underscore the necessity of incorporating lithofacies variability into HSA resource assessment. The interplay between mineral composition, lithotype, microstructures, and diagenetic processes collectively controls the petrophysical and thermal properties of the Chester Formation. Furthermore, the observed similarities between core and outcrop samples emphasise the potential for outcrop analogues in subsurface reservoir characterisation. A comprehensive understanding of these relationships is essential for accurately predicting reservoir quality and geothermal potential of a formation, in particular when extrapolating outcrop data to deep subsurface conditions.

The Chester Formation shares key diagenetic and petrophysical characteristics with analogous sandstone formations across Europe. The Rotliegend sandstones of the North Sea and Germany exhibit a comparable quartz-dominated framework where feldspar alteration led to clay mineral formation, impacting permeability and reservoir quality (Vincent et al., 2018). Similarly to the Chester Formation, these sandstones show substantial calcite cementation at depth, which is typically absent in outcrop equivalents due to meteoric dissolution at the surface. The Buntsandstein Group sandstones of France and Germany are also quartz-dominated, but exhibit variable porosity, largely controlled by feldspar content and clay mineral distribution (Bourquin et al., 2007; Bossennec et al., 2018; Bossennec

et al., 2021). In the Clare Basin sandstones of western Ireland, both compaction and feldspar dissolution are prominent diagenetic processes. In subsurface settings, diagenetic calcite plays a crucial role in cementation, contributing to the structural integrity of the rock. However, in surface exposures, this calcite cement is absent, likely due to meteoric dissolution (Tanner et al., 2018). Across all the western European sandstone formations mentioned, the interdependence of calcite cementation, feldspar dissolution, and secondary porosity emerges as a recurrent theme. These relationships influence the evolution of reservoir properties and underscore the critical role of diagenesis in reservoir quality predictions.

6.2.6. Conclusion

This study systematically evaluated the mineralogical, microstructural, petrophysical, and thermal properties of the Chester Formation, demonstrating significant similarities between surface (i.e., from outcrop exposures) and subsurface (i.e., from cores taken from depths up to 97 mbgl) samples and offering valuable insights for HSA reservoir characterisation. Four key findings emerge:

1. Mineralogical Variability: Quartz constitutes the dominant mineral phase in all samples, generally accounting for over 50% of the rock composition. The primary distinction between both sample types is the occurrence of calcite cementation in core samples, which has been dissolved in outcrop samples likely due to surface weathering. Overall, aside from the dominant mineral (quartz), the mineralogical composition exhibits a high variability between samples.

2. Petrophysical Variability: Core samples typically exhibit reduced porosity and permeability values compared to outcrop samples, principally because of calcite cementation. However, these petrophysical differences are not statistically significant which indicates that porosity and permeability values of outcrop and shallow-depth core samples are comparable. However, a

comparison between petrophysical properties of surface samples and deeper cores (e.g., >1 km) would likely yield statistically significant differences.

3. Thermal Conductivity Variability: Core samples generally demonstrate higher thermal conductivity compared to outcrop samples (2.1 W m^{-1} K^{-1} against 1.8 W m^{-1} K^{-1} on average), reflecting their lower porosity values. This difference was statistically validated through a t-test, confirming a significant disparity between both sample types. Pebble-rich lithotypes tend to exhibit slightly higher thermal conductivity values than other lithotypes. This variation is a product of the interplay of mineralogical composition, grain packing, and diagenetic processes.

4. The measurement of mineralogical, petrophysical and thermal properties of rocks can vary considerably based on sample size, observation scale, and the anisotropy or heterogeneity of the rocks studied. These factors must be carefully considered when evaluating potential geothermal reservoir rocks, particularly in the case of hot sedimentary aquifers.

These findings underscore the significance of initially assessing a HSA geothermal reservoir using cost-effective and readily available surface samples, before committing to the expense of drilling boreholes. Outcrop samples offer valuable insights into the depositional environment and mineralogical characteristics of the geological formation, providing a preliminary understanding of reservoir potential. By examining these surface samples, researchers can gain insightful information about lithological variations and diagenetic processes, thereby improving the accuracy of subsurface predictions and guiding subsequent geothermal exploration efforts.

CRediT Authorship Contribution Statement

Maëlle Brémaud: Conceptualization, Formal analysis, Investigation, Methodology, Validation, Visualization, Writing – original draft, Writing – review & editing. **Neil Murray Burnside:** Conceptualization, Funding Acquisition, Supervision, Writing –

review & editing. **Zoe Kai Shipton:** Conceptualization, Supervision, Writing – review & editing. **Claire Bossennec:** Investigation, Writing – review & editing. **Sven Fuchs:** Supervision, Writing – review & editing. **Fiorenza Deon:** Investigation, Writing – review & editing.

Competing Interests

The authors declare that they have no conflict of interest.

Data availability

Pictures and comprehensive descriptions of the samples are provided in the accompanying files.

Acknowledgements

MB was funded by a University of Strathclyde International Strategic Partner (ISP) Research PhD Studentship. The Strathclyde Hot Disk facility was funded by EPSRC Core Equipment award EP/X034895/1. The analysis at both laboratories was supported by Strathclyde EPSRC IAA funding (as part of award EP/X525820/1). For the purpose of open access, the authors have applied a Creative Commons Attribution (CC BY) licence to any Author Accepted Manuscript version arising from this submission. The authors express their gratitude to the British Geological Survey, particularly the Keyworth National Geological Repository, for providing access to the core samples.

References

Adl-Zarrabi, B., Christianson, R., Sundberg, J., & Wrafter, J. (2010). Measuring anisotropic thermal properties of metagranite at different scales. *Rock Engineering in Difficult Ground Conditions - Soft Rocks and Karst - Proceedings of the Regional Symposium of the International Society for Rock Mechanics, EUROCK 2009*.

Aigner, T., Asprion, U., Hornung, J., Junghans, W. D., & Kostrewa, R. (1996). Integrated outcrop analogue studies for Triassic alluvial reservoirs: examples from southern Germany. *Journal of Petroleum Geology*, *19*(4). https://doi.org/10.1111/j.1747-5457.1996.tb00446.x

A.P.I. (1998). Recommended practices for core analysis. *API Recommended Practice*, *40 ED. 2 REV.*

Bauer, J. F., Krumbholz, M., Meier, S., & Tanner, D. C. (2017). Predictability of properties of a fractured geothermal reservoir: the opportunities and limitations of an outcrop analogue study. *Geothermal Energy*, *5*(1). https://doi.org/10.1186/s40517-017-0081-0

Berkowitz, B. (2002). Characterizing flow and transport in fractured geological media: A review. Advances in Water Resources, 25(8–12). https://doi.org/10.1016/S0309-1708(02)00042-8

Bjørlykke, K. (2015). Petroleum geoscience: From sedimentary environments to rock physics, second edition. In Petroleum Geoscience: From Sedimentary Environments to Rock Physics, Second Edition. https://doi.org/10.1007/978-3-642-34132-8

Bloomfield, J. P., Brewerton, L. J., & Allen, D. J. (1995). Regional trends in matrix porosity and dry density of the Chalk of England. *Quarterly Journal of Engineering Geology*, *28*(Suppl. 2). https://doi.org/10.1144/gsl.qjegh.1995.028.s2.04

Bossennec, C., Géraud, Y., Böcker, J., Klug, B., Mattioni, L., Sizun, J. P., Sudo, M., & Moretti, I. (2021). Evolution of diagenetic conditions and burial history in Buntsandstein Gp. fractured sandstones (Upper Rhine Graben) from in-situ δ18O of quartz and 40Ar/39Ar geochronology of K-feldspar overgrowths. *International Journal of Earth Sciences*, *110*(8). https://doi.org/10.1007/s00531-021-02080-2

Bossennec, C., Géraud, Y., Moretti, I., Mattioni, L., & Stemmelen, D. (2018). Pore network properties of sandstones in a fault damage zone. *Journal of Structural Geology*, *110*. https://doi.org/10.1016/j.jsg.2018.02.003

Bourquin, S., Durand, M., Diez, J. B., Broutin, J., & Fluteau, F. (2007). The permian-triassic boundary and lower triassic sedimentation in western European basins: An overview. *Journal of Iberian Geology*, *33*(2).

Brémaud, M., Burnside, N. M., Shipton, Z., Willems, C. J. L., Pujol, M., & Bossennec, C. (2024). Global database of hot sedimentary aquifer geothermal projects: De-risking future projects by determining key success and failure criteria in the development of a valuable low-carbon energy resource. *Geoenergy*. https://doi.org/10.1144/geoenergy2024-031

Bridge, J. S., & Tye, R. S. (2000). Interpreting the dimensions of ancient fluvial channel bars, channels, and channel belts from wireline-logs and cores. *AAPG Bulletin, 84(8).* https://doi.org/10.1306/a9673c84-1738-11d7-8645000102c1865d

Brown, C. S. (2020). Modelling, characterisation and optimisation of deep geothermal energy in the Cheshire basin (Doctoral dissertation, University of Birmingham).

Cather, M. E., Morrow, N. R., & Klich, I. (1991). Characterization of Porosity and Pore Quality in Sedimentary Rocks. *Studies in Surface Science and Catalysis*, *62*(C). https://doi.org/10.1016/S0167-2991(08)61381-6

Clauser, C., & Huenges, E. (1995). Thermal conductivity of rocks and minerals. *Rock physics and phase relations: a handbook of physical constants*, *3*, 105-126.

Downing, R. A. (1993). Groundwater resources, their development and management in the UK: an historical perspective. *Quarterly Journal of Engineering Geology*, *26*(4). https://doi.org/10.1144/gsl.qjegh.1993.026.004.09

Downing, R. A., & Gray, D. A. (1986). Geothermal resources of the United Kingdom. Journal of the Geological Society, 143(3). https://doi.org/10.1144/gsjgs.143.3.0499

Eschard, E. R., & Doligez, B. (1993). Subsurface reservoir characterization from outcrop observations. Proceedings of 7th IFP Exploration and Production Research Conference, Scarborough, April 1992. *Subsurface Reservoir Characterization from Outcrop Observations. Proceedings of 7th IFP Exploration and Production Research Conference, Scarborough, April 1992*.

Filomena, C. M., Hornung, J., & Stollhofen, H. (2014). Assessing accuracy of gas-driven permeability measurements: A comparative study of diverse Hassler-cell and probe permeameter devices. *Solid Earth*, *5*(1). https://doi.org/10.5194/se-5-1-2014

Flint, S. S., & Bryant, I. D. (1993). The geological modelling of hydrocarbon reservoirs and outcrop analogues. *The Geological Modelling of Hydrocarbon Reservoirs and Outcrop Analogues*.

Gehringer, M., & Loksha, V. (2012). *Geothermal handbook: Planning and Financing Power Generation*. https://www.esmap.org/sites/esmap.org/files/DocumentLibrary/FINAL_Geothermal%20Handbook_TR002-12_Reduced.pdf

Gustafsson, S. E. (1991). Transient plane source techniques for thermal conductivity and thermal diffusivity measurements of solid materials. *Review of scientific instruments*, *62*(3), 797-804.

Holmes, I., Chambers, A. D., Ixer, R. A., Turner, P., & Vaughan, D. J. (1983). Diagenetic processes and the mineralization in the triassic of Central England. *Mineralium Deposita*, *18*(2 Supplement). https://doi.org/10.1007/BF00206485

Jackson, T. (2012). Geothermal potential in great Britain and northern Ireland. Sinclair Knight Merz: Sydney, NSW, Australia.

Li, K. Q., Chen, Q. M., & Chen, G. (2024). Scale dependency of anisotropic thermal conductivity of heterogeneous geomaterials. *Bulletin of Engineering Geology and the Environment*, *83*(3). https://doi.org/10.1007/s10064-024-03571-7

Mikkelsen, P. W., & Floodpage, J. B. (1997). The hydrocarbon potential of the Cheshire Basin. Geological Society Special Publication, 124. https://doi.org/10.1144/GSL.SP.1997.124.01.10

Moore, D. S., McCabe, G. P., & Craig, B. A. (2009). *Introduction to the Practice of Statistics* (Vol. 4). New York: WH Freeman.

Peacock, D. C. P., Sanderson, D. J., & Leiss, B. (2022). Use of Analogue Exposures of Fractured Rock for Enhanced Geothermal Systems. *Geosciences (Switzerland)*, *12*(9). https://doi.org/10.3390/geosciences12090318

Plant, J. A., Jones, D. G., & Haslam, H. W. (1999). The Cheshire Basin: basin evolution, fluid movement and mineral resources in a Permo-Triassic rift setting. *British Geological Survey*.

Plas, L., & Tobi, A. C. (1965). A chart for judging the reliability of point counting results. *American Journal of Science*, 263(1), 87-90.

Pugh, W. (1960). Triassic salt: discoveries in the Cheshire–Shropshire Basin. *Nature*, *187*(4734), 278-279.

Radley, J. D., & Coram, R. A. (2016). The Chester Formation (Early Triassic, southern Britain): sedimentary response to extreme greenhouse climate? *Proceedings of the Geologists' Association*, *127*(5). https://doi.org/10.1016/j.pgeola.2016.08.002

Reyer, D. (2014). Outcrop analogue studies of rocks from the Northwest German Basin for geothermal exploration and exploitation: fault zone structure, heterogeneous rock properties, and application to reservoir conditions (Doctoral dissertation, Niedersächsische Staats-und Universitätsbibliothek Göttingen).

Roduit, N. (2007). JMicroVision : un logiciel d'analyse d'images pétrographiques polyvalent. PhD thesis, Université de Genève. 149, 177, 275, 513

Rollin, K. E., Kirby, G. A., & Rowley, W. J. (1995). Atlas of geothermal resources in Europe: UK revision. British Geological Survey, Regional Geophysics Group.

Schön, J. H. (2011). Physical Properties of Rocks: A Workbook. In *Vasa*.

Schön, J. H. (2015). Physical Properties of Rocks: Fundamentals and Principles of Petrophysics (2nd edition). Developments in Petroleum Science (Elsevier), 65.

Steel, R. J., & Thompson, D. B. (1983). Structures and textures in Triassic braided stream conglomerates ('Bunter'pebble beds) in the Sherwood Sandstone Group, North Staffordshire, England. *Sedimentology*, *30*(3), 341-367.

Student. (1908). The Probable Error of a Mean. *Biometrika*, *6*(1). https://doi.org/10.2307/2331554

Thompson, D. B. (1970). Sedimentation of the Triassic (Scythian) Red Pebbly Sandstones in the Cheshire Basin and its margins. *Geological Journal*, *7*(1). https://doi.org/10.1002/gj.3350070111

Thompson, D. B., Pilling, D., & Macchi, L. (1985). *Field Excursion to the Permo-Triassic of the Cheshire-East Irish Sea-Needwood and Stafford Basins*. Poroperm-Geochem.

Vincent, B., Waters, J., Witkowski, F., Daniau, G., Oxtoby, N., Crowley, S., & Ellam, R. (2018). Diagenesis of Rotliegend sandstone reservoirs (offshore Netherlands): The origin and impact of dolomite cements. *Sedimentary Geology*, *373*. https://doi.org/10.1016/j.sedgeo.2018.06.012

Warrington, G. (1980). The Alderley Edge mining district. *Amateur Geologist*, *8*, 4-13.

Warrington, G., & Ivimey-Cook, H. C. (1992). Triassic. 97-106 in Atlas of palaeogeography and lithofacies. Cope JCW, Ingham J K & Rawson PF. Geological Society of London Memoir, 13.

Weydt, L. M., Bär, K., Colombero, C., Comina, C., Deb, P., Lepillier, B., Mandrone, G., Milsch, H., Rochelle, C. A., Vagnon, F., & Sass, I. (2018). Outcrop analogue study to determine reservoir properties of the Los Humeros and Acoculco geothermal fields, Mexico. *Advances in Geosciences*, *45*. https://doi.org/10.5194/adgeo-45-281-2018

Witter, J. B., Trainor-Guitton, W. J., & Siler, D. L. (2019). Uncertainty and risk evaluation during the exploration stage of geothermal development: A review. In Geothermics (Vol. 78). https://doi.org/10.1016/j.geothermics.2018.12.011

CHAPTER 7
Enhancing Assessment of Thermal Properties for HSA Reservoirs

7.1. Introduction

Chapter 6 demonstrated substantial similarities between surface (i.e., from outcrop exposures) and subsurface (i.e., from cores) samples of the Chester Formation from the Cheshire Basin (UK) regarding mineralogical, microstructural, petrophysical, and thermal properties. Quartz was identified as the predominant mineral phase in all samples, generally comprising over 50% of the rock composition. While core samples typically exhibited lower porosity and permeability than outcrop samples, the difference was not statistically significant. This suggested that permeability and porosity values of outcrop samples and shallow-depth core samples are comparable. In contrast, thermal conductivity was consistently higher in core samples than in outcrop samples. This variation was interpreted as a product of the interplay of mineralogical composition, grain packing, and diagenetic processes.

These findings emphasise the value of utilising cost-effective and readily available surface outcrop samples for preliminary assessments of HSA reservoirs before committing to the expense of drilling boreholes. Outcrop samples provide valuable insights into lithological variations and diagenetic processes of a geological unit, thereby enhancing the accuracy of subsurface predictions and guiding future geothermal exploration efforts.

Building on this foundation, the present chapter examines the thermal properties of the same Chester Formation samples under water-saturation and increasing temperature conditions. Thermal conductivity is a critical parameter influencing the efficiency of heat transfer within the reservoir, but is commonly measured under ambient laboratory conditions due to practical and economic constraints.

Such measurements may not accurately reflect in situ reservoir conditions, where temperature, pressure, and water saturation influence thermal transport processes. This chapter systematically compares thermal measurements conducted under ambient conditions with those performed under replicated in situ conditions (i.e., reservoir temperature and saturation). The implications of these findings for the assessment and characterisation of HSA reservoirs are discussed.

This chapter is being written up for publication. I contributed to the paper with: Writing – Original Draft, Writing – Review & Editing, Conceptualization, Methodology, Validation, Investigation, Data Curation, Visualization**.** Other Authors: **Neil Murray Burnside:** Conceptualization, Funding Acquisition, Supervision, Writing – review & editing. **Zoe Kai Shipton:** Conceptualization, Supervision, Writing – review & editing. **Sven Fuchs:** Supervision, Writing – review & editing. **Robert Peksa:** Methodology.

7.2. Publication

Comparative Evaluation of Thermal Conductivity in Sandstones: Ambient vs. In Situ Conditions for Geothermal Reservoir Assessment in the UK

Maëlle Brémaud[1,2], Neil M. Burnside[1], Zoe K. Shipton[1], Sven Fuchs[3], Robert Peksa[3]

[1]Department of Civil and Environmental Engineering, University of Strathclyde, Glasgow G1, 1XJ, UK

[2]JRG Energy, 6B Waipāhīhī Avenue, Hilltop, Taupō 3330, New-Zealand

[3]GFZ German Research Centre for Geosciences, Section 4.8, Geoenergy, Telegrafenberg, Potsdam, 14473, Germany

Correspondence to: Maëlle Brémaud (maelle.bremaud@strath.ac.uk)

Keywords

geothermal reservoir, hot sedimentary aquifer, thermal conductivity, sandstone, in situ experiment

Abstract

Thermal conductivity is a crucial parameter for geothermal resource and heat flow assessments. Although it is commonly determined under ambient laboratory conditions, such measurements may not accurately reflect in situ reservoir conditions due to changes in temperature, pressure, and water saturation with depth. This study investigates the impact of temperature and water saturation on the thermal conductivity of sandstone samples from the Cheshire Basin (UK) to enhance the accuracy of geothermal resource evaluations. Thermal conductivity measurements were conducted using optical scanning and transient plane source methods under both ambient and in situ temperature and saturation conditions. The results indicate that water saturation significantly increases the thermal conductivity of the samples (by c. 2.2 W m^{-1} K^{-1}), highlighting the importance of accounting for fluid content in geothermal evaluations. However, this magnitude of increase may not be solely attributable to fluid replacement effects and could be influenced by additional experimental factors, such as microstructural changes within the samples. The effect of water saturation on thermal conductivity is more pronounced in higher-porosity samples, underscoring the necessity of incorporating porosity measurements alongside thermal analysis for a more comprehensive geothermal assessment under in situ conditions. A gradual decrease in thermal conductivity is observed with increasing temperature (c. 0.1 W m^{-1} K^{-1} from 20°C to 90°C). The combined influence of water saturation and elevated temperature was explored using two innovative experimental setups which reveal a complex interaction. These findings emphasise the value of performing in situ thermal property measurements to better predict heat flow and geothermal resource potential. The results highlight how such measurements can improve the reliability of geothermal reservoir predictions, reduce uncertainties, and inform decision-making, thereby enhancing the economic feasibility and

sustainability of geothermal energy projects. Future research could incorporate pressure effects alongside temperature and water saturation to further refine geothermal reservoir assessments.

7.2.1. Introduction

Thermal processes are fundamental in controlling heat transfer within sedimentary basins, directly affecting the viability of geothermal systems (Huenges, 2010; Muffler and Cataldi, 1978). In hot sedimentary aquifers (HSAs) – defined as large and conductive sedimentary aquifers that are hot enough and have sufficient productivity to constitute a potential geothermal resource (Gillespie et al., 2013)− the thermal conductivity of reservoir rocks governs heat flow and reservoir performance in conjunction with the geothermal gradient. As a key thermophysical property of rocks, thermal conductivity is essential for reconstructing the thermal history of sedimentary basins (Liu et al., 2011; Clauser and Huenges, 1995). It plays a critical role in shaping the thermal structure of basins and facilitating the identification of geothermal targets at both regional and local scales (Fuchs et al., 2020). Additionally, thermal conductivity critically influences reservoir sustainability by controlling the rate at which heat is replenished from the surrounding formation into thermally depleted zones near production wells. Higher thermal conductivity enhances heat recharge, mitigating rapid cooling and prolonging the operational lifespan of the system (Blázquez et al., 2017; García-Noval et al., 2024; Marelis, 2017; Murthy et al., 2023; Sipio and Bertermann, 2018; van Rijn, 2018).

Measurement of rock sample thermal conductivity under ambient lab conditions is a well-established approach. Such measurements are valuable for preliminary assessments and offer an approximate estimate of the thermal conductivity of specific rock types. However, reservoir thermal values may differ significantly from ambient-condition laboratory measurements which fail to account for in situ saturation, temperature and pressure conditions at depth. It is well established that thermal conductivity of clastic rocks decreases with increasing temperature (e.g., Vosteen and Schellschmidt, 2003; Labus and Labus, 2018). While thermal

conductivity generally increases approximately linearly with pressure, likely due to enhanced grain-to-grain contact under higher pressures, this effect is less pronounced compared to the impact of temperature (e.g., Anand et al., 1973; Midttømme and Roaldset, 1999; Abdulagatov et al., 2006). Additionally, thermal conductivity tends to be higher in water-saturated samples, primarily because water has a higher thermal conductivity than air (Nagaraju and Roy, 2014; Midttømme and Roaldset, 1999). Variations in rock texture and mineral composition further contribute to discrepancies between thermal conductivity measured at ambient and reservoir conditions. Elevated temperatures at reservoir depths, for instance, can alter intergranular contacts and mineralogical properties by altering the intrinsic thermal conductivity of minerals, inducing thermal expansion, and promoting phase transitions or water-rock interactions. These effects can modify grain contacts, porosity, and heat transfer mechanisms, leading to differences in thermal conductivity between ambient and reservoir conditions (Seipold, 1998; Vosteen and Schellschmidt, 2003). As a result, it is important to establish if ambient-condition experiments adequately reflect the in situ behaviour of rocks, particularly in heterogeneous lithologies with diverse mineralogical and pore structures.

In this paper, we aim to (1) compare thermal conductivity measurements under ambient and in situ reservoir conditions, and (2) assess how the results can influence the evaluation of hot geothermal sedimentary reservoirs. Thermal conductivity measurements were performed on sandstone samples from the Cheshire Basin (UK) using two methods: optical scanning technology, and the transient plane source method. These techniques were selected to evaluate whether they yield consistent results, allowing for cross-validation and assessment of potential methodological discrepancies.

Currently, no standard laboratory device can reproduce simultaneously in situ temperature and pressure conditions on rock samples of representative sample size (Norden et al. 2020), although specific experimental setups led to limited measurements including the combined effect (Aliverdiev et al., 2024). Therefore,

only temperature and water saturation are used for simulating reservoir conditions in this study.

7.2.2. Data Collection

7.2.2.1. Study Area

The Cheshire Basin is a north-south trending rift system located in northwest England, that was initiated during Early Permian. The basin extends for approximately 105 km and varies between 30 and 50 km in width (Fig. 7-1). The development of the basin was controlled by major syn-depositional normal faults that delineate its boundaries. The Cheshire Basin contains a sedimentary infill of Permo-Triassic and Early Jurassic deposits, with thicknesses locally exceeding 4 km (Evans et al., 1993; Chadwick, 1997; Plant et al., 1999).

The main formations of the Sherwood Sandstone Group (SSG) include the Kinnerton Sandstone Formation, the Chester Pebble Beds Formation, the Wilmslow Sandstone Formation, and the Helsby Sandstone Formation (Warrington et al., 1980). The Late Permian to Middle Triassic Chester Pebble Beds, also referred to as the Chester Formation, is one of the lowermost stratigraphic units of the SSG. This formation comprises red-bed sequences deposited within a braidplain environment (Radley and Coram, 2016).

The Chester Formation is found at various depths and therefore different in situ temperatures within the Cheshire Basin. Using corrected bottom-hole-temperature (BHT) data (e.g., Burley et al., 1984; Rollin, 1995; Busby et al., 2011), Busby (2014) suggested a basin-wide geothermal gradient of 27°C/km. Considering this geothermal gradient with the reservoir depths of the Chester Formation, four regular temperature steps were selected for the thermal analyses to represent likely in situ reservoir conditions: 30, 50, 70, and 90 °C.

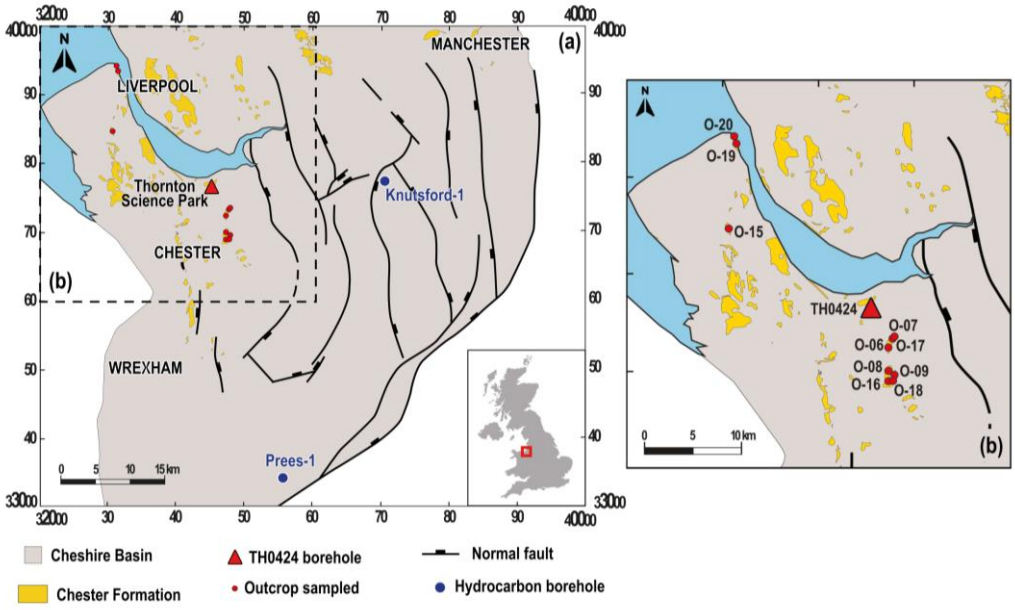

Figure 7-1: (a) Distribution of the Chester Formation outcrops in the Cheshire Basin and (b) area of interest with locations of the core samples (red triangle) and outcrop samples (red circles)(Brémaud et al., 2025, under review (Chapter 6)). Basin structure is reproduced from Mikkelsen and Floodpage (1997).

7.2.2.2. Location and Collection of the Samples

Samples of the Chester Formation were obtained from outcrop exposures and core material (Fig. 7-1). Outcrop locations were identified along roadways in the northern Cheshire Basin using BGS geological maps and the Street View feature in Google Maps. A total of 16 samples were collected at outcrop exposures. The core samples were acquired from an open bedrock borehole drilled for geophysical and hydrogeological research at the UKGEOS Cheshire site at Thornton Science Park (Kingdon et al., 2020). The TH0424 borehole, drilled to a depth of 100 m in 2021, targeted the Chester Formation. From the original borehole core, 21 sub-cores, each 2 inches in diameter, were extracted for analysis. A comprehensive comparative analysis of petrophysical, thermal and mineralogical properties of both sample types at ambient conditions was conducted in Chapter 6 (Brémaud et al., 2025, under review), therefore discrepancies in the results between core and outcrop samples are not further discussed in this Chapter.

7.2.3. Methods

Thermal conductivity measurements were performed using two methods: the optical scanning technology (thermal conductivity scanner, TCS; Popov et al., 1999), and the transient plane source method (TPS, Gustafsson, 1991). Table 7-1 summarises the experiments conducted using the TCS and TPS devices under various conditions, i.e., different temperatures and saturation states. The experiments were carried out at two facilities: The University of Strathclyde's Civil and Environmental Engineering (CEE) Laboratory, and GFZ Thermal Petrophysics Lab (Table 7-1).

Table 7-1: Devices and experimental conditions for the thermal conductivity experiments performed. TCS = thermal conductivity scanner; TPS = transient plane source.

Temperature	Sample state	Repeated measurements	Thermal kit used	Facility
Ambient (~20°C)	Dry	3	TCS	GFZ Lab
		3	TPS	GFZ Lab
Increasing temperature steps (50°C, 70°C, 90°C)	Dry	3	TPS	GFZ Lab
Ambient (~20°C)	Saturated	5	TCS	GFZ Lab
Increasing temperature steps (30°C, 50°C, 70°C, 90°C)	Saturated	5	TPS	GFZ Lab, CEE Laboratory

To prepare samples for measurements in the dry state, they were oven-dried at 60°C until they reach a constant weight (24 hours minimum). For thermal conductivity measurements on saturated rock samples, the specimens were first immersed in water within a sealed vacuum desiccator for 48 hours. For each sample, three identical scan cycles were performed on dry specimens, and five on water-saturated samples to enhance the statistical reliability of the measurements. The mean values from all cycles were averaged to the final conductivity value, with error bars in Figs. 7-6b, 7-7 and 7-8, or values in the text, representing the standard deviation of these repeated measurements.

7.2.3.1. Thermal Conductivity Scanner (TCS)

Optical scanning was performed using the TSCAN thermal conductivity scanner (TCS) manufactured by Lippmann Geophysical Instruments. This method required rock samples to be coated with black paint to unify the optical reflection coefficients across the rock (Popov et al., 1999). Samples remained stationery on a scanning platform, and the test was performed by moving the scanning unit (Fig. 7-2). Prior to heating, the initial temperature was recorded by the front sensor. The central heat source heated the sample, and the rear sensors *Th* and *Td* subsequently measured the peak temperature rise following the heating phase (Fig. 7-2). The mean thermal conductivity on the surface of sample along the scanning line was then derived. Several samples of similar thermal conductivity can be placed in parallel (and therefore measured) in the platform to speed up the process. Each scanning cycle required two to three minutes to complete. A total of 31 rock cores and outcrop samples were analysed under dry (oven-dried and air-saturated) conditions, and five samples were discarded due to their insufficient size. The systematic accuracy of the device was reported by Popov et al (1999) as 3% (for a confidence probability of 0.95) for thermal conductivity.

Thermal conductivity measurements on saturated samples involved an initial saturation process, as outlined previously. Following saturation, samples were removed from the water, and any excess water was removed by briefly pressing a paper towel against the bottom of the specimen. The samples were then positioned on the scanning platform, and the analysis was conducted following the same procedure as for the dry samples. A total of 30 samples were analysed under water saturation conditions, except for the mudstone sample (SSK153715).

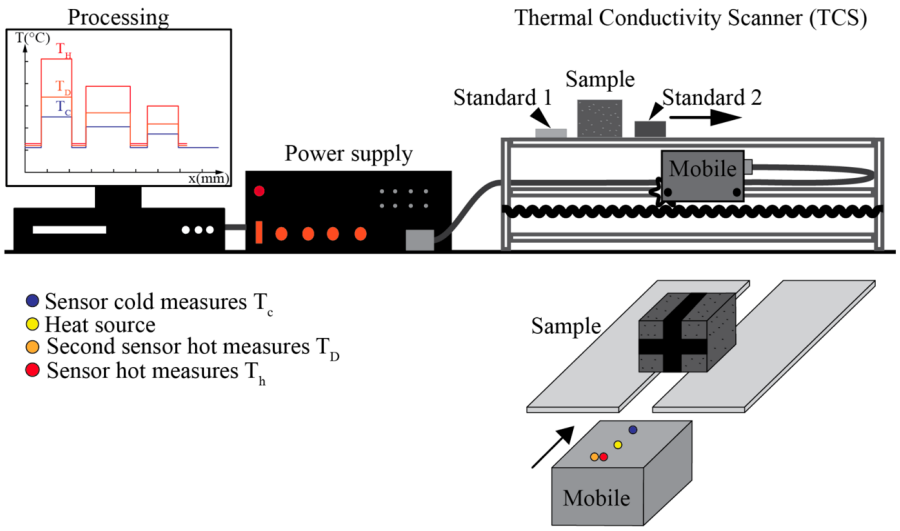

Figure 7-2: Scheme of the optical scanning apparatus (Navelot, 2018). The initial (cold) temperature Tc is recorded by the front sensor noted as Tc. Once the sample is heated by the heat source, the hot temperature is measured by two rear sensors to obtain Th and Td (the latter is utilised to determining thermal diffusivity).

7.2.3.2. Transient Plane-Source Technique (TPS)

TPS measurements were done using a Hot Disk TPS 1500 at GFZ Thermal Petrophysics Lab, and a TPS 2500 S at University of Strathclyde's CEE Laboratory. This method uses a transiently heated plane sensor with an electrically conducting circular double spiral teched out of a thin Nickel foil, that is used as both a resistance thermometer and a heat source. The disk was sandwiched between two thin sheets of Kapton (an electrical insulator). Two Kapton Hot Disk Sensors were used: 5501 F2 (radius: 6.4mm) for larger samples, and 5465 F1 (radius: 3.2mm) for thinner and/or smaller samples. The rule of thumb for choosing the right sensor is as follows: (1) the thickness of the sample should be at least equal to the sensor radius, and (2) the diameter of the sample must be at least equal to two times the sensor diameter. During the measurements, the sensor was fitted between two saw-cut pieces of the sample to be tested, and an electric current was run through the spiral which raised both its temperature and resistance (Fig. 7-3). Thermal properties (thermal conductivity, thermal diffusivity and specific heat capacity) of the sample were then deduced by monitoring this temperature increase

(Gustafsson, 1991). The accuracy of the Hot Disk device is given with +/- 5%, and the reproducibility of the measurements is within +/- 2%.

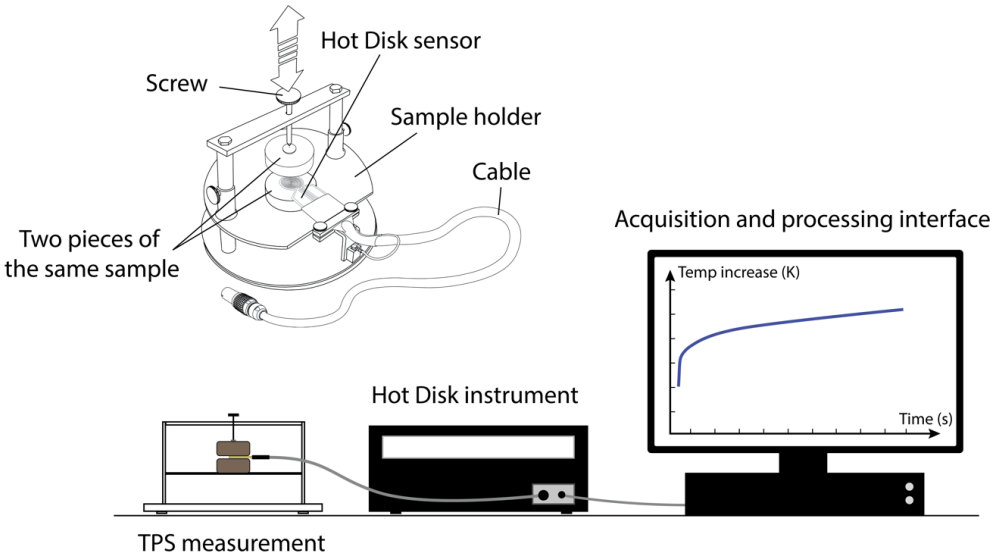

Figure 7-3: Schematic of a Hot Disk measurement at ambient temperature. Upper scheme shows the detailed setup (modified from Hot Disk, 2019)

7.2.3.2.1. Thermal measurements on dry samples

Thermal conductivity measurements under ambient temperature conditions were conducted at GFZ Thermal Petrophysics Lab on 31 samples, each sample undergoing three measurement runs. Five samples were excluded from analysis due to their insufficient size being incompatible with the available sensors.

Thermal conductivity analyses on dry samples under increasing temperature conditions required the use of a temperature control unit (TCU). The convection oven used for heating had a maximum chamber temperature of 600°C, with a temperature stability of ±0. 5°C. The heating process was automatically regulated via the Hot Disk Desktop application. A total of 29 samples were analysed at three elevated temperature levels: 50°C, 70°C, and 90°C. Three thermal conductivity measurements were performed at each temperature step.

7.2.3.2.2. Thermal measurements on water-saturated samples

Two novel experimental setups were developed for the analysis of saturated samples under elevated temperatures. Both consisted of TPS thermal conductivity measurements with a 5501 sensor.

Experiment A: Circulating water bath approach, GFZ Thermal Petrophysics Lab. Employed a Polystat CC2 heated circulating bath equipped with a temperature controller. To prevent submersion of the cable-sensor connection, the Hot Disk sensor was oriented vertically, and fully submerged, in the water and positioned between two sample pieces, all held in place by a single clamp. (Fig. 7-4a).

Experiment B: Convection water bath, Strathclyde's CEE Laboratory. Employed a JB Nova water bath, covered with a lid to minimise water loss from condensation, with a small gap to accommodate the sensor cable. An extended version of the 5501 sensor was used, allowing the connection between the cable and the sensor to be positioned 10 cm above the water level, to reduce risk of moisture ingress into the connection. Two clamps were used to securely fasten the sample pieces around the sensor (Fig. 7-4b).

These experimental configurations required manual control of temperature stability at four temperature steps : 30, 50, 70, and 90°C. A total of nine samples – four from outcrop exposures and five from cores – were analysed using both approaches, with five thermal conductivity measurements recorded per temperature step. Prior to thermal analysis, samples were submerged in a water-filled, sealed vacuum desiccator for 48h to ensure full saturation.

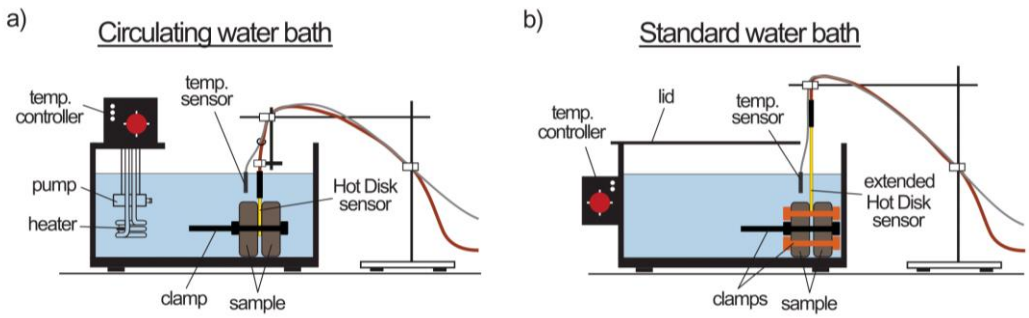

Figure 7-4: Comparison of the two experimental set ups designed to measure thermal conductivity under water-saturated conditions at different temperature steps. Temperature and Hot Disk sensor cables are connected to the Hot Disk instrument, as shown in Fig. 7-3. a) Circulating water bath with a pump and a heater deployed at GFZ Thermal Petrophysics Lab. b) Standard (convection) water bath with a lid and an extended Hot Disk sensor deployed at Strathclyde's CEE Laboratory.

7.2.3.3. Porosity measurements

In order to better assess the impact of water saturation on thermal conductivity, effective porosity was measured using the water immersion technique (WIP) that follows Archimedes' principle. Thirty-four samples were first oven-dried at 60°C for 24 hours (or until constant weight) and subsequently weighted to obtain the dry mass (m_{dry}). The samples were then placed in a desiccator, vacuum was applied, and the samples were saturated with distilled water. Following a 48h saturation period, the samples were weighted in two conditions: 1) under water to obtain the hydrostatic mass (m_{hydro}) and 2) in air while still saturated (m_{sat}). Porosity was then computed using Eq. (7-1) (Bloomfield et al., 1995; A.P.I., 1998):

$$\phi = \frac{m_{sat} - m_{dry}}{m_{sat} - m_{hydro}} \cdot 100 \qquad (7\text{-}1)$$

Two samples were excluded from the porosity measurements: the mudstone specimen (SSK153715) and a friable sample (16-2).

7.2.4. Results

7.2.4.1. Influence of Water Saturation

Porosity and thermal conductivity measurements at ambient temperature (approximately 21°C) are presented in Table 7-2. The porosity values ranged from 12.8% to 30.6%, with an average of 20.8% (Fig. 7-5a). Thermal conductivity measurements in the dry state varied between 1.63 and 2.99 W m^{-1} K^{-1} (TCS), and between 1.07 and 2.90 W m^{-1} K^{-1} (TPS), with mean values of 2.32 ± 0.02 W m^{-1} K^{-1}

(TCS) and 1.96 ± 0.02 W m^{-1} K^{-1} (TPS) respectively (Figs. 7-5b, 7-5c). Under water-saturated conditions at ambient laboratory temperature, thermal conductivity measurements obtained from optical scanning (TCS) ranged from 3.47 to 5.15 W m^{-1} K^{-1}, with a mean of 4.47 ± 0.05 W m^{-1} K^{-1} (Fig. 7-5d). Thermal conductivity was significantly higher under water-saturated conditions compared to dry conditions for the same samples (Fig. 7-6a). The average increase in thermal conductivity observed between the dry and water-saturated states was c. 2.2 W m^{-1} K^{-1}. The associated trendlines (Fig. 7-6a) showed a decrease in thermal conductivity with increasing porosity, with a more pronounced decrease observed in dry samples. None of the samples measured with the TCS aligned with the $\lambda_{dry} = \lambda_{sat}$ line, as they plot in the upper section of the graph (Fig. 7-6b). This observation confirmed that, for the sandstone specimens analysed, thermal conductivity was higher in water-saturated samples compared to their dry counterparts.

Table 7-2: Measured values of effective porosity, and thermal conductivity under dry and water-saturated conditions at ambient lab temperature conditions using the TCS and TPS techniques.

Sample ID	Sample Type	WIP (%)	Thermal conductivity (W m^{-1} K^{-1})		
			TCS		TPS
			λ_{dry}	λ_{sat}	λ_{dry}
SSK153718	Core sample	19.65	2.26	4.06	2.10
SSK153716	Core sample	20.79	2.18	4.25	1.93
SSK153729	Core sample	17.71	2.67	4.55	2.27
SSK153713	Core sample	24.52	2.23	3.9	1.68
SSK153724	Core sample	16.53	2.55	4.56	2.22
SSK153728	Core sample	19.80	2.25	4.91	2.17
SSK153717	Core sample	18.34	2.65	4.11	2.12
SSK153720	Core sample	22.49	2.34	4.65	2.01
SSK153711	Core sample	23.82	2.36	4.45	1.87
SSK153712	Core sample	25.25	2.26	4.15	1.80
SSK153722	Core sample	12.75	2.28	4.32	2.22
SSK153727	Core sample	17.84	2.47	4.74	2.35
SSK153714	Core sample	25.00	2.57	4.42	1.83
SSK153715	Core sample	-	1.75	-	1.60
SSK153707	Core sample	21.39	2.48	4.49	1.86
SSK153730	Core sample	18.18	2.86	5.13	2.28
SSK153723	Core sample	15.26	2.58	4.84	2.26
SSK153725	Core sample	13.93	2.43	3.91	2.07

SSK153719	Core sample	20.30	2.56	4.61	2.07
SSK153721	Core sample	14.74	2.99	4.88	2.90
SSK153726	Core sample	20.00	2.51	4.89	1.94
06-1	Outcrop sample	26.19	-	-	-
06-2	Outcrop sample	30.61	-	-	1.07
07-1	Outcrop sample	23.04	2.29	4.68	-
07-2	Outcrop sample	22.22	-	-	1.83
08-1	Outcrop sample	21.09	2.55	5.15	2.16
08-2	Outcrop sample	24.93	2.03	4.45	1.72
09-1	Outcrop sample	20.53	2.05	4.56	1.80
15-1	Outcrop sample	22.43	2.02	4.68	1.69
16-1	Outcrop sample	23.13	2.2	4.6	1.84
16-2	Outcrop sample		1.63	3.47	1.60
16-3	Outcrop sample	19.18	-	-	-
17-1	Outcrop sample	26.69	1.88	4.79	-
18-1	Outcrop sample	19.86	-	-	-
19-1	Outcrop sample	22.53	2.14	4.27	1.79
20-2	Outcrop sample	22.84	2.02	4.32	1.71

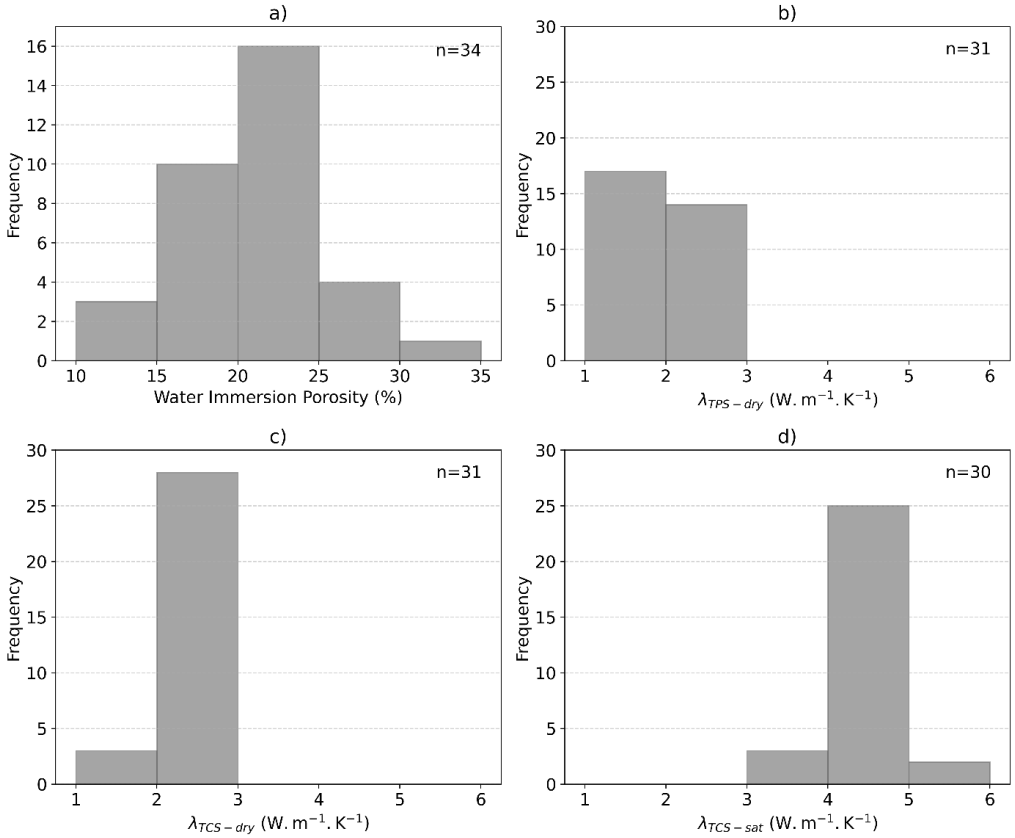

Figure 7-5: Histograms of the distribution of a) water immersion porosity; and thermal conductivity b) on dry samples using the TPS; c) on dry samples using the TCS; and d) on water-saturated samples using the TCS. The total number of samples analysed is presented in the upper-right corner of each figure.

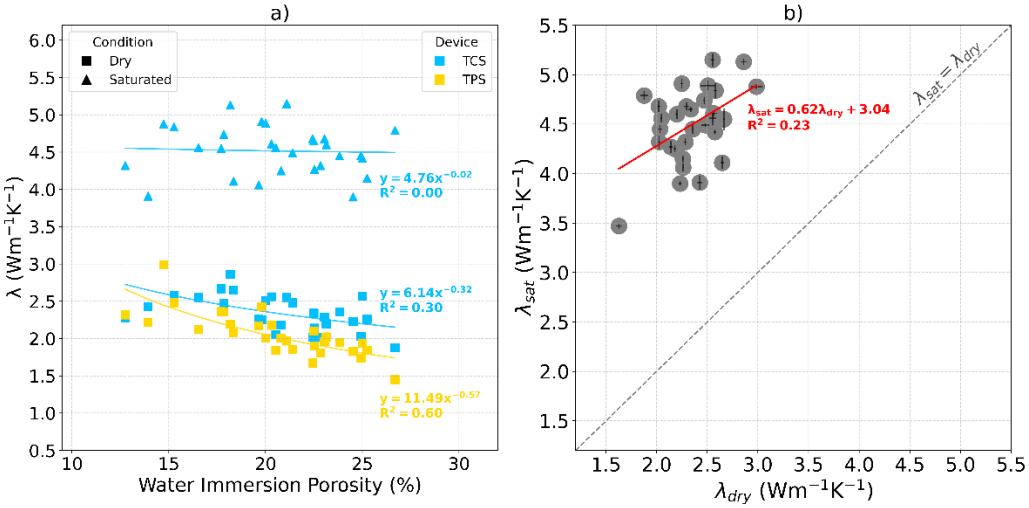

Figure 7-6: a) Thermal conductivity under dry (square symbol) and water-saturated conditions (triangle symbol) as a function of porosity. Conductivity measurements using the TCS and TPS are displayed in blue and gold respectively. The power regression lines for each data set are

displayed in the corresponding colour. b) Comparison of thermal conductivities measured under dry (λ_{sat}) and water-saturated (λ_{dry}) conditions using the TCS device. Standard deviations are indicated by black lines and a linear regression line is shown in red.

7.2.4.2. Temperature Effect

Results of thermal conductivity measurements at increasing temperatures are listed in Table 7-3, with values ranging between 1.12 and 2.73 W m^{-1} K^{-1}, 1.11 and 2.71 W m^{-1} K^{-1}, and from 1.12 to 2.67 W m^{-1} K^{-1} at 50, 70 and 90°C, respectively. The average thermal conductivity at 50°C, 70°C and 90°C was 1.97 ± 0.30 W m^{-1} K^{-1}, 1.95 ± 0.29 W m^{-1} K^{-1}, and 1.89 ± 0.28 W m^{-1} K^{-1}, respectively. These values were lower than those measured at ambient temperature (Table 7-2). A slight decline in thermal conductivity was observed with increasing temperature (Fig. 7-7), with a mean decrease of 0.1 W m^{-1} K^{-1} between ambient temperature (c. 21°C, Table 7-2) and 90°C.

Table 7-3: Dry sample thermal conductivity values at elevated temperature steps (50°C, 70°C, and 90°C). Measurements are done using the TPS device.

Sample ID	Thermal conductivity (W m^{-1} K^{-1})		
	50°C	70°C	90°C
SSK153718	2.07	2.01	1.95
SSK153716	1.9	1.89	1.84
SSK153729	2.22	2.18	2.09
SSK153713	1.65	1.67	1.6
SSK153724	2.22	2.14	2.11
SSK153728	2.31	2.26	2.15
SSK153717	2.06	2.07	1.95
SSK153720	1.94	1.92	1.83
SSK153711	1.88	1.86	1.73
SSK153712	1. 76	1.76	1.7
SSK153722	2.19	2.23	2.18
SSK153727	2.32	2.31	2.21
SSK153714	1.83	1.82	1.72
SSK153715	1.67	1.69	1.66
SSK153707	1.81	1.83	1.73
SSK153730	2.22	2.13	2.10
SSK153723	2.35	2.27	2.21
SSK153725	2.08	2.05	2.04

SSK153719	2.07	2.02	1.96
SSK153721	2.73	2.71	2.67
SSK153726	2.02	1.98	1.86
06-2	1.12	1.11	1.12
07-2	1.78	1.75	1.7
08-1	2.08	2.12	2.1
08-2	1.69	1.73	1.68
15-1	1.77	1.69	1.69
16-1	1.82	1.8	1.77
19-1	1.82	1.79	1.76
20-2	1.68	1.69	1.6

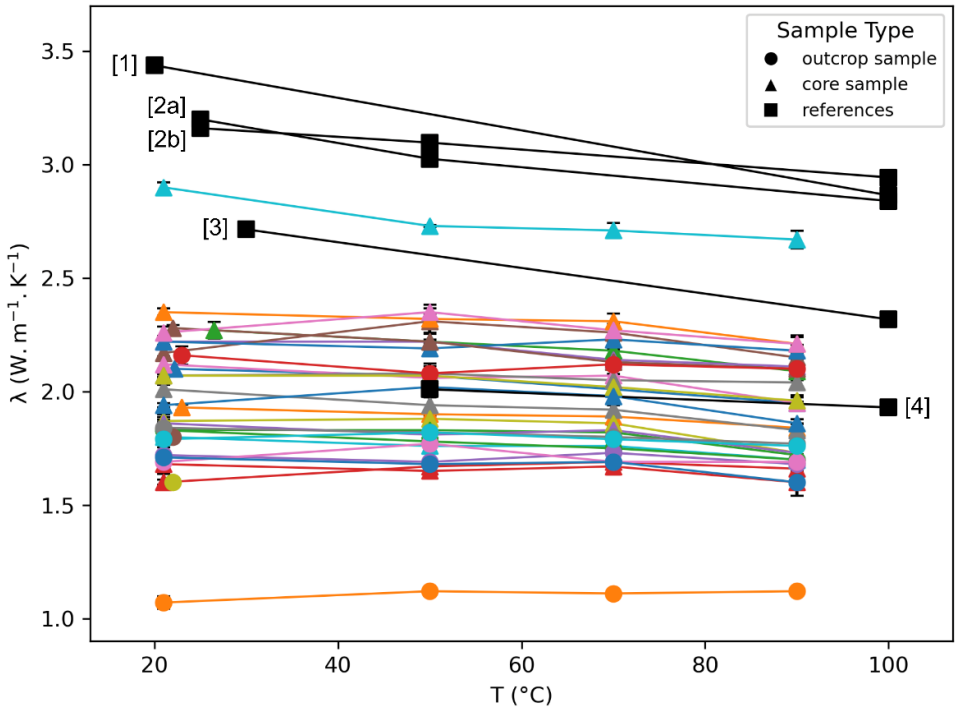

Figure 7-7: Thermal conductivity as a function of temperature for the 29 samples investigated. Sample types are differentiated with different markers: circles are outcrop samples and squares are core samples. Error bars (standard deviations) are shown at each temperature step for each sample. Black lines and markers correspond to previous results found in the literature, including [1] sandstone from a sedimentary basin in China (Hartlieb et al., 2015), [2a] a conglomerate of unknown origin (Chen et al., 2021); [2b] a sandstone of unknown origin (Chen et al., 2021); [3] a mix of sandstone and carbonate rocks from the Eastern Alps (Vosteen and Schellschmidt, 2003); and [4] a sandstone from a borehole in Aktash, Dagestan, Russia (Abdulagatov et al., 2006).

This decrease was more pronounced in samples showing higher thermal conductivity under ambient laboratory conditions, as illustrated by the difference in slopes between sample SSK153721 (blue upper line) and sample 06-2 (orange lower line). Additionally, samples collected from outcrop exposures typically exhibited lower thermal conductivity values compared to subsurface core samples (Fig. 7-7). The mean thermal conductivity of outcrop samples was 1.72 ± W m^{-1} K^{-1} at 50°C, 1.71 ± 0.26 W m^{-1} K^{-1} at 70°C, and 1.68 ± W m^{-1} K^{-1} at 90°C, whereas core samples displayed higher mean values of 2.06 ± 0.25 W m^{-1} K^{-1} at 50°C, 2.04 ± 0.24 W m^{-1} K^{-1} at 70°C, and 1.97 ± 0.25 W m^{-1} K^{-1} at 90°C. Some samples presented a slight increase in thermal conductivity between some temperature steps, which can be attributed to three primary factors: the ±5% error margin of the device, the measurement uncertainties indicated by black error bars in Fig. 7-7, and some minor inconsistencies encountered with the convection oven. Insufficient cooling time between successive measurement sets (i.e. thermal analysis from 50 to 90°C for a given sample) might have prevented the sensor from properly cooling down, leading to a slight upward shift in thermal conductivity values between measurements at ambient laboratory and at 50°C for some samples (SSK153728, SSK153715, SSK153723, SSK153725, SSK153726, 15-1, 19-1). This may account for the observed small increase in thermal conductivity between ambient conditions and the measurement at 50°C.

7.2.4.3. Combined Impact of Saturation and Temperature

Thermal conductivity measurements under water-saturated conditions at selected temperatures steps are listed in Table 7-4 and shown in Fig. 7-8.

Table 7-4: Thermal conductivity measurements under water-saturated conditions and progressively increasing temperature steps for Experiment A and B. The reported values represent the mean thermal conductivity derived from five repeated measurements. All measurements are included in a supplementary file to this paper (Appendix D). The thermal conductivity values of SSK153711 and 08-1 at 90°C were not reported as results were inconclusive (no definitive measurement could be obtained).

Sample ID	Sample Type	Experiment A				Experiment B			
		30°C	50°C	70°C	90°C	30°C	50°C	70°C	90°C
SSK153718	Core samples	3.20	3.19	3.11	3.05				
SSK153713		3.08	3.05	3.03	2.98				
SSK153730		4.4	4.24	4.13	3.95	4.39	4.26	4.13	4.12
SSK153711						3.44	3.28	3.2	-
SSK153723						4.04	3.87	3.85	3.73
08-1	Outcrop samples	2.96	2.83	3.00	-				
08-2						3.24	3.16	3.22	3.19
19-1		2.99	2.93	2.88	3.06	3.51	3.41	3.31	3.33
20-2						3.27	3.16	3.15	3.13

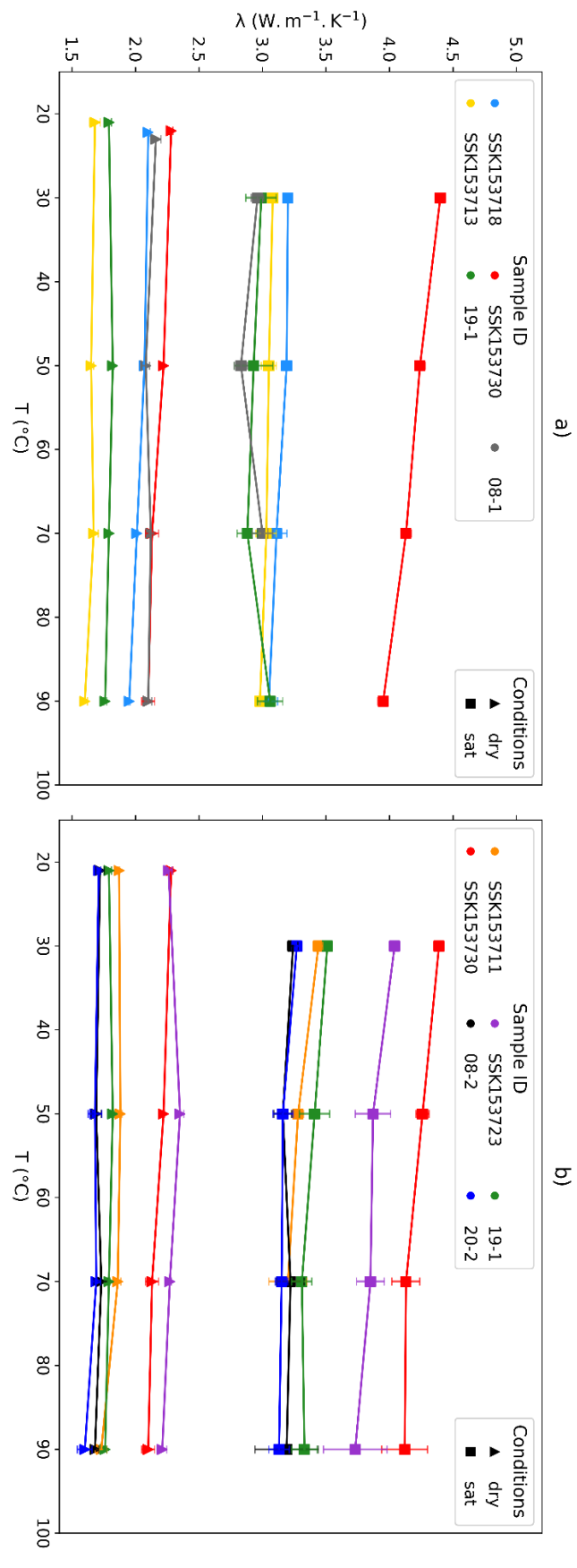

Figure 7-8: Thermal conductivity in the dry state (triangular marker) and water-saturated state (square marker) as a function of temperature for nine samples. Water-saturated measurements were done in a) Experiment A and b) Experiment B. Samples SSK153730 and 19-1 were analysed in both experiments to ensure the reliability of the setups and associated thermal conductivity measurements. Standard deviation bars representing repeated measurements are displayed for each sample. Thermal conductivity values in the dry state are presented in Table 7-3 and are displayed here for comparative analysis with water-saturated measurements.

A general decrease in the thermal conductivity of water-saturated samples with increasing temperature was observed, with a reduction of up to 0.3 W m^{-1} K^{-1} for SSK153723 between 30°C and 90°C. Measurements conducted on dry samples at varying temperatures (see Section 7.2.4.2) were also plotted in Fig. 7-8 to assess the combined effect of water saturation and temperature parameters. Water-saturated samples exhibited significantly higher thermal conductivity compared to their air-saturated counterparts.

As already outlined in Section 7.2.4.2, the decline in thermal conductivity with increasing temperature was more pronounced in samples that displayed higher thermal conductivity under relatively low-temperature or ambient conditions (Fig. 7-8). Samples collected from outcrop exposures showed relatively lower thermal conductivity values than core samples. Although all outcrop samples but one (sample 20-2) showed a slight increase in thermal conductivity between 30°C and 50°C, or 70°C and 90°C in the saturated state, this variation fell within the ±5% error margin of the TPS device. Furthermore, nearly all samples revealed higher standard deviations in thermal conductivity as temperature increased, suggesting that thermal conductivity values may be less reliable at high temperatures (Fig. 7-8). The minor increases in thermal conductivity between 50 and 90°C for water-saturated samples could likely be attributed to measurement and/or device errors.

The thermal properties of water-saturated SSK153730 and 19-1 were evaluated under increasing temperature conditions using both experimental setups, revealing distinct patterns. While SSK153730 exhibited very comparable thermal conductivity at all temperature increments in both experimental setups, 19-1 showed higher thermal conductivity when measured using Experiment B (Fig. 7-9). Overall, the thermal conductivity values from Experiment B exhibited less variability, as indicated by the generally smaller error bars compared to those in Experiment A (Figs. 7-8 and 7-9).

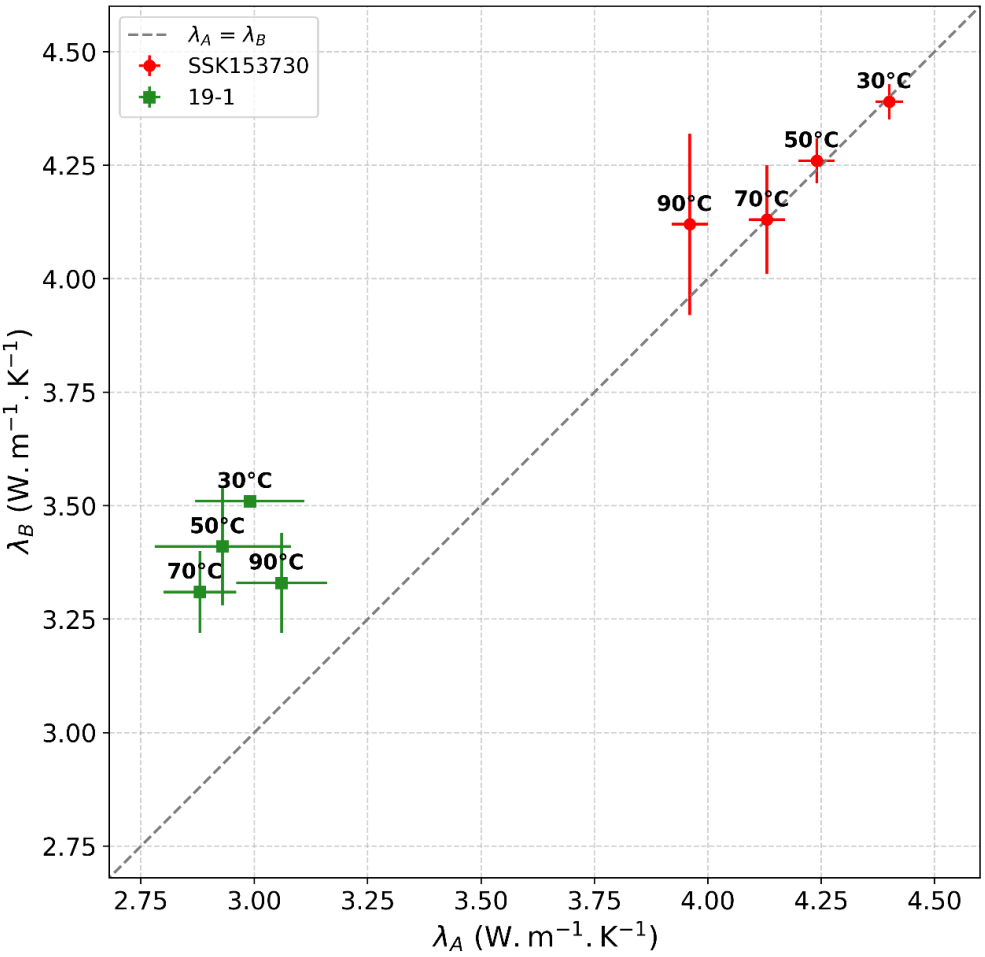

Figure 7-9: Comparison of the thermal conductivity of two samples under water-saturated conditions at elevated temperature steps for Experiments A and B. For each colour, individual data points represent thermal conductivity values at specific temperatures, with error bars indicating the variability derived from five repeated measurements.

7.2.5. Discussion

7.2.5.1. Comparison Between Thermal Conductivity at Ambient and Reservoir Conditions

In this study, we examined the influence of temperature and saturation on the thermal properties of sandstones, in particular the Chester Formation of the Cheshire Basin, UK. Under ambient temperature conditions, water-saturated samples exhibited higher thermal conductivity values compared to those measured in an air-saturated state (Fig. 7-6). The power regressions associated

with the data points in Fig. 7-6a indicated a decline in thermal conductivity with increasing porosity, with a more noticeable decrease observed in dry samples. This observation suggested that low-porosity rocks may exhibit relatively similar thermal conductivity values in both dry and water-saturated states, as also observed in previous studies (Fuchs et al., 2013; Nagaraju and Roy, 2014). To quantify the increase in thermal conductivity due to water saturation, the observed effect of water saturation (S_{obs}) was determined for each sample using the following equation Eq. (7-2):

$$S_{obs} = \frac{\lambda_{sat} - \lambda_{dry}}{\lambda_{dry}} \tag{7-2}$$

The observed (S_{obs}) values ranged from 55% to 154%, demonstrating a considerable increase in thermal conductivity under water-saturated conditions. In contrast, Rao (1976) reported S_{obs} values between 6% and 55% for sandstone samples in their study. Figure 7-10 displays a positive correlation between porosity and the effect of water saturation on thermal conductivity (S_{obs}). This observed relationship was subsequently compared to the theoretical effect of water saturation defined in Eq. (7-3):

$$S_{theor} = \frac{\lambda_{sat} - \lambda_{dry}}{\lambda_{dry}} = 20^{\phi} - 1 \tag{7-3}$$

The theoretical effect of water saturation on thermal conductivity (S_{theor}) was calculated using a geometric mixing law model (Lichtenecker, 1924). The corresponding values were depicted in Fig. 7-10 (grey line), along with +10% (red dashed line) and -10% (blue dashed line) uncertainty bounds. Amongst the analysed samples, 50% (14 out of 28) fell within the ±10% uncertainty interval. The remaining samples displayed substantial variability, indicating a discrepancy between observed and predicted values. Additionally, the slope of the linear regression was slightly lower than that of S_{theor} line. Several elements may contribute to this variability, including bulk porosity, the geometrical configuration of the pore network, and a partial saturation of the samples. In this study, porosity

was determined using the water immersion porosimetry (WIP) method, which measures effective rather than total porosity. Consequently, air –characterised by a lower thermal conductivity of c. 0.025 W m^{-1} K^{-1} compared to c. 0.604 W m^{-1} K^{-1} for water– could remain within isolated closed and dead-end pores, impacting the results. Previous studies (Clauser and Huenges, 1995; Jorand et al., 2011; Fuchs et al., 2021) observed that thermal conductivity of sandstones typically increases logarithmically with water saturation, a trend attributed to the connectivity and geometry of the pore networks (Schärli and Rybach, 1984). In sandstones containing clay minerals, capillary-bound water prevents complete drainage during drying, resulting in a constant residual water saturation. This residual saturation, which is governed by the clay content and pore structure, likely influenced thermal conductivity values in the dry state (Jorand et al., 2011).

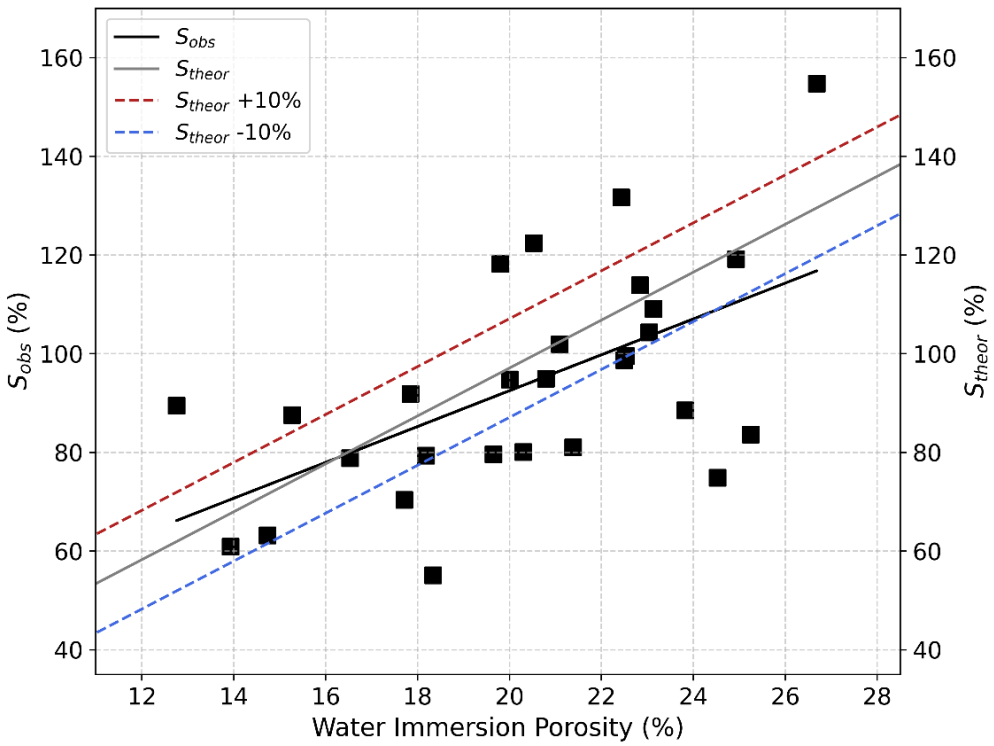

Figure 7-10: Effect of water saturation on thermal conductivity as a function of effective porosity. Black markers show the observed effect (Sobs) based on the thermal measurements done under dry and water-saturated conditions, with the black line corresponding to the associated linear regression. The grey line corresponds to the theoretical effect Stheor with ±10% uncertainty represented by red and blue dashed lines.

The discrepancy between S_{obs} values in this study (ranging from 55% to 154%), and those reported by Rao (1976) for sandstone samples (ranging between 6% and 55%) may suggest that additional factors may be influencing the experimental results. The average increase in thermal conductivity of c. 2.2 W m^{-1} K^{-1} between dry and water-saturated states cannot be fully attributed to the replacement of air (0.025 W m^{-1} K^{-1}) with water (0.604 W m^{-1} K^{-1}). Although this change does contribute to the increase, it is not sufficient to account for the full magnitude observed, suggesting that additional processes may be involved during sample saturation. For example, the increase in thermal conductivity of sample SSK153718 from dry to saturated states is notably high using both techniques (1.8 (TCS) vs. 1.1 (TPS) W m^{-1} K^{-1}; Tables 7-4 and 7-2), but even greater when measured using the TCS method. It is worth noting that the TPS measurement was taken at 30°C and might be slightly higher at ambient temperature. Three potential mechanisms are suggested to explain the elevated thermal conductivity observed in water-saturated samples:

(1) Water saturation of the rocks may induce microstructural changes and physicochemical interactions at mineral surfaces, especially in samples with clay content. Brémaud et al (2024) confirmed the presence of clay minerals in all the samples examined. The swelling of these clays may induce structural changes within the rock matrix, impacting thermal conductivity. However, such swelling is generally expected to reduce, rather than enhance, thermal conductivity (Guo et al., 2020).

(2) Surface wetting effects during thermal conductivity measurements of saturated samples using the TCS method. Following the saturation procedure, samples were removed from the water, and excess surface moisture was removed by briefly pressing a paper towel against the base of each specimen prior to placement on the scanning platform. This step aimed to minimise the influence of surface water films, which can alter thermal conductivity measurements. However, if this drying step was not fully effective, residual surface water may have affected the accuracy of the measurements.

(3) Influence of water bath setups. The first experiment utilised a circulating water bath and the second one a standard (convection) water bath. The use of these systems may have introduced heat fluxes, potentially inducing microscale convective processes within the pore space of the sample. Although this remains speculative, such effects could potentially enhance heat transfer beyond pure conduction, thereby influencing the measured thermal conductivity values. Further investigation would be necessary to determine the extent to which convective contributions may be present under these experimental conditions.

The impact of temperature on thermal conductivity in dry state is less significant than the effect of water saturation within the assessed temperature range (30°C to 90°C). A slight decrease in thermal conductivity with increasing temperature was observed (Fig. 7-7). This trend was consistent with findings from previous studies (Vosteen and Schellschmidt, 2003; Hartlieb et al., 2015; Chen et al., 2021), as illustrated by the trendlines in Fig. 7-7. Additionally, the decrease in thermal conductivity with temperature was more pronounced in samples exhibiting higher thermal conductivity at ambient temperature (Vosteen and Schellschmidt, 2003), as demonstrated by the sandstone sample in the upper part of Fig. 7-7 from Chen et al. (2021).

When examining the influence of both water saturation and temperature on the thermal conductivity of Chester Formation sandstone samples, we observed that these effects are combined. Water-saturated samples exhibited a higher thermal conductivity than dry samples, while thermal conductivity typically decreased with increasing temperature. Additionally, measurements on water-saturated samples at high temperatures using the TPS device showed a relative unreliability, characterised by significant errors bars (Figs. 7-8 and 7-9). This might be attributed to (1) the formation of bubbles on the sensor surface at elevated temperature, which likely created an interface gap between the sensor and the sample, and influenced heat transfer processes; and (2) the challenge of attaining temperature stabilisation in a partially or totally open system at high temperatures, particularly

in the presence of steam, leading to a temperature drift that affected the measurements. The smaller error bars observed in Experiment A compared to Experiment B could be related to the use of a circulating bath, which is more effective in maintaining temperature homogeneity. As previously discussed, the variation in thermal conductivity between dry and water-saturated conditions did not follow a consistent pattern (Fig. 7-6b). Samples exhibiting high thermal conductivity values under dry conditions did not necessarily show the highest values when water-saturated (Fig. 7-8). This reinforces the assumption that the effect of water saturation is inherently complex and governed by multiple interacting factors, and that the elevated values observed in water-saturated samples could be impacted by unforeseen experimental factors, as previously discussed.

7.2.5.2. Implications for Geothermal Reservoir Assessment

The evaluation of the thermal properties of the Chester Formation sandstones highlighted the substantial influence of temperature and water saturation on thermal conductivity. These factors must be carefully considered when assessing the thermal behaviour of rocks, particularly in the context of heat flow and heat transfer mechanisms within geothermal reservoirs. In this study, we focused on temperatures –up to 90°C– that represents the maximum temperature at which Chester Formation sandstones occur in the Cheshire Basin. The influence of temperature increases up to 90°C above ambient on thermal conductivity was relatively minor (decrease of c. 0.1 W m^{-1} K^{-1} on dry samples) compared to the effect of water saturation (increase of c. 2.2 W m^{-1} K^{-1}). However, previous studies (Vosteen and Schellschmidt, 2003; Hartlieb et al., 2015; Chen et al., 2021) examining thermal conductivity of dry samples at higher temperatures demonstrated that this parameter could have a significant impact on thermal conductivity, with a decrease of almost 2 W m^{-1} K^{-1} from 20 to 1000°C (Hartlieb et al., 2015). For a comprehensive review on the pressure and temperature effects, we recommend referring to Norden et al. (2020) and the references therein.

Thermal measurements on water-saturated samples indicated (1) a distinct increase in thermal conductivity between air-saturated and water-saturated samples, and (2) a general increase in the effect of water saturation (both observed S_{obs} and theoretical S_{theor}) with increasing effective porosity. Porosity therefore plays a key role in water saturation effects in the studied sandstone samples. Previous research showed that neglecting even a 5% porosity variation can result in thermal conductivity errors of approximately 15% (Popov et al., 2003; Nagaraju and Roy, 2014). While this study does not include samples with such low porosity values, our findings aligned with this trend (black S_{obs} line in Fig. 7-10). This observation is crucial as it directly affects heat flow estimations, which are partially derived from thermal conductivity measurements.

Conducting thermal measurements under in situ (i.e. both temperature and water saturation) conditions provides a more accurate representation of reservoir performance. Should thermal properties at depth be different than assumed, it could impact heat extraction efficiency and impact key parameters such as pumping rates, borehole placement and spacing, thereby resulting in suboptimal energy extraction strategies. The use of samples from outcrop exposures instead of subsurface cores in the thermal assessment of a potential geothermal reservoir can also reduce costs (Brémaud et al., 2025, under review (Chapter 6)). However, the reliability of outcrop-based approximations of subsurface conditions is closely linked to thorough consideration of temperature and fluid effects. As a consequence, water saturation and temperature must be carefully considered in thermal property measurements to ensure accurate geothermal reservoir characterisation.

7.2.6. Conclusion

This study highlights the significant influence of in situ geothermal hot sedimentary (HSA) reservoir conditions –in particular temperature and water saturation– on the thermal conductivity of Chester Formation rocks. The thermal analyses performed indicated the following:

1. Saturating samples with water increases the measured thermal conductivity of the samples investigated by c. 2.2 W m^{-1} K^{-1} on average, emphasising the necessity of accounting for fluid and porosity when evaluating geothermal reservoirs. However, this value may reflect not only fluid replacement effects but also other experimental influences, such as microstructural modifications, convective effects, and surface wetting effects.
2. The observed decrease in thermal conductivity with increasing temperature of c. 0.1 W m^{-1} K^{-1} aligns with previously established trends for sedimentary rocks. This demonstrates that ambient temperature measurements overestimate thermal conductivity at depth.
3. The combined effect of water saturation and elevated temperature reveals a complex interplay between these factors, highlighting the need for such in situ experimental setups.

These findings have crucial implications for geothermal exploration and resource assessment. Incorporating in situ thermal property measurements can enhance the reliability of heat flow predictions and geothermal resource characterisation, reducing uncertainty and investment risks in geothermal projects.

Future research includes the enhancement of the experimental setups for measuring thermal conductivity under both temperature and water-saturation conditions. Integration of pressure effects alongside temperature and water saturation to further refine in situ thermal conductivity measurements should be explored but could prove prohibitively costly for a minor gain in accuracy. The development of advanced laboratory setups that account for these parameters simultaneously might provide a more comprehensive approach of reservoir conditions. Improving our understanding of the thermal conductivity of deep subsurface geological reservoir rocks will contribute to the advancement of HSA resources and other sustainable low-carbon energy solutions, including other varieties of geothermal energy play, subsurface storage of heat energy, nuclear waste, and carbon dioxide.

Author Contributions

MB: Conceptualization, Formal analysis, Investigation, Methodology, Validation, Visualization, Writing – original draft, Writing – review & editing. **NMB:** Conceptualization, Funding Acquisition, Supervision, Writing – review & editing. **ZKS:** Conceptualization, Supervision, Writing – review & editing. **SF:** Supervision, Methodology, Writing – review & editing. **RP:** Methodology.

Competing Interests

The authors declare that they have no conflict of interest.

Acknowledgements

MB was funded by a University of Strathclyde International Strategic Partner (ISP) Research PhD Studentship. The Strathclyde Hot Disk facility was funded by EPSRC Core Equipment award EP/X034895/1. The analysis at both laboratories was supported by Strathclyde EPSRC IAA funding (as part of award EP/X525820/1). For the purpose of open access, the authors have applied a Creative Commons Attribution (CC BY) licence to any Author Accepted Manuscript version arising from this submission. The authors express their gratitude to the British Geological Survey, particularly the Keyworth National Geological Repository, for providing access to the core samples.

References

Abdulagatov, I. M., Emirov, S. N., Abdulagatova, Z. Z., & Askerov, S. Y. (2006). Effect of pressure and temperature on the thermal conductivity of rocks. Journal of Chemical and Engineering Data, 51(1). https://doi.org/10.1021/je050016a

Aliverdiev, A.A., Aliyev, R.M., Amirova, A.A. et al. (2024). Dependence of Effective Thermal Conductivity of Granites on Pressure and Temperature. High Temp 62, 160–165. https://doi.org/10.1134/S0018151X24700470

Anand, J., Somerton, W. H., & Gomaa, E. (1973). Predicting thermal conductivities of formations from other known properties. *Society of Petroleum Engineers Journal*, *13*(5). https://doi.org/10.2118/4171-pa

A.P.I. (1998). Recommended practices for core analysis. API Recommended Practice, 40 ED. 2 REV.

Bloomfield, J. P., Brewerton, L. J., & Allen, D. J. (1995). Regional trends in matrix porosity and dry density of the Chalk of England. Quarterly Journal of Engineering Geology, 28(Suppl. 2). https://doi.org/10.1144/gsl.qjegh.1995.028.s2.04

Brémaud, M., Burnside, N. M., Shipton, Z., Bossennec, C., Fuchs, S., & Deon, F. (2025). Bridging Surface and Subsurface: Comparative Analysis of Outcrop and Core Samples from the Chester Formation for Geothermal Exploration. *Geothermics*, under review. SSRN Preprint. 10.2139/ssrn.5177375

Burley, A. J., Edmunds, W. M., & Gale, I. N. (1984). Investigation of the geothermal potential of the UK: catalogue of geothermal data for the land area of the United Kingdom.

Busby, J. (2014). Geothermal energy in sedimentary basins in the UK. Hydrogeology Journal, 22(1). https://doi.org/10.1007/s10040-013-1054-4

Busby, J., Kingdon, A., & Williams, J. (2011). The measured shallow temperature field in Britain. Quarterly Journal of Engineering Geology and Hydrogeology, 44(3). https://doi.org/10.1144/1470-9236/10-049

Chadwick, R. A. (1997). Fault analysis of the Cheshire Basin, NW England. Geological Society Special Publication, 124. https://doi.org/10.1144/GSL.SP.1997.124.01.18

Chen, C., Zhu, C., Zhang, B., Tang, B., Li, K., Li, W., & Fu, X. (2021). Effect of Temperature on the Thermal Conductivity of Rocks and Its Implication for in Situ Correction. *Geofluids*, *2021*. https://doi.org/10.1155/2021/6630236

Clauser, C., & Huenges, E. (1995). Rock Physics & Phase Relations: A Handbook of Physical Constants. In American Geophysical Union (Ed.), *Thermal Conductivity of Rocks and Minerals* (Vol. 3, Issue Thermal Conductivity of Rocks and Minerals).

Evans, D. J., Rees, J. G., & Holloway, S. (1993). The Permian to Jurassic stratigraphy and structural evolution of the central Cheshire Basin. Journal - Geological Society (London), 150(5). https://doi.org/10.1144/gsjgs.150.5.0857

Fuchs, S., Balling, N., & Mathiesen, A. (2020). Deep basin temperature and heat-flow field in Denmark – New insights from borehole analysis and 3D geothermal modelling. *Geothermics*, *83*. https://doi.org/10.1016/j.geothermics.2019.101722

Fuchs, S., Förster, H.-J., Norden, B., Balling, N., Miele, R., Heckenbach, E. L., & Förster, A. (2021). Thermal diffusivity-porosity data used in the evaluation of the Goto-Matsubayashi modified geometric model for continental sedimentary rocks. https://doi.org/10.5880/GFZ.4.8.2020.003

Fuchs, S., Schütz, F., Förster, H.-J., Förster, A. (2013) Evaluation of common mixing models for calculating bulk thermal conductivity of sedimentary rocks: correction charts and new conversion equations. Geothermics, 47, 40-52. https://doi.org/10.1016/j.geothermics.2013.02.002

Guo, P., Bu, M., He, M., & Wang, Y. (2020). Experimental investigation on thermal conductivity of clay-bearing sandstone subjected to different treatment processes: Drying, wetting and drying II. *Geothermics*, *88*. https://doi.org/10.1016/j.geothermics.2020.101909

Gustafsson, S. E. (1991). Transient plane source techniques for thermal conductivity and thermal diffusivity measurements of solid materials. *Review of scientific instruments*, *62*(3), 797-804.

Hartlieb, P., Toifl, M., Kuchar, F., Meisels, R., & Antretter, T. (2016). Thermo-physical properties of selected hard rocks and their relation to microwave-assisted

comminution. *Minerals Engineering*, *91*. https://doi.org/10.1016/j.mineng.2015.11.008

Hot Disk. (2019). Hot Disk Thermal Constants Analyser - Instruction Manual.

Houseman, G. A., McKenzie, D. P., & Molnar, P. (1981). Convective instability of a thickened boundary layer and its relevance for the thermal evolution of continental convergent belts. Journal of Geophysical Research, 86(B7). https://doi.org/10.1029/JB086iB07p06115

Huenges, E. (2010). Geothermal Energy Systems: Exploration, Development, and Utilization. In Geothermal Energy Systems: Exploration, Development, and Utilization. https://doi.org/10.1002/9783527630479

Jorand, R., Fehr, A., Koch, A., & Clauser, C. (2011). Study of the variation of thermal conductivity with water saturation using nuclear magnetic resonance. *Journal of Geophysical Research: Solid Earth*, *116*(8). https://doi.org/10.1029/2010JB007734

Kingdon, A., Spence, M., & Fellgett, M. (2020). Cheshire Energy Research Facility Site (CERFS): A new experimental observatory location for geoscience energy research.

Labus, M., & Labus, K. (2018). Thermal conductivity and diffusivity of fine-grained sedimentary rocks. Journal of Thermal Analysis and Calorimetry, 132(3). https://doi.org/10.1007/s10973-018-7090-5

Lichtenecker, K. (1924). Der elektrische Leitungswiderstand künstlicher und natürlicher Aggregate. Physikalische Zeitschrift 25, pp. 169−181, 193−204, 226−233.

Liu, S., Feng, C., Wang, L., & Li, C. (2011). Measurement and analysis of thermal conductivity of rocks in the Tarim Basin, Northwest China. *Acta Geologica Sinica-English Edition*, *85*(3), 598-609. https://doi.org/10.1111/j.1755-6724.2011.00454.x

Marelis, A. A. (2017). *Energy capacity of a geothermal reservoir.*

Midttømme, K., & Roaldset, E. (1999). Thermal conductivity of sedimentary rocks: uncertainties in measurement and modelling. Geological Society Special Publication, 158. https://doi.org/10.1144/GSL.SP.1999.158.01.04

Mikkelsen, P. W., & Floodpage, J. B. (1997). The hydrocarbon potential of the Cheshire Basin. Geological Society Special Publication, 124. https://doi.org/10.1144/GSL.SP.1997.124.01.10

Muffler, P., & Cataldi, R. (1978). Methods for regional assessment of geothermal resources. Geothermics, 7(2–4). https://doi.org/10.1016/0375-6505(78)90002-0

Nagaraju, P., & Roy, S. (2014). Effect of water saturation on rock thermal conductivity measurements. Tectonophysics, 626(1). https://doi.org/10.1016/j.tecto.2014.04.007

Navelot, V. (2018). Caractérisations structurale et pétrophysique d'un système géothermique en contexte volcanique d'arc de subduction. Exemple de l'archipel de Guadeloupe. Phd thesis, Université de Lorraine. 11, 153, 170, 172, 503

Norden, B., Förster, A., Förster, H.-J., Fuchs, S. (2020). Temperature and pressure corrections applied to rock thermal conductivity: impact on subsurface temperature prognosis and heat-flow determination in geothermal exploration. Geothermal Energy, 8, 1. https://doi.org/10.1186/s40517-020-0157-0

Plant, J. A., Jones, D. G., & Haslam, H. W. (1999). The Cheshire Basin: basin evolution, fluid movement and mineral resources in a Permo-Triassic rift setting. British Geological Survey.

Popov, Y. A., Pribnow, D. F. C., Sass, J. H., Williams, C. F., & Burkhardt, H. (1999). Characterization of rock thermal conductivity by high-resolution optical scanning. *Geothermics*, *28*(2). https://doi.org/10.1016/S0375-6505(99)00007-3

Popov, Y., Tertychnyi, V., Romushkevich, R., Korobkov, D., & Pohl, J. (2003). Interrelations between thermal conductivity and other physical properties of

rocks: Experimental data. *Pure and Applied Geophysics*, *160*(5–6). https://doi.org/10.1007/PL00012565

Radley, J. D., & Coram, R. A. (2016). The Chester Formation (Early Triassic, southern Britain): sedimentary response to extreme greenhouse climate? Proceedings of the Geologists' Association, 127(5). https://doi.org/10.1016/j.pgeola.2016.08.002

Rao, G. V. (1976). Heat flow studies in some Gondwana basins of India (Doctoral dissertation, Ph. D. thesis, 178 pp., Osmania Univ., Hyderabad, India)

Rollin, K. E. (1995). A simple heat-flow quality function and appraisal of heat-flow measurements and heat-flow estimates from the UK Geothermal Catalogue. Tectonophysics, 244(1–3). https://doi.org/10.1016/0040-1951(94)00227-Z

Schärli, U., & Rybach, L. (1984). On the thermal conductivity of low-porosity crystalline rocks. *Tectonophysics*, *103*(1–4). https://doi.org/10.1016/0040-1951(84)90092-1

Seipold, U. (1998). Temperature dependence of thermal transport properties of crystalline rocks - a general law. *Tectonophysics*, *291*(1–4). https://doi.org/10.1016/S0040-1951(98)00037-7

van Rijn, S. (2018). *Breakthrough time of a geothermal reservoir.*

Vosteen, H. D., & Schellschmidt, R. (2003). Influence of temperature on thermal conductivity, thermal capacity and thermal diffusivity for different types of rock. Physics and Chemistry of the Earth, 28(9–11). https://doi.org/10.1016/S1474-7065(03)00069-X

Warrington, G., MG, A. C., RE, E., WB, E., HC, I. C., & PE, K. (1980). A correlation of Triassic rocks in the British Isles.

CHAPTER 8
Conclusions and Recommendations

Chapter-specific conclusions are provided at the end of Chapters 3, 6 and 7. This chapter provides broader overall conclusions and offers recommendations for the geothermal industry based on the major findings of the thesis. Last but not least, future research directions are explored.

8.1. Conclusions

Using a systematic literature review of publicly available data, geological fieldwork and laboratory analyses, the five research questions presented in Chapter 1 have been answered. The key findings for each research question are detailed below:

RQ 1: How much does geology contribute to project failure in HSAs?

The HSA database was developed using publicly available information on geothermal projects targeting HSA in eight countries: Australia, Croatia, Denmark, France, Germany, the Netherlands, Poland, and the UK. Amongst the 256 projects, 26% (n=67) were unsuccessful following at least one failure. The main reason for closure or suspension of the failed projects is related to hydrogeological or geological factors (39%), while financial decisions (26%), technical problems with the installations (25%), and policy decisions (7%) represent the remaining failure causes. Most issues in the geological and hydrogeological category are associated with borehole chemical degradation or unfavourable reservoir properties.

However, the results vary depending on the country and the timing of failure. Geological and hydrogeological issues prevailed (>50%) in the failures of Danish, Dutch, British and German HSA projects, while failures in Croatia and Australia

were dominated by financial aspects and policy respectively. Almost three quarters (72%) of the geological and hydrogeological failures occurred during the operational phase of HSA projects.

Although geological and hydrogeological data seem crucial for the success or failure of an HSA project, 56% of the database entries for these parameters are missing. Additionally, productivity index, thermal conductivity and heat flow only contain values for 13%, 1% and 1% of the HSA database entries respectively. This observation highlights a significant information gap in geological and hydrogeological data.

RQ 2: What approaches can be employed to facilitate the advancement of HSA systems?

Throughout the development and analysis of the HSA database, several key elements were identified that either support the successful implementation of such projects, or present challenges to their advancement, necessitating substantial improvements.

The geothermal community lacks standardised definitions and well-established boundaries for the various types of geothermal systems. While terminologies such as EGS, HSA, or Hot Dry Rocks are commonly used, certain definitions remain insufficiently specified, leading to multiple interpretations amongst researchers. In particular, a specific definition of HSAs has been established for the development of the database, as existing literature exhibited considerable variability in the depth and temperature thresholds used by authors. Moreover, classifications that are not recognised as international standards further contribute to ambiguity. The development and application of clear and internationally recognised definitions, as well as thresholds –based on parameters such as depth, temperature, or enthalpy– would significantly enhance the clarity, comparability, and broader adoption of geothermal energy, including HSAs.

During the development of the HSA database, substantial variability was identified in data reporting and availability, as well as in the regulatory frameworks governing

geothermal energy. France and the Netherlands provide the most comprehensive open-access databases, while Germany and some Australian states are progressively enhancing data accessibility. In contrast, countries such as Croatia, Denmark, Poland, and the UK lack publicly available and comprehensive repositories. Although growing interest in geothermal energy is driving greater data accessibility, further efforts are required to streamline access and facilitate the uptake of geothermal energy. Regulatory frameworks for geothermal energy vary significantly across the countries investigated. Poland and the UK lack dedicated geothermal regulations, which may hinder growth, whereas Germany has a structured legal framework under the Federal Mining Act that fosters increased geothermal development. Risk mitigation strategies, such as geothermal insurance schemes that were implemented in France, have significantly reduced failure rates and inspired similar policies in other European countries, including the Netherlands.

The mitigation and remediation measures implemented in some projects provide valuable insights into the advancement of HSAs. Such strategies were applied in 63 projects (25% of total projects) with 80% of them remaining operational as of 2022. The effective monitoring of both surface and borehole installations enhances infrastructure condition understanding and can help prevent failures. Remediation efforts included renovation or improvements to geothermal installations, reservoir management decisions such as adding boreholes to a current configuration, replacing old doublets, and altering heat use.

RQ 3: How well can outcrop samples data be used to predict subsurface conditions in HSA geothermal reservoirs?

In the preliminary stages of a geothermal project, outcrop samples offer cost-effective, readily available, and insightful data prior to committing to the significant investment required for drilling boreholes. Exploratory geothermal boreholes are expensive (>$1M USD), with costs escalating significantly as depth increases. This

financial constraint can be prohibitive, particularly for exploratory wells that might not yield viable resources.

Shallow subsurface core (up to 100m depth) and outcrop samples of the Chester Formation were collected in the Cheshire Basin, UK. The Chester Formation represents one of the basal units of the Sherwood Sandstone Group, a key target for geothermal development in the UK. Composed of river-sourced pebbly sandstones of Early Triassic age, the Chester Formation was sampled in the northwestern section of the basin, yielding 21 core and 16 outcrop samples for mineralogical, thermal, and petrophysical analysis. Quartz is the predominant mineral phase in all samples, with the principal difference between core and outcrop samples being the presence of calcite cementation in the core samples. Calcite has had been largely dissolved in outcrop samples, likely due to surface weathering. Beyond this distinction, both sample types exhibit similar diagenetic parasequences. Although core samples generally display lower porosity and permeability than outcrop samples, these differences are not statistically significant, suggesting comparable petrophysical properties between the two. However, outcrop samples exhibit statistically lower thermal conductivity compared to core samples, underestimating the reservoir thermal properties. Hence, outcrop samples offer valuable insights into the properties of a specific geological formation, providing a preliminary understanding of HSA reservoir potential.

RQ 4: How can thermal property assessments be improved to enhance the characterisation of HSA geothermal reservoirs?

Thermal conductivity is typically measured in laboratory settings under ambient conditions on dry rock samples. While such measurements provide a useful preliminary estimate of the rock thermal properties, they do not account for in situ reservoir conditions, where factors such as water saturation, temperature, and pressure can significantly alter thermal conductivity.

Using samples of the Chester Formation collected in the Cheshire Basin, UK, the impact of in situ geothermal hot sedimentary (HSA) reservoir conditions on the thermal conductivity of sandstones was assessed. In particular, the individual and combined effects of temperature and water saturation were evaluated and compared to measurements at ambient temperature conditions on dry samples. Thermal conductivity measurements were conducted in laboratories in Germany and the UK with three to five repeated measurements per sample to ensure data reliability and reproducibility. The findings demonstrate that water saturation significantly increases thermal conductivity, particularly in high-porosity samples, while increasing temperature reduces it slightly. The combined effects of water saturation and elevated temperature, examined using innovative experimental setups, reveal a complex interaction.

This underscores the necessity of accounting for reservoir conditions when measuring thermal properties to improve predictive accuracy and reduce uncertainties. Notably, the thermal conductivity measurements on water-saturated samples under elevated temperature conditions are relatively cost-effective, requiring only standard laboratory equipment that is widely available or can be acquired at a low cost. Thus, ambient measurements which provided less accurate representations of HSA in situ thermal conductivity are not as economically advantageous as previously assumed.

8.2. Recommendations

8.2.1. Recommendations for the Geothermal Industry

This section compiles a series of recommendations for the industry to de-risk and further develop geothermal resources found in hot sedimentary aquifers worldwide.

Pre-Drilling Geological Site Characterisation

Previous research (Gehringer and Loksha, 2012; Witter et al., 2019; Deinhardt et al., 2021) has identified geological risk as the primary challenge in geothermal

projects. In Chapter 3, geological and hydrological factors were found to account for 39% of the failures in HSA projects, primarily due to issues such as borehole degradation caused by chemical processes (e.g., corrosion, scaling, clogging) or unfavourable reservoir parameters (e.g., low transmissivity, temperature, or porosity). These findings highlight the necessity of conducting comprehensive and rigorous assessments of the geological and hydrogeological characteristics of prospective HSA reservoirs during the early stages of a geothermal project. A more thorough evaluation reduces uncertainties and risks, thereby decreasing the likelihood of project failure.

Consider the Influence of Fluids and Temperature when Assessing Thermal Properties of HSA Reservoirs

Thermal conductivity in sandstones decreases with increasing temperature (Vosteen and Schellschmidt, 2003; Labus and Labus, 2018), and is typically higher in water-saturated samples compared to dry samples, primarily due to the higher thermal conductivity of water relative to air (Nagaraju and Roy, 2014; Midttømme and Roaldset, 1999). Chapter 7 demonstrated that saturating Chester Formation sandstone samples with water leads to an increase in thermal conductivity of approximately 2.2 W m^{-1} K^{-1}, while a reduction in thermal conductivity with increasing temperature (20°C to 90°C) of 0.1 W m^{-1} K^{-1} is observed. The combined effect of water saturation and elevated temperature was measured using a novel experimental setup and revealed a complex interrelationship between these variables. Consequently, thermal property measurements conducted under ambient laboratory conditions do not accurately represent in situ rock behaviour, particularly in lithologically heterogeneous formations with diverse mineralogical compositions and pore structures. Whenever feasible, thermal conductivity assessments of HSA rocks should be conducted under in situ conditions, especially as this approach is relatively cost-effective and does not necessitate highly advanced equipment.

Outcrop Samples for Preliminary Geological Assessments of Subsurface HSA Reservoirs

Drilling exploratory boreholes into HSAs is costly, with a substantial risk that the resources may not demonstrate viable characteristics (Gehringer and Loksha, 2012). As discussed in Chapter 6, the application of outcrop samples to estimate in situ reservoir properties has been demonstrated to be feasible. Core and outcrop samples from the Chester Formation show comparative mineralogical and petrophysical (porosity and permeability) properties, while thermal conductivity is typically higher in core samples by c. 0.3 W m^{-1} K^{-1} on average. A notable difference between the two sample types is the presence of calcite cementation in core samples, which has been dissolved in the outcrop samples due to surface weathering. Overall, surface samples provide valuable insights into the thermal, mineralogical and petrophysical characteristics of a geological formation, offering an initial understanding of the HSA reservoir.

Accounting for the Scale of Investigation in Geological Evaluations

Sandstones, particularly from fluvial environments such as the Chester Formation, exhibit significant heterogeneity due to variable depositional processes like channel migration and floodplain dynamics (Bjørlykke, 2015; Bridge and Tye, 2000). These processes affect grain size, sorting, and lithological distribution, while diagenetic changes further contribute to variability. Chapter 6 explored the impact of sample heterogeneity on the variability of thermal and petrophysical measurements. Significant standard deviations in thermal conductivity were observed when the position of the Hot Disk sensor was altered across a sample, especially in pebbly sandstone specimens. The measurements of both petrophysical and thermal properties are also influenced by the scale of study. Small-scale measurements in core or outcrop samples typically reflect matrix properties, while larger-scale evaluations, such as well tests, capture additional fracture-related properties (Berkowitz, 2002). When evaluating the properties of a geological formation, factors it is crucial to consider factors such as the observation

scale, sample fracturing, heterogeneity and diagenesis, as these factors are likely to induce variations in permeability, porosity, and thermal conductivity values.

Constant Borehole Monitoring

Chapters 3 demonstrated that 39% of HSA projects failures are attributable to geological or hydrogeological factors, with nearly three-quarters of these 39% occurring during the operational phase of the project (i.e., from the commissioning of the project until its completion). The primary causes of these failures include issues with borehole integrity such as clogging or scaling, or the deterioration of the pump or the borehole. Therefore, insufficient monitoring of both surface and borehole installations can lead to significant problems regarding the conditions and efficiency of the infrastructures and represent a major risk for a project. Moreover, Chapter 3 underlined that projects that performed refurbishment or improvement work to their installations (representing 9% of all mitigation measures applied) addressed these issues proactively, preventing potential failures. A comprehensive and constant monitoring of both the borehole and the installations is crucial to ensure the viability of an HSA project.

Implementation of Risk Mitigation or Corrective Measures

In order to limit the likelihood of failures in a HSA project, a range of preventive strategies can be employed. Chapter 3 details seven mitigation or remediation techniques that have been implemented in over half of the projects within the HSA database. The most frequently used approaches include acid stimulation of the borehole to enhance reservoir permeability (59%), the drilling of sidetrack boreholes to address technical issues (14%), and refurbishment and or improvement of one or more boreholes (9%), as previously discussed. Of the projects that adopted these measures, 76 remained operational as of 2022. Among the 24% of projects that ultimately failed despite the implementation of mitigation strategies, only one of failed for a reason related to the strategy employed. This

demonstrates the effectiveness of these strategies in preventing failures and highlight their importance when facing difficulties in HSA geothermal projects.

Better Harmonisation of Geothermal Classification Systems

Chapters 2 and 3 identified a lack of standardised terminologies and definitions in the classification of geothermal systems. In particular, HSAs are alternatively referred to as *deep sedimentary aquifers* –without a clear definition of what constitutes "deep"– as well as *hydrothermal* or *hydrogeothermal* systems, with the latter terms sometimes encompassing systems targeting more than sedimentary formations. Additionally, Chapter 3 highlighted a considerable variation in the depth and temperature thresholds used to characterise HSAs. These inconsistencies, coupled with the introduction of multiple classifications and non-standardised classification frameworks, contribute to the ambiguity (Breede et al., 2015) and required the development of a clear and strict definition of HSA for this study. Achieving a better harmonisation of geothermal classification schemes through the adoption of precise and internationally recognised definitions is essential for the broader integration and uptake of geothermal energy.

Improved Regulatory Frameworks on Geothermal Data Availability and Reporting

The HSA database developed in Chapter 3 was incomplete, with c. 34% of the database cells unable to be completed. Notably, 56% of geological and hydrogeological values were lacking, whereas these variables were implicated in nearly 40% of failed projects. This underscores the limited accessibility and reporting of geothermal data, although it varies significantly based on the historical context and geographical location of geothermal projects. Chapter 3 examined eight countries throughout the development of the HSA database, revealing that France and the Netherlands provide exemplary access to comprehensive national databases that facilitate geothermal research and development. While Germany maintains an open-access database, it lacks raw

end-of-well reports and reservoir data. Energy policies differing by state, Australia offers various data access. In contrast, Croatia, Denmark, Poland, and the UK provide limited public geothermal data. Better data availability is essential for conducting robust risk assessments of HSA projects and, more broadly, for advancing geothermal energy development on a global scale.

Systematically Reporting and Learning from Failures

Organisational learning from failures is crucial in advancing the geothermal industry. Failing to identify and analyse small failures hinders the prevention of larger ones (Tucker and Edmondson, 2003; Sitkin, 1992). As demonstrated in Chapter 3, the implementation of remediation and mitigation strategies successfully prevented more than a hundred HSA projects from failing. In a "learning from failure" culture, the operators must consistently report and perform detailed failure analysis to ensure the proper lessons are learned (Edmondson, 2011). In contrast to the aviation industry, this practice is not widespread the geothermal industry, as evidenced by the lack of detailed failure reports in the HSA projects (Chapter 3). In sectors such as geothermal, accumulated experience plays a critical role in refining practices. Despite valuable lessons from industries like oil and gas, the poor reporting of failures in geothermal projects limits opportunities for learning and improvement.

Financial Schemes to Support Geothermal Development

Ultimately, all risks in geothermal project development translate into financial risks. Significant investment is often required before determining whether the geothermal resource has sufficient potential to recover the costs. Exploration and test drilling expenses can account for up to 15% of the overall capital cost (CAPEX), for a relatively high project risk (Gehringer and Loksha, 2012). The mid-range estimate of investment costs (DEVEX plus CAPEX) is c.US $4 M/MW (Gehringer and Loksha, 2012). Insurance and risk mitigation schemes can help limit these risks and reassure potential investors. As outlined in Chapter 3, such schemes have been

implemented in France since the 1980s, significantly benefiting the national geothermal industry. This successful model has inspired other countries –such as the Netherlands– to adopt similar risk insurances to boost geothermal development (Boissavy and Laplaige, 2018). Financial schemes are key for a global advancement of the geothermal industry.

8.2.2. Recommendations for Future Research

Building upon the work undertaken in this thesis, this section outlines some suggestions for future research.

Further Development and Improvement of the HSA Database (Chapter 3)

- While the HSA database is considered broadly representative of all HSA projects, analytical outcomes may be influenced by additional data from other countries, as demonstrated by the incorporation of French projects. A possible next step could be to expand the database by including a country with a large number of HSA projects, such as the USA or China, pending access to geothermal data. Ideally, a globally inclusive database encompassing all past and present HSA projects would provide a robust foundation for thorough analysis.

- Moreover, incorporating additional parameters such as borehole design (e.g., open or close-loop system), drilling technology, or total project cost, would significantly enhance the database and enable more comprehensive analyses. Refining existing parameters could also be beneficial. As suggested by one of the reviewers of the Chapter 3 publication, providing detailed information on the specific stage at which a project was discontinued –rather than broadly categorising it under 'development' or 'operational' stages–, would offer more valuable insights.

- To maximise the value of the database, the potential usage of multivariate statistical analyses was explored. While the focus was ultimately directed

toward other aspects of the study, a rigorous statistical examination of the dataset could reveal unexpected relationships between key parameters and enhance the robustness of the analysis.

- Given the growing adoption of geothermal energy and the relevance of such work to a wide range of industry stakeholders (including researchers, operators, and policymakers), there is potential interest in developing a similar database for Enhanced Geothermal Systems (EGS) and other geothermal systems to help de-risking all geothermal energy projects.

Enhanced Evaluation of Chester Formation Properties

- As evidenced in Chapter 6, the thermal conductivity of subsurface core samples is statistically higher than that of samples from surface exposures. This suggests that relying on outcrop samples to evaluate thermal conductivity at reservoir depths may lead to systematic underestimation. Further work could extend this investigation by replicating the study across additional boreholes of the UKGEOS Cheshire centre or at other sites. Such studies would help determine whether a systematic correction factor can be applied to thermal conductivity values of surfaces samples to more accurately estimate the thermal properties at the reservoir depth. This correction would likely be depth-dependent, as it is explored in the subsequent bullet point.

- The Chester Formation cores analysed were obtained from a shallow borehole at depths between 20 and 100m. Therefore, interpretations on the potential discrepancies or similarities between surface and subsurface properties must carefully account for this limited depth difference. Using cores from greater depths (i.e., 100m to 4 km depth) may change the relationships established in Chapter 6. Indeed, porosity and permeability typically decrease with depth, and while the difference in petrophysical values between core and outcrop samples were not statistically significant, such trends may become more pronounced with deeper cores. Future research could extend this investigation to deeper Chester Formation cores to evaluate these effects further. From a

broader perspective, replicating this study in other sedimentary basins, such as the Dogger carbonates of the Paris Basin, or expanding the scope to include other lithologies, such as volcanic rocks or granites from other geothermal systems, would provide valuable comparative insights.

- Due to time constraints, porosity measurements using the water immersion porosimetry method were not conducted multiple times. While this technique is recognised for its accuracy (±0.5% porosity, A.P.I., 1998), multiple successive measurements could be performed on the same sample set to enhance the reproducibility of the method and minimise uncertainty in the results.

- Additional thermal properties, including thermal diffusivity and specific heat capacity, were measured alongside thermal conductivity in Chapters 6 and 7. However, these data were not analysed as the primary focus was on thermal conductivity which is essential for heat flow measurements. A detailed examination of thermal diffusivity and specific heat capacity measurements could provide a more comprehensive assessment of the thermal processes governing HSA reservoirs.

- In situ thermal measurements conducted in Chapter 7 only considered temperature and water saturation, but additional parameters must be accounted to more accurately reproduce actual conditions found within an HSA reservoir. While pressure would likely have a relatively minor influence on thermal conductivity compared to temperature (Midttømme and Roaldset, 1999; Abdulagatov et al., 2006), it remains an important factor to consider. Moreover, preserving subsurface rock samples under ambient conditions may induce structural modifications, such as the formation of microfissures, as well as chemical and mineralogical transformations, such as mineral oxidation, which could influence thermal conductivity measurements. Future work could incorporate these factors and refine the experimental setup for measuring thermal conductivity under in situ conditions.

- The temperatures selected to simulate reservoir conditions in Chapter 7 are related to the depths at which the Chester Formations sandstones are found within the Cheshire Basin. However, other HSA reservoirs could exhibit significantly higher temperatures. Such conditions would likely present challenges related to temperature stabilisation during in situ measurements, requiring further methodological refinements to ensure both accuracy and reliability of the results.

- As presented in Chapter 7, two samples were measured under in situ conditions using both experimental setups. Conducting multiple repetitions of these experiments on the same set of rock samples would significantly enhance the reliability and robustness of the results, allowing for a more comprehensive assessment of whether the observed trends in Figure 7-9 are consistently reproduced. Additionally, the experimental set up could be enhanced by integrating the most effective aspects of each configuration (as outlined in Table 5-1) and be further tested and validated through measurements on a broader range of lithologies.

8.3. References

Abdulagatov, I. M., Emirov, S. N., Abdulagatova, Z. Z., & Askerov, S. Y. (2006). Effect of pressure and temperature on the thermal conductivity of rocks. Journal of Chemical and Engineering Data, 51(1). https://doi.org/10.1021/je050016a

A.P.I. (1998). Recommended practices for core analysis. API Recommended Practice, 40 ED. 2 REV.

Berkowitz, B. (2002). Characterizing flow and transport in fractured geological media: A review. Advances in Water Resources, 25(8–12). https://doi.org/10.1016/S0309-1708(02)00042-8

Bjørlykke, K. (2015). Petroleum geoscience: From sedimentary environments to rock physics, second edition. In Petroleum Geoscience: From Sedimentary

Environments to Rock Physics, Second Edition. https://doi.org/10.1007/978-3-642-34132-8

Boissavy, C., & Laplaige, P. (2018). The successful geothermal risk mitigation system in France from 1980 to 2015. Transactions - Geothermal Resources Council, 42.

Breede, K., Dzebisashvili, K., & Falcone, G. (2015). Overcoming challenges in the classification of deep geothermal potential. In Geothermal Energy Science (Vol. 3, Issue 1). https://doi.org/10.5194/gtes-3-19-2015

Bridge, J. S., & Tye, R. S. (2000). Interpreting the dimensions of ancient fluvial channel bars, channels, and channel belts from wireline-logs and cores. AAPG Bulletin, 84(8). https://doi.org/10.1306/a9673c84-1738-11d7-8645000102c1865d

Deinhardt, A., Dumas, P., Schmidle, V., Antoniadis, A., Boissavy, C., Bozkurt, C., Garabetian, T., Hamm, V., Karytsas, S., Kasztelewicz, A., Kepinska, B., Keramiotis, C., Kujbus, A., Leguenan, T., Link, K., Lupi, N., Mendrinos, D., Miecznik, M., Nador, A., … Yildirim, C. (2021). Why de-risking is key to develop large geothermal projects? GEORISK Projet. https://www.georisk-project.eu/wp-content/uploads/2021/07/Final-Report.pdf

Edmondson, A. C. (2011). Strategies for learning from failure. Harvard Business Review, 89(4), 48–55.

Gehringer, M., & Loksha, V. (2012). Geothermal handbook: Planning and Financing Power Generation. https://www.esmap.org/sites/esmap.org/files/DocumentLibrary/FINAL_Geothermal%20Handbook_TR002-12_Reduced.pdf

Labus, M., & Labus, K. (2018). Thermal conductivity and diffusivity of fine-grained sedimentary rocks. Journal of Thermal Analysis and Calorimetry, 132(3). https://doi.org/10.1007/s10973-018-7090-5

Midttømme, K., & Roaldset, E. (1999). Thermal conductivity of sedimentary rocks: uncertainties in measurement and modelling. Geological Society Special Publication, 158. https://doi.org/10.1144/GSL.SP.1999.158.01.04

Nagaraju, P., & Roy, S. (2014). Effect of water saturation on rock thermal conductivity measurements. Tectonophysics, 626(1). https://doi.org/10.1016/j.tecto.2014.04.007

Sitkin, S. B. (1992). Learning Through Failure: The Strategy of small losses. In Research in organizational behavior (Vol. 14).

Tucker, A. L., & Edmondson, A. C. (2003). Why hospitals don't learn from failures: Organizational and psychological dynamics that inhibit system change. In California Management Review (Vol. 45, Issue 2). https://doi.org/10.2307/41166165

Vosteen, H. D., & Schellschmidt, R. (2003). Influence of temperature on thermal conductivity, thermal capacity and thermal diffusivity for different types of rock. Physics and Chemistry of the Earth, 28(9–11). https://doi.org/10.1016/S1474-7065(03)00069-X

Witter, J. B., Trainor-Guitton, W. J., & Siler, D. L. (2019). Uncertainty and risk evaluation during the exploration stage of geothermal development: A review. In Geothermics (Vol. 78). https://doi.org/10.1016/j.geothermics.2018.12.011

APPENDIX A.
WGC 2023 Publication

Proceedings World Geothermal Congress 2023
Beijing, China, April 17 – 21, 2023

De-risking database for Hot Sedimentary Aquifers

Maëlle Brémaud[1], Neil M. Burnside[1], Zoe K. Shipton[1], Cees J.L. Willems[2]

[1]Department of Civil and Environmental Engineering, University of Strathclyde, Glasgow, UK

[2]Huisman Equipment B.V., Schiedam, The Netherlands

maelle.bremaud@strath.ac.uk

Keywords: deep geothermal, hot sedimentary aquifers, risk mitigation, failure, database

ABSTRACT

At the COP26 Summit in 2021, the world's largest greenhouse gas emitting nations have committed to Net Zero or carbon neutrality targets between the years 2045 to 2060. In parallel, there is an increasing investment in geothermal energy technology to diversify the power mix and decarbonise energy generation. Hot Sedimentary Aquifers (HSAs) are underdeveloped geothermal resources with plenty of renewable heat and investment potential. These large and hydraulically conductive groundwater systems, typically occurring in large sedimentary basin settings away from more conventional geothermal resources in fault zones or volcanic regions. They are hot enough and have sufficient productivity to provide significant low-carbon resources for heating or electricity generation, and often need no or limited well stimulation reducing public acceptance challenges. However, due to subsurface uncertainty and key information gaps there can be an unpalatable level of risk associated with delivery of HSA projects. This paper introduces a new database that captures publicly available information for 45 successful and failed HSA exploration and energy generation projects, enabling a robust assessment of predictive parameters for de-risking prospective HSA developments. The database enables comparison of factors within specific sedimentary basins (e.g., specific to the geological setting of a basin), between nations (e.g., specific to the regulatory regime), and location-independent technical aspects (e.g., drilling technology). We summarise findings from the first phase of data collection, encompassing a suite of project information such as reservoir properties and exploration and operation encountered risks. Case studies are discussed from the UK, the Netherlands, Denmark and Poland and preliminary recommendations for best practice in both HSA project development and data curation are presented.

1. INTRODUCTION

Geothermal energy is an important contribution to diversification of power and heat mix away from fossil fuels in many countries. The geothermal potential of Hot Sedimentary Aquifers (HSAs) has gained great interest in the last 20 years. HSAs are conduction-dominated hydrothermal systems in permeable sedimentary strata at depths of more than 200m and down to 4km (Gillepsie et al., 2013). In contrast to hot dry rock systems, HSAs do not usually require significant well stimulation to establish economically sustainable production rates. Temperatures of geothermal wells that currently produce from HSA usually range from 20°C to 80°C and the hot water produced is suitable for heating applications or occasionally electricity generation when the resource temperature exceeds 100°C. The heat from hydrothermal systems can be exploited via several types of well systems, in accordance with reservoir properties, project strategy and environmental regulations. A so-called "doublet system" includes a production well that extracts hot water and an injection well that re-injects cooled water back into the geothermal reservoir to maintain reservoir pressure or comply with local environmental regulations. Geothermal well systems utilising a single borehole (i.e. that pumps and discharges water) are rarer, with thermally spent water discharged to local water course or into the sea, such as at Southampton, UK (Downing et al., 1984). This configuration was especially selected for old (1970s, 1980s and 1990s) projects but its use is now restricted (or not permitted anymore) in many countries for environmental reasons e.g. high levels of TDS (salinity) or other constituents (Finster et al., 2015). A so-called "triplet" well configuration involves either two production wells and an injection well, such as at Fresnes, France or a single producer with two injection wells such as at Champigny-sur-Marne, France. Sometimes, other configurations such as "quadruplet" or "quintet" systems can be used depending on the thermal properties of the geothermal system exploited.

Countries that have potential HSA resources differ in their strategy of geothermal resource exploitation. The Netherlands has developed many HSA projects since the 2000s, especially in the West Netherlands Basin (Mijnlieff, 2020). The uptake of HSA geothermal projects was fuelled by the rise in gas prices and the crucial need for decarbonised energies. Indeed, the theoretical potential for direct use of geothermal energy in the Netherlands is substantial, at around 90,000 PetaJoule of heat in place (HIP) in the major reservoirs in Permian, Lower Triassic and Lower Cretaceous sandstones (Van Heekeren and Bakema, 2015). Italy is the global birthplace of geothermal industry with the first extraction of boric acid from volcanic mud using geyser steam that took place Larderello in 1880. In contrast to the Netherlands, since the 1900s, the country has mainly focused on exploring hot dry rock systems for electricity generation. One of the reasons for the very low growth of geothermal production for direct uses of the heat in Italy is the lack of effective support schemes and regulation (Manzella et al., 2019).

In addition to economic or legislative boundary conditions, the understanding of properties of the geothermal resource (or uncertainty thereof) is a major factor that facilitates uptake of geothermal development. Those uncertainties, together with financial and technical risks, and paucity of data, increase the risk exposure of projects and contribute to stakeholder reluctance to invest in HSA developments. If not mitigated, such risks can lead to the closure of a well, the abandonment of a geothermal project or a change in the purpose of the well.

Here we present a comprehensive assessment of currently operational and past HSA projects to highlight the most important predictive parameters for success, inform risk mitigation strategies and encourage the development of HSA technology.

2. METHODS

2.1 Systematic Literature Review

A systematic literature review synthesises the current state of knowledge in a specific field, by aggregating data systematically collected from peer-reviewed and grey literature (Figure 1). By examining pertinent literature, this research method allows an understanding of the scope and depth of the field studied as well as identification of research gaps and developing new theories (Xiao and Watson, 2019). Stewart (2004) defined a good review as comprehensive, fully referenced, selective, relevant, balanced, critical, analytical and a synthesis of key themes and ideas.

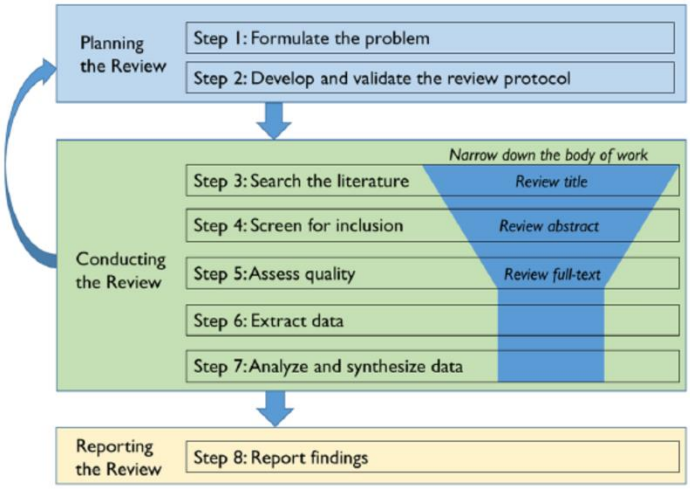

Figure 1: Process of a systematic literature review (from Xiao and Watson, 2019)

An initial HSA de-risking database was constructed using information from various sources (including online databases, research publications and websites). At the time of writing, it covers four countries: the UK, the Netherlands, Poland, and Denmark.

2.1.1 Various Data Sources

The identification and screening process is presented in Figure 2 and is adapted from the Preferred Reporting Items for Systematic Reviews and Meta-Analyses (PRISMA) protocols (Moher et al., 2010; Nguyen et al., 2019). For each search term, the first 10 pages of each utilized search engine were investigated.

Databases were found using search terms in Google including the name of the country investigated as well as keywords such as “geothermal database”, “public geothermal data” or “online dataset geothermal projects” “geological survey” (Figure 2). The number of results differed according to the country investigated.

Research articles were searched through search engines like Google, Google Scholar, university or private libraries, in scientific journals and research databases. The search words used included “hot sedimentary aquifer projects”, “geothermal energy” “geothermal projects” “geothermal sedimentary projects” together with the name of the

country studied. Only articles and abstracts that contained specified keywords and that were properly addressing the research objectives were selected to be further studied (Figure 2).

In the absence of project-related publications or reports, websites could represent a useful data source and can contain borehole reports and details on existing projects that will not be found anywhere else online. The search words are the same than for research articles but using Google. Websites can be projects, such as the trans-European PERFORM project (https://www.geothermperform.eu) whose main objectives are to improve geothermal plant performance, lower operational expenses and extend the lifetime of infrastructure, by combining data collection, predictive modelling, innovative technology development and in situ validation. Some operators also publicly share data about their power or heat plants on their website. The screening process for website selection is detailed in Figure 2.

Overall, the systematic review process took between one day and one week per country. Most of the time, a second review was performed afterwards, to gain more details for a specific project or well discovered during the first assessment. Specific search words including the name of a well (ex: “PNA-GT-02”), a project (ex: “Thisted”), parameters such as “porosity” or” depth” as well as the words “well report”, “project”, “final report” or “production test” were then used in Google and Google Scholar. A single key data collection source for all projects cannot be highlighted, as each country has its own political, regulatory and economic circumstances. However, a new trend is materialising in the last decade, with increased nations planning to massively invest in geothermal energy and therefore providing a wide access to the actual state of play of the technology and existing projects. The World Geothermal Congress (WGC) also created in 1995 the “country update” category of papers for the same purpose, that provides an up-to-date review of the geothermal development of a country (Krieger et al., 2022). In WGC 2000 and 2005, 72 countries have reported projects utilising geothermal energy for direct-heat applications or power generation (Lund, 2009), against 88 reports for WGC 2020 (Rumberg, 2020). However, Lund (2009) indicated that not all countries submit regular updates to the WGC, with at least 5 countries that develop geothermal projects for direct heating purposes not included in the Proceedings for WGC 2005.

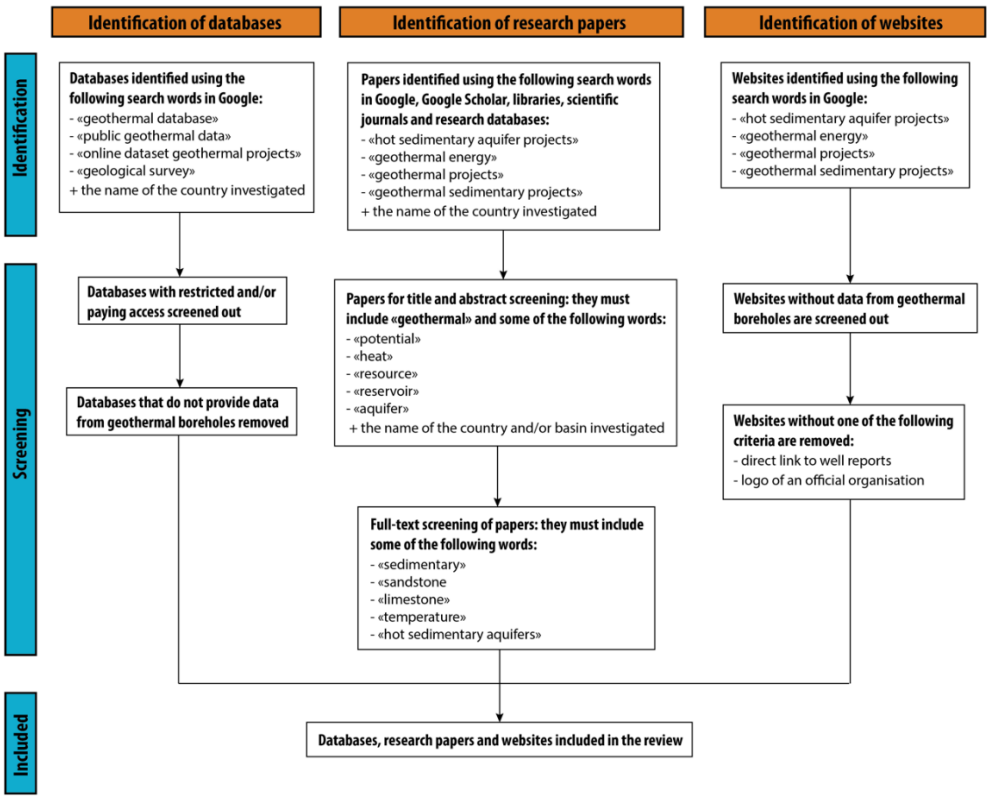

Figure 2: PRISMA flowchart of databases, research papers and website selection for the systematic literature review

2.1.2 A Country-Dependent Approach

Dataset availability is often related to the regulatory regime of a nation and these are dissimilar between the four countries studies in this paper. The methodology applied was therefore somewhat different for each country.

In the Netherlands, the geological survey (TNO) manages an open access database for geothermal projects which encompasses many parameters. General data such as the name and the starting date of the project, the number of wells, and the system type and use of the project are also commonly specified in Dutch scientific papers. Overall, the research process for this nation data was relatively simple and many data were found in a short amount of time.

Poland and Denmark have been more complicated countries to investigate for HSA data. Polish and Danish databases do not provide many geothermal data and information was mainly collected through Google Scholar and Google. However, it took much more time and search words including the name of the wells investigated + “well report” had to be used to obtain further details for the projects. In a third phase, search words were typed in Polish and Danish which increased the number of results.

Data research for HSA projects of the UK mostly involved scientific articles. The latter were found without difficulty using the search words specified in the previous section. Data provided is usually very detailed with parameters for each geothermal resource or reservoir. Although the British Geological Survey has an online database including energy

and water datasets, the data can only be displayed in map viewers, which makes aggregating the data very time-consuming.

2.1.3 Data Quality Appraisal

Assessment of data quality is an integral part of a systematic literature review and was performed throughout the entire process. Quality assessment implies checking that the values stored are correct, that there is no erroneous information and evaluation of the quality of the data sources. Most of the data collected comes from either well reports or published papers, and the information provided is therefore considered to be trustworthy. However, a few data could only be found in websites conducting an inventory of currently operational geothermal plants in a given country, with details on some parameters such as well depths, temperature and target formation. Even if only websites that are part of an official organization and/or displayed links to official project or well reports were selected during the systematic literature review process, the information provided is not entirely reliable. In several research papers and reports some variables are only provided as a range of values, which lowers their precision. For instance, a geothermal well drilled in 1981 in Larne, Northern Ireland, gave a porosity range from 15% to 25% for the target Sherwood Sandstone reservoir (Busby, 2014). Such ranges make any comparison or conclusion difficult and reduce data quality as they can only be included in the database as a mean (porosity of 20% for this example). Overall, around 7% of the numerical values of the hydrogeological dataset was reported as a range. Moreover, many boreholes have been drilled several decades ago when drilling, logging and testing techniques were not as advanced as more recent example, resulting in higher chances of inaccurate results and technical issues.

2.2 HSA Database

The HSA de-risking database encompasses a range of parameters that have been classified into four main categories: (1) general project information; (2) geological setting data; (3) hydrogeological property data; and (4) any risks encountered during the project (Figure 3). 36 parameters have been selected to describe each geothermal project as comprehensively as possible.

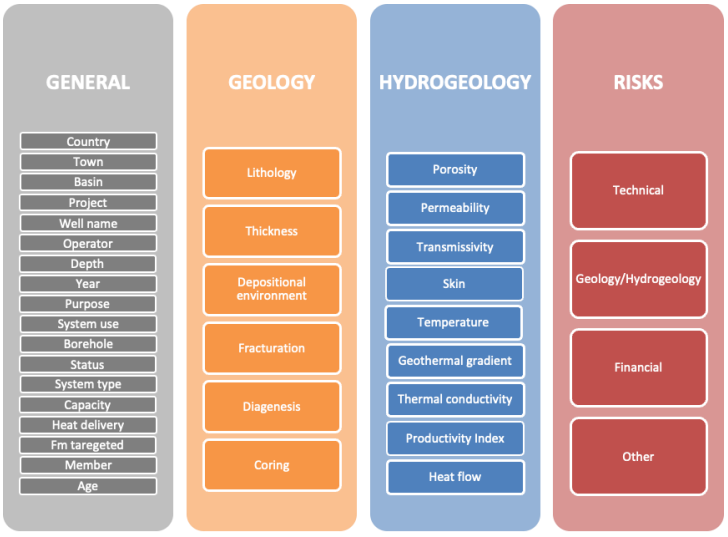

Figure 3: Listing of main parameters researched for each HSA project

General information includes typical variables found for each project, regardless of the field, such as project name, year(s) active, country, host sedimentary basin and targeted geological formation, and drilled borehole data (e.g. depth, name, status, system use, capacity). Within the geology category, parameters assessed included reservoir lithology, thickness (gross and net), and any information related to diagenesis and structural evolution. Collated reservoir information incorporates a suite of fluid and heat flow properties, all of which are strongly corelated with one of three key parameters: porosity, permeability and reservoir temperature. The last category gathers the diverse types of risks that can be faced when conducting a geothermal project. In most cases, risk is related to technical aspects, geological or petrophysical parameters, or project financing.

3. RESULTS AND DISCUSSION

3.1 Data availability and reporting

Interesting findings regarding availability were discovered during the systematic literature review process. The type of data and reports available strongly depends on the country, often driven by regulatory regime. In the Netherlands, the institution of the Mining Law in 2003 considerably improved the availability of information. Since 2003, all geothermal and oil and gas operators are required to publish geological and production data online in an open access database (www.nlog.nl) within 5 years of acquisition rather than 10 years as it was previously the case (Kombrink et al., 2012). The database, managed by the Geological Survey of the Netherlands (TNO) on the behalf of the Ministry of Economic Affairs and Climate, holds various data types such as 2D and 3D seismic lines, licences, oil and gas fields and borehole data. For most Dutch geothermal boreholes, the online database provides well reports, well test results, lithological logs and occasionally descriptions of core or cutting samples. The database access is public, free of charge and detailed. However, only raw data like lithological logs must be published in the online database, while interpreted data such as well tests are exempt from the rule. Developers only have to publish data several years after acquisition, and therefore the database is not fully up to date. The projects completed in the range 2018-2022 are not yet available online as it appears that companies and operators usually wait until the end of the embargo period (i.e., 5 years after acquisition) to publish the data. In old wells, regardless of the country, many petrophysical parameters were not evaluated and very little well or production test data is typically available. Consequently, both recent (2018 and after) and old (1960-1990) projects can lack published data. The Netherlands appears to be the exception when it comes to freely accessible geothermal data repositories, operators in most countries are not required by law to publish project related results.

The Croatian Hydrocarbon Agency (AZU) also provides a free of charge access to reports of Croatian geothermal wells, seismic data, and GIS data through the Croatian Geothermal Virtual Data Room (VDR). However, the VDR is a controlled-access database: it is available for investors only and access is not provided for academic purposes.

In the UK, the British Geological Survey (BGS) retains a wide range of general geoscience data, through datasets, borehole reports and map viewers of the whole nation. However, the available information is not as detailed (i.e. with exact values for many parameters) as the Dutch database as not all reports (and thus data) can be accessed online. The same observation can be applied to both Danish and Polish geothermal databases that usually

only provide general data, such as project and well name, depth, coordinates, and drilling date.

Information on geothermal wells drilled in the UK is conventionally published in research articles, most of the time by way of the BGS. Detailed data is usually provided, with parameters for each geothermal resource or reservoir, and information accuracy can be tested by cross-checking multiple articles. The abundance of geological variables in UK papers could be explained by a political desire to facilitate access to data in order to develop HSA projects.

Danish and Polish research papers provide a good overview of existing plants and projects with common parameters included, such as reservoir temperature and total depth of the well, but they do not always specify petrophysical data like porosity or permeability, which are critical for the assessment of a geothermal aquifer. The same observations can be applied to the Netherlands, where a number of scientific articles listing existing hot sedimentary aquifer projects and potential targets can be found, but without details regarding the related geological and reservoir parameters.

Nevertheless, it should be noted that not all projects targeting HSAs were included into the database. As previously stated, there are only little data available on very recent projects, so it was decided to not incorporate any borehole (1) drilled after 2018 and (2) that does not include basic project information (i.e. name, system type, depth, year). Moreover, this study was focused on deep sedimentary reservoirs only, thus shallow technologies such as ground source heat pumps (GSHP) or flooded mine workings are not covered. Aquifer Thermal Energy Storage (ATES) systems were not included either, but as an emergent technology they could represent, if hot and deep enough, an excellent opportunity to enrich the database in the future.

3.2 Development of Geothermal Energy Technology

The database currently includes 88 geothermal boreholes associated with HSAs in the UK, the Netherlands, Denmark and Poland. These boreholes are from a total of 45 HSA projects: one borehole can reach several target aquifers and one project may involve a doublet or triplet (or more) system of boreholes. Fifty-three (60%) of the boreholes were drilled in the Netherlands, 19% in Poland while the other countries represent approximately the same percentage of wells, with 9% for the UK and 11% for Denmark. However, as outlined in the previous section, none of these borehole records have data for every variable, leading to gaps in the database.

The types of wells systems utilised in the compiled HSA projects are reported in Figure 4. More than half of the wells (56%) exploit the reservoir via a doublet or a double-doublet (quadruplet) system, 31% use a single well system and the triplet configuration is utilised in only four projects (9%). A geothermal project in the Carpathian (Poland) is currently exploiting a sedimentary aquifer using a quintet system including two injectors and three producers. The septet borehole system (Figure 4) will be used in another Polish system, that is currently extracting heat using a triplet but whose project assumes the production of four new geothermal wells in the coming years (Cloudzynska, 2019).

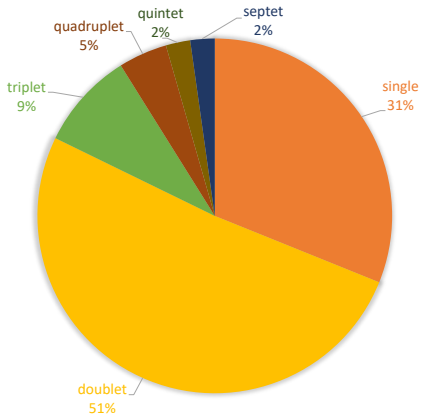

Figure 4: Proportion of borehole system types used in database-included projects

The variation in technical approach in each country can be assessed by looking at the difference between the number of new boreholes versus the number of new projects. The total number of HSA projects increased through time, with almost twice as many new projects developed throughout 2011-2019 than during the previous decade (Figure 5). However, each country shows different progress during the last 50 years with a much greater increase in projects in the Netherlands than any other country.

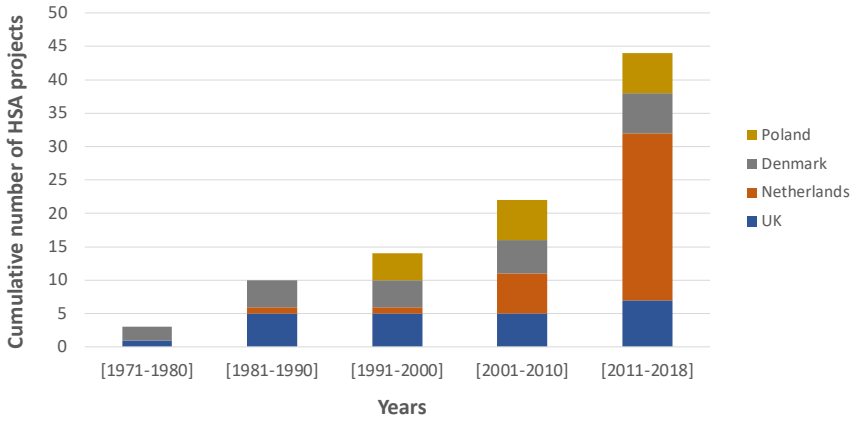

Figure 5: Cumulative number of HSA projects per 10-year interval, including projects that are currently running and shut projects.

In the Netherlands, the first exploration well for geothermal development (Asten-2) was drilled in 1987 in the in the Roer Valley Graben (Kombrink et al., 2012). Dufour and Heederik (2019) suggested that a large amount of natural gas reserves proven in 1986-1987 as well as a lack of support and cooperation between oil companies and the government slowed down geothermal energy development. The legislative framework to explore geothermal energy was unclear due to lack of knowledge and experience of permitting and licencing. Since the end of the 1990s, especially following the Kyoto protocol (1997), geothermal energy received a renewed interest in the Netherlands and steps were taken to create a pertinent legislation (Lokhorst and Wong, 2008). Figure 5 shows that 4 projects were initiated between 2001 and 2010 while only the Asten project pre-dates this period. The emergence of new techniques such as basin modelling, 3D seismic interpretation and subsurface temperature assessments kickstarted a series of studies to estimate geothermal resources (Kombrink et al., 2012). In the middle of the 2000s, high gas prices as well as the pressing need to reduce CO2 emissions further

convinced Dutch authorities and companies of the need to invest in geothermal energy. The number of exploration licenses considerably increased in subsequent years with 93 applications by August 2011, most of them in the West Netherlands Basin (Kombrink et al., 2012). By January 2019, the Netherlands counted 51 exploration licences and 12 production licences. Between 2011 and 2018, the Netherlands have experienced the fastest development of geothermal energy in Europe. Willems and Nick (2019) suggest that geothermal production from the Lower Cretaceous reservoirs could cover up to 20% of heat demand in Zuid-Holland province by 2050. The results from our study show the same trend with only Asten-2 starting in the 1980s and the 1990s, then almost four times more projects between 2011-2018 than 2001-2010 (Figure 5). This pattern is seen in all exploited reservoir units: Lower Cretaceous, Carboniferous and Lower Permian aquifers.

Figure 6 illustrates the evolution of the number of new HSA wells (first bar for each decade), compared to the evolution of the number of new HSA projects since the 1970s (second bar for each decade), giving a ratio of the number of wells per project throughout the decades. The ratio of single to multi-well systems has evolved with time in the Netherlands, with twice as many boreholes as projects between 2011 and 2019 (Figure 6). This feature can probably be explained by increased use of doublet systems with producer and injector wells. However, Willems and Nick (2019) suggest that Dutch doublet deployment has not been efficient and predict that only 1% of potential heat within Lower Cretaceous aquifers will be recovered within 30 years. They also state that individual operators develop individual doublet systems which focus on small and decentralised heat grid demands (such as greenhouse agriculture), while a regional coordinated approach, matching up wider scale and interlinked heat demand, could increase potential heat recovery by several orders of magnitude.

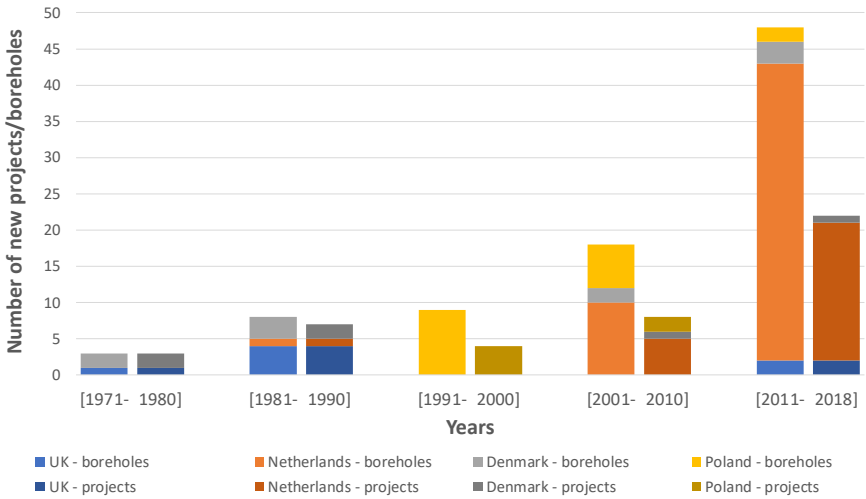

Figure 6: Evolution of the number of new HSA boreholes compared to the number of new HSA projects per 10-year interval. UK is in shades of blue, the Netherlands in shades of orange, Denmark in shades of grey and Poland in shades of yellow. Lighter shades are fore boreholes while darker shades relate to projects

In the UK, the government and the European Commission funded the Geothermal Energy Program following the increase in oil prices between 1977 and 1994 to assess the potential of British HSA resources (Downing and Gray, 1986). Four deep geothermal boreholes were drilled but by the end of the 17-year Program, the only commercial use occurred at

Southampton to provide heat to a district heating scheme (Barker et al., 2000). In 2004, the UK became a net-importer of energy due to the decline of the North Sea hydrocarbon production. As fossil fuel supply became restricted and more expensive and the drivers for decarbonization became stronger in the 2000s, geothermal exploration efforts were made to diversify the UK power mix and develop geothermal energy for direct use applications (Busby, 2010). Aforementioned developments and technological drilling advances enhanced the case for exploitation of HSA resources in the UK (Busby, 2014). However, the Southampton District Energy Scheme remains the only deep commercial geothermal project in the UK to date. The borehole was drilled in 1987 to a depth of 1.827 km and is targeting Triassic Sandstones. The Southampton borehole was located at a coastal site so the brine could be discharged directly to the sea and no reinjection borehole was required (Barker et al., 2000). Since then, most new boreholes drilled in the UK have been for demonstration or exploration purposes, resulting in a UK borehole to project ratio of 1:1 (Figure 6). The number of HSA related boreholes peaked in the 1980s (n = 5), with no new wells in the 1990s or 2000s, and two new projects in the 2010s. With a total of one active project (and another one only used for research purposes), the UK lags behind the other countries in the present study in the development of HSAs.

Denmark hosts a large geothermal potential, with estimated HSA resources sufficient to cover household heating supplies for more than 100 years (Sørensen et al., 1998). Since the mid-1990s, the Danish government has focused on low-CO2 producing heating sources and increased fossil fuel taxes (Mahler and Magtengaard, 2005), leading to increased development of renewable energies. The target is to reach 100% renewable energy by 2050 with a specific focus in some regions such as the Copenhagen area, which holds a substantial geothermal potential and should be carbon-neutral by 2025 (Mathiesen et al., 2010). Technological improvements in the 2000s increased the interest in aquifers with good porosity and permeability properties and high productivity (Nielsen et al., 2004). Figure 6 shows that since the 2000s, there is around twice as many boreholes as HSA projects reported in Denmark (Figure 6), meaning that Danish geothermal systems are mainly doublets plus three single wells. The number of Danish HSA projects increased from beginning of the 1970s to the end of the 1980s (Figures 5 and 6). This trend slowed in the 1990s but resumed from the 2000s and will likely continue in the following decade. Despite those encouraging results, only a fraction of the Danish geothermal resources is being exploited at present, with only six projects reported in this study. Indeed, there are very few options for risk hedging and the regulation for shallow plants is still complex even though it is currently being revised (Røgen et al., 2015).

In Poland, four HSA projects were initiated in the 1990s and two in the 2000s, and development of new projects has since stagnated (Figure 6). However, several Polish projects developed their well systems in the 2010s to meet the ever-increasing heat demand. For example, a new producer well was drilled in 2013 in the Podhale geothermal project that was first initiated in 1992 (Sliwa et al., 2021). Slow growth of new projects is mainly due to a lack of financial support as well as economic and legal barriers (Sowizdzal, 2018). The Central Fund for Water Management and Environment Protection provided financial support for geothermal investments and, as a result, 30 applications were submitted in 2016 (Sowizdzal, 2018). Furthermore, many positive decisions on financing new research drillings for geothermal were issued at the end of the 2010s, and therefore around 10 new geothermal wells are expected in the coming years (Kępińska, 2019). Polish

geothermal exploitation has so far focused on small scale heating applications such as space heating, balneotherapy, or bathing (Sowizdzal, 2018). Technology has evolved over the decades: vertical geothermal boreholes made of steel pipes have been gradually replaced by directional wells (Sliwa et al., 2021). Furthermore, many geothermal or former oil wells were reconstructed over the years and may have both prevented the closing of some projects and allow for the lifetime extension of others (Bujakowski et al., 2020). Overall, there is not a widely used well system in Poland. Conversely, they are exploiting HSA utilizing a wide range of systems (single, triplet, quadruplet, quintet, septet) (Figure 6).

3.3 Causes of Failure in HSA Projects

The data analysis showed that HSA projects are subject to four dominant types of risk during geothermal development (Table 1).

Risk	Details
Technical	Well integrity issues: corrosion, formation damage, clogging, wellbore deviation
Geology/Hydrogeology	Changing groundwater chemistry, ground deformation, fault reactivation, aquifer uncertainties, temperature colder than expected, low petrophysical values, insufficient water flow or productivity or injectivity, water pollution, induced seismicity
Financial	Lack of funding, bankrupt, project not commercially attractive, insufficient number of subscribers
Other	No demand for the water nearby, wrong decisions, timing, scheduling

Table 1: Detailed classification of the 4 types of risks catalogued in the database: drilling, geology and hydrogeology, financial and any other risk

A project is defined as failed when at least one of the risks cannot be mitigated leading to abandonment of the project and/or a change in the purpose of the wells. For example, a project drilled for heating purposes that failed to flow water to surface or shows an unexpected low permeability, that is now used for research purposes is considered as having failed. just like a project abandoned because of a well that experienced corrosion deposits, or due to a lack of funding. A project can be abandoned due to one of several of the risks listed in Table 1. Amongst the 45 projects gathered in the database, 40% experienced at least one failure. The proportion of failed HSA projects varies between the UK, Denmark, Poland and the Netherlands (Figure 7). The highest failure rate of all countries is observed in the UK, with six out of eight projects that either are no longer active or never launched. These projects were drilled for research purposes (n=7) or to provide heat to a district heating scheme (n=3). Denmark shows a success rate of 66% with only two out of six projects that experienced at least one issue. 40% of Dutch projects experienced some form of failure, while Poland shows 100% success: none of the six HSA projects that were launched in Poland experienced a single failure. Technological improvements for geothermal energy in Poland such as well reconstructions that have been undertaken in the 1990s, 2000s and 2010s on abandoned or damaged boreholes

(Bujakowski et al., 2020), or lack of reporting of failed projects could explain the success rate.

Figure 7: Total number of HSA projects (blue) versus the number of projects experiencing 1 or more failure during project development (red), for each country assessed

4. CONCLUSION

Hot sedimentary aquifers (HSA) have significant potential to provide a low-carbon heat source, but projects must cope with a large number of uncertainties and risks. A database was created to capture key information from HSA-related projects in four countries: the UK, the Netherlands, Denmark, and Poland. The database includes information gathered from 88 boreholes, with the number of recorded parameters for each borehole or project ranging from 11 to 28. Preliminary analysis shows interesting trends regarding the type of borehole systems used for HSA development: each country has its most common system type that highly depends on both technical evolutions as well as the legal framework in place. 51% of the 45 HSA projects employ a doublet system with an injector and a producer. On the other hand, a single well configuration was selected in 31% of the projects (mainly old or/and exploration wells) versus 9% for a triplet system. Regarding project successes, 18 of them experienced one or more failures during their development with a substantial difference in success rate for each country studied.

This paper presents the initial findings of the HSA database development. Future work will expand the geographical reach of the database, expand on the number of factors that may have influenced failure, as well as examining different modes of project failure. Learning from project failure will ensure a rapid roll-out of this exciting new technology to help meet decarbonisation targets and secure energy supplies.

REFERENCES

Barker, J. A., Downing, R. A., Gray, D. A., Findlay, J., Kellaway, G. A., Parker, R. H., and Rollin, K. E.: Hydrogeothermal studies in the United Kingdom, Quarterly Journal of Engineering Geology and Hydrogeology, 33(1), (2000), 41-58.

Bujakowski, W., Bielec, B., Miecznik, M., and Pająk, L.: Reconstruction of geothermal boreholes in Poland, Geothermal Energy, 8(1), (2020), 1-27.

Burgers, C., Brugman, B. C., and Boeynaems, A.: Systematic literature reviews: Four applications for interdisciplinary research, Journal of Pragmatics, 145, (2019), 102-109.

Busby, J.: Geothermal prospects in the United Kingdom, (2010).

Busby, J.: Geothermal energy in sedimentary basins in the UK. Hydrogeology journal, 22(1), (2014), 129-141.

Cloudzynska, A: Stargard Geothermal Development Plans!, Globenergia, (2019), Retrieved October 20, 2022, from https://globenergia.pl/plany-rozwoju-geotermii-stargard/

Downing, R. A., Allen, D. J., Barker, J. A., Burgess, W. G., Gray, D. A., Price, M., and Smith, I. F.: Geothermal exploration at Southampton in the UK: a case study of a low enthalpy resource, Energy Exploration & Exploitation, 2(4), (1984), 327-342.

Downing R. A., Gray D. A (Eds.).: Geothermal energy: the potential in the United Kingdom, HM Stationery Office, (1986).

Dufour, F. C., and Heederik, J. P.: Early Geothermal Exploration in the Netherlands 1980 – 2000, Proceedings, European Geothermal Congress 2019, Den Haag, The Netherlands, (2019).

Finster, M., Clark, C., Schroeder, J., & Martino, L: Geothermal produced fluids: Characteristics, treatment technologies, and management options, Renewable and Sustainable Energy Reviews, 50, (2015), 952-966.

Gillespie, M. R., Crane, E. J., and Barron, H. F: Study into the potential for deep geothermal energy in Scotland, British Geological Survey Commissioned Report, (2013).

Kępińska, B.: Geothermal energy use - Country update for Poland, 2016–2018, Proceedings, European Geothermal Congress 2019, Den Haag, The Netherlands, (2019).

Kombrink, H., Ten Veen, J. H., and Geluk, M. C.: Exploration in the Netherlands, 1987-2012, Netherlands Journal of Geosciences, 91(4), (2012), 403-418.

Krieger, M., Kurek, K. A., and Brommer, M.: Global geothermal industry data collection: A systematic review, Geothermics, 104, (2022), 102457.

Lokhorst, A., and Wong, T. E.: Geothermal energy, (2008).

Lund, J. W.: Utilisation of geothermal resources, Proceedings of the Institution of Civil Engineers-Energy, 162(1), (2009), 3-12.

Mahler, A., and Magtengaard, J. Geothermal Development in Denmark, Country Update 2005, Proceedings, World Geothermal Congress 2005, Antalya, Turkey, (2005).

Manzella, A., Serra, D., Cesari, G., Bargiacchi, E., Cei, M., Cerutti, P., ... and Vaccaro, M.: Geothermal energy use, country update for Italy, Proceedings, European Geothermal Congress 2019, Den Haag, The Netherlands, (2019), 11-14.

Mathiesen, A., Nielsen, L. H., and Bidstrup, T.: Identifying potential geothermal reservoirs in Denmark, GEUS Bulletin, 20, (2010), 19-22.

Merz, S. K.: Geothermal Energy Potential in Great Britain and Northern Ireland, (2012).

Mijnlieff, H. F.: Introduction to the geothermal play and reservoir geology of the Netherlands, Netherlands Journal of Geosciences, (2020), 99.

Moher, D. L. A., Liberati, A., Tetzlaff, J., Altman, D.G., and Prisma Group.: Preferred reporting items for systematic reviews and meta-analyses: the PRISMA statement, International Journal of surgery (London, England), 8(5), (2010), 336–341.

Nguyen, H., Manolova, G., Daskalopoulou, C., Vitoratou, S., Prince, M., and Prina, A.M.: Prevalence of multimorbidity in community settings: A systematic review and meta-analysis of observational studies, Journal of Comorbidity, 9, (2019), 1–15.

Nielsen, L. H., Mathiesen, A., and Bidstrup, T.: Geothermal energy in Denmark, GEUS Bulletin, 4, (2004), 17-20.

Okoli, C., and Schabram, K.: A guide to conducting a systematic literature review of information systems research, Sprouts: Working Papers on Information Systems, 10(26), (2010).

Røgen, B., Ditlefsen, C., Vangkilde-Pedersen, T., Nielsen, L. H., and Mahler, A.: Geothermal energy use, 2015 country update for Denmark, Proceedings, World Geothermal Congress 2015, Melbourne, Australia, (2015).

Rumberg, G.: World Geothermal Congress 2020 – Virtual event and global updates, IGA, (2020), Retrieved October 19, 2022, from https://www.lovegeothermal.org/world-geothermal-congress-2020-virtual-event-global-updates-april-27-2020/

Sliwa, T., Sapińska-Śliwa, A., Gonet, A., Kowalski, T., and Sojczyńska, A.: Geothermal Boreholes in Poland - Overview of the Current State of Knowledge, Energies, 14(11), (2021), 3251.

Sørensen, K., Nielsen, L. H., Mathiesen, A., and Springer, N.: Geotermi i Danmark: Geologi og ressourcer, Danmarks og Grønlands Geologiske Undersøgelse Rapport, 123, (1998), 24.

Sowizdzal, A.: Geothermal energy resources in Poland - overview of the current state of knowledge. Renewable and Sustainable Energy Reviews, 82, (2018), 4020-4027.

Steward, B.: Writing a literature review, British Journal of Occupational Therapy, 67(11), (2004), 495-500.

Van Heekeren, V., and Bakema, G.: The Netherlands Country Update on Geothermal Energy, Proceedings, World Geothermal Congress 2015, Melbourne, Australia, (2015).

Willems, C. J. L., and Nick, H. M.: Towards optimisation of geothermal heat recovery: An example from the West Netherlands Basin, Applied energy, 247, (2019), 582-593.

Xiao, Y., and Watson, M.: Guidance on conducting a systematic literature review, Journal of planning education and research, 39(1), (2019), 93-112.

Younger, P. L., Feliks, M. E., Westaway, R., McCay, A. T., Harley, T. L., Elliott, T., ... and Waring, A. J.: Renewing the exploration approach for mid-enthalpy systems: Examples from northern England and Scotland, Proceedings, World Geothermal Congress 2015, Melbourne, Australia, (2015).

APPENDIX B.
Supporting Information for Chapter 3

The database for "Global database of hot sedimentary aquifer geothermal projects: De-risking future projects by determining key success and failure criteria in the development of a valuable low-carbon energy resource" contains 57 components of HSAs projects in Australia, Croatia, Denmark, France, Germany, Poland, the Netherlands, and the UK that were extracted. Collated data especially include technical information on the project and the boreholes, geology and hydrogeology parameters, and the risks associated with each project.

The dataset can be found here: https://doi.org/10.15129/19dfb2af-13f6-45f5-a406-497ab15950b9

APPENDIX C.
Supporting Information for Chapter 6

Picture of the samples

Sample n°SSK153707

Sample n°SSK153713

Sample n°SSK153711

Sample n°SSK153714

Sample n°SSK153712

Sample n°SSK153715

Sample n°SSK153716

Sample n°SSK153717

Sample n°SSK153718

Sample n°SSK153719

Sample n°SSK153720

Sample n°SSK153721

Sample n°SSK153722

Sample n°SSK153723

Sample n°SSK153724

Sample n°SSK153725

Sample n°SSK153726

Sample n°SSK153727

Sample n°SSK153729

Sample n°SSK153730

Sample n°SSK153728

Sample n°06-1

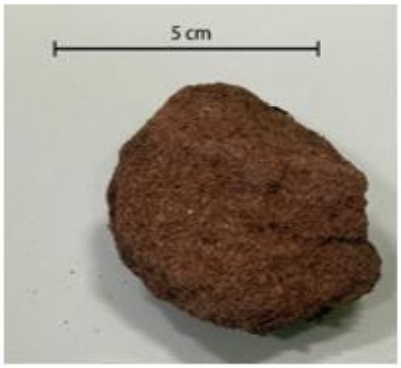

Sample n°06-2

Sample n°06-3

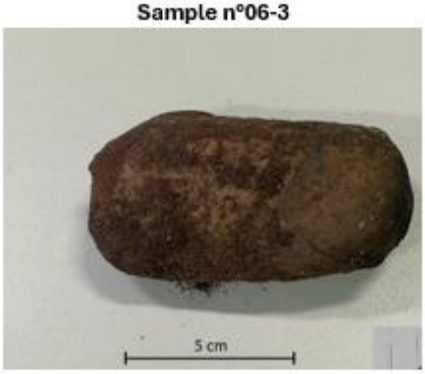

Sample n°07-1

Sample n°07-2

Sample n°08-1

Sample n°08-2

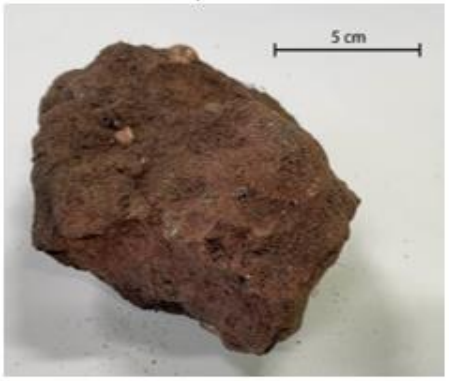

Sample n°09-1

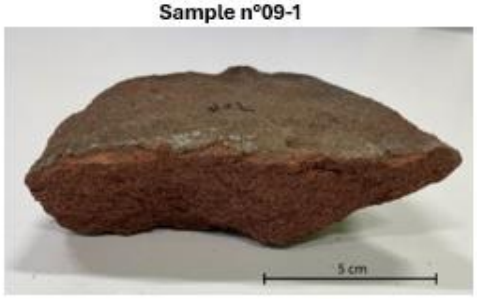

Sample n°15-1

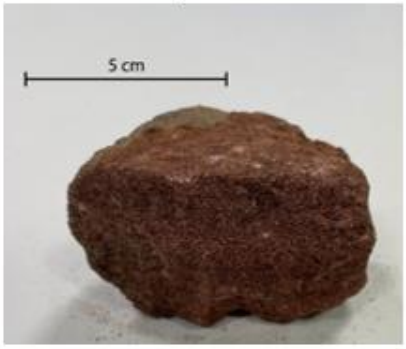

Sample n°16-1

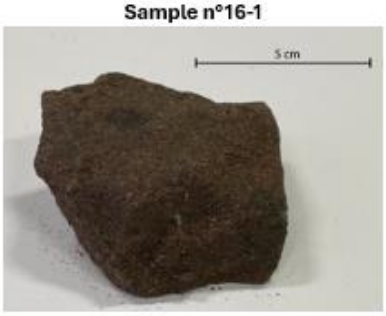

Sample n°16-2

Sample n°16-3

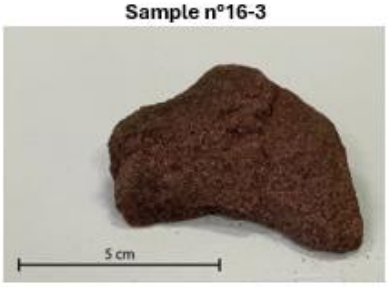

Sample n°17-1

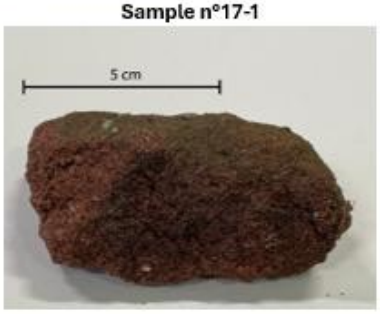

Sample n°18-1

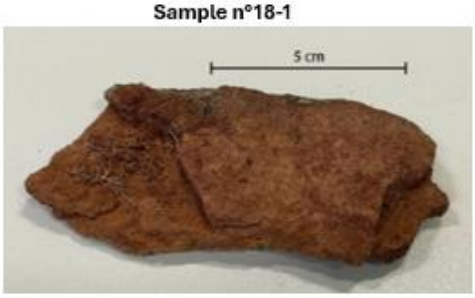

Sample n°19-1

Sample n°20-2

Description of the core samples

Borehole name/Well number	Sample Number	Acid Test (10% HCl)	Depth top (m)	Depth base (m)	Diameter	Length (cm)	Drilling direction	Color	Grain size	Grain shape	Grain sorting	Sedimentary features	Fractures/faults	Pebbles
UKGEOS CHESHIRE TH0424	SSK153707	No reaction	22.82	22.87	2"	3	Vertical	red-brown	fine	subrounded	Well sorted	trough cross bedding	Fault zone with very closely-spaced fractures, clay filled	
UKGEOS CHESHIRE TH0424	SSK153711	No reaction	26.37	26.42	2"	5	Vertical	red-brown	fine-medium	rounded	Moderately sorted	some mud clasts		
UKGEOS CHESHIRE TH0424	SSK153712	No reaction	27.55	27.6	2"	5	Vertical	red-brown	fine-medium	subrounded	Well sorted			
UKGEOS CHESHIRE TH0424	SSK153713	No reaction	31.53	31.58	2"	5	Vertical	red-brown	fine-medium	subangular	Moderately sorted	mud clasts		mm scale pebble
UKGEOS CHESHIRE TH0424	SSK153714	No reaction	32.67	32.72	2"	5	Vertical	red-brown	medium	rounded	Very well sorted			
UKGEOS CHESHIRE TH0424	SSK153715	No reaction	34.01	34.06	2"	5	Vertical	brown	clay			soft-sediment deformation	fractured	
UKGEOS CHESHIRE TH0424	SSK153716	Moderate reaction	34.78	34.83	2"	5	Vertical	red-brown	fine-medium	subrounded	Moderately sorted	low angle cross bedding		
UKGEOS CHESHIRE TH0424	SSK153717	Strong reaction	37.77	37.82	2"	5	Vertical	red-brown	fine-medium	subangular	Well sorted	low angle cross bedding		
UKGEOS CHESHIRE TH0424	SSK153718	Moderate reaction	39.61	39.66	2"	5	Vertical	red-brown	fine-medium	subrounded	Moderately sorted	low angle cross bedding		
UKGEOS CHESHIRE TH0424	SSK153719	Strong reaction	39.87	39.92	2"	5	Vertical	red-brown	fine-medium	subangular	Well sorted	low angle cross bedding		some mm pebbles
UKGEOS CHESHIRE TH0424	SSK153720	Strong reaction	44.04	44.09	2"	5	Vertical	red-brown	fine-medium	subrounded	Well sorted			
UKGEOS CHESHIRE TH0424	SSK153721	Strong reaction	56.39	56.44	2"	5	Vertical	red-brown pale green grey and	medium-coarse	subangular	Well sorted			a few mm to cm sub-rounded pebbles
UKGEOS CHESHIRE TH0424	SSK153722	No reaction	60.25	60.3	2"	5	Vertical	red-brown banding	very fine-fine	subrounded	Well sorted	low angle cross bedding		
UKGEOS CHESHIRE TH0424	SSK153723	Strong reaction	73.39	73.45	2"	6	Vertical	red-brown	fine-medium	subangular	Moderately sorted			cm scale sub-rounded pebbles
UKGEOS CHESHIRE TH0424	SSK153724	Moderate reaction	78.25	78.3	2"	5	Vertical	red-brown	fine-medium	subrounded	Moderately sorted	low angle cross bedding, soft sediment deformation		
UKGEOS CHESHIRE TH0424	SSK153725	Moderate reaction	79.12	79.17	2"	5	Vertical	red-brown	fine	subangular	Moderately sorted	low angle cross bedding		
UKGEOS CHESHIRE TH0424	SSK153726	Weak reaction	80.62	80.69	2"	7	Vertical	red-brown	medium	subrounded	Well sorted	low angle cross bedding		large variability in sub-rounded pebble
UKGEOS CHESHIRE TH0424	SSK153727	Strong reaction	83.7	83.75	2"	5	Vertical	red-brown	medium-coarse	subrounded	Well sorted	low angle cross bedding		few mm scale sub-rounded pebbles
UKGEOS CHESHIRE TH0424	SSK153729	Moderate reaction	87.1	87.15	2"	5	Vertical	red-brown	medium	rounded	Well sorted	low angle cross bedding		few mm scale sub-rounded pebbles
UKGEOS CHESHIRE TH0424	SSK153730	Moderate reaction	91.1	91.18	2"	8	Vertical	red-brown	medium	subangular	Moderately sorted	rare mud clasts		rare mm scale sub-rounded pebbles
UKGEOS CHESHIRE TH0424	SSK153728	Strong reaction	96.55	96.6	2"	5	Vertical	red-brown	medium	subrounded	Well sorted	low angle cross bedding		rare mm scale sub-rounded pebbles

Description of the outcrop samples

Sample Number	Thickness (cm)	Width (cm)	Length (cm)	Acid Test (10% HCl)	Outcrop condition	Outcrop Facies	Texture	Induration	Color	Grain shape	Grain sorting	Faults/fracturing	Amount	Pebbles Size (cm)	Layered (Y/N)	Other structures
06-1	1.5	2.5	2.5	No reaction	medium	massive	Matrix-supported conglomerate with medium grains	Soft	brown	Rounded	Well sorted	Outcrop fractured (fault?)	A few	2-3	N	
06-2	2.5	2.5	4.0	No reaction	medium	massive-layered	Matrix-supported conglomerate with medium grains	Soft	brown	Rounded	Well sorted		Many	2-3	N	
06-3	4.5	4.0	9.5		medium	layered	Matrix-supported conglomerate with medium grains	Hard	brown	Rounded	Moderately sorted		Many	3-4	N	
07-1	2.5	4.0	7.0	No reaction	good	massive-layered	Matrix-supported conglomerate with coarse grains	Medium	brown	Subrounded	Well sorted	Vertical fractures	A few	4-5	N	
07-2	1.5	3.5	3.5	No reaction	good	massive	Coarse sand	Soft	brown	Subangular	Moderately sorted	fractures	None			Cross bedded, N10 7NE
08-1	6.0	5.0	11.0	No reaction	medium	massive-layered	Matrix-supported conglomerate with medium grains	Medium	brown	Subrounded	Well sorted	fractures	Many	3-4	N	
08-2	2.0	2.5	4.5	No reaction	medium	layered	Matrix-supported conglomerate with coarse grains	Soft	brown	Subrounded	Moderately sorted	Vertical fractures	A few	1-2	Y	
09-1	4.0	5.0	11.5		good	massive-layered	Medium sand	Hard	brown	Subangular	Well sorted	Vertical fractures	Almost none	1	N	
15-1	2.0	3.0	6.0	No reaction	good	massive-layered	Medium sand	Medium	brown	Rounded	Well sorted	fractures	None			Cross bedded
16-1	4.0	3.0	3.5	No reaction	good	massive-layered	Medium sand	Hard	brown	Subangular	Well sorted	fractures	None			Cross-bedded
16-2	1.4	7.0	10.0	No reaction	good	massive-layered	Medium sand	Hard	brown	Subrounded	Moderately sorted	fractures	None			Cross-bedded
16-3	2.0	1.5	2.5	No reaction	good	massive-layered	Medium sand	Hard	brown	Subangular	Well sorted	fractures	None			Cross-bedded
17-1	3.5	2.5	3.5	No reaction	medium	massive	Matrix-supported conglomerate with coarse grains	Soft	brown	Rounded	Well sorted	Fractures	A few	2-3	Y	
18-1	1.0	4.0	9.0	No reaction	medium	layered	Medium sand	Soft	brown	Angular	Well sorted	Small faults	None			
19-1	2.5	2.0	4.5	No reaction	good	massive	Fine sand	Soft	brown	Subrounded	Moderately sorted		None			
20-2	5.5	3.0	8.0	No reaction	good	massive	Medium sand	Hard	brown	Rounded	Well sorted		None			

APPENDIX D.
Supporting Information for Chapter 7

Thermal conductivity measurements under water-saturated conditions and progressively increasing temperature steps for Experiment A and B.

	sample ID	λ at 30°C (W/(mK))					λ at 50°C (W/(mK))					
		measurements			mean	sd	measurements			mean	sd	
Experiment A	SSK153718	3.199	3.185	3.197	3.210	**3.20**	0.01	3.165	3.221	3.210	3.148	3.211	**3.19**	0.03
	SSK153713	3.038	3.090	3.097	3.098	3.085	**3.08**	0.02	3.107	3.036	3.090	2.937	3.075	**3.05**	0.06
	SSK153730	4.430	4.427	4.423	4.342	4.390	**4.40**	0.03	4.298	4.192	4.228	4.206	4.254	**4.24**	0.04
	08-1	2.948	3.041	2.971	2.889	2.963	**2.96**	0.05	2.868	2.767	2.802	2.907	2.801	**2.83**	0.05
	19-1	2.997	2.917	3.197	3.021	2.839	**2.99**	0.12	2.866	2.705	3.109	3.068	2.883	**2.93**	0.15
	SSK153730	4.445	4.39	4.347	4.416	4.369	**4.39**	0.03	4.277	4.237	4.298	4.185	4.309	**4.26**	0.05
Experiment B	SSK153723	4.054	3.957	4.051	4.087	4.067	**4.04**	0.04	3.784	4.145	3.769	3.894	3.776	**3.87**	0.14
	SSK153711	3.481	3.403	3.469	3.421	3.44	**3.44**	0.03	3.256	3.237	3.245	3.343	3.296	**3.28**	0.04
	20-2	3.264	3.251	3.293	3.248	3.307	**3.27**	0.02	3.206	3.218	3.128	3.018	3.247	**3.16**	0.08
	08-2	3.266	3.245	3.286	3.187	3.212	**3.24**	0.04	3.191	3.073	3.27	3.176	3.075	**3.16**	0.07
	19-1	3.51	3.512	3.524	3.495	3.505	**3.51**	0.01	3.394	3.276	3.627	3.346	3.416	**3.41**	0.12

	sample ID	λ at 70°C (W/(mK))					λ at 90°C (W/(mK))					
		measurements			mean	sd	measurements			mean	sd	
Experiment A	SSK153718	3.130	3.194	3.180	3.079	2.967	**3.11**	0.08	2.989	3.051	2.966	3.161	3.073	**3.05**	0.07
	SSK153713	3.177	2.972	2.998	2.993	2.984	**3.03**	0.08	2.968	3.003	2.955	2.993	2.971	**2.98**	0.02
	SSK153730	4.103	4.166	4.072	4.137	4.170	**4.13**	0.04	3.908	3.934	3.978	4.020	3.918	**3.95**	0.04
	08-1	2.836	3.061	2.998	3.056	3.041	**3.00**	0.08							
	19-1	2.903	2.739	2.921	2.852	2.963	**2.88**	0.08	2.999	3.125	3.212	2.998	2.942	**3.06**	0.10
	SSK153730	3.966	4.101	4.259	4.082	4.232	**4.13**	0.11	3.931	4.018	4.233	4.413	4.003	**4.12**	0.18
Experiment B	SSK153723	3.929	3.776	3.687	3.98	3.86	**3.85**	0.11	3.957	3.549	4.094	3.418	3.645	**3.73**	0.25
	SSK153711	3.397	3.25	3.293	3.04	3.018	**3.20**	0.15							
	20-2	3.124	3.186	3.076	3.15	3.233	**3.15**	0.05	3.089	3.062	3.268	3.068	3.164	**3.13**	0.08
	08-2	3.185	3.124	3.433	3.179	3.154	**3.22**	0.11	2.946	3.546	3.442	3.025	2.976	**3.19**	0.25
	19-1	3.373	3.28	3.429	3.198	3.272	**3.31**	0.08	3.352	3.403	3.375	3.498	3.184	**3.33**	0.10